Die approbierte Originalversion dieser Dissertation ist an der Hauptbibliothek der Technischen Universität Wien aufgestellt (http://www.ub.tuwien.ac.at).

The approved original version of this thesis is available at the main library of the Vienna University of Technology (http://www.ub.tuwien.ac.at/englweb/).

DISSERTATION

"The dual role of the Alzheimer disease protein ß-Amyloid: Anti-oxidative ß-Amyloid (1-40) becomes a pro-oxidant during self-aggregation and damages the plasma membrane of neurons"

ausgeführt zum Zwecke der Erlangung des akademischen Grades eines Doktors der technischen Wissenschaften/der Naturwissenschaften unter der Leitung von

O.Univ.Prof. Dipl.-Ing. Dr.techn. Helmut Stachelberger

E1667

Institut für Verfahrenstechnik, Umwelttechnik und Techn. Biowissenschaften
Naturstoff- und Lebensmittelchemie

eingereicht an der Technischen Universität Wien

Fakultät für technische Naturwissenschaften und Informatik

von

DI Erich Pusch

e9226487

Quellenplatz 6/13
A-1100 Wien/Österreich

Wien, am 20.09.2003

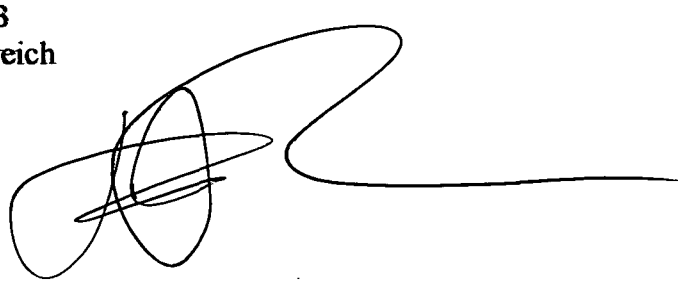

ausgeführt am

Department for Chemical Engineering
College of Engineering
University of Wisconsin-Madison
USA

unter der Leitung von

Regina Murphy, PhD

und an den

Forschungslaboratorien der Universitätsklinik für Neurologie
Allgemeines Krankenhaus Wien AKH
Österreich

unter der Leitung von

Dr. Mark Schiefermeier

CONTENT

Deutsche Kurzfassung der Dissertation 1
Summary 2

INTRODUCTION 3
Alzheimer disease (for review, see Nussbaum and Ellis, 2003) 3
The Alzheimer disease protein ß-Amyloid 4
The different forms of ß-Amyloid 5
ß-Amyloid peptide in Alzheimer disease 6
Influence of ß-Amyloid structure on function 7
ß-Amyloid assembled structures 9
Peptide domain requirements for ß-Amyloid association 9
Constitutive level of ß-Amyloid in healthy individuals and
Alzheimer disease patients 10
Mechanisms of toxicity of ß-Amyloid aggregates 11
Membrane-disrupting effects of ß-Amyloid 11
Oxidative stress 12
Lipid and protein oxidation 13
ß-Amyloid and reactive oxygen species 14
ß-Amyloid and activation of Nuclear Factor-κB 15
Alternative hypothesizes for ß-Amyloid toxicity 17
The "choline autocannibalism" theory (for review, Wurtmann, 1992) 17
Modification of Ion channels 18
Inhibitors of ß-Amyloid aggregation 19
Our hybrid-compound inhibitors 21

GOAL OF THE WORK 22

MATERIAL & METHODS 23
The Alzheimer disease protein ß-Amyloid (1-40) 23
Preparation of ß-Amyloid (1-40) samples 23
DMSO-conditions 23
Urea-conditions 23
Addition of [^{125}I]-ß-Amyloid (1-40) as tracer 24
Inhibitors KLVFFK$_6$ and KLVFFE$_4$ 25
Liposomes as artificial model membranes 26

Preparation of liposomes....26
Preparation of calcein-encapsulated liposomes....27
Uptake of ß-Amyloid (1-40) in liposomes....27
Membrane fluidity in liposomes by measurement of DPH-anisotropy....29
Calcein Leakage Assay....33
Cell Culture....35
The human neuroblastoma cell line SH-SY5Y....35
The human astrocytoma cell line GOS-3....38
Determination of cell number and cellular viability....40
Cellular toxicity assay....41
[^{125}I]-ß-Amyloid (1-40)-uptake assay....43
Incorporation of 1,6-diphenyl-1,3,5-hexatriene into SH-SY5Y cells....48
Lipid release in SH-SY5Y....53
DPH as marker for lipid in SH-SY5Y and GOS-3 cells....53
FITC-DHPE as marker for lipid in SH-SY5Y cells....54
ß-DPH-HPC as marker for lipid in SH-SY5Y and GOS-3 cells....56
Steward assay....57
Measurement of lipid peroxidation by determination of TBARS....58
Measurement of intracellular level of reactive oxygen species....61
Measurement of the NFκB-activity in the human neuroblastoma cell line SH-SY5Y....63
Determination of free, soluble ß-Amyloid (1-42)....66
Ex vivo oxidative stress in whole blood....67

RESULTS....68
Characterization of ß-Amyloid (1-40)....68
Qualitative estimation of the hydrophobicity of ß-Amyloid (1-40)....68
Qualitative estimation of the aggregation state of ß-Amyloid (1-40)....70
Studies of ß-Amyloid (1-40) effects on liposomes as model membranes....72
ß-Amyloid (1-40)-membrane binding....72
ß-Amyloid (1-40) decreases membrane fluidity....74
ß-Amyloid (1-40) induces calcein-leakage....77
Toxicity studies in the human neuroblastoma SH-SY5Y and the astrocytoma GOS-3 cell line....79
H_2O_2-induced toxicity....79
H_2O_2-induced toxicity in SH-SY5Y-cells....79
H_2O_2-induced toxicity in GOS-3-cells....80
Influence of ß-Amyloid (1-40) on the cellular viability....81

ß-Amyloid (1-40) decreases the cellular viability in SH-SY5Y cells 82
The Inhibitor KLVFFK$_6$ circumvents successfully the
ß-Amyloid (1-40)-induced toxicity in SH-SY5Y cells 84
No effect of ß-Amyloid (1-40) on the cellular viability of GOS-3 cells 84
ß-Amyloid (1-40) uptake in SH-SY5Y cells 86
Deposition of ß-Amyloid (1-40) on polystyrene surface 86
Association of ß-Amyloid (1-40) with the cellular membrane 87
Internalization of ß-Amyloid (1-40) 89
Degradation of ß-Amyloid (1-40) 91
Quantification of degraded ß-Amyloid (1-40) 91
Characterization of degradation of ß-Amyloid (1-40) 92
Evaluation of the distribution of extracellular
and intracellular degradation of ß-Amyloid (1-40) 93
Intracellular degradation of ß-Amyloid (1-40) 94
Aggregates of ß-Amyloid (1-40) decrease the membrane fluidity in SH-SY5Y cells 97
Preliminary experiment 98
ß-Amyloid (1-40)-induced decrease of membrane fluidity in SH-SY5Y 99
No effect of the inhibitor KLVFFK$_6$ on the ß-Amyloid (1-40)-induced
increase in DPH-anisotropy 101
Aggregates of ß-Amyloid (1-40) induce lipid leakage in SH-SY5Y 102
DPH-release induced by aggregated ß-Amyloid (1-40) 102
Fluorescence intensity and anisotropy of DPH in the supernatant 102
Remaining fluorescence intensity of DPH in the cellular membrane 104
No effect of KLVFFK$_6$ on the ß-Amyloid (1-40)-induced DPH-release 105
Comparison of DPH-release in SH-SY5Y and GOS-3 cells 106
Fluorescent lipids as probes for cellular membrane lipids 108
FITC-DHPE as probe for cellular membrane lipids 108
ß-DPH-HPC as probe for cellular membrane lipids 109
Determination of lipid-release with the Stewart-assay 110
Aggregates of ß-Amyloid (1-40) enhance H_2O_2-induced lipid peroxidation
in SH-SY5Y cells 112
H_2O_2-induced lipid peroxidation in SH-SY5Y and GOS-3 cells 113
ß-Amyloid (1-40) does not induce significantly lipid peroxidation 114
Aggregates of ß-Amyloid (1-40) enhance H_2O_2-induced lipid peroxidation
in SH-SY5Y cells 115
Pretreatment with ß-Amyloid (1-40) aggregates increases H_2O_2-induced
lipid peroxidation 117

ß-Amyloid (1-40) circumvents H_2O_2-induced increase of oxidative stress 118
Induction of oxidative stress by H_2O_2 in SH-SY5Y and GOS-3 cells 118
ß-Amyloid (1-40) reduces the level of iROS in SH-SY5Y cells 120
ß-Amyloid (1-40) pretreatment circumvents H_2O_2-induced increase of oxidative stress 122
Aggregated ß-Amyloid (1-40) induces Nuclear Factor-κB activation in SH-SY5Y cells 123
Constitutive level of NFκB activity in SH-SY5Y cells 123
Aggregated ß-Amyloid (1-40) induces NFκB-activation in SH-SY5Y 124
No effect of the inhibitor KLVFFK$_6$ on the ß-Amyloid (1-40)-induced activation of NFκB 126
Oxidative stress induces the release of ß-Amyloid (1-42) in SH-SY5Y and GOS-3 cells 127
Ex vivo addition of H_2O_2 to whole blood induces the release of ß-Amyloid (1-42) 129

DISCUSSION 131
Is ß-Amyloid the key element of Alzheimer disease? 131
ß-Amyloid and its impact on membrane integrity 133
ß-Amyloid: pro-oxidant or antioxidant? 142
Neurons play an active role in Alzheimer disease 148
Does blood plasma ß-Amyloid contribute to the accumulation of ß-Amyloid deposits in the brain? 153
A new model for the development of Alzheimer disease 155

REFERENCES 158

Curriculum vitae 175

Deutsche Kurzfassung der Dissertation

DAT (Demenz vom Alzheimer-Typ) ist eine Erkrankung des Gehirns, bei der langsam aber stetig Nervenzellen sterben. In Österreich sind etwa 100.000 Personen von dieser Demenz betroffen. Das pathologische Hauptmerkmal sind extrazelluläre Ablagerungen im Gehirn des Patienten, die vorwiegend aus ß-Amyloid, dem Abbauprodukt des "amyloid precursor protein" (APP) bestehen. *In vitro* und *in vivo* Ergebnisse unterstützen die Hypothese, dass ß-Amyloid in aggregierter Form neurotoxische Eigenschaften besitzt und eine entscheidende Rolle in der Entstehung und dem Verlauf der Krankheit spielt.

Im Rahmen dieser Arbeit untersuchten wir den Einfluss der Isoform ß-Amyloid (1-40) auf die Integrität der Plasmamembran neuronaler Zellen, am Beispiel der Zelllinie SH-SY5Y. In Liposomen und SH-SY5Y Zellen bewirkte die Zugabe von aggregiertem ß-Amyloid (1-40) eine Erniedrigung der Membranfluidität (gemessen durch DPH-Anisotropie) und eine Reduzierung der Membranimpermeabilität (gemessen durch Freisetzung von DPH und fluoreszierenden Membranbestandteilen), sowie einen Anstieg oxidierter Membranlipide (gemessen durch TBARS). Letztere Beobachtung ist von besonderem Interesse, da ß-Amyloid (1-40) unabhängig des Aggregationszustandes eine Abnahme intrazellulärer Peroxyde in ruhenden und H_2O_2-behandelten SH-SY5Y Zellen induzierte und daher antioxidative Eigenschaften zeigte.

Weiters untersuchten wir die neuronale Aufnahme und Freisetzung von ß-Amyloid durch SH-SY5Y Zellen. Wir beobachteten die quantitative Aufnahme und den Abbau von ß-Amyloid (1-40), sowie die Freisetzung der Isoform ß-Amyloid (1-42) durch H_2O_2-Stimulation. Diese Ergebnisse bekräftigen die Annahme, dass Neuronen eine aktive Rolle im ß-Amyloid-Metabolismus spielen. Zudem zeigten wir, dass die *ex vivo* H_2O_2-Zugabe zu frischem Vollblut eine Erhöhung des Plasma-Spiegels von ß-Amyloid (1-42) bewirkte.

Schlussendlich führen unsere gewonnenen Daten zu folgendem Modell: Um gegen den erhöhten oxidativen Stress im Alter anzukämpfen, setzen Neuronen (und andere im Blut vorhandene Zellen) antioxidatives, monomeres ß-Amyloid frei. Bei fortdauerndem oxidativen Einfluss aggregiert akkumuliertes ß-Amyloid und erlangt dadurch prooxidative und toxische Eigenschaften, die sich beispielsweise in Schädigungen der Membranintegrität manifestieren.

Summary

Alzheimer disease is a devastating neurodegenerative disease that afflicts approximately 100.000 elderly people in Austria. The major pathological hallmark is the abundance of extracellular plaques found in the brain of patients upon autopsy, constituted to more than 90% of the peptide ß-Amyloid, a 39- to 43-residue proteolytic product of a membrane-associated precursor protein. Mounting *in vitro* and *in vivo* data supports the hypothesis that ß-Amyloid, and more specifically, aggregated (fibrillar) ß-Amyloid, is neurotoxic and thus likely plays a substantial causative role in the Alzheimer disease pathology.

How ß-Amyloid exerts its toxic impact on neurons remains an open question. Within the framework of this study, we focused on the impact of the 40-residue ß-Amyloid (1-40) on the integrity of the plasma membrane in the cell line SH-SY5Y as a model for neurons.

In liposomes and in viable SH-SY5Y cells, addition of ß-Amyloid (1-40) altered the fluidity of the plasma membrane (as measured by DPH-anisotropy), induced the leakage of certain membrane constituents (as measured by the release of DPH and fluorescent lipids), and oxidized membrane lipids (as measured by the TBARS-assay) only if aggregated. The latter is of interest, as the peptide also decreased the concentration of intracellular reactive oxygen species (iROS) and circumvented H_2O_2-mediated increase in iROS independent of its aggregation state in the cells, thereby acting as anti-oxidant.

In view of this dual role of ß-Amyloid on neurons, we further characterized the uptake and release of ß-Amyloid by SH-SY5 cells. Our data supports the hypothesis that neurons play an active role in ß-Amyloid metabolism. The cells degraded a significant amount of ß-Amyloid (1-40) and released measurable amounts of the (1-42) isoform into the extra-cellular fluid upon addition of H_2O_2 to generate oxidative stress, thereby contributing actively to the increased burden of ß-Amyloid in the brain of Alzheimer disease patients.

Finally our observation that *ex vivo* addition of H_2O_2 to whole blood also increased the concentration of plasma ß-Amyloid leads us to the following model: Monomeric ß-Amyloid itself has anti-oxidative capacities and it is released by neurons and other agents in order to fight against the oxidative stress that occurs in the elderly. Ultimately, accumulated ß-Amyloid self-associates and becomes neurotoxic by acting as a pro-oxidant and damaging the neuronal membrane.

INTRODUCTION

Alzheimer disease (for review, see Nussbaum and Ellis, 2003)

Alzheimer disease is a devastating neurodegenerative disease that afflicts approximately 100.000 elderly in Austria, with more than 10.000 new incidents per year. Worldwide, the number is expected to grow to more than 20 millions in the next few decades. Alzheimer disease is thereby clearly the most common neurodegenerative disease and constitutes about two thirds of cases of dementia overall (numbers vary from 41 to 81 percent in various studies, e.g. Helmer et al., 2001).

Excluding persons with clinically questionable dementia, Alzheimer disease has a prevalence of approximately one percent among those 65 to 69 years of age. The incidence rate increases then to 40 to 50 percent among persons 95 years of age or over. The frequency in women is slightly higher than in man (approximately 10 percent higher in women than in men). Although the mean age at the onset of dementia is approximately 80 years, early-onset disease, defined arbitrarily and variously as the illness occurring before the age of 60 to 65 years, can occur but is rare, making up about 6 to 7 percent in total of all cases of Alzheimer disease. A small percentage of early-onset Alzheimer disease (less than 10 percent) is familiar, in an autosomal dominant manner.

Diagnosis is based on neurological examination and the exclusion of other causes of dementia; but the definitive diagnosis can be made only at autopsy.

The clinical hallmarks are progressive impairment in memory, judgment, decision-making, orientation to physical surrounding, and language; as well as increased libido.

Pathological features of the disease are, in addition to irreversible synapse and neuronal loss, extracellular senile plaques and intraneuronal fibrillary tangles (NFT), both abnormal features found in the brain of patients upon autopsy (Katzman and Saitoh, 1991) and first described and published by the Bavarian psychiatrist Alois Alzheimer himself in the year 1906 (Alzheimer, A. (1906). Über einen eigenartigen schweren Krankheitsprozess der Hirnrinde, *Zentralblatt für Nervenkrankheiten*, **25**, 1134). Whereas 10 to 15 percent of brain autopsies have been reported to show very little or no cortical

NFT, neuritic plaque formation is seen in all cases of Alzheimer disease (Joachim et al., 1987).

The senile plaques consist of a proteinaceous amyloid deposit surrounded by degenerating neurites. The predominant protein component of the amyloid deposit is ß-Amyloid, a 4kDa peptide derived from a much larger transmembrane precursor protein. ß-Amyloid deposits are fibrillar, with a diameter of ~10 nm and a cross-ß structural motif.

Mounting *in vitro* and transgenic mouse data support the hypothesis that ß-Amyloid, and more specifically, aggregated (fibrillar) ß-Amyloid, is neurotoxic and thus likely plays an essential role in the onset and/or progression of Alzheimer disease pathology.

Nevertheless, nearly 100 years after the discovery of this neurodisease and 20 years after the discovery of ß-Amyloid and intense scientific scrutiny, the question, how ß-Amyloid exerts its toxic effect, remains unanswered and is still a matter of debate.

The Alzheimer disease protein ß-Amyloid

ß-Amyloid is the major protein component of senile plaques and cerebrovascular amyloid deposits from Alzheimer disease patients (Glenner and Wong, 1984; Masters et al., 1985; Wong et al., 1985). The ß-Amyloid peptide is a 39- to 43-residue proteolytic product of a membrane-associated precursor protein. ß-Amyloid contains sequences from both extracellular and transmembrane regions of the parental protein (Kang et al., 1987; Masters et al., 1985). Proteolysis of the precursor protein proceeds via sequential cleavage by ß- and γ-secretase at the N- and C-termini of the peptide product (Mills and Reiner, 1999). The sequence and the putative position of ß-Amyloid in the precursor are shown in Figure 1.

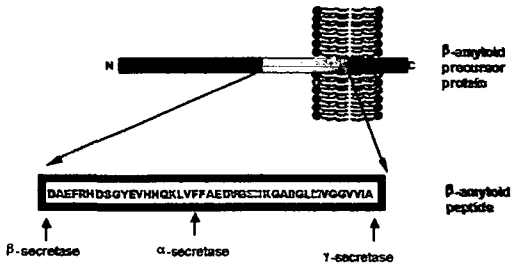

Fig.1: ß-Amyloid (1-40) sequence and its position in precursor protein

ß-Amyloid spontaneously self-assembles into amyloid fibrils, which are characterized by cross-ß sheet conformation, diameters of ~10 nm, and birefringence upon staining with congo red (Jimenez et al., 1999; Kirschner et al., 1986; Merz et al., 1983), see figure 2 for an electron micrograph of ß-Amyloid aggregates. These extracellular depositions of this processed peptide in senile plaques are the one defining characteristic of Alzheimer disease, Down's syndrome and hereditary cerebral hemorrhagic disease, HCWA-D (Dutch type).

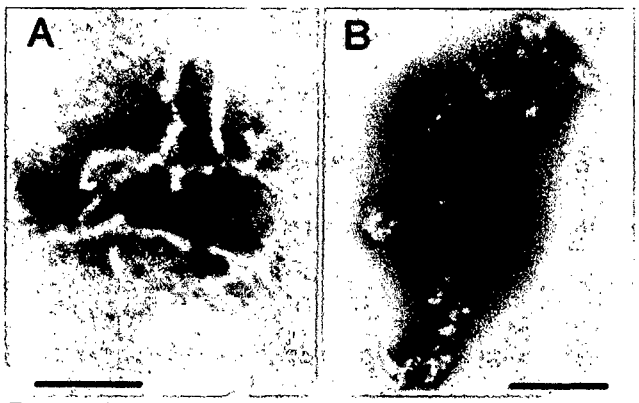

Fig.2: Electron micrographs of ß-Amyloid aggregated for 2 days at neutral and acidic pH. (A) pH 7 fibrillar aggregates, scale bar = 50 nm; (B) pH 6 agglomerated aggregates; scale bar = 200 nm (Ghanta et al., 2000)

The different forms of ß-Amyloid

Cleavage of the amyloid precursor protein at different sites by the secretases leads to different isoforms of ß-Amyloid. Major isoforms found in the Alzheimer disease brain are ß-Amyloid (1-40) and ß-Amyloid (1-42).

The relative contribution of ß-Amyloid (1-40) and ß-Amyloid (1-42) to Alzheimer disease pathogenesis has been the subject of numerous studies. There is evidence that ß-Amyloid (1-42) is important in the early development of Alzheimer disease pathology because of its association with diffuse plaques, loosely aggregated deposits of amyloid protein (Hardy, 1997; Iwatsubo et al., 1996; Selkoe, 1997). In addition, as compared with ß-Amyloid (1-40), the (1-42) isoform has been shown to have a greater aggregation potential (Jarett and Lansbury, 1993; Jarett et al., 1993) and is produced in relatively higher amounts in familial forms of the disease, including presenilin and amyloid

precursor genetic alterations (for reviews see Selkoe, 1997; Yankner, 1996). However, immunohistochemical studies have shown that ß-Amyloid (1-40) is the predominant form in neuritic, mature plaques, a lesion that develops later in the disease process (Iwatsubo et al., 1995, 1996; Suzuki et al., 1994). Studies by Shin and coworkers (1997) suggest that ß-Amyloid (1-42) is essential to the early development of Alzheimer disease pathology, but not sufficient to promote the formation of mature, neuritic plaques unless succeeded by ß-Amyloid (1-40) deposition.

These findings support a "seeding" hypothesis, that ß-Amyloid (1-42) aggregates act as the initiation factors for early, diffuse plaque formation followed by progressive accumulation of ß-Amyloid (1-40) in the Alzheimer disease brain.

ß-Amyloid peptide in Alzheimer disease

Many researchers believe that ß-Amyloid plays a major role in the onset and/or progression of Alzheimer disease (Joachim and Selkoe, 1992; Rosenberg, 1993). The lack of rigorous evidence for another toxic agent, loss of trophic factor(s), or specific defect in intermediary metabolism that can initiate the Alzheimer disease cascade has allowed the "amyloid cascade hypothesis" (Hardy and Higgins, 1992), that ß-Amyloid overproduction and subsequent deposition is a major causative factor in the onset of Alzheimer disease, to emerge as the ethiopathogenetic mechanism with arguably the most extensive and compelling supportive data. To date, it is supported by strong biochemical, genetic, and transgenic evidence (e.g., Games et al., 1995; Hsiao et al., 1996; Holcomb et al., 1998; Mattson et al., 1992; Rubinsztein, 1997; Yankner et al., 1990). For example, multiple studies have shown that addition of synthetic ß-Amyloid can be directly neurotoxic to cultured cortical cells (Busciglio et al., 1993b; Ueda et al., 1994; Yankner et al., 1990; Zamani et al., 1997) and can increase neuronal vulnerability to a variety of insults including enhanced susceptibility to excitotoxicity (Koh et al., 1990; Mattson et al., 1992), glucose deprivation (Copani et al., 1991), and free radicals (Goodman and Mattson, 1994). Direct injection of ß-Amyloid in rat and monkey cerebral cortex produced localized necrosis and neuronal loss (Frautschy et al., 1991; Kowall et al., 1992). More recently, transgenic mice have been developed that produce human ß-

Amyloid precursor protein, secrete ß-Amyloid, develop ß-Amyloid deposits, and possess neuronal pathology and learning deficits (Games et al., 1995; Hsiao et al., 1996; Johnson-Wood et al., 1997; Moran et al., 1995).

These and other results have considerably strengthened the "amyloid hypothesis" (Joachim and Selkoe, 1992; Rosenberg, 1993).

Influence of ß-Amyloid structure on function

A subsidiary to the amyloid hypothesis is that ß-Amyloid is toxic only when it is aggregated into fibrils. A substantial body of biophysical, biochemical, and cell biological data (for review, see Iversen et al., 1995) support this idea, which links the physical state of ß-Amyloid with its biological activity.

Simmons and coworkers (1994) found that variability in the toxicity of synthetic ß-Amyloid (1-40) to hippocampal cultures correlated with the extent of ß-sheet formation of the peptide in solution, suggesting that the conformation of ß-Amyloid influences its activity. A significant role for peptide conformation in self-assembly also was found by Maggio and coworkers (1992). Using ^{1}H NMR spectroscopy to probe peptide conformation, they observed that the conformation adopted by ß-Amyloid fragments capable of forming plaques was different from that adopted by those that were inactive (Lee et al., 1995). In other studies, "aged" ß-Amyloid (generated by incubation at 37°C for several days) formed stable insoluble amyloid aggregates and induced neurodegeneration *in vitro* (Pike et al., 1991a, 1991b, 1993). Treatment of aggregated ß-Amyloid with hexafluoro-2-isopropanol not only resolubilized the peptide but also reduced its cellular toxicity (Pike et al., 1993). Lorenzo and Yankner (1994) demonstrated that fibrillar ß-Amyloid (1-42) was toxic to rat hippocampal cultures, but amorphous aggregated ß-Amyloid (1-42) was not, lending further support for the importance of ß-Amyloid conformation and aggregation. Seilheimer and coworkers (1997) demonstrated a strong positive correlation between conversion of ß-Amyloid monomers to elongated fibrils, as measured by electron microscopy and circular dichroism spectroscopy, and ß-Amyloid cellular toxicity, as measured by the MTT

reduction assay. These results indicate that both the conformational and aggregational state of ß-Amyloid influence its activities.

Observations from genetically linked cases of early-onset Alzheimer disease also support the premise that ß-Amyloid aggregation is necessary for ß-Amyloid toxicity (Selkoe, 1996). Specifically, several missense mutations in the gene encoding the ß-Amyloid precursor protein are associated with the inherited form of the disease. Each of these changes result in increased production of ß-Amyloid variants in cell culture, especially the more aggregation-prone isoform ß-Amyloid (1-42).

Further evidence comes from a study probing the biological role of the presenilins, proteins identified by their linkage to familial Alzheimer disease. Mice producing a presenilin 1 variant associated with early onset Alzheimer disease were found to have an increased level of ß-Amyloid (1-42) relative to that of ß-Amyloid (1-40) (Duff et al., 1996).

An alternative hypothesis, that a soluble intermediate in the fibrillogenesis pathway, not the final insoluble product, is the toxic moiety, has gained significant exposure in recent years (Koo et al., 1999; Lansbury, 1999). It is possible that soluble rather than precipitated ß-Amyloid oligomers are the active species in accomplishing neurotoxicity. As examples, dimeric (Roher et al., 1996), oligomeric (Lambert et al., 1999), nonfibrillar (non-thioflavin-T staining, Pillot et al., 1999), and "protofibrillar" (Hartley et al., 1999; Ward et al., 2000) ß-Amyloid are reportedly toxic to cultured cells. For example, aggregated ß-Amyloid added directly to cell culture medium is toxic, but fibrillar ß-Amyloid displayed on a solid substrate exhibited no cellular toxicity (Wujek et al., 1996). ß-Amyloid oligomers (about 4-10 monomers) were toxic to mouse brain slices (Lambert et al., 1999). Adding the peptide $KLVFFK_6$ to ß-Amyloid (1-40) during aggregation enhances the rate of aggregation while reducing ß-Amyloid-induced toxicity in PC12 cells (Lowe et al., 2001). Observations in post-mortem human studies also support the notion that soluble ß-Amyloid forms may make a previously unrecognized contribution to early synaptotoxicity in Alzheimer disease (Klein et al., 2001).

ß-Amyloid assembled structures

Given the biological relevance of ß-Amyloid fibrillogenesis, several detailed studies have been conducted to further investigate the conformational and aggregational characteristics of ß-Amyloid. ß-Amyloid adopts a wide range of secondary structure depending on solvent conditions and peptide segment. Under aqueous conditions, ß-Amyloid contains a significant amount of α-helical character (Barrow et al., 1992; Kohno et al., 1996) and can undergo conformational transition to a ß-rich structure if bound to membranes (Choo-Smith and Surewicz, 1997), containing negatively charged lipids (Terzi et al., 1994). In physiological buffers, both random coil and ß-sheet secondary structure is observed, with the ß-sheet content increasing dramatically with increasing ß-Amyloid length and peptide concentration (Barrow and Zagorski, 1991; Barrow et al., 1992; Hilbich et al., 1991). ß-Amyloid conformation shows strong pH dependence, with the greatest ß-sheet content in the pH 4-7 range (Fraser et al., 1991). ß-sheet content is concentration-dependent, indicating that the ß-sheet-containing conformers are oligomeric. Recent studies suggest that the dimer/tetramer population lacks regular secondary structure, but larger spherical oligomers (~20mers), stable at pH 3, possess ß-structure similar to mature fibrils (Huang et al., 2000).

Peptide domain requirements for ß-Amyloid association

Biophysical studies of ß-Amyloid provide insight into how the structural features of the peptide influence its self-assembly. At physiological pH, ß-Amyloid aggregates into fibrils, which possess a cross-ß-sheet structure (Kirschner et al., 1986). The rate-determining step in the aggregation process appears to be nucleation with fibril elongation proceeding rapidly (Harper and Lansbury, 1997; Jarrett et al., 1993; Lomakin et al., 1996; Shen and Murphy, 1995). In support of this model, the concentrations of ß-Amyloid required to initiate fibril formation are higher than those necessary for deposition onto pre-existing aggregates (Maggio et al., 1992). Coincident with the conversion of monomeric to fibrillar ß-Amyloid is a transition from random coil to ß-sheet (Terzi et al., 1995), indicating that a conformational change is involved in the rate-determining step. The rate of aggregation is exquisitely sensitive to small changes in

peptide length or sequence. For example, ß-Amyloid is an amphiphilic peptide possessing a hydrophilic N-terminus and a hydrophobic C-terminus; increasing the length of the latter greatly increases the rate of aggregate formation (Jarrett et al., 1993). One region that plays an important role in the rate of aggregation is the short hydrophobic strech ranging from residue 17 to 21, which appears to be critical in the formation of fibrillar structure (Esler et al., 1996; Fraser et al., 1991; Hilbich et al., 1992). Electrostatic effects also contribute to fibril formation, as charged residues adjacent to this region affect the process (Fraser et al., 1991, 1994). Thus, residues 17-21 and the C-terminus are two sections of ß-Amyloid that play key roles in its self-assembly. Another region of ß-Amyloid that is supposed to contribute circumstantially to ß-Amyloid aggregation and toxicity is the stretch 25-35 (Pike et al., 1995).

Constitutive level of ß-Amyloid in healthy individuals and Alzheimer disease patients

In vitro, ß-Amyloid aggregation is only observed at high concentrations in the µM-range. Driven by these findings, researchers have focused on determining the *in vivo* concentration of ß-Amyloid in the human blood plasma and in the cerebrospinal fluid.

Measurements in blood plasma revealed that ß-Amyloid (1-40) and (1-42) are expressed constitutively in healthy people and mean values are statistically not altered in Alzheimer disease (Vanderstichele et al., 2000).

Moreover, no correlation between the concentration of the ß-Amyloid (1-40) isoform in the cerebrospinal fluid and the degree of dementia has been observed so far. Recent studies suggest that the concentration of the (1-42)-isoform in the cerebrospinal fluid, which lies in the nM-range, is reduced in Alzheimer disease patients in comparison to healthy people (Andreasen et al., 2001; Jellinger, 1996; Sunderland et al., 2003). The sensitivity and specificity of these measures are high for separation of Alzheimer disease patients from controls, but their specificity against other dementias is only moderate.

The question, to what extent blood plasma ß-Amyloid is contributing to the progression of the ß-Amyloid plaques in the brain is not yet clear. Data about the migration of ß-Amyloid through the blood-brain-barrier are to date contradictory. Blanc and coworkers

(1997) observed ß-Amyloid-induced albumin permeability in vascular endothelial cells and suggest blood-brain barrier breach, confirming results of others (Matilla et al., 1994; Perlmutter, 1994). Saito and coworkers (1995) observed only marginal transport of radiolabeled ß-Amyloid (1-40) through the brain capillary endothelial wall, which makes up the blood-brain barrier *in vivo*. No correlation between concentration of ß-Amyloid (1-42) in plasma and in cerebrospinal fluid has been observed so far (Fukumoto et al., 2003).

Mechanisms of toxicity of ß-Amyloid aggregates

Mounting circumstantial evidence supports the hypothesis that extracellular ß-Amyloid in a self-associated state is toxic to cells, but how ß-Amyloid interacts with cells to cause degeneration remains an open question.

Membrane-disrupting effects of ß-Amyloid

Binding to trypsin-sensitive sites has been observed (Lambert et al., 1999), and a few candidate receptors have been identified (Deane et al., 2003; El Khoury et al., 1996; Joslin et al., 1991; Kimura and Schubert, 1993; Kuner et al., 1998; Schultz et al., 1998; Yan et al., 1996, 1997, 1999). However, it remains doubtful whether specific ß-Amyloid binding to receptors is responsible for the toxicity (Chung et al., 1999; Liu et al., 1997). The findings, that both D- and L-enantiomers of ß-Amyloid have similar biological activity (Cribbs et al., 1997), and that fibrils consisting of either amylin or ß-Amyloid, with similar structure but distinct sequence, induce similar changes in gene expression (Tucker et al., 1998), argue strongly against a specific ß-Amyloid-receptor association.
An alternative is that extracellular ß-Amyloid interacts rather nonspecifically with cell membranes (Kanfer et al., 1999). This hypothesis rests on the notion that the perturbation of membrane physical properties causes an abnormal functioning of membrane-embedded proteins. Given the amphiphilic nature of the peptide and its origin as a product of a membrane-protein, it is reasonable to postulate that ß-Amyloid-lipid interactions might be significant. Indeed, membrane surface ruffling, increases in

membrane conductance, decreases in membrane fluidity, fusion of small unilamellar vesicles, leakage of encapsulated dyes from phospholipid vesicles, formation of pores as for example cationic-selective ion channels, and loss of impermeability in mitochondrial, lysosomal, and endosomal membranes have been variously observed following ß-Amyloid addition to synthetic membranes, cortical homogenates, or whole cells (Arispe et al., 1993; Carette et al., 1993; Choo-Smith et al., 1997; Engstrom et al., 1995; Galdzicki et al., 1994; Li et al., 1995; Lin et al., 1998; Maestre et al., 1993; McLaurin and Chakrabartty, 1996, 1997; McLaurin et al., 1998; Müller et al., 1998; Pillot et al., 1996; Simmons and Schneider, 1993).

Any satisfactory mechanisms for ß-Amyloid toxicity must explain the connection to the ß-Amyloid assembled state. There is limited evidence which links ß-Amyloid-membrane interactions with ß-Amyloid aggregation: fibrillar but not monomeric ß-Amyloid bound to lipid components of cortical homogenates (Good and Murphy, 1995), binding of fibrils but not unaggregated ß-Amyloid to cell membranes (Sadler et al., 1995), and decreases in lipid bilayer fluidity correlated with ß-Amyloid aggregation state (Kremer et al., 2000). Furthermore, circular dichroism studies have shown that acidic phospholipids induce specifically a conformational change in ß-Amyloid from random-coil to toxicity-prone ß-structure (McLaurin and Chakrabarrty, 1997).

Despite significant efforts in recent years, there is as yet no broad consensus as to the molecular basis for ß-Amyloid cellular toxicity, and the exact relationship between ß-Amyloid aggregation and ß-Amyloid-cell associations remains relatively unexplored.

Oxidative stress

> *Oxidative stress can be defined as a surplus of oxidants over antioxidants or as the production of reactive oxygen species (e.g. $O_2^{\cdot-}$, H_2O_2, $OH^{\cdot}$, and $ONOO^{-}$) beyond the capacity of the cell to neutralize them.*

Once bound specifically to a putative membrane-bound receptor or in unspecific fashion to the cellular membrane, the question how ß-Amyloid induces neuronal cell death

remains widely open. It has been observed that the brain of Alzheimer disease patients is under extensive oxidative stress (Markesbery, 1997; Swerdlow et al., 1997), manifested by lipid peroxidation and protein oxidation, among other markers of oxidative stress (for reviews, see Mark et al., 1996; Smith and Perry, 2002). Moreover, decreases in the activity of oxidation sensitive enzymes and increased protein carbonyl content in the brains of Alzheimer disease patients have been documented (Smith et al., 1991). Connecting this increase of oxidative burst to the amyloid cascade hypothesis - that aggregation generates toxic species of ß-Amyloid - leads to the promising hypothesis that neurodegeneration in Alzheimer disease brain is based on free radical oxidative stress associated with, or even induced by ß-Amyloid.

Lipid and protein oxidation

Extensive evidence for lipid peroxidation being an important mechanism of neurodegeneration in Alzheimer disease brain exists. Lipid peroxidation studies of Alzheimer disease brains demonstrated that free radical-induced lipid peroxidation is widespread. Interestingly, increased lipid peroxidation is found in the frontal cortex and hippocampus, areas that show neuritic plaques (ß-Amyloid (1-40)-rich), whereas no increase in membrane oxidative damage is found in the cerebellum, where only diffuse plaques (ß-Amyloid (1-42)-rich) have been observed (McClure et al., 1994). Furthermore, it has been shown that ß-Amyloid can cause lipid peroxidation in brain cell membranes and that this oxidation can be at least partially circumvented by addition of antioxidants (Avdulov et al., 1997; Bruce-Keller et al., 1998; Butterfield et al., 1994; Daniels et al., 1998; Gao et al., 2001; Gridley et al., 1997; Mark et al., 1997, 1999). Lipid oxidation has also been observed in cultured neurons (Behl et al., 1994; Butterfield et al., 1994; Goodman and Mattson, 1994).

More *in vivo* evidence for lipid peroxidation in Alzheimer disease is coming from analysis of total phospholipids and compositional alterations in the brain. Levels of fatty acids vulnerable to free radical attack, as polyunsatursated fatty acids (PUFA), including arachidonic and docosohexanoic acid, are predicted to decrease in Alzheimer disease brain if lipid peroxidation increases. Consistent with this prediction, a decrease in these

fatty acids has been shown in several studies (Miatto et al., 1986; Nitsch et al., 1992), as well as a decrease of PUFA-rich phosphatidylinositol and phosphatidylethanolamine (Guan et al., 1999; Prasad et al., 1998).

Free radical attack on PUFA can ultimatively lead to multiple aldehydes, for example acrolein and 4-hydroxy-2-nonenal (HNE) (Esterbauer et al., 1991). These lipid peroxidation products are able to alter the conformation of membrane proteins (Pocernich et al., 2001; Subramaniam et al., 1997), and are toxic to neurons, possibly by disrupting Ca^{2+} homeostasis and reducing Na^{+}/K^{+}-ATPase activity (Lovell et al., 2001; Mark et al., 1997; Subramaniam et al., 1997). Elevated levels of HNE, one of the major products of lipid peroxidation, in the Alzheimer brain and cerebrospinal fluid, have been shown several times (Markesbery and Lovell, 1998; Sayre et al., 1997). Furthermore, it has been shown that ß-Amyloid can induce the formation HNE and acrolein in rat hippocampal neurons (Mark et al., 1997). In line with these observations is a decrease in activity of glutathione S-transferase (Lovell and Markesbery, 1998), an enzyme that shows high detoxifying activity against HNE (Bruns et al., 1999). These results suggest that, in addition to direct damage to neuronal membranes from reactive oxygen species, products of lipid peroxidation as HNE may contribute to an indirect mechanism of cell damage.

Taken together, these findings are consistent with the notion that ß-Amyloid-induced lipid peroxidation may in part account for neurodegeneration in Alzheimer disease: soluble aggregates of ß-Amyloid could insert into neuronal membranes, where, in processes that are inhibited by chain-breaking oxidants, lipid peroxidation, protein oxidation and formation of reactive oxygen species occur. This oxidative damage or membrane modification, resulting from the reaction of lipid peroxidation products as HNE with enzymatic membrane-bound enzymes, could alter synaptic membrane functioning (for example voltage-dependent calcium channels or plasma membrane ion-motive ATPases) and eventually lead to neuronal cell death.

ß-Amyloid and reactive oxygen species

Reactive oxygen species (ROS) have been implicated in many aspects in Alzheimer disease and other neurodegenerative diseases (Coyle and Puttfarcken, 1993; Smith et al.,

1992). The neurotoxicity of ß-Amyloid appears to involve ROS: ß-Amyloid generates free radicals in solution (Hensley et al., 1994) and induces peroxide accumulation in cultured neuroblastoma cells (Behl et al., 1994) and primary hippocampal neurons (Goodman and Mattson, 1994). It has been observed that ß-Amyloid toxicity and increased intracellular calcium are quantitatively blocked by antioxidants (Behl et al., 1994; Goodman and Mattson, 1994; Goodman et al., 1994), but other researchers observed only limited success to no impact at all in ß-Amyloid-toxicity circumvention by use of antioxidants (Lockhart et al., 1994; Pike et al, 1997; Yao et al., 1999), suggesting that ß-Amyloid-toxicity is not solely mediated by ROS.

Nevertheless, it is still unclear how ß-Amyloid induces ROS in cells. Specific inhibitors of an NADPH-linked oxidase similar to that found in neutrophils have successfully blocked ß-Amyloid toxicity (Behl et al., 1994). Electron paramagnetic resonance spectroscopy data indicate that the peptide itself is a free radical that can propagate radicals to proteins and membrane lipids (Butterfield et al., 1994; Hensley et al., 1994, 1995a, 1995b). Butterfield and coworker (2002) postulate a critical role of methionine residue 35 for the oxidative stress and neurotoxic properties of ß-Amyloid (1-42). Another postulated site is located in the hydrophilic N-terminal part of the peptide and consists of three histidine (at positions 6, 13, and 14) and one tyrosine (at position 10) residues, all of which are known to efficiently chelate transition metal ions (Kontush, 2001).

ß-Amyloid and activation of Nuclear Factor-κB

Recently, more compelling evidence for an involvement of ROS in Alzheimer disease is coming from observations that ß-Amyloid can induce the Nuclear Factor-κB (NFκB), a transcriptional factor that can be activated posttranslationally by oxidative stress (Schreck et al., 1992). Typically sequestered in the cytoplasm in an constitutively and inducible form as a cytoplasmatic p50-p65 heterodimer bound to the inhibitor subunit IκB, NFκB represents a ubiquitous, rapid system for responding in a transcriptional-dependent manner to stimuli from a variety of sources, including pathogenic agents, pro-inflammatory cytokines, phorbol esters, UV irradiation, and oxidants (Rothwarf and

Karin, 1999). Activation of the heterodimer is achieved by phosphorylation of IκB by different IκB kinases, followed by ubiquitination and proteasomal degradation of phospho-IκB. Liberation of the IκB subunit unmasks nuclear localization sequences on the NFκB-heterodimer, allowing it to traverse the nuclear pore, migrate into the nucleus, and sit down on its cognate DNA consensus sequence, thereby initiating de novo transcription. Target genes regulated by NFκB include many cytokines, acute phase proteins, immunoreceptors, and oxidative stress-compensatory proteins such as Mn-superoxide dismutase (see figure 3). Thereby, NFκB can increase cellular antioxidant capacity (Schreck et al., 1992).

NFκB-activation by ß-Amyloid has been demonstrated in primary rat astrocytes (Akama et al., 1998; Smits et al., 2001), mouse glial cells (Bales et al., 1999, 2000; Bonaitu et al., 1997; Heese et al., 1998), oligodendrocytes (Xu et al., 2001), and neuroblastoma cells (Bales et al., 1998; Behl et al., 1994; Kaltschmidt et al., 1997). Moreover, NFκB-immunoreactivity is observed in the nuclei of neurons in the vicinity of diffuse plaques in the brain of Alzheimer disease patients (Ferrer et al., 1998).

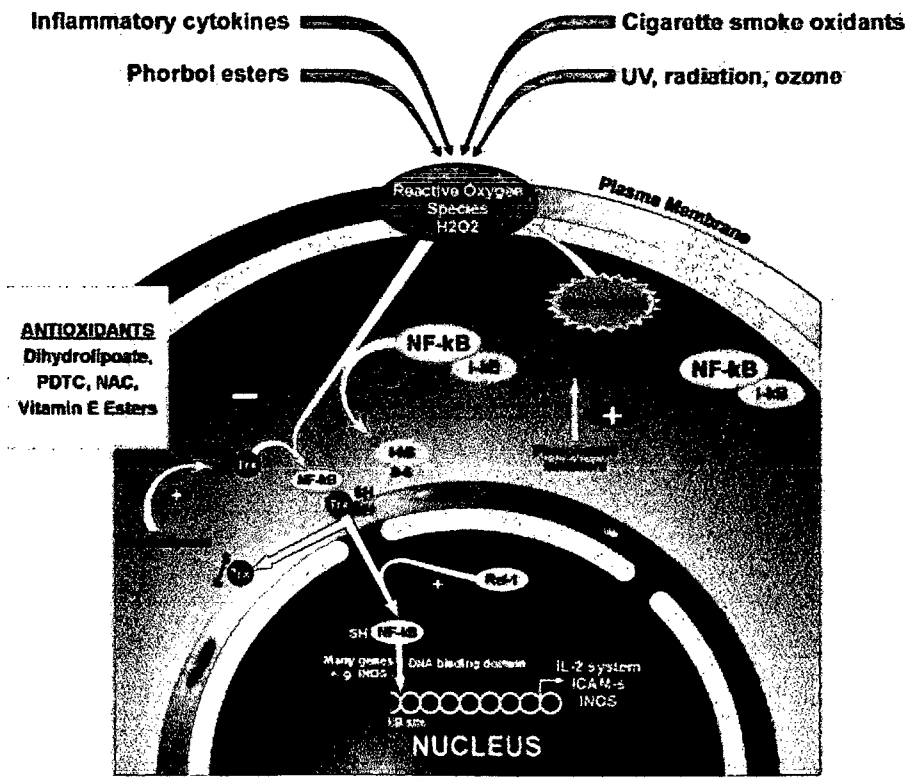

Fig.3: NFκB-activation pathway (Network Anti-oxidantsTM)

Alternative hypothesizes for ß-Amyloid toxicity

After more than a decade and extensive research, the question, if ß-Amyloid-induced oxidative stress in Alzheimer disease brain is occurring and/or relevant, or at least one dominant feature of the disease, is still heavily debated and alternative hypothesizes have emerged and gained significance.

The "choline autocannibalism" theory (for review, see Wurtmann, 1992)

The findings that cigarette smoking is positively correlated with the delayed onset of Alzheimer disease (van Duijn and Hofman, 1991) and that nicotine inhibits cell loss induced by ß-Amyloid (Zamani et al., 1997, for review, see Zamani and Allen, 2001) argue against the oxidative stress hypothesis, as it is known that nicotine is a well-known inducer of ROS and therefore a potential enhancer of ß-Amyloid-induced toxicity via ROS. It is assumed that nicotine binding to the nicotinic acetylcholine receptor, a ligand-gated calcium-permeable receptor that is linked to cognitive function and development, is able to circumvent partially the cholinergic deficit in Alzheimer disease. Dramatic abnormalities in the cholinergic system have been shown several times and are so far the primary target for drugs fighting Alzheimer disease.

The "choline autocannibalism" theory unifies acethylcholine deficit and membrane disruption: Under resting conditions, the free choline pool seems to be sufficient to maintain acethylcholine synthesis, but during enhanced function other pools are then mobilized. Although the nature and sites of these pools have not yet been characterized, the possibility that in certain circumstances the membrane phospholipids are able to liberate choline has been postulated. When free choline is in short supply relative to the amount needed for acetylcholine synthesis, cholinergic neurons may break down the phosphatidylcholine in their membranes more rapidly than they can synthesize it, thereby either diminishing membrane phosphatidylcholine levels relative to other phospholipids or reducing the ability of the cell to synthesize new membrane. Either change might be

expected to impair membrane functions, especially on the aged brain, whose membranes already contain abnormal quantities of cholesterol and phospholipids other than phosphatidylcholine, decrease the quantity of membrane per cell, and lead eventually to disruption of the membranes and ultimately to the neuron's demise. Moreover, membrane disruption reduces membrane-bound acetylcholinesterase activity, as observed by Piasecka and coworkers (2000).

Modification of Ion channels

One early physiologic action of ß-Amyloid is an increase in intracellular calcium concentration. This ß-Amyloid-induced upregulation has been found in neurons and neuron-like cells (Hartmann et al., 1993). How ß-Amyloid induces increase of intracellular calcium has been subject of several studies. Mark and coworkers (1995) found evidence for a reduced activity of ion-motive ATPases following ß-Amyloid treatment inducing loss of neuronal Ca^{2+} homeostasis. Ca^{2+}-blockers have been shown to reduce neuronal degeneration (Weiss et al., 1994). Using artificial membranes, it has been found that ß-Amyloid has a tendency to insert itself into liposomes and forming membrane ionophores permeable to calcium. *In vivo*, the situation is less evident, as ß-Amyloid is found to enhance the activity of ligand-gated or voltage-dependent calcium-channels. In NIE-115 cells, L-channel blockers have been found to prevent an increase in intracellular Ca^{2+} without reducing the amount of ß-Amyloid-induced ROS, arguing for a causative role of calcium-deregulation in ß-Amyloid-induced toxicity (Ueda et al., 1997). Moreover, deregulation of calcium signaling and neurotoxicity were abolished by the membrane stabilizing properties of cholesterol (Hartmann et al., 1994). Other researchers (Whitson and Appel, 1995) observed that ß-Amyloid neurotoxicity and calcium homeostasis were insensitive to Ca^{2+}-channel blockers but sensitive to antioxidants such as vitamine E, arguing against the calcium-channel theory.

Inhibitors of ß-Amyloid aggregation

Given the mounting circumstantial evidence linking ß-Amyloid toxicity to its aggregation state, molecules that inhibit ß-Amyloid aggregation are needed to directly address the role of this peptide in Alzheimer disease. Moreover, such inhibitors may serve as therapeutic leads for treatment of this debilitating disease (John et al., 1997; Lansbury, 1997; Schenk et al., 1995). Strategies for interfering with protein aggregation may find broad use for treatment of a growing number of diseases that appear to be caused by such events (Kelly, 1996).

One strategy for identifying lead candidates is to screen compounds that block ß-Amyloid aggregation, and, presumably, the peptide's toxicity. Progress in this area has been hampered by the difficulties associated with the development of effective screening protocols and the interpretation of the assay results (Esler et al., 1997; Lansbury, 1997; Schenk et al., 1995; Wood et al., 1996). Despite these difficulties, several classes of small molecules have been reported to possess anti-aggregation and/or anti-toxicity activity.

The cationic surfactant hexadecyl-N-methylpiperidinium bromide, when mixed with ß-Amyloid at approximately equimolar quantities, appeared to alter aggregation. Specifically, ß-Amyloid mixtures treated with the surfactant showed decreased Congo red binding and turbidity, and the morphology of aggregates observed by electron microscopy was altered (Wood et al., 1996). In these solutions, ß-Amyloid was not monomeric and no loss of ß-sheet structure could be detected by circular dichroism spectroscopy.

Other molecules shown to inhibit aggregation are conjugated and/or aromatic systems, like the dyes used for amyloid plaque detection.

Rifampicin and related naphtahydroquinones caused a reduction in thioflavin-T fluorescence intensity of ß-Amyloid solutions, reduced the density of fibrils observed on electron microscopy, and decreased the cytotoxicity of ß-Amyloid; but these effects were only observed at ratios of 5:1 or greater molar excess of rifampicin (Tomiyama et al., 1996).

Daunomycin and related anthracyclines (Howlett et al., 1999a) are postulated to interfere with ß-Amyloid toxicity via binding to ß-Amyloid monomer, whereas benzofuran's mode of action was via binding ß-Amyloid oligomers (Howlett et al, 1999b).

Some sulfonated dyes, such as Congo red and related sulfonate anions, reportedly disrupt ß-Amyloid aggregation and reduce ß-Amyloid toxicity (Kisilevsky et al., 1995; Klunk et al., 1998; Sadler et al., 1995) possibly by inhibiting association with cell membranes (Sadler et al., 1995).

Similarly, the cationic aromatic compound pyronine Y has been identified as an inhibitor of ß-Amyloid aggregation (Esler et al., 1997), and the heterocyclic amine nicotine and related compounds inhibited ß-sheet formation and precipitation of ß-Amyloid (1-42), possibly by stabilizing a α-helical conformation (Salomon et al., 1996).

Other compounds are ß-cyclodextrin, which has a cavity that binds hydrophobic groups and partially reduces ß-Amyloid toxicity (Camilleri et al., 1994), or heterocyclic pyridones (Kuner et al., 2000).

None of these agents, however, is likely to specifically target ß-Amyloid or its aggregates because of the affinities of these putative inhibitors for hydrophobic sites. A more specific approach was taken by Solomon and colleagues (1997), who showed that a monoclonal antibody directed against the N-terminal region of ß-Amyloid protected PC-12 cells from ß-Amyloid toxicity.

A recent study using aggregated ß-Amyloid (1-42) (Elan/Wyeth-Ayerst AN1792 vaccine) in Alzheimer disease patients was suspended after 17 of the 300 study participants developed meningoencephalitis. Data analysis is not yet finished, but those participants whose immune systems made antibodies against the injected ß-Amyloid preparation indeed enjoyed a clinical benefit. However, generation of self proteins in humans is rarely of benefit. The immune complexes that result can lead to inflammatory immune complex diseases such as nephritis and vasculitis, and autoantibodies have been shown to contribute to the pathology of neurodegenerative diseases such as multiple sclerose, Rasmussen's encephalitis, and Guillian-Barré disease (for example, see Genain et al., 1999).

Our hybrid-compound inhibitors

ß-Amyloid is an amphiphilic self-associating peptide whose sequence is known. To self-associate, ß-Amyloid must be able to "recognize" other copies of itself. This self-recognition feature of ß-Amyloid allows exploiting an alternative approach to develop more specific inhibitors: molecules that borrow partial sequences from ß-Amyloid could also associate specifically with, or recognize, ß-Amyloid. Such sequences would be useful as means to target ß-Amyloid (Ghanta et al., 1996; Findeis et al., 1999; Soto et al., 1996, 1998; Tjernberg et al., 1996). These recognition sequences could then be coupled to elements that are capable of disrupting ß-Amyloid aggregation. The hybrid compounds, containing both recognition and disrupting functionality, could potentially prevent ß-Amyloid neurotoxicity.

As judged by electron microscopy, the pentapeptide KLVFF (16-20 sequence of full length ß-Amyloid) binds to and disrupts fibril formation (Tjernberg et al., 1996). Elaborating on their initial results, this group screened peptide libraries composed of pentapeptide sequences derived from D-amino acids to identify specific sequences that bind to the KLVFF motif. They found several candidates that bind the target region, and two of these were found to inhibit fibril formation when added in 10-fold excess over ß-Amyloid (Tjernberg et al, 1997).

In our laboratories, we showed that a compound containing the 16-20 (KLVKK) sequence of ß-Amyloid coupled to a charged string of amino acids as a "disrupting" domain (lysine hexamer or glutamate tetramer) altered ß-Amyloid aggregation kinetics and inhibited ß-Amyloid cellular toxicity (Lowe et al., 2001; Pallitto et al., 1999).

Thereby, a highly sophisticated tool is provided by our inhibitors, which will unravel which biological effects of ß-Amyloid are linked to toxicity, as these effects have to be circumvented by our inhibitors in the sole case of a causative connection between effect and cell death. Cell death induction competence of ß-Amyloid can easily be manipulated by adjusting incubation time and concentration, as well as addition of inhibitors in order to generate non-toxic species of ß-Amyloid (monomeric ß-Amyloid or ß-Amyloid preaggregated with one of our inhibitors) or toxic species of ß-Amyloid (ß-Amyloid preaggregated alone at 70µM or 140µM).

GOAL OF THE WORK

Recently, we showed that aggregated ß-Amyloid (1-40) decreased membrane fluidity in liposomes as model for membranes, whereas monomeric ß-Amyloid (1-40) had no effect (Kremer et al., 2000). Moreover, only aggregates of ß-Amyloid (1-40) were toxic to the rat adrenal pheochromocytoma cell line PC-12 as reported previously (Lowe et al., 2001). Addition of our designed hybrid-compound peptides altered ß-Amyloid aggregation kinetics and inhibited ß-Amyloid-induced toxicity successfully (Lowe et al., 2001).

Driven by these findings, we first addressed the question to which extent ß-Amyloid (1-40)-induced membrane disruption in liposomes is of *in vivo* relevance for the development of Alzheimer disease. Thus, we determined the effect of ß-Amyloid (1-40) on the integrity of membranes in the human neuroblastoma cell line SH-SY5Y as model for neurons and compared these effects with its toxicity.

Furthermore, as more evidence emerged for the involvement of oxidative stress in Alzheimer disease, we examined the role of reactive oxygen species (ROS) and lipid peroxidation in ß-Amyloid (1-40)-induced membrane properties alterations and cellular toxicity.

Thereby, we can define a matrix of

- two sets of actors:
  - toxic ß-Amyloid (1-40) species (aggregated ß-Amyloid alone) and
  - non-toxic ß-Amyloid (1-40) species (monomeric ß-Amyloid alone and aggregates of ß-Amyloid with inhibitors),
- their effects on two postulated mechanisms of toxicity:
  - membrane-disruption and
  - generation of oxidative stress,
- in two different settings:
  - liposomes as artificial models for membranes and
  - human, neuronal, ß-Amyloid-toxicity sensitive cell line SH-SY5Y

Investigations in this matrix gave new insights into the role of the enigmatic peptide ß-Amyloid in neuronal toxicity and Alzheimer disease.

The Alzheimer disease protein ß-Amyloid (1-40)

Lyophilized ß-Amyloid (1-40) was purchased from AnaSpec, Inc. (San Jose, California, product number 24236) in glass vials of 1mg net peptide weight and used without further purification. Identity and peptide purity were measured by mass spectrometry and amino acid analysis done by the vendor. The reported molecular weight was 4330.9 and the reported purity was greater than 95%. The amino acid sequence is DAEFRHDSGYEVHHQKLVFFAEDVGSNKGAIIGLMVGGV. Lyophilized ß-Amyloid was stored at -70°C until use.

Preparation of ß-Amyloid (1-40) samples

DMSO conditions

ß-Amyloid (1-40) was prepared essentially as described previously (Kremer et al., 2000). Briefly, ß-Amyloid (1-40) was dissolved for no less than 60 min at 10 mg/mL in filtered (pore size of poly-carbonate filters 0.2µm) DMSO (Sigma), which was previously dried using molecular sieves (Sigma) overnight. This treatment disrupts ß-sheet structure (Shen and Murphy, 1995) and renders ß-Amyloid (1-40) apparently monomeric (Snyder et al., 1994). A ß-Amyloid (1-40) stock solution was diluted 20-fold in PBSA (pH 6 or 7) and allowed to aggregate for two days at room temperature at 0.5 mg/mL (115µM equivalent monomer concentration). Freshly diluted ß-Amyloid (1-40) samples were kept in DMSO (at 10 mg/mL) until direct dilution into the sample.

Urea conditions

Lyophilized ß-Amyloid (1-40) was dissolved in filtered 8 M urea prepared in 10 mM glycine-NaOH buffer (pH 10, sterile filtered) to a concentration of 12 mg/mL, incubated 10 minutes at room temperature, then diluted to 70 or 140µM equivalent monomer concentration with sterile filtered PBS (final solutions contained 0.4 M urea). 8 M urea at pH 10 condition was chosen as a solvent for lyophilized ß-Amyloid as it has strong

denaturation and solubilizing potential, particularly for hydrophobic domains, and as ß-Amyloid aggregation is hindered at basic pH (Burdick et al. 1992). To reduce the possibility of chemical modification of the peptide, ß-Amyloid was incubated at 8 M urea, pH 10 for only 10 minutes before dilution. This is sufficient to produce fully monomeric peptide. By circular dichroism, urea-denaturated ß-Amyloid is random coil (unpublished results). Samples were allowed to aggregate at room temperature for one day, and then diluted with appropriate media. Freshly diluted ß-Amyloid (1-40) samples were dissolved in 8 M urea as above, diluted directly into media containing PBS in the same concentration as aggregated ß-Amyloid (1-40) samples, and immediately added to cells.

Addition of [^{125}I]-ß-Amyloid (1-40) as tracer

For aggregation and uptake studies, radiolabeled [^{125}I]-ß-Amyloid (1-40) from Amersham Pharmacia Biotech Int. (Product number IM294, 10µCi, specific activity: 2000Ci/mmol at activity reference date) was added to non-radiolabeled ß-Amyloid (1-40) from AnaSpec, Inc. (San Jose, California, product number 24236) prior to aggregation. It has been shown that traces of radiolabeled ß-Amyloid (1-40) are a reliable and easily detectable marker for non-radiolabeled ß-Amyloid (1-40). Moreover, it has been shown that radiolabeled [^{125}I]-ß-Amyloid (1-40) can bind to preexisting amyloid plaques in frozen sections of Alzheimer disease brains (Maggio et al., 1992).

10µCi of [^{125}I]-ß-Amyloid (1-40) were dissolved in 200µL dried and sterilfiltered (pore size of poly-carbonate filters 0.2µm) DMSO, incubated for one hour at room temperature, aliquoted in 20µL and stored at 4°C until use.

Aliquots of [^{125}I]-ß-Amyloid (1-40) were added to non-labeled ß-Amyloid (1-40) dissolved under urea-conditions prior to dilution in PBS. After brief vortexing to mix radioactive and non-radioactive ß-Amyloid (1-40), the solution was used directly as fresh, monomeric ß-Amyloid (1-40), or incubated for 24 hours at room temperature to generate ß-Amyloid (1-40) aggregates.

Inhibitors $KLVFFK_6$ and $KLVFFE_4$

The inhibitor peptides $KLVFFK_6$ and $KLVFFE_4$ were hand synthesized or automatically synthesized on a Synergy peptide synthesizer (Applied Biosystems, Model 432A) using standard solid phase synthesis; Fmoc-protected amino acids and either HBTU or HOBt mediated coupling reactions. Deprotected peptides were cleaved from resin with trifluroacetic acid (TFA) and purified by reversed-phase HPLC on a Vydac C4 peptide column (MacMod Analytical) using linear gradients of water and acetonitrile, containing 0.1% TFA. Peptides were analyzed by MALDI mass spectrometry at the University of Wisconsin-Madison Chemistry Instrument Center (molecular weight 1409g/mol) for purity, lyophilized and stored at -70°C. HBTU, HOBt, protected amino acids and resin were purchased from Novabiochem or Advanced ChemTech and HPLC grade acetonitrile was purchased from Fisher Scientific. Electrophysiology/molecular biology grade urea was purchased from Boehringer-Mannheim. All other chemicals were purchased from Sigma-Aldrich. The lyophilized inhibitors were dissolved in 20μL PBS, and then diluted into freshly diluted 70 or 140μM ß-Amyloid (1-40) samples to achieve a 1:1 molar ratio prior to aggregation.

Liposomes as artificial model membranes

In this work, large unilammelar vesicles, produced by repeated extrusion of hydrated phospholipids through polycarbonate membranes of defined size serve as artificial model membranes.

Preparation of liposomes

1-Palmitoyl-2-oleyl-sn-glycero-3-phosphocholine (POPC) and 1-palmitoyl-2-oleyl-sn-glycero-3-[phospho-rac-(1-glycerol)] (POPG) were purchased from Avanti Polar Lipids. Use of POPC and POPG allows a comparison between net neutral (zwitterionic) and anionic polar head groups. POPC and POPG contain mono-unsaturated acyl chains (16 and 18 carbons long); liposomes made from these phospholipids closely mimic the bilayer thickness of biological membranes. Dimethyl sulfoxide (DMSO), poly-L-lysine (molecular mass of 280 000 Dalton), bovine serum albumin (BSA) were purchased from Sigma Chemical Co. Lipids were stored at -20°C in chloroform. Cholesterol was purchased from Sigma, stored as lyophilized solid at -20°C, and diluted in chloroform. Single-component large unilammelar vesicles were prepared by extrusion. After mixing different lipid solutions for the preparation of multicomponent-vesicles, the lipid solutions were dried using a N_2 stream, followed by vacuum desiccation for one hour and overnight storage in a desiccated container. Dried samples were stored at -20°C till use. Lipid solutions were then resuspended in PBSA (10mM KH_2PO_4/K_2HPO_4, 150mM NaCl, 0.02% NaN_3 (mg/ml) at pH 6.0 or pH 7.0, allowed to equilibrate for at least 30 minutes, and passed through an extruder (Avanti Polar Lipids) with a 1000nm pore size membrane at least 19 times. This generates liposomes of approximately 1000-1250nm in diameter. Liposomes were extruded at room temperature, as the transition temperature of the liposomes was below room temperature. Lipid concentration was determined using the Stewart assay (Steward et al., 1980).

Preparation of calcein-encapsulated liposomes

POPC- and POPC-monocomponent liposomes and POPG-POPC-cholesterol-multicomponent-liposomes (at molar ration 45:45:10) were prepared by extrusion. Briefly, lipids were rehydrated to a concentration of 10 mg/mL in an aqueous calcein (50 mM) solution at pH 6.0 or pH 7.0 in PBS buffer. After equilibration for 30 minutes, the hydrated lipid suspension was subjected to 4-5 freeze-thaw cycles in an ethanol-dry ice bath and warm water bath, then passed through a 1000nm polycarbonate filter (Avanti Polar Lipids) at least 19 times. Liposomes were separated from unencapsulated calcein by Sephadex G-50 size exclusion chromatography. Lipid concentration was determined using the Stewart assay (Steward et al., 1980).

Uptake of ß-Amyloid (1-40) in liposomes

ß-Amyloid (1-40)-uptake was measured with a modified magnetic bead assay, providing an easy tool to separate liposomes attached to the beads from the medium using radiolabeled ß-Amyloid.

[^{125}I]-radiolabeled ß-Amyloid (1-40) was purchased from Amersham Pharmacia Biotech Int. (Product number IM294, 10µCi, specific activity: 2000Ci/mmol at activity reference date) and used as marker by adding small amounts to a surplus of non-labeled ß-Amyloid (AnaSpec, product number 24236).

1-palmitoyl-2-oleyl-sn-glycero-3-[phospho-rac-(1-glycerol)] (POPG, Avanti Polar Lipids, product number 840457) and 1,2-Dioleoyl-3-Trimethylammonium-Propane (DOTAP, Avanti Polar Lipids, product number 890890) liposomes doped with biotinylated phospholipids (1-(12-biotinyl(aminododecanoyl))-rac-Glycerol, Avanti Polar Lipids, product number 860555) at a 1/500-1/1000 ratio were extruded with a 1000nm pore size membrane as described above at pH 7.0. The lipid concentration was adjusted to 325µM. To quantify the concentration of lipid, liposomes were also doped with DPH prior to extrusion. Exposure to light was minimized during the loading with the dyes.

Streptavidin-coated (SA) magnetic beads (Spherotech, product number SVM-08-10, or Pierce, product number 21344) were rinsed two times in PBS-buffer by applying the magnetic field to the beads on a magnetic separator (Spherotech, FlexiMag Separator,

product number FMJ-1000) for 15 minutes, removing the ambient buffer carefully without disturbing the pellet, adding an equivalent amount of buffer, and repeating the procedure. Special care was taken to not disturb the "pellets" of magnetic beads. Therefore, only glass pipettes were used to remove the "supernatant" solution without excessively mixing the solution.

The POPG and DOTAP liposomes were then mixed with the PBS-washed SA beads in a total volume of 200μL/sample. During equilibration for 30 minutes, the solution was gently vortexed every 10 minutes to keep beads/liposomes in solution. Then, excess non-bound liposomal solution was removed by applying the magnet for 15 minutes. The excess solution was collected to quantify the concentration of lipid using DPH-fluorescence. Then, beads/liposomes were rinsed two times with PBS and the excess solutions again collected and used for lipid-quantification to verify that lipids are fully immobilized.

Lipids were now resuspended in PBS with different amounts of ß-Amyloid (1-40) with or without the inhibitor $KLVFFK_6$. After equilibration for 30 minutes with occasional gentle vortexing, the beads were placed on the magnetic separator for additional 10 minutes. 80% of the buffer with free, unbound ß-Amyloid (1-40) were gently removed and transferred into 5mL tubes for gamma-counting. The remaining 20% plus beads were transferred into a separate 5mL tube. The original centrifuge tube was rinsed two times with excess of PBS to collect all ß-Amyloid (1-40). As control, the bottom of the tube was cut off on occasion to ensure very little ß-Amyloid (1-40) was attached to the centrifuge tube (usually less than 5%). The amount of ß-Amyloid (1-40) in the supernatant was corrected for the 20% volume loss, as well as the amount of liposome-bound ß-Amyloid (1-40).

This procedure has the advantage to avoid any centrifugation, which would not only pellet liposomes, but possibly also larger unbound ß-Amyloid-aggregates, and moreover to work reproducibly and quantitatively.

Control experiment

To determine the binding of the lipids to the beads, we added the DPH-coated liposomes to the beads and incubated for 30 minutes. After separation, we retained the supernatant and washed two times with PBS. Washing solutions after separation were retained as well. Then, the intensity of fluorescence of the membrane-bound DPH in the supernatant and the washing solutions was determined on a spectrofluorometer by measuring DPH fluorescence.

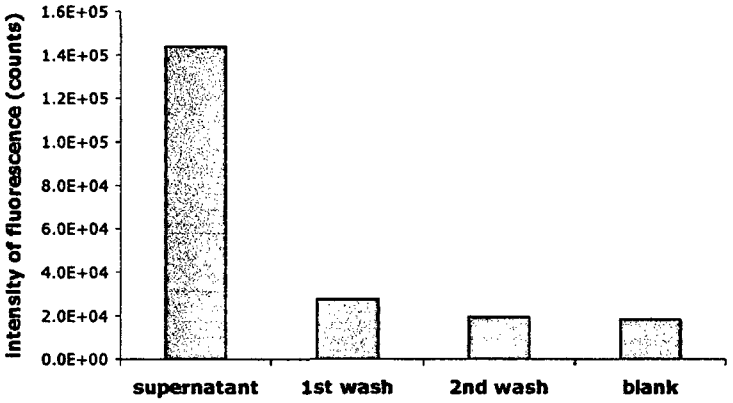

Fig.4: Intensity of the DPH-fluorescence of the remaining, unbound liposomes is rapidly decreasing with successive washing of the magnetic beads

The intensity of fluorescence of the dye DPH incorporated in the unbound, free liposomes decreased rapidly with successive washing of the magnetic beads (figure 4). After the second wash step, the solution was quantitatively void of any DPH, therefore also void of any bead-unbound, free liposomes.

Membrane fluidity in liposomes by measurement of DPH-anisotropy

1,6-diphenyl-1,3,5-hexatriene (DPH) is a rigid anisotropic molecule that localizes deep within the hydrophobic core of the lipid bilayer and therefore it is an extrinsic fluorophor for membranes (see figure 5). Its low solubility and quenched emission in water makes it an ideal probe for membranes. In this hydrophobic environment, it has strong fluorescence intensity. It is generally assumed that DPH, once incorporated into the membrane, is oriented parallel to the lipid acyl chain axis (see figure 6). Its rotational

freedom is compromised in highly viscous surroundings, such as might be found in the gel phase of a lipid bilayer. As DPH is a cylindrically shaped molecule, absorption and fluorescence emission transition dipoles are aligned approximately parallel to their long molecular axis. Consequently, their fluorescence polarization is high in the absence of rotational motion and is very sensitive to reorientation of the long axis resulting from interactions with surrounding lipids. Steady-state fluorescence polarization measurements report thereby on the relative rotation (or, conversely, anisotropy) of DPH embedded in the hydrophobic core, thereby yielding information about the fluidity of the acyl chains. These properties have led to their extensive use for membrane fluidity measurements.

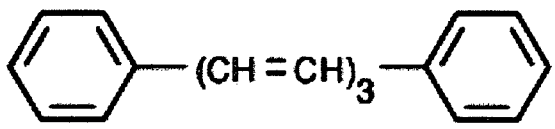

Fig. 5: Molecular structure of DPH

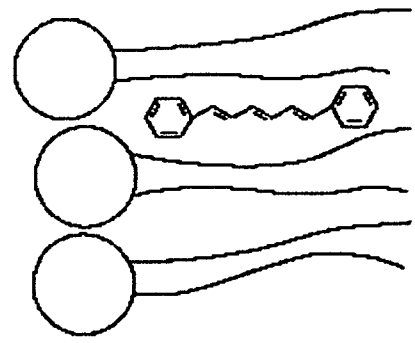

Fig. 6: Orientation of DPH in the membrane

We have previously shown that aggregates of ß-Amyloid (1-40) altered the membrane fluidity in liposomes as measured by DPH-anisotropy (Kremer et al., 2000, 2001). These liposomes were prepared by adding DPH to the rehydrated lipids before preparation of the liposomes by extrusion. We chose for this work another approach by adding a DPH-solution to already extruded, preformed liposomes. The comparison of results of these two different procedures allowed us to strengthen the liability of the results in case of conformity. Furthermore, this approach was chosen as preliminary work for an eventual DPH-staining of neuronal cells in order to measure the effect of ß-Amyloid (1-40) on viable neurons.

Protocol

Liposomes were prepared as described above and diluted to 250µM with PBSA (10mM KH_2PO_4/K_2HPO_4, 150mM NaCl, 0.02% NaN_3 (mg/ml)) at pH 7.0. A stock solution of DPH (Sigma, product number 43050) in tetrahydrofuran (THF, Sigma) at 3mM was

suspended in PBS at a ratio of 1:100 and the emulsion shaken vigorously for one hour before addition to the liposomes at a volume ratio of 1:30 to achieve a molar ratio of 1:250 (dye:lipid). After incubation for one hour, equilibration was achieved and PBS with ß-Amyloid (1-40) aggregated under different conditions was added to the liposomes. After 30 minutes, the anisotropy of DPH was measured.

As controls, BSA and poly-L-lysine solutions in PBS were used at 5mg/mL (10 times surplus of highest applied concentration of ß-Amyloid (1-40)). BSA is known to lack any effect on membrane structure and dynamics; poly-L-lysine is known to associate with the surface of negatively charged membranes, but to not penetrate into the hydrophobic core. Exposure to light was minimized during the entire procedure.

DPH-fluorescence was measured on a M-3 Alphascan spectrofluorometer (Photon Technology International) with Felix software, version 1.2X. Prior to fluidity measurements, alignment of the polarizers was checked as follows:

A stock-solution of glycogen at 1mg/mL in PBS, stored at 4°C, was diluted 1:20 with PBS and transferred into a clean cuvette. The slit widths of the spectrofluorometer were opened to 1nm, excitation wavelength set to 400nm, and emission wavelength set to 280-420nm (wavelength scan modus). Then, the P-factor was determined with equation 1,

$$P = \frac{I_{par} - I_{perp}}{I_{par} + I_{perp}} \qquad (1)$$

where I_{par} and I_{per} are parallel and perpendicular orientated polarizers respectively and I is the maximum emission intensity at 400nm. Polarizators were judged as aligned for P-values greater than 0.97.

For DPH-anisotropy measurements, the excitation wavelength was set to 360nm and emission to 430nm. The slit widths were set to 5 nm to get values of approx. 200000counts/sec. After checking the g-factor, samples of 1mL of treated DPH-loaded liposomes were transfered to cuvettes, which were cleaned overnight with acid solution. Then, the anisotropy was measured. Exposure to light during measurement was minimized to avoid bleaching.

Anisotropy (r) was calculated with equation 2,

$$r = \frac{I_{VV} - gI_{VH}}{I_{VV} - 2gI_{VH}} \qquad (2)$$

where I_{VV} and I_{VH} correspond to vertically polarized excitation and vertically, respectively horizontally polarized emission, and g corresponds to the g factor, see equation 3,

$$g = \frac{I_{HV}}{I_{HH}} \qquad (3)$$

where I_{HV} and I_{HH} correspond to horizontally polarized exctitation and vertically, respectively horizontally polarized emission.

Anisotropy increases as acyl chain fluidity decreases.

Titration of the molar ratio dye:lipid

To evaluate the minimum concentration of DPH required to stain the liposomes quantitatively and reliably, we added different volumes of DPH-solution to POPG-liposomes. After incubation for one hour to achieve steady state equilibrium, we measured the intensity of fluorescence and the anisotropy of DPH.

Figure 7 shows clearly that concentrations of DPH below a molar ratio of 1:250 were associated with low intensities of fluorescence. More important, the values of measured anisotropies at these low molar ratios are known to be incorrect. Higher amounts of added DPH increased the intensity of fluorescence and thereby the signal/noise ratio, but were possibly already affecting the physical properties of the liposomes as a result of the high amount of DPH. Therefore, we chose a molar ratio of 1:250 as the minimal concentration of DPH leading to reproducibility and reliability.

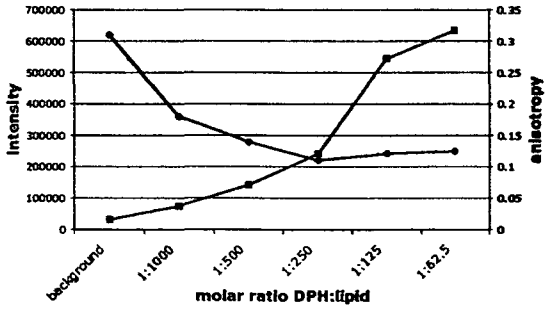

Fig.7: Titration of DPH shows clearly an optimal molar ratio of 1:250 for the staining of POPG-liposomes

Verification of the method

To verify that we were indeed gathering information about membrane fluidity by measuring the anisotropy of DPH, we measured the effect of increasing the concentration of cholesterol in liposomes on the anisotropy of DPH. It is well known that cholesterol disrupts the ordered conformation of the lipid bilayer and thereby increases the rigidity, which should be reflected in an increase of the measured anisotropy of DPH (Yip et al., 2001).

Therefore, we prepared POPG-liposomes with different amounts of cholesterol at pH 7.0, added a DPH-solution for final molar ratio of 1:250 (dye:lipid), incubated for one hour to achieve steady-state and measured the anisotropy of DPH at room temperature.

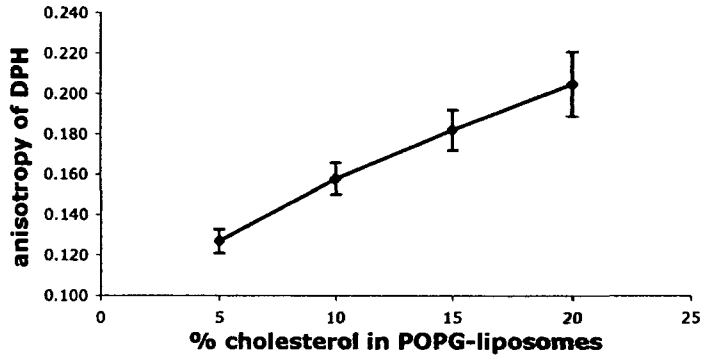

Fig. 8: POPG-liposomes with high percentage of cholesterol have a higher constitutive membrane rigidity as measured by DPH-anisotropy

As predicted, liposomes prepared with higher amounts of cholesterol had a significantly higher DPH-anisotropy (see figure 8). We therefore assumed that addition of DPH to preformed liposomes was an easy and reliable method for measuring membrane fluidity in liposomes.

Calcein Leakage Assay

Leakage of encapsulated calcein from different liposomes (monocomponent POPG and POPC, multicomponent POPG-POPC-Cholesterol at molar ratio 45:45:10) was used to determine the lytic ability of ß-Amyloid (1-40).

Calcein is a self-quenching dye; release of encapsulated calcein from liposomes into buffer causes an intraliposomal reduction in concentration and a corresponding increase

in fluorescence intensity as a result of reduced self-quenching. Exposure to light was minimized during the preparation of the liposomes, the ß-Amyloid (1-40) incubation, and the measuring of fluorescence.

Fluorescence measurements were collected using a model M-3 Alphascan spectrofluorometer (Photon Technology International, South Brunswick, NJ), with Felix software, version 1.2X, with excitation set to 490nm and emission set to 520nm. Samples were prepared by mixing calcein-encapsulated liposomes (final lipid concentration 250 μM) with different concentrations of ß-Amyloid (1-40) in PBS at pH 6.0 or pH 7.0, 1% (v/v) Triton-X 100 (100% leakage), or PBS at pH 6.0 or pH 7.0 (0% leakage) alone. Samples were briefly vortexed, and then left quiescent for 24 hours at room temperature except measurements after one hour, 4 hours and finally after 24 hours. Fluorescent intensity (Fl) measurements were normalized with equation 4.

$$\%leakage = \frac{Fl_{sample} - Fl_{buffer}}{Fl_{triton} - Fl_{buffer}} \times 100 \qquad (4)$$

Cell Culture

The human neuroblastoma cell line SH-SY5Y

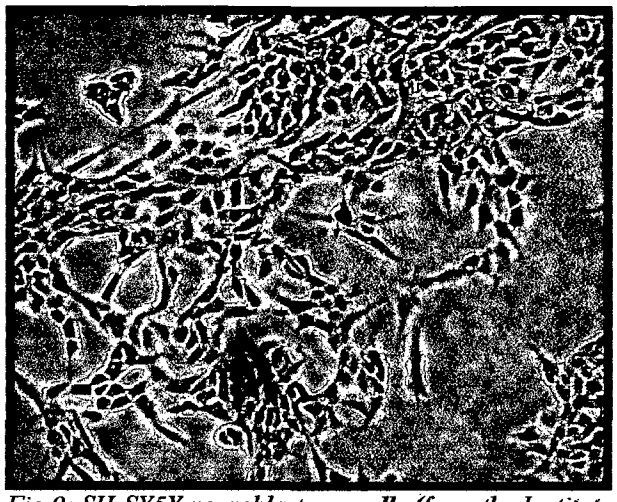

Fig.9: SH-SY5Y neuroblastoma cells (from the Instituto de Investigaciones Biomédicas de Barcelona, CSIC, Spain)

In this work, the cell line SH-SY5Y served as a model for human neurons (see figure 9). It is widely used in Alzheimer disease research and it has, in comparison to the rat adrenal pheochromocytoma cell line PC-12, the advantage to originate from human tissue. The cell line SH-SY5Y is a thrice-cloned (SK-N-SH → SH-SY → SH-SY5 → SH-SY5Y, see ATCC CLR-2266, DSMZ No ACC 209) subline of the neuroblastoma cell line SK-N-SH (see ATCC HTB-11), which was established in 1970 from a metastatic bone tumor of a Caucasian four years old female. The cells present a neuroepithelial-like morphology (Biedler et al., 1973; Jalava et al., 1990), and grow as clusters of neuroblastic cells with multiple, short, fine cell processes (neurites). Cells aggregate, form clumps and float. The whole cell population can thereby be defined as a combination of floating and adherent cells.

Cultivation of SH-SY5Y

Cells were cultured to confluence on poly-L-lysine coated T-flasks (Costar) in SH-SY5Y-cultivation-medium.

SH-SY5Y-cultivation-medium:

44.5% minimal essential medium (MEM) (GIBCO)

44.5% Ham's modification of F-12 medium (GIBCO)

10% fetal bovine serum (FCS) (GIBCO)

Supplemented with 1% penicillin/streptomycin (Pen.10000U/mL, Str. 10mg/mL, HyClone)

Sterilfiltered and stored at 4°C

Cultivation was under standard conditions: incubation in a humidified 37°C, 5% CO_2 environment (Incubator from Heraeus). Cells were fed every third day with fresh cultivation medium till confluence. Addition of 10µM retinoic acid (Sigma, R-2625, all trans, stock solution dissolved in DMSO at 3mg/mL, kept in the dark at -20°C) dissolved in medium did not induce any further morphological differentiation.

Thawing SH-SY5Y-cells

2mL cryo-vials (Bibby Sterilin Ltd or Corning, product number 1430659) stored in liquid nitrogen, containing aliquots of SH-SY5Y-cells in freezing-medium, were shortly thawed and quickly diluted with 6mL 37°C preheated thawing-medium (SH-SY5Y-cultivation-medium with 20% FCS instead of 10%). After brief mixing, cells were harvested at 300G for 5 minutes (centrifuge Hettich Rotanta) and the supernatant discarded to remove the DMSO from the storage-medium. Pellet was then suspended in 14mL thawing-medium till no clumps were detected on the microscope. 7mL of the cell suspension were then transferred in one T25 cell culture flasks (Costar), and incubated in a humidified 37°C, 5% CO_2 environment.

Passaging SH-SY5Y-cells

At a confluence of approximately 90% or more, which corresponds to a density of 1.10^6 cells/cm^2, the supernatant with the floating cells was removed and the cells recovered by centrifugation at 700G for 5 minutes. The monolayer was then rinsed with 3mL of 37°C preheated trypsin-solution. After removing of the trypsin-solution, 2mL trypsin-solution was added to detach the cells from the well.

Trypsin-solution:

40mg EDTA (GIBCO)

4mL 2.5% Trypsin-stock-solution (GIBCO)

200mL PBS

Sterilfiltered, and stored in aliquots of 4mL at –20°C

Then, the culture was let sit at room temperature until detachment of the first cells. The trypsin-solution was then removed and 7mL of fresh medium were added. After mild aspiration, the solution was then combined with the floating cells recovered above and again aspirated till no clumps were detected on the microscope. A small aliquot was used for trypan-blue determination of cell number and viability. Then, the solution was dispensed into two new flasks with each additional 3.5mL fresh medium and incubated in a humidified 37°C, 5% CO_2 environment.

Freezing SH-SY5Y-cells

Cells were detached from the flask bottom as above, suspended in 2mL of freezing-medium, and mildly aspirated.

Freezing-medium

4mL SH-SY5Y-medium

0.5mL FCS

0.5mL DMSO (Sigma)

After mild aspiration, the cells were aliquoted into two cryo-vials and stored one to three days at -80°C, then stored under liquid nitrogen.

The human astrocytoma cell line GOS-3

Fig.10: Astrocytoma cell line (from the University of British Columbia, Dept. of Neuroscience, Canada)

In this work, the cell line GOS-3 was used a model for human astrocytes, residing in the brain (see figure 10). The cell line GOS-3 is a human astrocytoma/oligodendroglioma cell line (see DSMZ ACC 408) established from the tumor material of brain from a 55-year-old man with a mixed astro-oligodendroglioma (grade II/III). The morphology of GOS-3 is fibroblastoid. The adherent cells grow as monolayer (Halfter et al., 1998a, 1998b).

Cultivation of GOS-3-cells

Cells were cultured to confluence on poly-L-lysine coated T-flasks in GOS-3-medium.

GOS-3 medium:

90% Dulbecco's Minimal Essential Medium (MEM)

10% fetal bovine serum (FCS)

2% L-glutamine (200mM)

Supplemented with 1% penicillin/streptomycin (Pen.10000U/mL, Str. 10mg/mL, HyClone)

Sterilfiltered and stored at 4°C

Cultivation was done under standard conditions: incubation in a humidified 37°C, 5% CO_2 environment. Cells were passaged every third day.

Thawing GOS-3-cells

2mL cryo-vials (Bibby Sterilin Ltd) stored in liquid nitrogen, containing aliquots of GOS-3 cells in freezing-medium, were shortly thawed and quickly diluted with 6mL 37°C preheated thawing-medium (GOS-3 cultivation-medium with 20% FCS instead of 10% FCS). After brief mixing, cells were harvested at 300G for 5 minutes and the supernatant removed. Pellet was then suspended in 14mL thawing-medium till no clumps were detected on the microscope. 7mL of the cell suspension were then added in T25 cell culture flasks and incubated in a humidified 37°C, 5% CO_2 environment.

Passaging GOS-3

At a confluence of approximately 90% or more, which corresponds to a density of $1.5 \cdot 10^6$ cells/cm^2, the supernatant with the floating cells was removed and the cells recovered by centrifugation at 700G for 5 minutes. The monolayer was then washed for one minute with 3mL of 37°C preheated PBS. After removing of the PBS, 2mL trypsin-solution was added.

Trypsin-solution:

40mg EDTA
4mL 2.5% Trypsin-stock-solution (GIBCO)
200mL PBS
Sterilfiltered, and stored in aliquots of 4mL at –20°C

Then, the culture was let sit at room temperature until detachment of the first cells. The Trypsin-solution was then removed and, after one minute, 7mL of fresh medium were added. The cells were aspirated till no clumps were detected on the microscope. Then, the solution was dispensed into two new flasks with each additional 3.5mL fresh medium and incubated in a humidified 37°C, 5 % CO_2 environment.

Freezing GOS-3-cells

Cells were detached from the flask bottom as above, suspended in 2mL of freezing-medium, and mildly aspirated.

Freezing-medium

4mL GOS-3-medium

0.5mL FCS

0.5mL DMSO

After mild aspiration, the cells were aliquoted into two cryo-vials and stored one to three days on -80°C, then stored under liquid nitrogen.

Determination of cell number and cellular viability

The determination of cell number and cellular viability on a routine basis was carried out through trypan-blue-dye exclusion and cell counting in a hemacytometer. An aliquot of 10µL of cell suspension was added to a well of a micro-titer-plate and gently mixed with the same amount of the trypan-blue-solution (0.25% trypan-blue (Sigma) in PBS (Sigma)). After one minute, the cell suspension was transferred into the chamber. Viable cells appear colorless due to the dye-exclusion, whereas dead cells appear blue due to incorporation of trypan-blue. Counting of statistically located squares was repeated to achieve greater accuracy.

Cell number was defined as (equation 5):

$$Cells(cells/\mu L) = \frac{cells_{counted}}{area(sqmm) \times chamber\ depth \times dilution} \quad (5)$$

Viability was defined as (equation 6):

$$Viability(\%) = \frac{cell\ number\ viable}{cell\ number\ (viable + dead)} \times 100 \quad (6)$$

Cellular toxicity assay

As the physiological effects of ß-Amyloid aggregates are still being elucidated and debated (Felician and Sandson, 1999), it is difficult to relate the effect of inhibitors on the biological function of ß-Amyloid. Since significant technical and economic issues remain with the use of transgenic mouse models as screening tools, the current practice relies on *in vitro* cell toxicity screening for identification of inhibitory compounds.

The most widely adopted measure of *in vitro* ß-Amyloid cellular toxicity is the inhibition of the reduction of 3-[4,5-dimethylthiazol-2-yl]-2,5 diphenyltetrazolium bromide (MTT) to formazon. This assay has proven to be reliable, reproducible, and specific (Shearman et al., 1994, 1995), and has found widespread use in evaluation of compounds designed to inhibit ß-Amyloid toxicity (for example, Klunk et al., 1998; Seilheimer et al., 1997; Tomiyami et al., 1996; Yu et al., 1998). MTT is generally believed to be a measure of mitochondrial activity. The major site of MTT reduction is thought to be at two stages of electron transport, the cytochrome oxidase and ubiquinone of mitochondria, although recent evidence suggests that significant MTT reduction occurs in endosomes, and that ß-Amyloid inhibits MTT reduction by altering intracellular vesicle trafficking (Liu et al., 1998). Whatever the mechanism of initial insult, mitochondrial dysfunction is prevalent in Alzheimer's disease (Cassarino et al., 1998; Mecocci et al., 1997; Sheehan et al., 1997). Mitochondrial dysfunction can activate apoptotic or necrotic cell death, but most data point towards an apoptotic mode of cell death following exposure to aggregates of ß-Amyloid (Loo et al., 1993; Tucker et al., 1998; Li et al., 1996; Wernyj et al., 1999).

Techniques such as DNA-laddering assays detect apoptosis, but these methods have only rarely been used to evaluate activity of inhibitors of ß-Amyloid toxicity (Kim et al., 1998).

Protocol

Cells were cultivated till confluence, harvested, and plated in 96-well poly-L-lysine-coated plates (Falcon) with 100,000 cells SH-SY5Y or 50,000 cells GOS-3 per 100µL medium per well and incubated for 48 hours at 37°C, 5% CO_2 to reach confluence. After 48 hours, 80µL of medium was removed and 80µL of medium containing ß-Amyloid

(aggregated in urea conditions or freshly diluted), ß-Amyloid aggregated with inhibitor, or control medium (containing the same concentration of urea as ß-Amyloid-samples) were added. Cells were incubated for additional 24 hours, then viability was measured using MTT (Sigma, catalog number M5655): 20μL of 2.5 mg/mL MTT in cultivation-medium were added to each well. Cells were then incubated at 37°C for additional 5 hours. Then, 100μL of 50% DMF, 20% SDS (pH 4.7) at 37°C were added to each well to dissolve the formazan crystals produced only by healthy mitochondria. 8-12 hours after SDS/DMF addition, absorbance at 570nm was measured with a microplate reader (Bio-Tek Instruments) using background subtraction at 620nm. Cell viability was calculated as follows (equation 6):

$$Viability(\%) = \frac{Abs_{sample} - Abs_{background}}{Abs_{control} - Abs_{background}} \times 100 \qquad (6)$$

Sample, background and control absorbances were averaged over 5 replicates. Background samples without cells contained cell culture medium, MTT, and the SDS/DMF solution at same concentrations as samples. Control samples were untreated cells, cell culture medium, MTT, and the SDS/DMF solution at same concentration.

[^{125}I]-ß-Amyloid (1-40)-uptake assay

By means of the [^{125}I]-ß-Amyloid (1-40)-uptake assay, we were able to quantify the amount of ß-Amyloid that is incorporated into neurons and degraded.

Briefly, SH-SY5Y cells were plated into 6-well plates and after 24 hours, radioactive ß-Amyloid (1-40) was added to the cells. After different times, the supernatant was removed and retained to measure the amount of free, unbound and not internalized ß-Amyloid (1-40). Furthermore, the supernatant was submitted to a trichloroacetic acid (TCA)-precipitation to differentiate between degraded and not degraded ß-Amyloid (1-40) in the supernatant. Then, the protease trypsin was added to the cells in order to degrade and solubilize ß-Amyloid (1-40) on the outer membrane. Thereby, we can quantify the amount of cell-associated ß-Amyloid (1-40) in the "trypsin-fraction". Finally, the amount of internalized ß-Amyloid (1-40) was determined by measuring the remaining radioactivity in the cells.

Material

ß-Amyloid (1-40) was prepared as described above with [^{125}I]-ß-Amyloid (1-40) as tracer for ß-Amyloid (1-40) material. TCA-solution: 10% in PBS. The trypsin-solution was identical to the one of cell culture and was used cold. BSA-solution: 10mg/mL in PBS. Binding medium is a low serum medium with 1% FCS instead of 10%. Chloroquine was purchased from Sigma (product number C6628).

Preliminary experiments

Determination of necessary sample volume

It is known, that cells in culture internalize extracellular ß-Amyloid (1-40) only marginally. To determine the minimum cell number necessary to achieve reliability and reproducibility in the results, SH-SY5Y cells were plated either in 96-well, 24-well or 6-well plates and grown to confluence. After 24 hours, the cultivation-medium was removed and fresh media supplemented with preaggregated ß-Amyloid (equivalent

monomer concentration 10μM) was added to the cells. 24 hours later, the supernatant with free ß-Amyloid (1-40) was removed and the cell monolayer washed extensively. Then, the trypsin-solution was added for two minutes to detach the cells from the well bottom. Cells were then transferred into a centrifuge tube. To remove cells quantitatively, the wells were eventually washed twice with PBS and the washing solutions collected with the cell suspension.

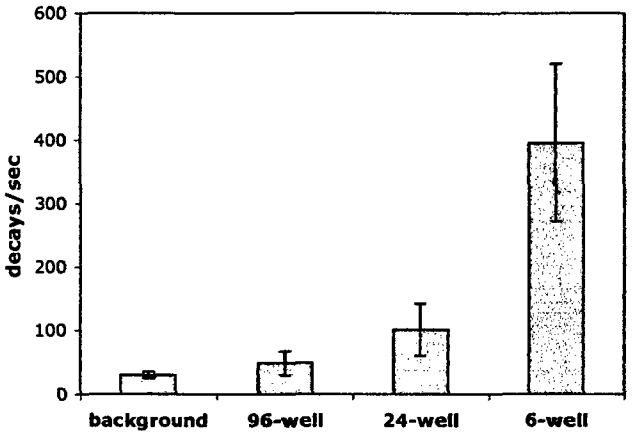

Fig.11: 6-well plates are necessary and sufficient to get reproducibility and high signal/noise-ratio

It was obvious that a sufficient sensitivity could only be achieved with a rather large sample volume by use of 6-well plates (see figure 11). Smaller sample areas/volumes did not provide measurements noticeably different from the background radioactivity, thereby not leading to statistically relevant results. This experiment also explained the use of an applied concentration of ß-Amyloid (1-40) of rather low 10μM, as higher concentrations were economically impossible.

Determination of necessary trypsin-incubation time

It has been shown that trypsin degrades membrane-bound ß-Amyloid quantitatively (Knauer et al., 1992). Therefore, we decided to remove the outer-cell-membrane-associated ß-Amyloid (1-40) by means of a trypsin-degradation. Thereby, membrane-bound ß-Amyloid (1-40) was degraded and solubilized, and moved into the supernatant phase. Thereby the peptide was separated from the cell-fraction. As extended trypsin-incubations are potentially harmful to cells and lead to loss of membrane integrity and

possible leakage of incorporated ß-Amyloid, we optimized the duration of the trypsin-incubation.

We added radioactive ß-Amyloid (1-40) to the adherent cells in 6-well plates and removed the supernatant after 24 hours. Then, the cells were washed extensively and 2mL of trypsin-solution was added. Cells were then incubated for different amounts of time on ice and afterwards the amount of ß-Amyloid (1-40) in the cell-free trypsin-solution and the amount of ß-Amyloid internalized was measured on a gamma-counter.

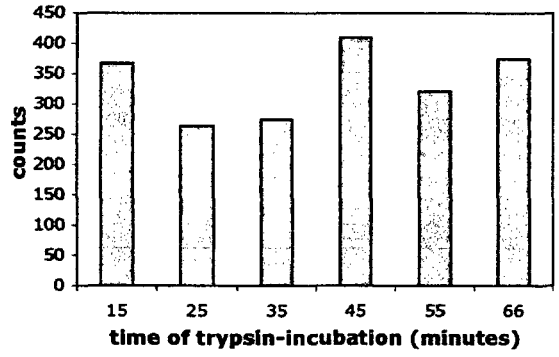

Fig.12: Trypsin-degraded ß-Amyloid (1-40)

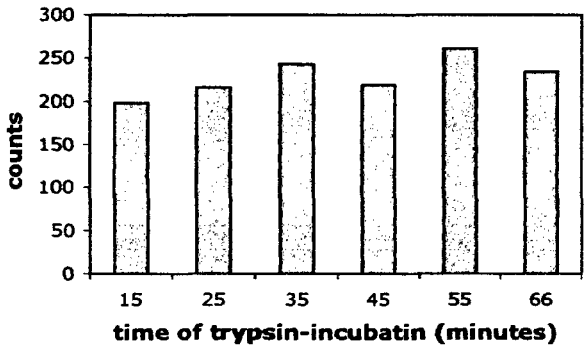

Fig.13: Internalized ß-Amyloid (1-40)

We can see in figures 12 and 13 that a trypsin-incubation of 15 minutes was sufficient to solubilize quantitatively cell membrane-bound ß-Amyloid (1-40), as a prolonged incubation did not lead to higher signal. As trypsin-incubation of 66 minutes did not lead to decreased amount of internalized ß-Amyloid (1-40), which would reflect membrane-integrity loss and ß-Amyloid (1-40)-leakage, we decided to incubate the cells with trypsin for 30 minutes for the following experiments.

Protocol

SH-SY5Y-cells were cultured till confluence and plated into 6-well plates at 2E6 cells/well in 2 mL cultivation media with 10% FCS. To determine non cell-specific adhesion and precipitation of ß-Amyloid (1-40) at the bottom of the well, as well as the non cell-specific degradation of ß-Amyloid (1-40), cultivation medium without cells was added into one well. After 24 hours, the cultivation medium was removed, the cells washed briefly with 1mL binding media (1% FCS), and 2mL of radioactive ß-Amyloid (1-40) diluted in binding media added. Control wells without cells were treated identically. Experiments were done at an applied concentration of 10µM ß-Amyloid (1-

40) (sub-lethal concentration), to avoid uptake and release effects due to cell death. Three wells (two wells with SH-SY5Y cells for duplicate, one well without cells) at three different time points were used for each experiment. After one, 12 and 24 hours, the supernatant (2mL) was removed and retained. 1mL of the supernatant was used as reference to measure the total amount of radioactivity. 200µL of the supernatant were used for the TCA-preparation to differentiate between degraded and non-degraded ß-Amyloid (1-40): Therefore, 200µL of the retained supernatant were added to a solution containing 200µL BSA-solution and 400µL TCA-solution, vortexed and incubated for one hour on ice. Then, the solution was centrifuged at high speed (10000rpm for 10 minutes) and the supernatant removed from the pellet. Radioactivity in the supernatant that was soluble in 10% TCA was taken to represent degraded ß-Amyloid (1-40). The pellet consisted of intact, non-degraded ß-Amyloid (1-40). The cell pellet was then washed 4 times with 1mL PBS to remove unbound ß-Amyloid (1-40). Then 700µL of ice-cold trypsin-solution were added to each well. After 30 minutes of incubation, the trypsin-solution with floating, detached cells was collected and the well washed with 300µL PBS. Trypsin-solution and wash-PBS were pooled to collect the cells quantitatively. An aliquot of 900µL was centrifuged at 5000rpm for 5 minutes to harvest the cells and separate them from the trypsin-solution containing free, unbound, and soluble ß-Amyloid (1-40).

Diluted ß-Amyloid (1-40) was also used for aggregation-studies. Therefore, an aliquot of 500µL of the binding medium with ß-Amyloid (1-40) was filtered through micro-centrifuge tubes (pore size of 1µm) at the time point t=0h and at t=24h to determine the aggregation kinetics of ß-Amyloid (1-40) aggregates at 10µM in medium. Three washing steps with PBS were required to remove any soluble ß-Amyloid (1-40) from the filter.

To calculate the amount of internalized, degraded, and membrane-associated ß-Amyloid (1-40) per cell, a preliminary experiment without addition of radioactive ß-Amyloid (1-40) was carried out and the cell number determined after 24 hours by means of a cell counting chamber. This experiment revealed that the cell number is fairly constant, as the applied conditions (relatively short incubation time of 24 hours, 1% FCS, and 10µM ß-Amyloid) prevented cell growth.

To characterize the origin of the degradation of ß-Amyloid (1-40), conditioned medium was used instead of fresh media in some experiments for control wells without cells. Conditioned medium was obtained by plating cells in a 6-well plate at a cell number of 2E6 cells/well in 2mL. After 24 hours, the supernatant was removed and replaced by 1% FCS-binding medium without ß-Amyloid (1-40). After 24 hours, the binding-medium was retained, centrifuged at low speed (1200rpm at Beckmann-centrifuge for 5 minutes) to remove cells, then centrifuged at high speed (3000rpm for 10 minutes) to remove any remaining cells and cell fragments. This media was stored at 4°Celsius for no longer than 24 hours prior to use. For some experiments, conditioned medium from cell cultivation was used. Therefore, cell culture medium was removed from fully-grown cells in T75-flasks, and the medium treated as the conditioned medium before.

To further characterize the origin of the degraded ß-Amyloid (1-40), cells were pretreated with chloroquine, a known inhibitor of lysosomal degradation (e.g. Kounnas et al., 1995). Therefore, chloroquine was added to the cells one hour prior to addition of ß-Amyloid (1-40). Furthermore, chloroquine was also added to the binding medium containing ß-Amyloid (1-40).

As this procedure dealt with fairly low amounts of radioactivity, and therefore with a low signal-to-noise ratio, special care was taken to control that the washing steps after removal of the supernatant were sufficient. It was shown that 4 washing steps were necessary, but also sufficient to remove free, unbound ß-Amyloid (1-40) quantitatively.

Radioactivity as a measure for ß-Amyloid (1-40) amount was determined on a gamma counter in gamma counting tubes. Measured radioactivity was converted into radioactivity at reference date to compensate for the natural radioactive decay of ^{125}I and to compare results from three different batches of [^{125}I]-ß-Amyloid (1-40).

Incorporation of 1,6-diphenyl-1,3,5-hexatriene into SH-SY5Y cells

Material

1,6-diphenyl-1,3,5-hexatriene (DPH, product number 43050) and tetrahydro-furan (THF) were purchased from Sigma-Aldrich. ß-Amyloid (1-40) from Anaspec (product number 24236, 1mg) was dissolved in 8 M urea (in glycine-buffer, pH 10) for 10 minutes to achieve quantitative monomerization with subsequent dilution into PBS-buffer (pH 7.4) to desired concentration of aggregation as described above. Diluted glycogen-solution at approximately 1mg/mL in PBS from Sigma-Aldrich was used to calculate and check the alignment of the polarizators of the spectrofluorometer. Special care was taken to clean the fluorescence cuvettes with acid solution overnight before each experiment. As controls, BSA and poly-L-lysine were used. DPH-fluorescence was measured on a M-3 Alphascan spectrofluorometer (Photon Technology International) with Felix software, version 1.2X. For anisotropy measurements, the excitation wavelength was set to 360nm and emission to 430nm. The slit widths were set to 8 to10nm to get values of approximately 200000 counts/sec. For more details, see Material&Methods: Membrane fluidity in liposomes by measurement of DPH-anisotropy.

Protocol

DPH was dissolved in THF at 3mM and kept at 4°C as a stock in a glass vial in the dark. This stock-solution is stable for several months. Aliquots of the DPH-stock solution were suspended at a volume-ratio of 1:100 in PBS containing 5% glucose in glass vials and shaken vigorously for at least 30 minutes at 37°C on a thermo-mixer, or till no absorption of DPH was detectable on a photometer (data not shown). Therefore, 5µL of the DPH-stock-solution were added to 500µL of PBS supplemented with 5% glucose in one glass vial. Meanwhile, SY5Y-cells at confluence were harvested and suspended at 0.5E6 cells/mL in HBSS supplemented with 5% glucose. Then, the cell suspension was carefully mixed with the diluted DPH-solution at a volume ratio of 1:1. Therefore, for each sample 500µL of the cell suspension were added to one glass vial containing 500µL of the diluted DPH-solution. The solution was kept at room temperature or 37°C for 30 minutes (no difference could be detected). Slow shaking on a rotor was applied to keep

the cells in suspension. Staining was thereby achieved at a cell density of 250,000 cells/mL at 15μM DPH applied concentration. The cells were then washed 4 times with PBS (supplemented with 5% glucose) to remove any non-incorporated DPH in solution. Therefore, cells were suspended with a syringe and the suspension transferred into an eppendorf tube. After harvesting the cells, the supernatant was discarded and fresh PBS with 5% glucose added to the cells. Finally, the cells were resuspended with a syringe, and the washing repeated three times. Cells were considered now ready for stimulation/treatment.

After treatment of the cells (in our case incubation with ß-Amyloid (1-40) aggregated under different conditions with or without inhibitor for one hour), the cells were suspended with a syringe to disrupt any cell clumps and to ensure isotropic distribution. Then, the fluorescence intensity and the anisotropy were measured on the spectrofluorometer without or with polarizators respectively. The DPH-labeled systems were exposed to the excitation light for less than 5 seconds, which eliminated the possibility of reversible bleaching of DPH that presumably originates from reversible photo-isomerization. In both cases, the measure chamber was preheated to 37°C in a thermostatically controlled bath. Sample temperature of 37°C was checked with a thermometer immersed in the analyzed solution, which minimized the errors in the recorded temperature to less than 0.2°C.

A wavelength scan was done with an excitation wavelength of 360nm and an emission wavelength region from 429nm to 431nm (The emission maximum of DPH is at 430nm), with the excitation and emission slit widths opened to approximately 7nm to get intensity values around 200000 events/sec. For measuring the anisotropy of DPH, 4 measurements were carried out to get values for the 4 possible positions of the two polarizators (vertical/vertical, vertical/horizontal, horizontal/horizontal, and horizontal/vertical). Measurement of a wavelength scan allowed the exclusion of false values originating from light scattering. Signs of light scattering were great differences between emission at 429nm and 431nm, as these wavelengths should have comparable intensities.

Titration of DPH

Optimal concentration of DPH for cell staining was determined by titrating of the concentration of DPH.

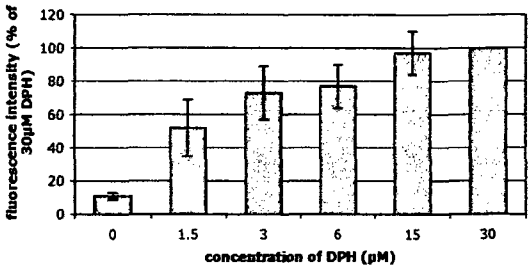

Fig.14: Successful staining of the cellular membrane with the fluorescent dye DPH

As we can see in figure 14, the incorporation of DPH into the cell membranes was successful. The fluorescence intensity increased with higher DPH-concentration and leveled off at approximately 15µM. Ultimately, at higher concentrations than 30µM, the signal decreased due to self-quenching (data not shown). Therefore, a DPH-concentration of 15µM was chosen for all experiments. Increasing the incubation time and simultaneously decreasing DPH-concentration showed no further amelioration and was therefore avoided to shorten the duration of the protocol and to avoid cell death. Furthermore, by limiting the incubation time to 30 minutes, migration of DPH into inner membranes was avoided in order to target the plasma membrane.

Influence of temperature on the membrane fluidity

It is believed that once DPH is incorporated into the inner core of the cellular membrane, it is a reliable marker for membrane fluidity. We confirmed the validity of the method by inducing membrane fluidity alterations in SH-SY5Y cells by means of different incubation temperatures, as it is well known that higher temperature (hyperthermia) renders the membrane more fluid, which should be reflected in a reduced anisotropy, and lower temperatures (hypothermia) more rigid, reflected by increased anisotropy.

Briefly, the cells were stained for 30 minutes with 15µM DPH as described above and afterwards incubated directly in the thermo-regulated measure chamber till medium-temperature reached 4°C, 37°C, or 42°C to achieve hypothermia, cell cultivation

temperature, or hyperthermia respectively. Then, any cell clumps were quickly disrupted with a syringe to avoid light scattering and the anisotropy measured afterwards.

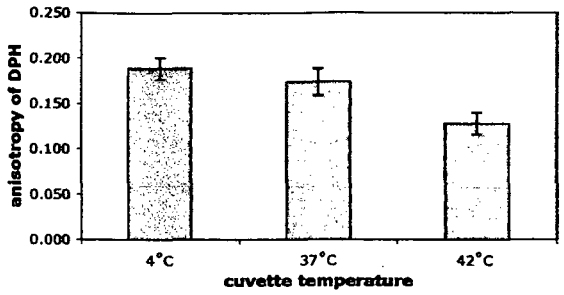

Fig.15: DPH anisotropy is altered by hypo- and hyperthermia successfully

Figure 15 shows clearly that hyperthermia of 42°C induced a decrease of anisotropy (higher fluidity), whereas hypothermia of 4°C induced an increase of anisotropy (higher membrane rigidity) in comparison with 37°C. From this experiment, we concluded that the method was suitable to measure membrane fluidity alterations in SH-SY5Y cells.

Control experiment

Before investigating the effect of ß-Amyloid (1-40) on the DPH-anisotropy, the influence of BSA and Poly-L-lysine (0.5mg/mL in PBS) on the DPH-anisotropy was measured. It has been shown that both agents have no influence on DPH-anisotropy.

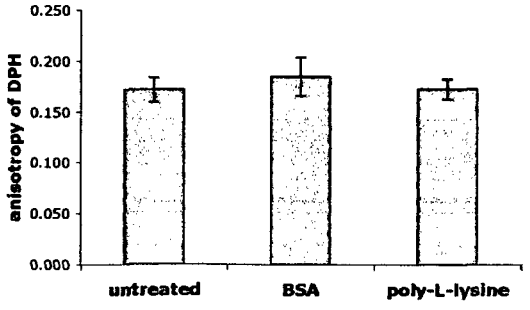

Fig.16: No effect of BSA or poly-L-lysine on the measured DPH-anisotropy in SH-SY5Y

As we see in figure 16, neither BSA nor poly-L-lysine was able to alter the DPH-anisotropy. This indicates, that simple charge-effects (e.g. between the positively charged lysine and the negatively charged plasma membrane) were not able to alter DPH-anisotropy.

Cellular viability

We ensured that the cellular viability of the SH-SY5Y cells did not decrease during the procedure. By means of trypan-blue exclusion, we observed that the average percentage of stained (dead) cells after accomplishment of the entire procedure was less than 5%.

Qualitative determination of ß-Amyloid-incorporation into the membrane of SH-SY5Y cells

After loading the cellular membrane of SH-SY5Y cells with DPH successfully, we used the fluorescent dye as a probe for membrane lipid. Therefore, we loaded the cells with DPH as described above and added ß-Amyloid (1-40) aggregated under different conditions as before with or without inhibitor. Then, cells were separated from the supernatant. Therefore, the cells were harvested at 700G for 7 minutes and the supernatant retained. Cells were now washed 4 times to remove any rests of supernatant. The retained supernatant was centrifuged at higher rotation (5000G for 15 minutes) to remove any cell fragment remnants. By this, we were able to quantify the amount of DPH in the cells and in the supernatant by measuring each fraction separately with and without polarizators to determine the anisotropy of DPH and the intensity of fluorescence as values for ß-Amyloid (1-40)-DPH-interaction and DPH-amount respectively.

Control experiment

Special care was taken to control that the supernatant of ß-Amyloid (1-40)-untreated cells was void of any non-bound DPH. Therefore, we incubated the cells after DPH-staining in PBS for one hour, removed the cells and collected the supernatant. Then, we extracted any DPH with n-octanol and measured the anisotropy of the hydrophobic phase. This step was necessary, as DPH does not have any measurable fluorescence intensity in an aqueous environment. As negative control, we measured the supernatant of cells, which were not labeled with DPH. As positive control, we added DPH to n-octanol at a concentration of 0.1µM. There was no difference in intensity between DPH-loaded and DPH-unloaded cells, confirming that the supernatant of DPH-loaded cells is void of any DPH indeed.

Lipid-release in SH-SY5Y-cells and GOS-3 cells

Lipid-release in SH-SY5Y and GOS-3 cells was determined via different approaches.

DPH as marker for lipid in SH-SY5Y and GOS-3 cells

Protocol

Determination of 1,6-diphenyl-1,3,5-hexatriene (DPH)-release induced by ß-Amyloid (1-40) can be estimated by measuring the fluorescence signal of the supernatant after ß-Amyloid (1-40) incubation, as described above. To exclude the possibility that DPH-release induced by ß-Amyloid (1-40) is connected to the unusual environment for SH-SY5Y cells kept in suspension, we modified the assay to determine the release of DPH in adherent cells.

Therefore, SH-SY5Y and GOS-3 cells were grown to confluence, harvested, and plated into 96-well plates (Falcon) at 100,000, respectively 50,000 cells/well in 200µL per each well. After 48 hours, cells reached confluence and were stained with DPH (Molecular probes, product number D-202, stock solution at 3mM in THF) at a concentration of 5µM (SH-SY5Y) or 2.5µM (GOS-3) dissolved in cultivation medium. After one hour, the cells were washed 4 times with medium and incubated with ß-Amyloid (1-40) diluted in PBS, low serum medium, or high serum medium. After incubation of one hour, we transferred an aliquot of 150µL from the supernatant into an empty well and measured the intensity of fluorescence of DPH on a fluorescence plate reader (Cytofluor 2350, Millipore). Excitation and emission bandwidth of the wavelength filters was chosen as technically possible (cut-off wavelength of excitation 330nm and 390nm and of emission 410nm and 450nm).

Optimizing the concentration of DPH

To determine the optimal staining concentrations of DPH, we added different amounts of DPH diluted in medium to adherent SH-SY5Y and GOS-3 cells grown in 96-well plates.

After 30 minutes, we removed the supernatant and washed the cells twice with PBS. Then, we measured the intensity of fluorescence of DPH on a fluorescence plate reader with appropriate settings.

Figure 17 shows that DPH was also incorporated into adherent cells. Based on this experiment, we chose a concentration of 2.5µM or 5 µM DPH for GOS-3, respectively SH-SY5Y cells for the studies using ß-Amyloid (1-40).

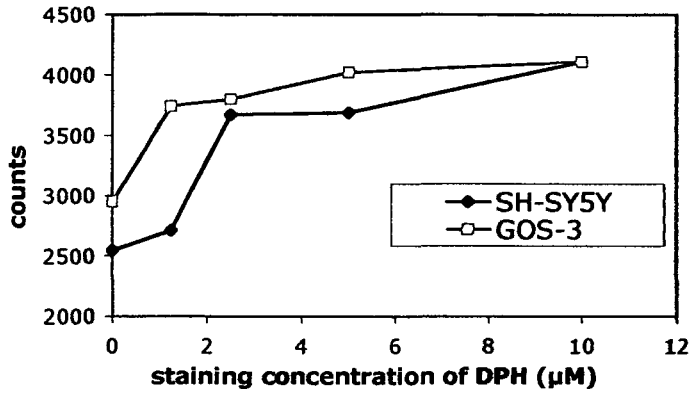

Fig.17: Successful incorporation of the fluorescent dye DPH into adherent SH-SY5Y and GOS-3 cells

FITC-DHPE as marker for lipid in SH-SY5Y

Protocol

N-(fluorescein-5-thiocarbamoyl)-1,2-dihexadecanoyl-sn-glycero-3-phosphoethanolamine triethylammonium salt (fluorescein DHPE, Molecular probes, product number F-362) was used as a probe for the cellular membrane of SH-SY5Y cells. Lyophilized FITC-DHPE was diluted in ethanol at 1mg/mL and served as a stock solution. SH-SY5Y cells were plated at 0.5E6 cells/mL in 24-well-titer plates at 1mL/well. After 24 hours, the supernatant was removed and 1mL 1:200 diluted FITC-DHPE-solution (5µg lipid/mL) was added to the cells for 20 minutes at 4°C in the dark. Then, cells were washed twice with HBSS to remove any non-incorporated lipid.

Titration of FITC-DHPE

To optimize the incorporation of lipids into the cellular membrane, cells were plated as described above and different amounts of lipid were added to the cells. Then, cells were washed twice with HBSS as described above to remove free lipid and solubilized by adding a 10% triton-solution to the cells. The fluorescence was then measured on the spectrofluorometer (extinction 495nm, max. emission at 519nm).

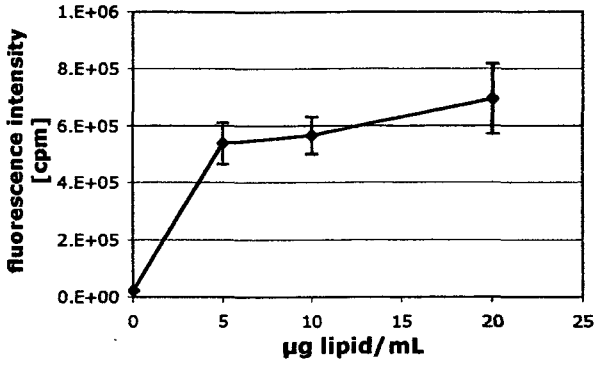

Fig.18: A lipid concentration of 5µg/mL is necessary for successful staining of the membrane of SH-SY5Y cells

Figure 18 shows the fluorescence of FITC-lipid incorporated into the membrane in variation with different concentrations of FITC-lipid. As we can see, a concentration of 5µg lipid/mL was sufficient to load the cells with the FITC-lipid successfully. Higher concentrations of the fluorescent lipid did not lead to higher signal and were therefore avoided to minimize the harmful effects of the ethanol.

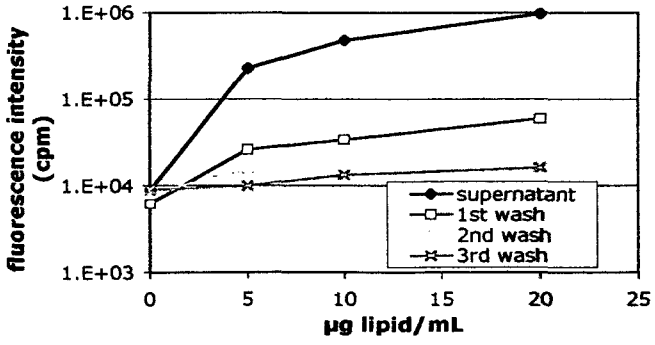

Fig.19: Remaining unbound lipid in supernatant and wash solutions after successful FITC-DHPE-staining of SH-SY5Y cells

Successive washing removed the non-incorporated lipid successfully (see figure 19). After the third washing step, the supernatant was almost void of any free lipid.

ß-DPH-HPC as marker for lipid in SH-SY5Y and GOS-3 cells

Protocol

2-(3-(diphenylhexatrienyl)propanoyl)-1- hexadecanoyl-*sn*-glycero-3- phosphocholine (ß-DPH HPC) from Molecular Probes (product number D-476) was used as another probe for lipid in the cellular membrane of SH-SY5Y and GOS-3 cells. The lyophilized lipid was diluted in ethanol at 1mg/mL as a stock solution. Cells were cultivated till confluence, harvested, and plated in 96-well poly-lysine-coated plates (Falcon) at a cell number of 100,000 SH-SY5Y or 50,000 GOS-3 cells per well in 100µL and incubated for 48 hours at 37°C, 5% CO_2 to reach confluence. Then, the medium was removed and fresh medium supplemented with ß-DPH-HPC at 10µM (SH-SY5Y) or 5µM (GOS-3) added. After one hour, the supernatant was removed and the cells washed twice with medium. ß-Amyloid (1-40) diluted in PBS, low serum medium, or high serum medium was then added to the cells for one hour. Then, an aliquot of 100µL from the supernatant was transferred into an empty well and the intensity of fluorescence of DPH measured on a fluorescence plate reader. Excitation and emission bandwidth of the wavelength filters was chosen as technically possible (cut-off wavelength of excitation 330nm and 390nm and of emission 410nm and 450nm).

Titration of ß-DPH-HPC

To determine to optimal concentration of ß-DPH-HPC for lipid-loading, we added different amounts of ß-DPH-HPC to the cells and incubated for one hour. Then, the supernatant was removed and the cells washed twice with PBS. The fluorescence intensity of DPH was measured in the wells containing cells on a fluorescence plate reader.

Figure 20 shows clearly the optimal ß-DPH-HPC concentrations of 10µM and 5 µM for membrane labeling in SH-SY5Y, respectively GOS-3 cells.

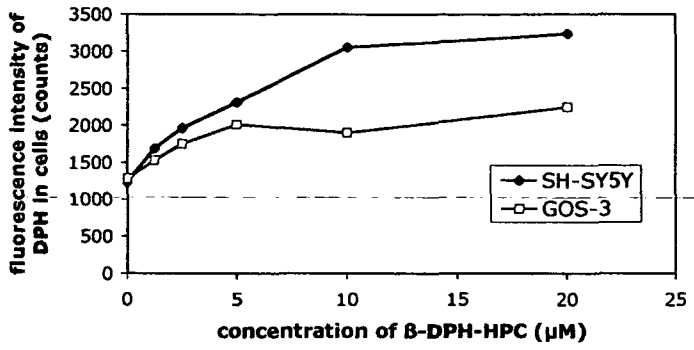

Fig.20: Successful incorporation of ß-DPH-HPC into the membranes of SH-SY5Y and GOS-3 cells

Stewart assay

Besides addition of specific lipids to cells, we also determined the amount of total lipid released by ß-Amyloid (1-40) by means of the Steward assay (Stewart, 1980). Hereby, the ability of phospholipids to form a complex with ammonium ferrothiocyanat in organic solution was utilized. The advantage of this method is that the presence of inorganic phosphate does not interfere with the assay. A simple conversion factor was used to translate absorbance values into milligrams of phospholipids. An ammonium ferrothiocyanate solution at 0.1 M was prepared by dissolving ferric chloride hexahydrate and ammonium thiocyanate in bdH_2O. This solution was stored at room temperature and was stable for several months.

2mL of cell culture supernatant were added to 2mL of ferrothiocyanate-solution and the solution vortexed vigorously for 30 seconds. Then, the solution was centrifuged at 1000rpm for 5 minutes in a bench centrifuge and the lower layer removed with a Pasteur pipette and retained. Then, the absorbance at 485nm was measured on a photometer.

For the standard curve, POPG-lipids were dissolved in chloroform at a concentration of 0.1mg/mL.

Measurement of lipid peroxidation by determination of TBARS

Aldehydes are produced when lipids are oxidized and eventually the lipid hydroperoxides break down. Lipid peroxidation research focused mostly on 4-hydroxynonenal, the major product of the peroxidative decomposition of polyunsaturated fatty acids, and malondialdehyde, the most abundant individual aldehyde resulting from lipid peroxidation.

One measure to quantify the amount of malondialdehyde (MDA) is the determination by thiobarbituric acid (TBA). Malondialdehyde forms a 1:2 adduct with thiobarbituric acid at high temperature and low pH and produces a pink pigment (see figure 21). The chromogen can be measured by fluorometry or spectophotometry at 532nm (see Esterbauer and Cheeseman, 1991). As the TBA-test is not specific for MDA, but also for a great variety of aldehydes and other substances applicable, the test is today known as the TBARS (TBA-reactive substances)-test. The validity of the TBARS-assay as an index for lipid peroxidation is still debate of controversy, but attracts widespread interest.

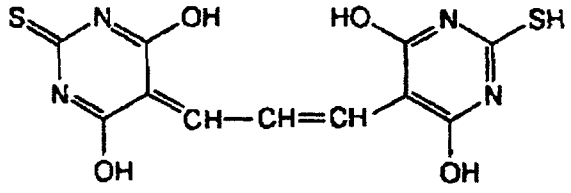

Fig.21: Molecular structure of the pink 1:2 adduct of MDA and TBA

Protocol

SH-SY5Y and GOS-3 cells were grown till confluence and plated into 12-well-plates (Falcon) at 0.5E6 (SH-SY5Y) or 0.25E6 (GOS-3) cells/well in 2mL per well. After 48 hours, cells reached confluence and were stimulated with ß-Amyloid (1-40) or H_2O_2 for different times. Then the stimulation medium was removed and the cells washed 4 times with 37 °C preheated PBS. 300µL of bdH_2O with added butylated hydroxytolene (0,01%) and EDTA (10mM) were added to each well to inhibit lipid-peroxidation during the procedure. After addition of 1800µL of a sodium dodecyl sulfate (SDS)-solution (0.1%) with 1% H_3PO_4 for achieving an acid milieu at approximately pH 3.5, the solution was suspended with a syringe to break up cell clumps. Then, ultrasound water-bath was

applied for 5 minutes for quantitative cell lysis. After addition of 2000µL of a 0.67% thiobarbituric acid solution, an aliquote of 1500µL was transferred into a 2mL eppendorf tube and the solution vortexed vigorously and boiled for 60 minutes on a thermo-heater. After cooling, the pink chromogen was extracted with 400µL of n-buthanol and pyridine (15:1 v/v). After centrifugation at 1500rpm for 15 minutes, the organic layer (upper phase) containing the colored MDA-thiobarbituric acid complex was retained and the absorbance assessed on a photometer at 532nm at room temperature. A blank sample containing pure n-butanol was measured in parallel and the absorbance subtracted from samples. Standard MDA was prepared by hydrolysis of 1,1,3,3-tetraethoxypropane. Therefore, 220mg of the MDA precursor were dissolved with stirring in 100mL of 1% (v/v) sulfuric acid at room temperature for two hours. Then, 1mL of this solution was diluted to 100mL with 1% (v/v) sulfuric acid and this solution used to construct a standard curve using the same procedure as above. The standard curve was used to indicate MDA equivalents in each sample (see figure 22 for an example of a standard curve).

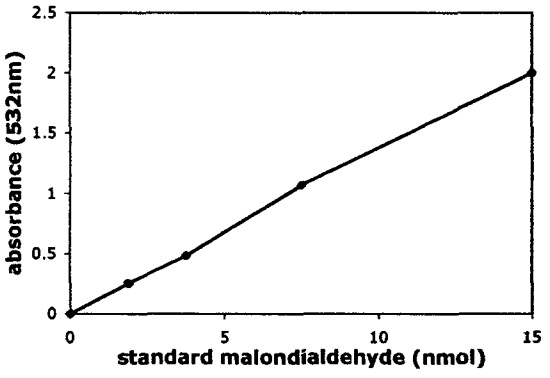

Fig.22: Example of a standard curve of the TBARS-assay using tetraethoxy-propane as precursor of MDA

Determination of the concentration of SDS

After personal communication with Mr. Chien-Tsai Lai, it was evident that it is crucial to determine the amount of SDS needed to extract MDA quantitatively of the cellular material. Therefore, we titrated the concentration of SDS in a preliminary experiment.

As we see in figure 23, the absorbance greatly depended on the amount of added SDS. Addition of 0.1% SDS to extract MDA from cells was necessary to measure significant

amounts of the TBARS. Increased concentration of SDS reduced the absorbance. Therefore, we estimated that a SDS-concentration of 0.1% was needed as well as sufficient to determine TBARS reproducibly and quantitatively.

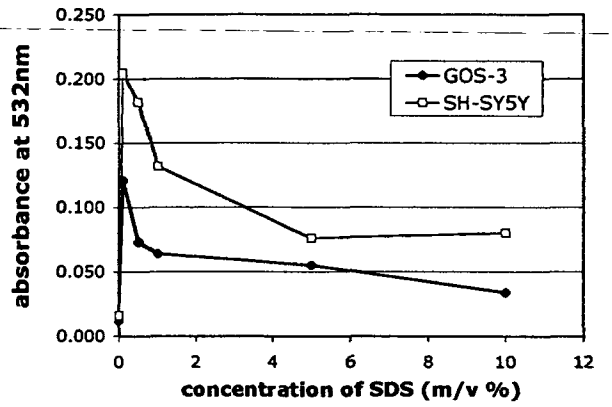

Fig.23: Cell extraction of MDA depends greatly on the SDS-concentration

Determination of the optimal boiling time

In order to achieve formation of the 1:2 adducts of TBARS (MDA and equivalent reactive aldehydes) with TBA, samples of SH-SY5Y cell lysate containing TBARS were incubated with TBA on a thermo-heater at 95°C. The samples were boiled for different amount of times and quickly cooled down to stop the reaction. Then, the chromogens were detected on a photometer at 532nm.

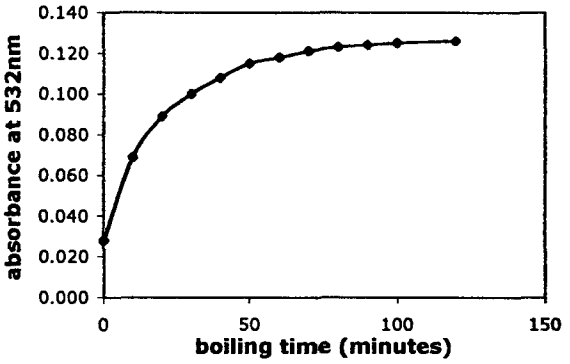

Fig.24: Incubation for 60 minutes at 95°C is necessary for quantitative formation of TBARS-TBA adducts

We see in figure 24 that an incubation time of 60 minutes lead to quantitative formation of the desired 1:2 adduct of TBARS with TBA. Therefore, we chose a duration of 60 minutes as optimal time for the experiments.

Measurement of intracellular level of reactive oxygen species

Cellular peroxides can be quantified by loading cells with 2,7-dichlorofluorescein diacetate (DCFH-DA) as shown previously in cell cultures of hippocampal (Barger et al., 1995). DCFH-DA is freely permeable to cells and diffuses across the cell membrane. It is then trapped by cellular deacetylation. Intracellular hydrogen peroxide (and presumably other peroxides as well) oxidizes this compound to 2',7'-dichlorofluorescein (DCF), which is highly fluorescent and readily detectable on a spectrofluorometer (Keston and Brandt, 1965).

DCF fluorescence is widely believed to be a measure for estimation of reactive oxygen species (ROS) formation or oxidative metabolism, since hydrogen peroxide is an intermediate in the oxidative metabolism. Thus, the superoxide anion is converted by superoxide dismutase to hydrogen peroxide. Furthermore, Fe^{2+} reacts with hydrogen peroxide to produce hydroxyl radicals. Therefore, it is assumed that DCF is suitable for estimating the level of intracellular ROS formation. Loading SH-SY5Y cells with DCFH-DA was already successfully achieved (Amoroso et al., 1999).

Protocol

To measure the intracellular level of ROS in SH-SY5Y and GOS-3 cells, cells were grown to confluence, harvested, and plated into 96-well flat bottom plates (Falcon, product number 35/3072) at 100.000 cells (SH-SY5Y) or 50.000 cells (GOS-3) per well in 200µL cultivation medium. After 48 hours, cells reached confluence. Then, 100µL of the supernatant was removed and 100µL medium with 6-carboxy-2',7'-dichlorohydrofluorescein diacetate, di(acetoxymethyl ester) (DCFH-DA, Molecular probes, product number C-2938) was added to the cells for final concentration of 15µM DCHF-DA in GOS-3 and 10µM DCFH-DA in SH-SY5Y. After one hour, supernatant with not incorporated DCFH-DA was removed. The cells were washed twice and incubated with medium containing H_2O_2 or ß-Amyloid (1-40) in cultivation conditions in an incubator. After one hour, the 96-well plate was removed from the incubator and the intensity of fluorescence of DCF measured on a fluorescent plate reader (Cytofluor 2350, Millipore). The wavelength filters were chosen appropriately: excitation filter was set to

495nm to ensure excitation of DCF at 488nm; emission filter was set to 510nm to ensure emission light passage at 532nm to the detector.

Determination of optimal DCFH-DA concentration for cell-labeling

Optimal concentration of DCFH-DA for cellular labeling was determined by applying different amounts of DCFH-DA to SH-SY5Y and GOS-3 cells for one hour, successive washing, and oxidation of DCFH to DCF by means of H_2O_2 for one hour. As we can see in figures 25 and 26, 15µM DCHF-DA in GOS-3 and 10µM DCFH-DA in SH-SY5Y were the optimal concentrations providing greatest signal/noise ratio and were therefore used for experiments.

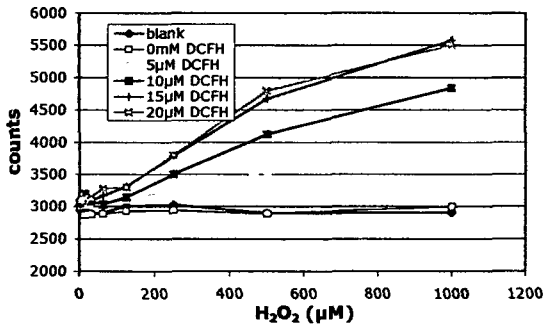

Fig.25: Titration of DCFH in GOS-3 cells

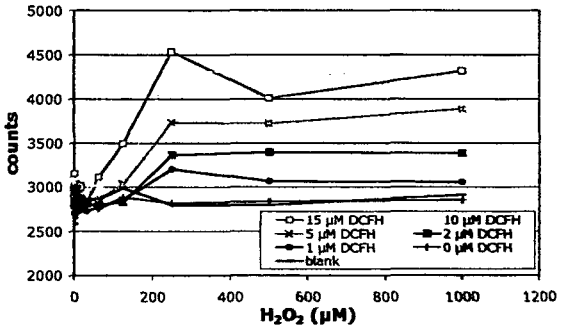

Fig.26: Titration of DCFH in SH-SY5Y cells

Determination of optimal incubation time with DCFH-DA

Optimal cell-labeling time was determined by adding DCFH-DA at optimal concentrations to the cells (15µM DCHF-DA in GOS-3 and 10µM DCFH-DA in SH-SY5Y), removing the supernatant after different time points, cell washing, and oxidizing DCFH to DCF by means of addition of 1mM H_2O_2-solution. Thereby, we observed that after 30 minutes, no further incorporation of DCFH into the cells was observed. As the staining was undergone in cultivation environment and therefore not obviously harmful to the cells, we chose an optimal time of one hour to achieve quantitative staining (data not shown).

Protocol variant

In addition, cells were also alternatively stimulated first and then stained with DCFH-DA for 30 minutes. Then, supernatant was removed, the cells washed twice, and the DCF

fluorescence measured on a fluorescent plate reader with appropriate settings. This procedure avoided possible leakage of DCFH into the extracellular, oxixdizing medium during the treatment and thereby falsifying results. Furthermore, we assume that this method allowed measuring the level of intracellular ROS (iROS) right after addition of DCFH, thereby measuring the level of iROS after treatment.

Measurement of the NFκB-activity in the cell line SH-SY5Y

NFκB-activity in the cell line SH-SY5Y was measured by means of immunofluorometry. A monoclonal antibody recognizing the active p65 subunit of NFκB was used and detected with a FITC-conjugated secondary antibody.

Material

Paraformaldehyd, sucrose and saponin were purchased from Sigma. The mouse IgG_3 anti-NFκB, p65 subunit monoclonal antibody was purchased from Chemicon Int (Product number MAB3026, formerly Roche 1697838). Lyophilized anti-mouse IgG3, FITC-conjugated antibody was purchased from Chemicon Int. and reconstituted to 1mg/mL with bdH_2O. The Isotype-control Mouse IgG_3 Ab-1 monoclonal antibody was purchased from NeoMarkers (Clone NCG3.01, Product number NC-1357).

Protocol

SY5Y-cells were plated into 24-well plates (Falcon) at 0.75E5 cells per well in 1.5mL cultivation medium. After 24 hours, the supernatant was removed and SH-SY5Y cultivation-media (10% FCS) with ß–Amyloid (1-40) was added. At different time points, the supernatant was removed, the cells washed briefly with 1mL HBSS at room temperature, and then fixed with 4% paraformaldehyd in PBS with 5% sucrose for 15 minutes at room temperature. Then, the cells were washed again with 1mL HBSS and stored in 1mL HBSS at 4°C until staining for no longer than 48 hours. For staining, the storage-HBSS was removed and the cells washed three times with 1mL PBS/saponin (0.1%) for 10 minutes. Then, unspecific binding was blocked by PBS with additional 3% BSA and 1% FCS at pH 7.4, NaN_3 and 0.1% saponin for one hour at room temperature.

Then, the cells were again washed briefly with 1mL PBS/saponin. Staining with primary antibody was done in a sample volume of 150µL solution at a 1:100 dilution in PBS/saponin, overnight at 4°C. Unspecific binding was determined by means of a negative control consisting of 150 µL of IgG_3 Isotype-control at the same dilution of 1:100 in PBS/saponin. As a positive control, NFκB was induced in one sample with 100µM H_2O_2 instead of ß-Amyloid (1-40) treatment. After washing three times with PBS/saponin for 10 minutes, unspecific binding was blocked again for one hour at room temperature with the same blocking solution as above and the cells washed briefly with 1mL PBS/saponin. Then, the cells were stained with a FITC-conjugated secondary antibody (anti-mouse IgG3, FITC-conjugated, from Chemicon Int.) in a sample volume of 150µL, diluted 1:350 in PBS/saponin for one hour. Cells were then washed three times with PBS/saponin and additionally two times with HBSS. Cells were kept finally in 1mL HBSS containing NaN_3 and stored at 4°C for no longer than 48 hours or until imaging. In case of prolonged storage, storage-HBSS was removed and fresh HBSS was added prior to imaging. Fluorescence microscopy and digital image collection were performed using a Leitz Diavert fluorescence microscope equipped with a Photometrics (Tucson) cooled CCD camera. Fluorescence intensity quantification was carried out with a 25× objective to obtain a large number of cells per field, whereas the images for visualization purposes were obtained at higher magnification (63×, NA 1.4 objective). Fields used for fluorescence quantification were selected random throughout the dish and focused using phase contrast optics. All such fields were included in the quantitative analysis. Imaging time was limited to no longer than 10 seconds to ensure limited photobleaching of the fluorophore. Wavelength filters were chosen appropriately to ensure excitation of FITC at 490nm and emission of FITC at 525nm. Adobe Photoshop was used to quantify the intensity of fluorescence.

Titration of secondary antibody

To evaluate the unspecific binding of the secondary antibody, a titration of the second antibody was done by omitting the use of the primary antibody. Therefore, cells were treated as described before, incubated with the secondary antibody and washed several

times to remove unbound secondary antibody. Then, the samples were immediately afterwards measured.

Figure 27 clearly shows that dilutions of the secondary antibody greater than 1:300 increased the unspecific binding of the secondary antibody. At a dilution of 1:400, the fluorescence signal was almost reduced to the auto-fluorescence of the sample. Therefore, we used a dilution of 1:350 to titrate the primary antibody.

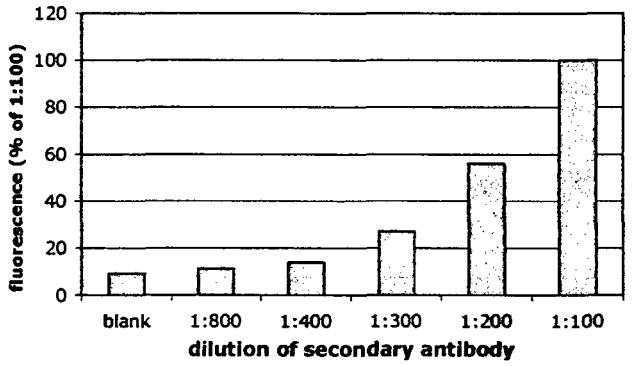

Fig.27: Titration of the secondary antibody reveals that at dilutions greater than 1:300 unspecific binding is not significant

Titration of primary antibody

To optimize the dilution of the primary antibody, the dilution of the primary antibody was varied with a fixed dilution of the secondary antibody of 1:350. We can see in figure 28 that increase of the concentration of the primary antibody caused an increase of the fluorescence signal. A dilution of 1:100 was considered as optimal due to the high signal, not significantly lower than at a dilution of 1:50.

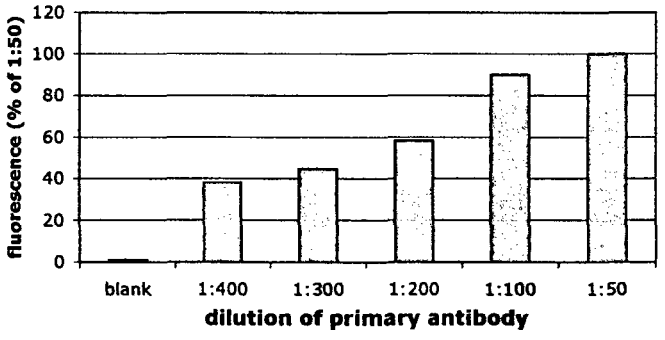

Fig.28: Titration of the primary antibody reveals that a dilution of 1:100 is necessary to achieve strong fluorescence signal

Determination of free, soluble ß-Amyloid (1-42)

A direct, "solid-phase" enzymatic immunoassay from Innogenetics N. V. was used to quantify free, soluble, ß-Amyloid (1-42) (Vanderstichele et al., 2000). Briefly, ß-Amyloid (1-42) was bound on a monoclonal antibody (MAB 21F12) linked to the solid phase, which recognized an epitope on the C-terminus of ß-Amyloid (1-42). Then, a second biotinylated monoclonal antibody (3D6) was added, recognizing the N-terminus of ß-Amyloid (1-42). For detection of bound antibody, HPR-marked streptavidin was used. The substrate TMB (tetra methyl benzidine) was added to the sample and the peroxidase-reaction stopped with sulfuric acid. The yellow stain was detected at 450nm.

Procedure

The manufacturer protocol for high sensitivity was followed to determine soluble ß-Amyloid (1-42). 100μL of sample, ß-Amyloid (1-42) standard or blank were added into the wells of the anti-ß-Amyloid (1-42)-coated plate and incubated for three hours at room temperature on a slow rotor. Then, the wells were washed 5 times with washing solution and then incubated with the high sensitivity conjugate 1 (C1HS) for one hour at room temperature. After washing as before, conjugate 2 (C2, HPR-linked streptavidin) was added and incubated for 30 minutes at room temperature. After washing, substrate was added to the wells and the reaction stopped after 30 minutes with sulfuric acid. Samples were immediately afterwards measured on an ELISA-plate reader (Dynatech MR 7000) at 450nm, with reference wavelength set to 595nm. Parallel to each experiment, a standard curve with known concentrations of ß-Amyloid (1-42) was measured to determine the actual concentrations of ß-Amyloid (1-42) in the samples (see figure 29).

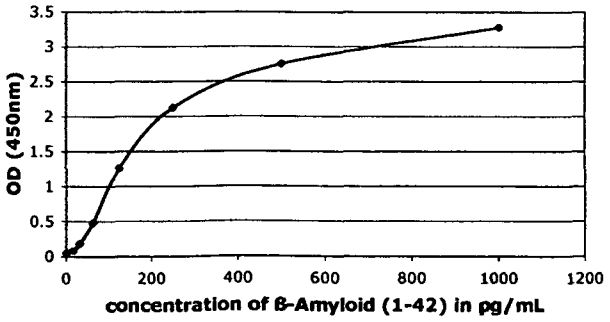

Fig.29: Example of a standard curve

Ex vivo oxidative stress in whole blood

Fresh blood was collected from 10 randomly selected healthy people in sodium EDTA blood tubes (purple cap). *Ex vivo* oxidative stress in whole blood was induced by the addition of H_2O_2 in PBS for final concentration of 500µM and incubation at 37°C for 5 hours. Then, the blood tube was submitted a centrifugation step at 4000rpm for 10 minutes on a bench centrifuge to pellet cells quantitatively. An aliquot of 1mL serum was retained and stored at -20°C for not longer than one month.

As control, fresh blood was either centrifuged immediately (not longer than one hour) after blood collection or either incubated at 37°C for 5 hours without supplementation of H_2O_2 prior to centrifugation.

Control experiment

The measurement of concentration of ß-Amyloid (1-42) in blood plasma is not yet standardized. The question, to what extent detection methods of soluble ß-Amyloid are providing quantitative results, remains widely open. It has been shown that only a small fraction of ß-Amyloid in human biological fluids is free, whereas up to 5% of ß-Amyloid is bound to lipoproteins and the vast majority bound to albumin (Biere et al., 1996). To detect as much soluble ß-Amyloid as possible in whole blood, we collected blood from one healthy individual in different blood tubes and measured the concentration of ß-Amyloid (1-42) by means of the ELISA-kit (Innogenetics N. V.) as described above.

Cap color	Anticoagulant	Supernatant after centrifugation	ß-Amyloid (pg/mL)
Purple	EDTA	EDTA-Plasma	87.2
Red	-	Serum	22.5
Green	Heparin	Heparinized plasma	76.4
Light blue	Sodium-citrate	Citrate-plasma	56.4

We see that the values for the concentration of free, soluble ß-Amyloid (1-42) greatly differed and depended on the type of blood tube. EDTA-tubes with purple caps were considered as best suited for measuring the concentration of free, soluble ß-Amyloid (1-42), as the measured values were maximal.

RESULTS

Characterization of ß-Amyloid (1-40)

Qualitative estimation of the hydrophobicity of ß-Amyloid (1-40)

Various methods (e.g. circular dichroism) give insight into the secondary structure of ß-Amyloid aggregates. Thereby, it has been shown that hydrophobic domains are formed during aggregation. ß-Amyloid aggregates, but not monomers of ß-Amyloid, bind to dyes that recognize hydrophobic sites, such as thioflavin-T and congo red. Driven by the recent findings of Chauhan et al (2000), who showed that fibrillar ß-Amyloid (1-40) forms membrane-like hydrophobic domains, as measured by DPH fluorescence anisotropy, we determined DPH fluorescence intensity and anisotropy in the presence of different species of ß-Amyloid (1-40).

It is known that DPH fluorescence emission is only detectable if DPH is located in a hydrophobic environment, typically in the inner core of cellular membranes or liposomes, whereas there is essentially no emission of DPH if suspended in an aqueous solution.

To quantify ß-Amyloid (1-40)-DPH association in an aqueous solution, we suspended DPH diluted in THF in PBS at a concentration of 15µM. The suspension was vigorously shaken till no emission was detectable on a photometer (data not shown). Then, we added ß-Amyloid (1-40) aggregated under different conditions after solubilization in the urea-system at an applied concentration of 20µM and incubated for one hour with occasional gentle vortexing to enhance ß-Amyloid (1-40)-DPH association without disturbing and breaking up ß-Amyloid (1-40) aggregates. Fluorescence intensity and anisotropy were then measured on a spectrofluorometer without and with polarizators respectively. As controls, BSA and poly-L-lysine were added to DPH-solutions at a concentration of 0.5mg/mL. Results are mean of three experiments.

As we can see clearly in figures 30 and 31, freshly dissolved, non-aggregated ß-Amyloid (1-40) had no influence on fluorescence intensity or anisotropy of DPH. This shows that

freshly diluted ß-Amyloid (1-40) had no measurable hydrophobicity. We therefore assume that freshly diluted ß-Amyloid (1-40) was mostly monomeric.

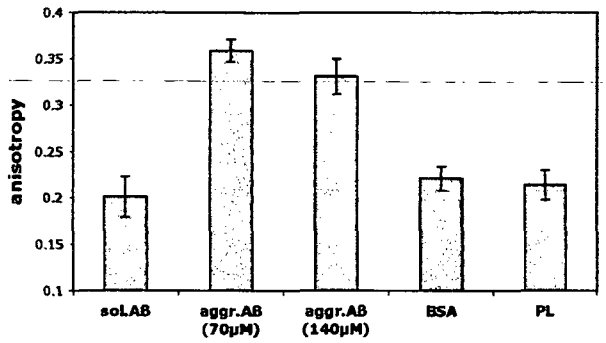

Fig.30: DPH-anisotropy of DPH increases in the presence of aggregated ß-Amyloid (1-40) significantly

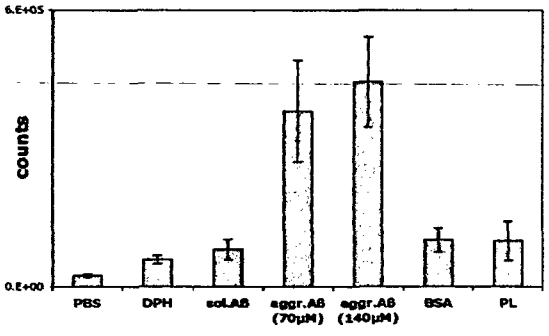

Fig.31: Intensity of fluorescence of DPH increases in the presence of aggregated ß-Amyloid (1-40) significantly

In comparison to freshly diluted ß-Amyloid (1-40) ("sol. Aß"), preaggregated ß-Amyloid (1-40) (preaggregation at 70µM or 140µM equivalent monomer concentration for 24 hours, "aggr. Aß") induced a significant increase of fluorescence intensity of DPH. We can conclude thereby that aggregates of ß-Amyloid (1-40) had a certain extent of hydrophobic domains bound by DPH. No significant difference between ß-Amyloid (1-40) preaggregated at 70µM or 140µM was observed (see figure 31).

The anisotropy values of DPH showed a significant increase only if DPH was incubated with preaggregated ß-Amyloid (1-40) (see figure 30). Measured values were approximately 0.33 and confirmed thereby the results from Chauhan et al (2000), who observed an anisotropy of ~0.33 if DPH was incubated with fibrillar ß-Amyloid (1-40). This increase in anisotropy suggests a loss of rotational freedom of the small molecule DPH if associated with large aggregates of ß-Amyloid (1-40), as anisotropy values of ~0.35 are correlated with nearly complete rigidity

The controls BSA and poly-L-lysine ("PL") did not affect DPH fluorescence or anisotropy.

Based on these results, we regarded in the following experiments freshly dissolved ß-Amyloid (1-40) as "monomeric" ß-Amyloid (1-40), whereas preaggregated ß-Amyloid (1-40) was then considered as "aggregated" ß-Amyloid (1-40), even though we could not

rule out completely that after each preparation procedure, the peptide was present in aggregated and monomeric form simultaneously.

Qualitative estimation of the aggregation state of ß-Amyloid (1-40)

It has been shown that ß-Amyloid is toxic to neurons and neuron-like cells if aggregated. Usually, ß-Amyloid is incubated at high concentration (e.g. 140µM) for a certain time to generate aggregates and later applied to cells at lower concentration (e.g. 35µM equivalent monomer concentration). After certain incubation time, the cellular viability is then determined with different methods and the impact of ß-Amyloid on cell survival correlated to the aggregation size applied initially. But very little is known about the fate of the aggregates during the incubation at low concentration.

To get further insights into the aggregation size of ß-Amyloid as a result of preaggregation as well as during incubation with cells at low concentration, we preaggregated ß-Amyloid (1-40) alone or in the presence of an inhibitor (either $KLVFFK_6$ of $KLVFFE_4$) for 24 hours at 140µM. As a tracer for ß-Amyloid (1-40), an aliquot of [^{125}I]ß-Amyloid (1-40) was added prior to aggregation, as it has been shown that [^{125}I]ß-Amyloid (1-40) was successfully incorporated into the aggregates and did not alter the aggregation kinetics significantly, thereby being a reliable tracer for ß-Amyloid (1-40) aggregates. Then, we diluted the ß-Amyloid (1-40) samples into low serum medium (1% FCS) for a final concentration of 10µM and incubated at room temperature. After one and 24 hours, an aliquot was withdrawn and submitted to a filtration using microcentrifuge tubes. Therefore, 0.5mL of the ß-Amyloid (1-40) sample was submitted to a centrifugation. Three washing steps were required to wash away loosely membrane-bound monomeric ß-Amyloid (1-40) quantitatively (data not shown). Results are the average of 6 or 15 experiments for ß-Amyloid (1-40) with or without inhibitor respectively.

As we see in figure 32, there was less than 5% ß-Amyloid (1-40) bound on the filter in freshly dissolved ß-Amyloid (1-40) samples. This strengthened our hypothesis that

freshly dissolved ß-Amyloid (1-40) in urea-conditions was predominantly present in monomeric form. No increase in membrane-bound ß-Amyloid (1-40) was observed 23 hours later; we therefore assume that a concentration of 10µM was below an assumed threshold for ß-Amyloid (1-40) aggregation.

This result gives hint that the *in vivo* aggregation of ß-Amyloid can only be achieved if ß-Amyloid is concentrated in certain compartments, e.g. lysosomes of microglia, or on the outer surface of neurons, as the extracellular concentration of ß-Amyloid in the cerebrospinal fluid and blood plasma is far below the µM range.

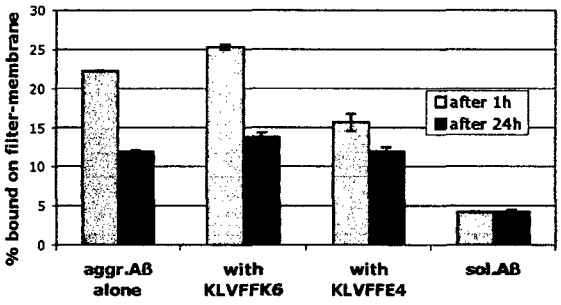

Fig.32: Ratio ß-Amyloid (1-40) bound on filter to ß-Amyloid (1-40) washed away: Incubation for 24 hours at 10µM induces partial deaggregation

Predictably, preaggregation of ß-Amyloid (1-40) at 140µM for 24 hours lead to higher binding of ß-Amyloid (1-40) to the filter as shown in figure 32. Incubation of the different aggregates in low serum cultivation medium at 10µM for 24 hours lead to a lower percentage of ß-Amyloid (1-40) bound on the filter-membrane. This shows that aggregates of synthetic ß-Amyloid (1-40) can partially resolubilize at an equivalent monomer concentration of 10µM. Such process of deaggregation of the peptide could be of relevance in the designing of drugs fighting Alzheimer disease.

Studies of ß-Amyloid (1-40) effects on liposomes as model membranes

ß-Amyloid (1-40)-membrane binding

As more evidence for ß-Amyloid-induced membrane-disruption emerges, the interactions between ß-Amyloid and membranes become more important. It has been shown that the extent of ß-Amyloid-lipid binding not only depends on the aggregation state of ß-Amyloid, but also on the nature of the fatty acids chains of the lipids.

Previously, we reported that our inhibitors were most potent in circumventing ß-Amyloid (1-40)-induced toxicity in PC-12 cells if the disrupting element consisted of charged residues (Lowe et al., 2001). Therefore we addressed the question whether a charge-effect was also a driving force in ß–Amyloid (1-40)-lipid binding.

To determine the amount of ß-Amyloid (1-40) that associated with the lipid layer of liposomes as model for cellular membranes, we used a quantitative approach by attaching the liposomes to magnetic beads. Thereby, membrane-bound ß-Amyloid (1-40) aggregates could easily be separated from free, soluble ß-Amyloid (1-40) aggregates by application of a magnetic field separating the liposomes from the supernatant.

To determine if the uptake of ß-Amyloid (1-40) aggregates to the membranes was a result of charge-effects, we used either aggregates of ß-Amyloid (1-40) alone (net neutral) or aggregates of ß-Amyloid (1-40) in the presence of our inhibitor $KLVFFK_6$ (6 positively charged lysine residues) and applied these aggregates to either POPG-liposomes (as model for anionic lipids) or DOTAP-liposomes (as model for cationic lipids).

Briefly, we prepared POPG- and DOTAP-liposomes and attached them to magnetic beads as described in Material&Methods. Then, we added preaggregated ß-Amyloid (1-40) (preaggregation at 140µM for 24 hours) supplemented with radioactive [^{125}I]ß-Amyloid (1-40) as tracer with or without the inhibitor $KLVFFK_6$ (at molar ratio 1:1) to the liposomes and incubated the solution for one hour at room temperature to attain equilibrium. After separation of the liposomes from the solution, we quantified the amount of free ß-Amyloid (1-40) in solution and bound ß-Amyloid (1-40) to the liposomes by measuring the corresponding radioactivity of [^{125}I] on a gamma-counter and

calculated the percentage of bound ß-Amyloid (1-40) to the total amount of ß-Amyloid (1-40). As control, we applied ß-Amyloid (1-40) aggregates with and without the inhibitor $KLVFFK_6$ at 20µM equivalent monomer concentration to non-coated magnetic beads (without liposomes). The experiment was done two times with one replicate per sample. Values are the average of the 4 results.

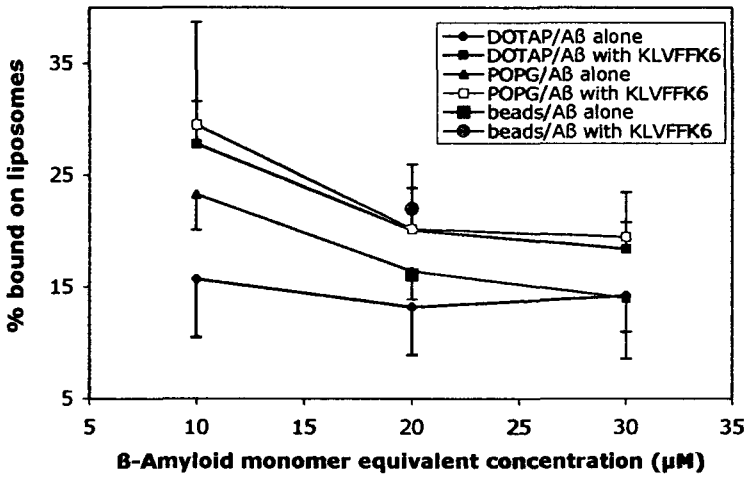

Fig.33: Membrane binding of ß-Amyloid aggregates with and without the inhibitor $KLVFFK_6$ on DOPTAP- and POPG-liposomes: Presence of $KLVFFK_6$ induces increased binding of ß-Amyloid aggregates to DOTAP- and POPG-liposomes

The general shape of the curves shows an inverse dose-relationship: The percentage of ß-Amyloid (1-40) aggregates bound to liposomes decreased with increased concentration of added ß-Amyloid (1-40). At an equivalent monomer concentration of 30µM ß-Amyloid (1-40) saturation was mostly achieved.

When comparing the binding of ß-Amyloid (1-40) aggregates to POPG- and DOTAP-vesicles, it is evident that the net charge of the lipids was not of relevance, as there was no significant difference in ß-Amyloid (1-40) binding to either POPG- or DOTAP-vesicles. This is even more obvious if the positively charged inhibitor $KLVFFK_6$ was added to ß-Amyloid (1-40): binding of ß-Amyloid (1-40)/$KLVFFK_6$ aggregates was identical in DOTAP- and in POPG-vesicles. We can therefore exclude any charge-effect as driving force for ß-Amyloid (1-40)-membrane associations.

Furthermore, we observed a greater amount of binding to the liposomes if the inhibitor $KLVFFK_6$ was added to ß-Amyloid (1-40) prior to aggregation. Assuming that the

membrane-binding of ß-Amyloid (1-40) aggregates was at least partially driven by simple deposition of large, pseudo-soluble aggregates, this difference is expected as the presence of the inhibitor $KLVFFK_6$ generated larger aggregates, more prone to deposition.

Interestingly, the amount of bound aggregates was not affected by omitting the attachment of liposomes to the magnetic beads, thereby presenting the silanized iron oxide surface of the magnetic beads instead of the lipid surface of the liposomes to the ß-Amyloid (1-40) aggregates. In the presence of blank, uncoated beads, the percentage of bead-bound ß-Amyloid (1-40) aggregates was nearly identical to the percentage of ß-Amyloid (1-40) aggregates bound to liposomes attached to the beads. This is further evidence for a simple deposition effect of large ß-Amyloid (1-40) aggregates as the ultimate driving force for ß-Amyloid (1-40)-membrane association.

ß-Amyloid (1-40) decreases membrane fluidity

One important structural feature of the cellular membrane is the fluidity of the bilayer, because of its influence on proper functioning of membrane-bound proteins. Numerous membrane-bound enzymes have been shown to have activities depending on the membrane fluidity (Gould and Ginsberg, 1985). A few inconsistent results have emerged regarding the effect of ß-Amyloid on membrane fluidity. Müller and coworkers (1995, 1998) observed a decrease in membrane fluidity when ß-Amyloid was added to mouse brain or human cortex membrane homogenates embedded with DPH. Sonication of ß-Amyloid with phospholipids and cardiolipin also induced a decrease in membrane fluidity (Chauhan et al., 1993). In contrast, when ß-Amyloid was mixed with rat synaptic plasma membrane constituents embedded with the fluorescent dye pyrene, increases in annular and bulk fluidity were observed (Avdulov et al., 1997; Chochina et al., 2001; Mason et al., 1999).

Several of the published investigations of ß-Amyloid-membrane interactions have used sonication or other mechanical means of mixing ß-Amyloid with lipids. Given the amphiphilic nature of ß-Amyloid, sonication is likely to facilitate incorporation of ß-

Amyloid into the lipid phase. We preferred to prepare the liposomes separately, and then contact liposomes without agitation with ß-Amyloid (1-40) solutions, as a more physiologically relevant contact mode.

Previously, we were able to show that aged (aggregated) ß-Amyloid (1-40) under DMSO-conditions decreased membrane fluidity in DPH-embedded mono- and multi-component liposomes in a dose-dependent way, whereas there was no effect of fresh, monomeric, ß-Amyloid (1-40) on membrane fluidity (Kremer et al., 2000).

Effect of ß-Amyloid (1-40) on the membrane fluidity

First, we addressed the question whether ß-Amyloid (1-40) is also altering membrane fluidity in liposomes if aggregated under urea-conditions.

Therefore, ß-Amyloid (1-40) was monomerized in 8 M urea and either applied directly or allowed to aggregate at 140µM for 24 hours prior to addition to DPH-coated POPG-liposomes. DPH-anisotropy was measured after one hour. Data are the mean of three replicates of one experiment.

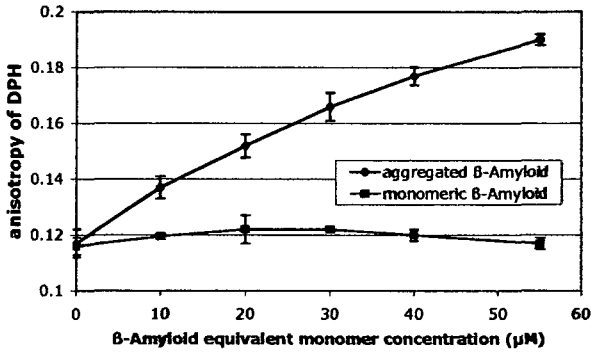

Fig.34: Aggregates of ß-Amyloid (1-40) decrease membrane fluidity in POPG-liposomes as measured by DPH-anisotropy

We see clearly that ß-Amyloid (1-40) induced in POPG-liposomes an increase in DPH-anisotropy, corresponding to a decrease of membrane fluidity, only if aggregated, whereas monomeric ß-Amyloid (1-40) had no effect (see figure 34).

We also determined the effect of ß-Amyloid (1-40) on the membrane fluidity of POPC-liposomes. The same, monomeric ß-Amyloid (1-40) did not alter membrane fluidity, whereas aggregated ß-Amyloid (1-40) increased the DPH-anisotropy to values of

approximately r~0.33 (data not shown). These anisotropy values are observed in POPC-liposomes at temperatures just below the gel transition temperature (Mitchell and Litman, 1998).

Effect of the Inhibitor $KLVFFK_6$ on the ß-Amyloid (1-40)-induced alteration of membrane fluidity in POPG-liposomes

To elucidate the role of ß-Amyloid (1-40)-induced alterations of membrane fluidity in ß-Amyloid (1-40)-induced neuronal toxicity, we added our inhibitor $KLVFFK_6$ to ß-Amyloid (1-40) in order to determine if the inhibitor is able to circumvent the ß-Amyloid (1-40)-induced alteration of membrane fluidity in POPG-liposomes. ß-Amyloid (1-40) with or without inhibitor was applied at 20µM equivalent monomer concentration and the DPH-anisotropy was measured after one hour. Data are the mean of three replicates of one experiment.

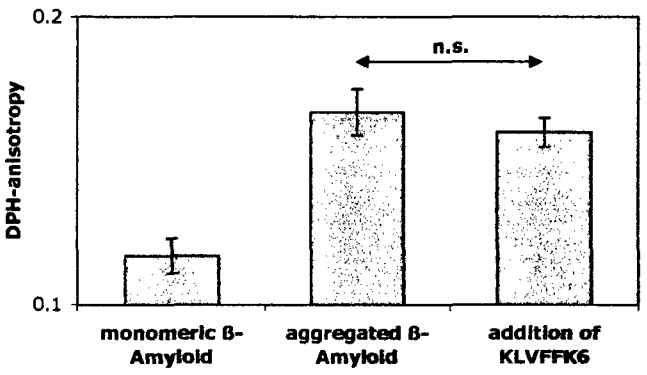

Fig.35: The inhibitor $KLVFFK_6$ is not able to circumvent the ß-Amyloid (1-40)-induced decrease in membrane fluidity in POPG-liposomes

We can clearly see in figure 35 that the inhibitor $KLVFFK_6$ was not able to circumvent the ß-Amyloid (1-40)-induced decrease in membrane fluidity in POPG-liposomes. Similar results were obtained in POPC-liposomes (data not shown).

Control experiment

To quantify the fluorescence signal of free DPH (not embedded into the liposomes) bound to aggregates of ß-Amyloid (1-40), we added ß-Amyloid (1-40) to a 1µM DPH-

solution without liposomes. A 1μM DPH-solution was equivalent to the total amount of DPH added to liposomes in previous experiments and therefore exceeded the concentration of free, liposome-unbound DPH in the previous experiments. Using the same widths of the shutters on the fluorometer, no DPH-specific fluorescence signal was detected with intensities equal to background. This strengthens our hypothesis, that at the DPH-concentration used in these experiments, we measured indeed the membrane fluidity of the liposomes.

ß-Amyloid (1-40) induces calcein-leakage

It has been shown that ß-Amyloid is able to damage the membrane integrity. In liposomes, different authors have reported leakage of an encapsulated dye if the liposomes were incubated with aggregated ß-Amyloid (e.g. McLaurin and Chakrabarrty, 1996). Some authors postulate that ß-Amyloid itself forms cation-permeable channels rather than altering the activity of membrane-bound cation-channels that are cell-inherent (Mirzabekov et al., 1994). In mitochondria, ß-Amyloid induced cytochrome c release from the intermembrane space of mitochondria (Rodrigues et al., 2001).

To determine if ß-Amyloid (1-40) by itself can induce liposomal leakage of an encapsulated dye, we prepared either monomeric ß-Amyloid (1-40) species or aggregates of ß-Amyloid (1-40) and applied these samples to different calcein-encapsulated liposomes. Moreover, we aggregated ß-Amyloid (1-40) in the presence of $KLVFFK_6$ to generate non-toxic aggregates of ß-Amyloid (1-40) to get new insights into the role of ß-Amyloid-induced loss of membrane integrity in Alzheimer disease.

We prepared freshly dissolved, monomeric ß-Amyloid (1-40) and aggregates of ß-Amyloid (1-40) (preaggregation for 24 hours at 140μM with or without the inhibitor $KLVFFK_6$) and applied these different species to monocomponent (POPC or POPC) and multicomponent (POPG-POPC-Cholesterol at molar ratio 45:45:10) calcein-encapsulated liposomes. ß-Amyloid (1-40) was applied to liposomes suspended in PBS at pH 7 as model for the cell membrane, and in PBS at pH 6 as model for the intracellular

compartments. Calcein-fluorescence as marker for dye-release was measured after one hour, 4 hours, and 24 hours as described in Material&Methods.

There was no effect of monomeric or aggregated ß-Amyloid on monocomponent liposomes (POPG and POPC liposomes at pH 6 and pH 7, data not shown), whereas there was a small, but significant amount of dye-leakage in multicomponent liposomes induced by aggregates of ß-Amyloid (1-40) alone as shown in figures 36 and 37. The calcein-leakage in these multicomponent liposomes was more prominent at pH 6 (see figure 36), mimicking internal vesicular environment, than at pH 7, as model for extracellular or plasma membrane environment (see figure 37). This pH-dependence confirms data of McLaurin and Chakrabarrty (1997), whereas the long incubation time to achieve leakage and the low amount of released dye are in strong contradiction to previous works, showing dye-leakage as soon as after one minute and leading to quantitative dye leakage (McLaurin and Chakrabarrty, 1997, 1998). The faster and quantitative dye-leakage measured by McLaurin and Chakrabarrty was presumably the result of their different preparation of liposomes by sonication, leading to less stable liposomes: Whereas untreated sonicated liposomes have a dye-leakage of 10% after 5 minutes, there was virtually no dye-leakage in our liposomes prepared by extrusion even after 24 hours.

Addition of the inhibitor $KLVFFK_6$ did not circumvent the ß-Amyloid (1-40)-induced dye-release. The amount of released calcein at pH 6 and pH 7 was virtually identical if the inhibitor $KLVFFK_6$ was present or not. This suggests that membrane disruption leading to a reduction of membrane impermeability is not the ultimate driving force for the toxic impact of ß-Amyloid (1-40) in our cell culture studies.

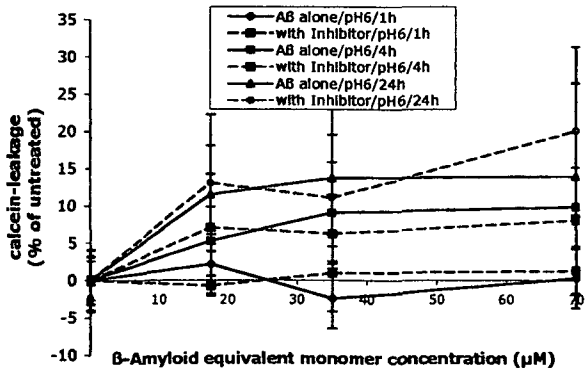

Fig.36: ß-Amyloid (1-40) induces calcein-leakage in multicomponent-liposomes at pH 6

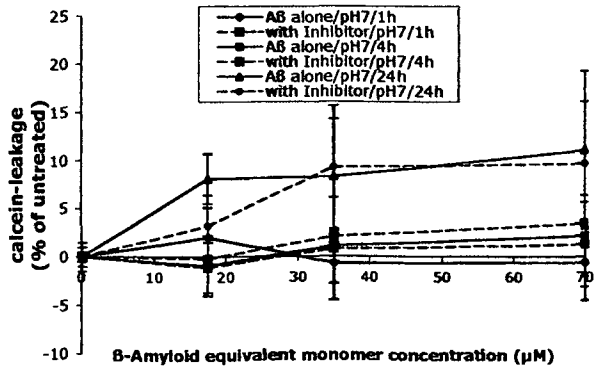

Fig.37: ß-Amyloid (1-40) induces calcein-leakage in multicomponent-liposomes at pH 7

Toxicity studies in the human neuroblastoma SH-SY5Y and the astrocytoma GOS-3 cell line

H_2O_2-induced toxicity

A great part of this work addressed the relationship between ß-Amyloid and oxidative stress. It is believed that neurons are more vulnerable to multiple insults such as extracellular applied ß-Amyloid or generation of oxidative stress than astrocytes or microglia.

Therefore, we wanted to characterize the cellular response of a human neuronal (SH-SY5Y) and a human astrocytoma (GOS-3) cell line to oxidative stress before investigating the effect of ß-Amyloid (1-40) on cellular viability of these two cell lines. Hydrogen peroxide, H_2O_2, was used as an inducer of oxidative stress, as it is widely used in research in relation to oxidative stress and often serves as reference. To correlate the cellular viability to the induction of oxidative stress, exogenous H_2O_2 was applied to the two cell lines at different concentrations for 24 hours to determine the effective concentrations of H_2O_2. Then, the cellular viability was determined by means of MTT reduction.

H_2O_2-induced toxicity in SH-SY5Y-cells

Briefly, cells were plated into 96-well plates and cultivated for 48 hours to reach confluence. Then, the supernatant was removed and H_2O_2 at different concentrations in either fresh medium with 10% FCS or 1% FCS, or in PBS alone was added to the cells. The cells were then incubated for 24 hours with H_2O_2 before assessment of the cellular viability by MTT-reducing activity. Results are the average of three experiments made in 7 replicates each.

The figure 38 displays the H_2O_2-induced cell death in the neuronal cell line SH-SY5Y. Impact of H_2O_2 on cellular viability after 24 hours incubation was already detected at concentrations as low as 30µM H_2O_2. As expected, the cells were more vulnerable in PBS than in low (1% FCS) or high serum (10% FCS) concentration cultivation medium respectively. LD_{50} were approximately 75, 185, and 215µM H_2O_2 for PBS, low serum, and high serum medium respectively. MTT-reducing activity was almost quantitatively abolished with 500µM H_2O_2. These values are in good correlation with work of Misonou and coworkers (2000), observing an LD_{50} of approximately 200µM H_2O_2, but in strong contradiction to results from Lee and coworkers (2000), observing neither morphological changes nor decrease in cellular viability at concentrations up to 1mM of H_2O_2, actually even observing a slight increase in viability. These differences are presumably attributable to differences in cultivation conditions of the neuronal cell line SH-SY5Y and illustrate the difficulties in comparing data from different laboratories using this cell line.

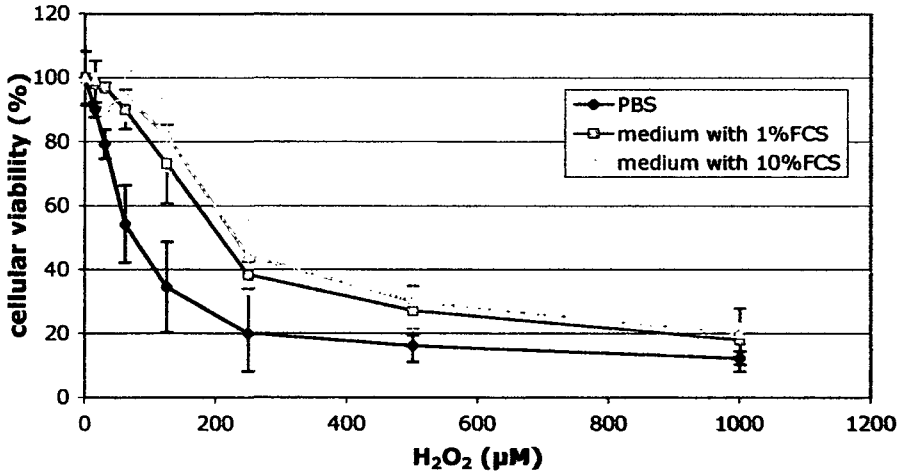

Fig.38: H_2O_2-induced toxicity in SH-SY5Y cells as measured by MTT reduction

H_2O_2-induced toxicity in GOS-3-cells

Cells were plated into 96-well plates and cultivated for 48 hours to reach confluence. Then, the supernatant was removed and fresh medium with 10% FCS or 1% FCS or PBS

alone with added H_2O_2 in different concentrations was added. After 24 hours, cellular viability was determined by means of the MTT assay. Results are the average of three experiments made in 7 replicates each.

We can clearly see in figure 39 that H_2O_2 also induced cell death in GOS-3 cells, but at higher concentrations as previously observed in SH-SY5Y cells (for comparison, SH-SY5Y response to H_2O_2 is represented in dashed lines in fugure 39). The GOS-3 cells appeared less vulnerable to H_2O_2 toxicity, with LD_{50} values of approximately 285, 325, and 340µM H_2O_2 for PBS, low serum (1% FCS), and high serum (10% FCS) medium respectively.

Moreover, the effect of reduced or lack of nutrients (1% FCS or PBS) on the viability was also less prominent than in SH-SY5Y cells.

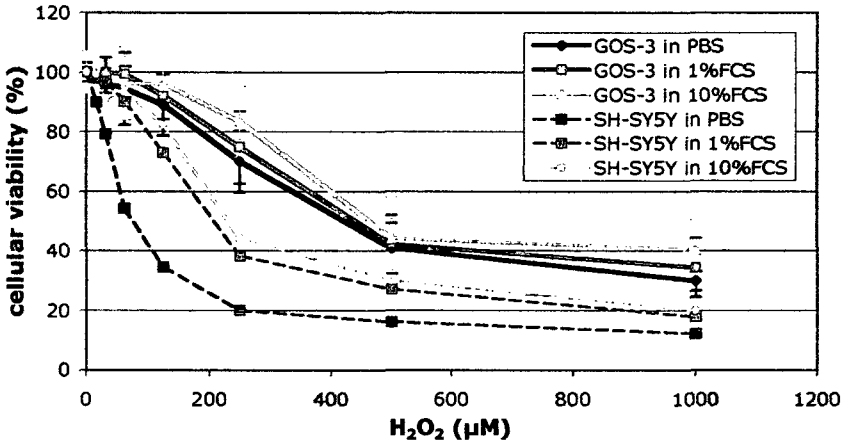

Fig.39: H_2O_2-induced toxicity in GOS-3 cells as measured by MTT reduction

Influence of ß-Amyloid (1-40) on the cellular viability

Early work of Whitson and coworkers (1989) demonstrated a trophic effect of ß-Amyloid in rat hippocampal neurons *in vitro*. Only later, it was shown that the aggregation state of ß-Amyloid is important whether ß-Amyloid exerts trophic or toxic impact on neurons. To date, multiple papers described ß-Amyloid as a neurotoxic agent to primary neurons (e.g. Pike et al., 1992; Yankner et al., 1990) or neuroblastoma cell lines in culture (e.g. Behl et

al., 1994; Busciglio et al., 1995; Lane et al., 1998; Mattson et al., 1993; Pike et al., 1993; Yankner et al., 1989, 1990), but the molecular pathway and the extend to which ß-Amyloid induces neuronal cell death are still heavily debated.

Whereas many researchers believe that this inconsistency in the literature is a result of different protocols and procedures in preparing ß-Amyloid samples and measuring toxicity, other researchers believe that the observed decreases in cellular viability induced by ß-Amyloid are just artificially constructed results under specific circumstances that are irrelevant for the understanding of Alzheimer disease and the situation *in vivo* (Rottkamp et al., 2001). This alternative hypothesis is strengthened by observations that neither isolated senile plaques nor immobilized ß-Amyloid elicit neurotoxicity *in vivo* or *in vitro* (Canning et al., 1993; DeWitt et al., 1998; Frautschy et al., 1992).

As many researchers struggle with great batch-to-batch variability when determining the toxic impact of ß-Amyloid on a cell line (personal communication from various colleagues), we purchased ß-Amyloid (1-40) from one single vendor (AnaSpec) and used one batch per set of experiments if possible.

ß-Amyloid (1-40) decreases the cellular viability in SH-SY5Y cells

Previously, we have shown that ß-Amyloid (1-40), preaggregated under urea-conditions, was toxic to rat PC-12 cells and that our inhibitors were able to circumvent the induced toxicity of ß-Amyloid (1-40) to different extents.

To better understand the effect of ß-Amyloid (1-40) on human neurons and its correlation with Alzheimer disease, we applied the same samples of ß-Amyloid (1-40) to a neuronal cell line. We chose the neuronal cell line SH-SY5Y, as it is a well-characterized cell line, often used in ß-Amyloid research. Preliminary experiments seemed to confirm data of PC-12 cells.

It has been shown that retinoic acid induces differentiation of SH-SY5Y into cells with neuron-like morphological, neurochemical, and electrophysiological phenotype (Morton et al., 1992; Pahlman et al., 1990) and that differentiated SH-SY5Y cells are more sensitive to ß-Amyloid toxicity (Zhang et al., 1994). Cell death occurred via an apoptotic pathway and only when ß-Amyloid was aggregated (Lambert et al., 1994; Li et al., 1996).

Furthermore, it has been shown that congo red inhibits ß-Amyloid induction of apoptosis measured by DNA fragmentation in SH-SY5Y cells (Li et al., 1996). Thus, this cell line, while easy to grow and maintain, provides an *in vitro* model system that may more closely reproduce the human disease than do rat-derived PC-12 cells.

Prior to the determination of the effect of ß-Amyloid (1-40) aggregated under our conditions on SH-SY5Y cell survival, we compared the morphology of SH-SY5Y cells grown under our culture conditions, cultivation without retinoic acid, and grown under the same conditions, but with addition of retinoic acid at an applied concentration of 10µM. We did not observe any morphological difference; the cultivation on poly-styrene-coated flasks without retinoic acid also lead to a neuronal differentiation. Therefore, we omitted the supplementation of retinoic acid during our toxicity experiments. Moreover, it has been shown that differentiation of PC 12 cells by nerve growth factors altered the toxicity mechanisms of ß-Amyloid and the circumventive impact of antioxidants (Sung et al., 2003).

Briefly, cells were plated into 96-well plates and cultivated for 48 hours to reach confluence. Then, the supernatant was removed and fresh medium with 10% FCS or 1% FCS containing preaggregated ß-Amyloid (1-40) (preaggregation at 70 or 140µM for 24 hours) or freshly dissolved ß-Amyloid (1-40) in different concentrations was added. After 24 hours, cellular viability was determination by means of the MTT assay. Results are the average of two experiments made in 4 replicates each.

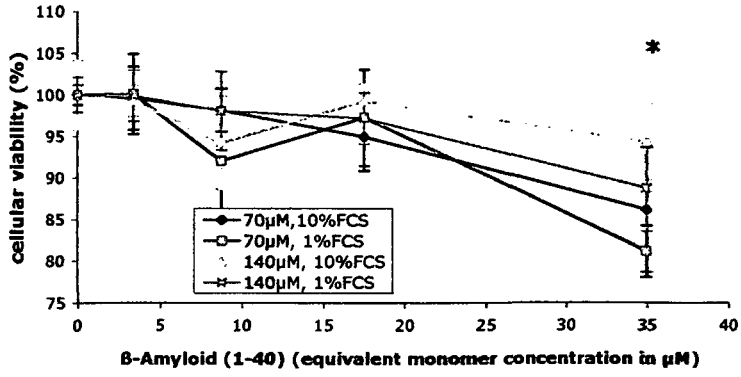

Fig.40: Aggregated ß-Amyloid (1-40) is toxic to SH-SY5Y neuroblastoma cells in a dose-dependent fashion (P<0.01)*

In figure 40, we see the effect of aggregated ß-Amyloid (1-40) on the cellular viability of SH-SY5Y after 24 hours. There was a dose-dependent toxic effect of aggregated ß-

Amyloid (1-40), significant at an applied concentration of 35μM. Preaggregation at 70μM lead to more toxic species than preaggregation at 140μM. Moreover, low serum medium rendered the neurons more vulnerable to ß-Amyloid (1-40) toxicity.
Addition of freshly dissolved ß-Amyloid (1-40) did not affect cellular viability (data not shown).

The Inhibitor $KLVFFK_6$ circumvents successfully the ß-Amyloid (1-40)-induced toxicity in SH-SY5Y cells

Next, we preaggregated ß-Amyloid (1-40) in the presence of $KLVFFK_6$ before application to SH-SY5Y cells. A molar ratio of 1:1 (inhibitor to ß-Amyloid) was chosen, as the circumvention of ß-Amyloid-induced toxicity was maximal at this molar ratio in PC-12 cells. Data are the average of 4 experiments. We see in figure 41 that the Inhibitor $KLVFFK_6$ was able to circumvent the toxic effect of preaggregated ß-Amyloid (1-40) partially.

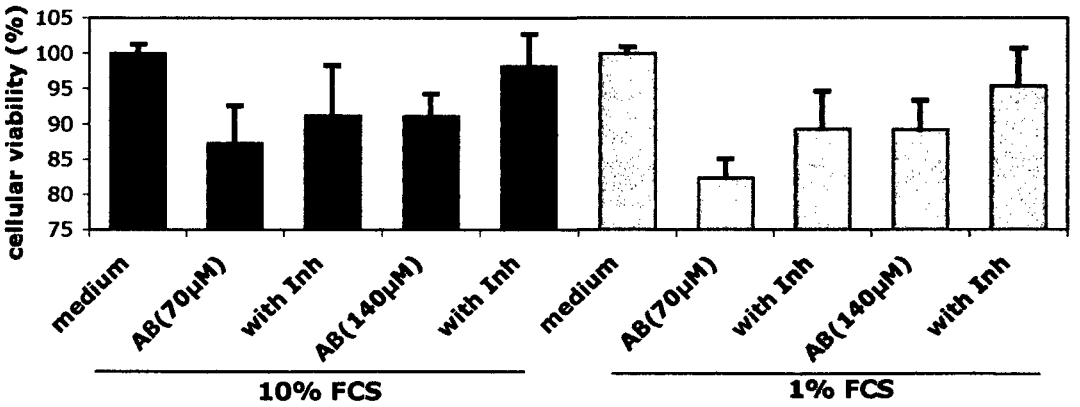

Fig.41: The inhibitor $KLVFFK_6$ ("Inh") is able to circumvent the ß-Amyloid (1-40)-induced toxicity in the neuroblastoma cell line SH-SY5Y partially

No effect of ß-Amyloid (1-40) on the cellular viability of GOS-3 cells

It has been shown multiple times that the ß-Amyloid peptide exerts a toxic effect on neurons or neuron-like cell lines. But little is known on the effect of ß-Amyloid on astrocytes and microglia. It has been shown that amyloid deposits are associated not only

with neurons, but also with reactive astrocytes and activated microglia (Duffy et al., 1990; Mandybur and Chuirazzi, 1990; Selkoe, 1991), and that both cell types also express the amyloid precursor protein APP and secrete low levels of ß-Amyloid (Busciglio et al., 1993a; Haass et al., 1992; Siman et al., 1989). Salinero and coworkers (1997) have shown that the 25-35 fragment of ß-Amyloid induces morphological changes in cultures astrocytes and is moderately cytotoxic. Similar morphological changes have been observed in glial cultures after treatment with ß-Amyloid (1-42) (Pike et al., 1994).

To determine the effect of ß-Amyloid (1-40) on astrocytes, we applied the same aggregates of ß-Amyloid (1-40) as before to GOS-3 cells, as this cell line is routinely grown in our lab, under the same experimental conditions as previously in the SH-SY5Y cell line. The experiment was repeated once using the same ß-Amyloid (1-40) samples, but aggregated for 48 hours. Results are the average of the two experiments using either 24 hours or 48 hours aggregated ß-Amyloid (1-40).

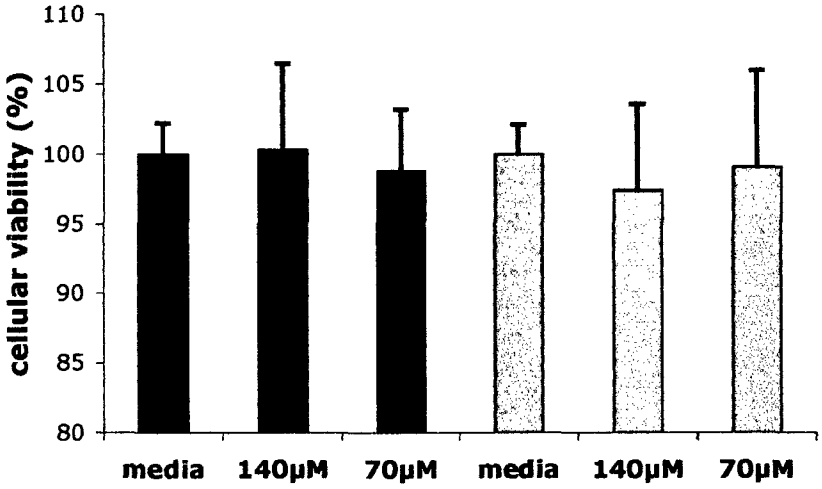

Fig.42: No effect of ß-Amyloid (1-40) on cellular viability in astrocytoma GOS-3 cells as determined by MTT-reduction capability

As we can see, there was no measurable effect of ß-Amyloid (1-40) on the cellular viablility of GOS-3 cells (see figure 42). These results provide further evidence that ß-Amyloid is firstly neuro-toxic, even though we recognize the possibility that certain, to date unknown preaggregation conditions could generate ß-Amyloid (1-40) aggregates that are toxic to non-neuronal cells, for example to GOS-3 cells as model for astrocytes.

ß-Amyloid (1-40) uptake in SH-SY5Y cells

When synthetically prepared ß-Amyloid is added to cells, little is known about the fate of ß-Amyloid, once added to the cells. Work using microglia cells has shown that microglia are able to internalize and to degrade ß-Amyloid partially. ß-Amyloid uptake in microglia has been shown to proceed via the family of scavenger receptors (Chu et al., 1998; Paresce et al., 1996).

Whether neurons can participate in ß-Amyloid clearance is unknown. Ida and coworkers (1996) have shown that ß-Amyloid added to SH-SY5Y cells is partially incorporated. ß-Amyloid was detected by means of SDS-polyacrylamide gel electrophoresis/western blot and a quantitative approach showed that a great part of ß-Amyloid was not detectable after incubation, suggesting ß-Amyloid degradation.

For our investigations, we chose another approach by adding radioactive [^{125}I]ß-Amyloid (1-40) as tracer to non-labeled ß-Amyloid (1-40) prior to aggregation, thereby generating aggregates, that are easily detectable quantitatively by means of a gamma-counter. Furthermore, this approach not only allowed to determine the amount of ß-Amyloid (1-40) internalized by SH-SY5Y cells, but also provided a tool for measuring the amount of ß-Amyloid (1-40), that was deposited onto the surface, meaning the monolayer of cells. Moreover, degradation of radioactive ß-Amyloid (1-40) leads to free radioactive iodide or amino acid-bound iodide that can be separated from ß-Amyloid (1-40) peptide-bound iodide by means of a trichloroacetic acid (TCA)-precipitation.

Thereby, we were able to get new insights into the role of neurons in ß-Amyloid (1-40) clearance.

Deposition of ß-Amyloid (1-40) on polystyrene surface

Prior to determine the ß-Amyloid (1-40)-cell-specific interactions, we determined the amount of deposited ß-Amyloid (1-40) on the polystyrene surface of the wells.

Therefore, we added ß-Amyloid (1-40)-solutions to empty wells and removed the supernatant after one hour, 12 hours, and 24 hours. Extensive washing ensured the

removal of any remainder of ß-Amyloid (1-40) in the supernatant. Then, trypsin-degradation was applied for 30 minutes to solubilize deposited ß-Amyloid (1-40). Then, the radioactivity of the trypsin-solution was measured on a gamma-counter. Results are the average of three experiments.

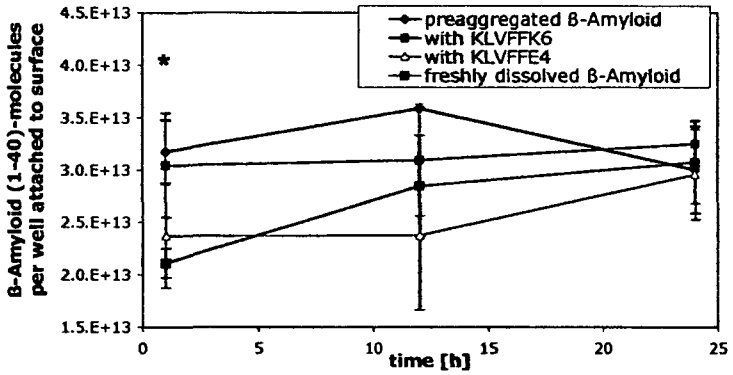

*Fig.43: Binding/deposition of different species of ß-Amyloid (1-40) on the poly-styrene surface of the wells depends on the aggregation state and the incubation time (*P<0.01)*

We see in figure 43 that after one hour, monomeric and ß-Amyloid (1-40)/$KLVFFE_4$-aggregates were deposited in significantly lower quantity than aggregates of ß-Amyloid (1-40) alone or in the presence of $KLVFFK_6$ on the polystyrene surface. This suggests that ß-Amyloid (1-40) deposition depends on the aggregate size, as larger aggregates are more prone to sediment than smaller.

After 24 hours, the different aggregates were deposited on the bottom of the well in approximately the same quantity of 3E+13 peptides per well. Assuming aggregates with a length of 200nm, a diameter of 12nm, and a molecular weight of 3000kDa (Kremer et al., 2000), 20% of the surface was covered with ß-Amyloid (1-40). Taking into consideration the inaccuracy of these numbers, a monolayer of ß-Amyloid (1-40) aggregates covering the surface was highly probable.

Association of ß-Amyloid (1-40) with the cellular membrane

Much work was done so far to identify a postulated ß-Amyloid membrane receptor. So far, various receptors were found to bind ß-Amyloid specifically. If there were a specific

ß-Amyloid-receptor, one would believe that binding of ß-Amyloid to the receptor would greatly depend on the aggregation state, as the aggregation state defines the shape, size, and epitope of the ß-Amyloid species.

Furthermore, unspecific binding to the membrane as cause of deposition is highly probable, as we have seen that ß-Amyloid (1-40) binds to liposomes driven rather by deposition than by specific ß-Amyloid (1-40)-lipid interaction as a result of a charge-effect, and as we have observed that ß-Amyloid (1-40) aggregates are also deposited unspecifically on the bottom of the well. A specific binding of ß-Amyloid (1-40) to a supposed receptor could increase the amount of membrane-deposited ß-Amyloid (1-40).

Briefly, we incubated SH-SY5Y cells at confluence with different ß-Amyloid (1-40) species. After one, 12, and 24 hours, we removed the medium, washed the cell monolayer 4 times to remove any unbound ß-Amyloid (1-40), and solubilized the membrane-bound ß-Amyloid (1-40) by trypsin-degradation for 30 minutes. Results are the average of three experiments made in duplicates.

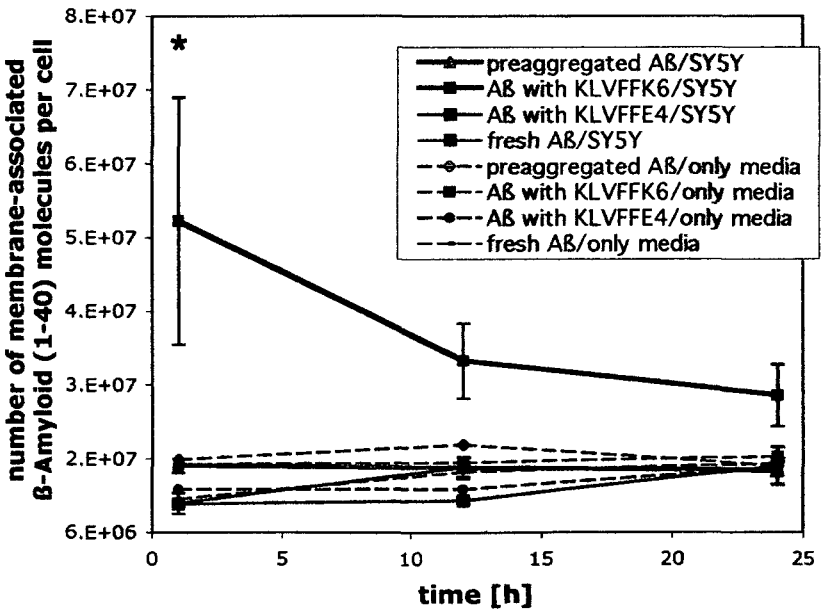

*Fig.44: Impressive amount of ß-Amyloid (1-40) molecules asscociated on the outer membrane of SH-SY5Y cells only if preaggregated with the Inhibitor $KLVFFK_6$ (*P<0.001)*

We can see in figure 44 that the amount of cell-associated ß-Amyloid, if preaggregated alone, was nearly equal the amount of deposition on cell-free wells (data from the previous experiment, measuring deposition on the bottom of the well in the absence of

cells represented in dashed lines). This strengthens the idea that ß-Amyloid (1-40) was rather deposited unspecifically on the membrane surface of cells rather than bound to specific receptor.

Aggregates containing $KLVFFK_6$ showed a strongly increased membrane binding after one hour. This suggests a complete coverage of the cellular surface exposed to the medium containing the ß-Amyloid (1-40) aggregates. This highly increased deposition is believed to be either the result of charge interaction between the positively charged lysines of the inhibitor incorporated in the ß-Amyloid (1-40) aggregates and the negatively charged cellular membrane or the result of an increase in size of ß-Amyloid (1-40) aggregates if $KLVFFK_6$ is added. Interestingly, the amount of cell-surface bound ß-Amyloid (1-40) aggregates with $KLVFFK_6$ decreased with time and leveled off in the range observed for the other aggregates. More work has to be done to understand completely this strong binding of ß-Amyloid (1-40) if preaggregated with this inhibitor. However, non-toxic aggregates of ß-Amyloid (1-40) with the Inhibitor $KLVFFE_4$ did not bind in similar fashion to the cellular membrane, we can rule out that the strong binding of ß-Amyloid (1-40)/$KLVFFK_6$ aggregates is linked to the circumvention of ß-Amyloid (1-40)-toxicity of our inhibitors.

The lack of increased amount of membrane-bound ß-Amyloid (1-40) as a function of time argues against a "seeding theory" of ß-Amyloid at the membrane surface, as postulated previously (Yanagisawa et al., 1995, Yip and McLaurin, 2001; Yip et al., 2001), even though we cannot rule out the possibility that specific interactions between ß-Amyloid (1-40) and receptors and ß-Amyloid (1-40)-fibrillogenesis at the surface of the membrane were masked by the considerable unspecific deposition on the surface.

Internalization of ß-Amyloid (1-40)

As we have observed that the aggregation state defines partially the amount of membrane-associated ß-Amyloid (1-40), it is of interest if this difference affects the amount of internalization of ß-Amyloid (1-40). Whereas large aggregates of ß-Amyloid (1-40) with $KLVFFK_6$ are probably not as easily taken up as smaller aggregates or

monomers, we have observed a 5 times higher amount of these large ß-Amyloid (1-40)/ $KLVFFK_6$ aggregates on the cell surface, prone to internalization.

To determine the amount of internalized ß-Amyloid (1-40), we incubated SH-SY5Y cells for 24 hours with ß-Amyloid (1-40). After one, 12 and 24 hours, we removed the medium by aspiration, washed the cells, removed the membrane-associated peptide by trypsin-degradation and measured the remaining radioactivity of ^{125}I in the cells. Results are the average of three experiments in duplicates.

Surprisingly, loading the cells with different species of ß-Amyloid (1-40) did not affect the amount of ß-Amyloid (1-40) that was internalized (see figure 45). As the total amount of internalization of toxic (preaggregated ß-Amyloid (1-40) alone) and non-toxic (monomeric ß-Amyloid (1-40), aggregated ß-Amyloid (1-40) with inhibitors $KLVFFK_6$ or $KLVFFE_4$) ß-Amyloid (1-40) species was identical, we assume that toxicity of ß-Amyloid (1-40) in SH-SY5Y cells did not depend on the total amount of internalized ß-Amyloid (1-40).

However, we cannot rule out that ß-Amyloid (1-40)-induced toxicity is correlated to the internalization of one specific species of ß-Amyloid (1-40) aggregates, and that the amount of internalization of these specific aggregates is masked by the overall internalization of the peptide.

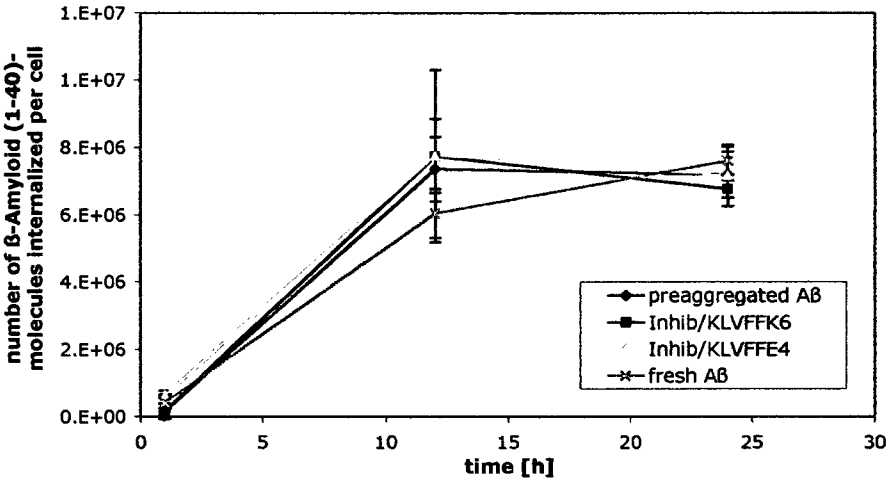

Fig.45: No difference in internalization of different species of ß-Amyloid (1-40) in SH-SY5Y cells

Quantification of degraded ß-Amyloid (1-40)

Next, we addressed the question if the neuronal cell line SH-SY5Y is able to degrade ß-Amyloid (1-40) in order to elucidate the role of neurons in ß-Amyloid clearance *in vivo*. Therefore, we incubated different species of ß-Amyloid (1-40) at 37°C for 24 hours with and without cells and determined the amount of free, peptide-unbound ^{125}I by means of a TCA-precipitation, as well as the total amount of ^{125}I in the supernatant. Results are the average of three experiments made in duplicates.

Figure 46 shows the degradation of the different ß-Amyloid (1-40) species in cultivation medium without cells at 37°C. After 24 hours, approximately 1.5% of the total amount of ß-Amyloid (1-40) was detected in the TCA-soluble fraction, representing degraded peptide. As expected, there was no difference in thermal stability between monomeric, aggregated ß-Amyloid (1-40) with or without the inhibitors $KLVFFK_6$ or $KLVFFE_4$.

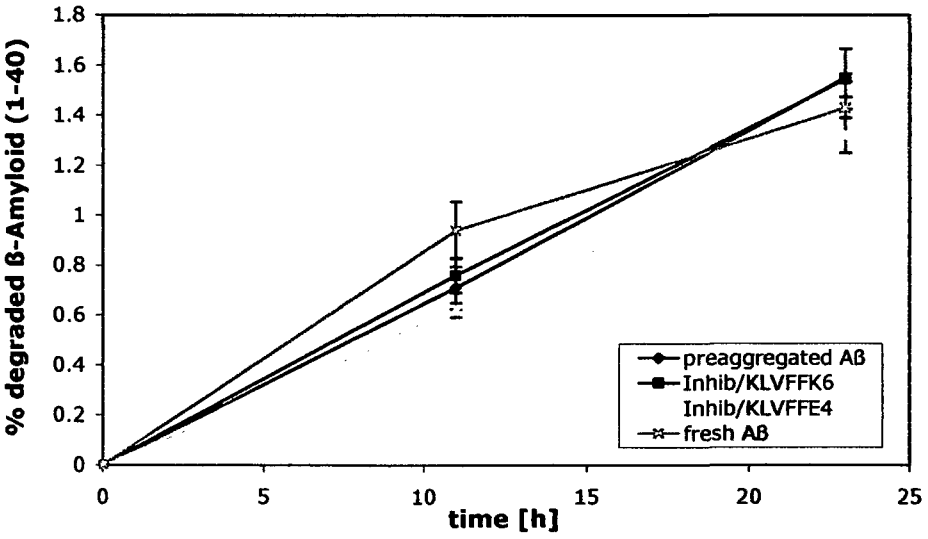

Fig.46: Thermodynamic degradation of different ß-Amyloid (1-40) species in cell-free cultivation medium shows no difference in stability of the different ß-Amyloid (1-40) species

The amount of cell-specific degradation is represented in figure 47. Cell-specific degradation was defined as the difference of the measured amount of degraded ß-Amyloid (1-40) in samples with cells and the measured amount of degraded ß-Amyloid

(1-40) in samples without cells (prior experiment). We observed no significant difference in the resistance to cell-specific degradation of the different ß-Amyloid (1-40) species. Moreover, we observed that approximately 2% of the total amount of ß-Amyloid (1-40) in the supernatant was degraded in a cell-specific manner in addition to the 1.5% degraded ß-Amyloid (1-40) in the absence of cells after 24 hours.

As the amount of cell-specifically degraded ß-Amyloid (1-40) did not decrease with time (the curve suggest more an exponential time-course), we assume that there was no limitation in ß-Amyloid (1-40)-degradation capacity of SH-SY5Y cells in our settings, giving some hints for an active role of neurons in ß-Amyloid-clearance *in vivo*.

From these data, we can estimate a half-life time $t_{1/2}$ of approximately one hour. This is in good correlation with Savage and coworkers (1998), who measured a $t_{1/2}$ for brain ß-Amyloid in mice between 1.0 and 2.5 hours, and with Knauer et al. (1992) and Burdick et al. (1997), observing a half-life of ß-Amyloid (1-40) of one hour in PC12 cells.

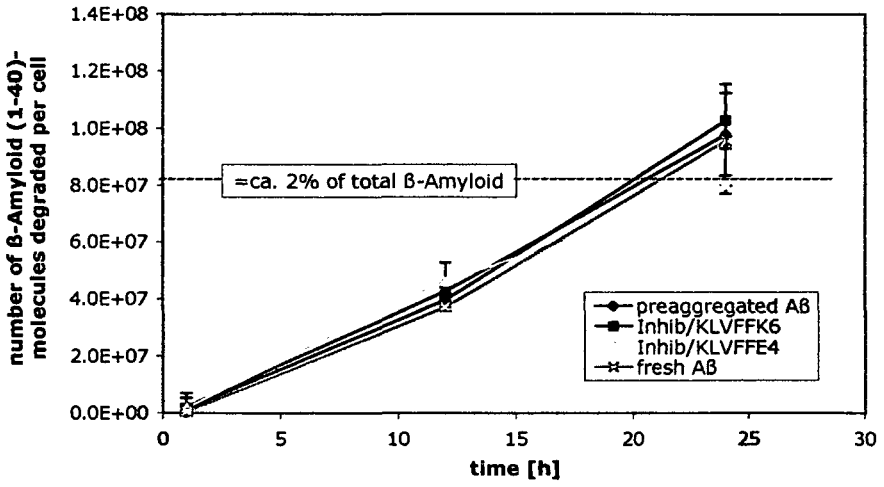

Fig.47: SH-SY5Y cell-specific degradation of different ß-Amyloid (1-40) species reveals no difference in the extent of degradation

Characterization of degradation of ß-Amyloid (1-40)

Next we addressed the question whether the cell-specific degradation of ß-Amyloid (1-40) was from extracellular or intracellular origin. To determine if extracellular degradation occured, we added preaggregated ß-Amyloid (1-40) alone (at 140µM for 24 hours) to conditioned medium from routine cell culture instead of fresh cultivation

medium. Then, after 24 hours, we determined the amount of degraded ß-Amyloid (1-40) in this cell-free conditioned medium by means of a TCA-precipitation and compared data to ß-Amyloid (1-40) degradation in fresh medium without cells and fresh medium with cells. Results are the average of two experiments.

We observed a strong degradation of ß-Amyloid (1-40) aggregates if incubated in conditioned medium overnight at 37°C (see figure 48: 16.3% degraded ß-Amyloid (1-40) in condition medium in comparison to 10% in fresh medium with cells). This is strong evidence for the existence of proteases in the extracellular matrix, released by SH-SY5Y cells, able to degrade ß-Amyloid (1-40)-aggregates.

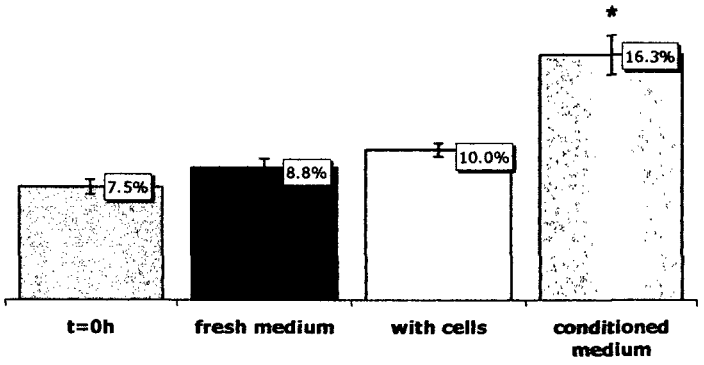

*Fig.48: Percentage of degraded ß-Amyloid (1-40) aggregates in fresh medium with or without the presence of cells, and in cultivation medium without cells gives evidence for extracellular degradation of ß-Amyloid (1-40) (*P<0.001)*

Evaluation of the distribution of extracellular and intracellular degradation of ß-Amyloid (1-40)

As we have observed that preaggregated ß-Amyloid (1-40) was degraded extracellularly by SH-SY5Y-released proteases, we wanted to quantify the amount of extracellularly degraded ß-Amyloid (1-40) in our system.

Therefore, we collected cultivation medium from cells cultivated for 24 hours in 6-well plates ("dry run" without ß-Amyloid (1-40)) and diluted ß-Amyloid (1-40) samples into this conditioned medium, thereby mimicking the extracellular matrix that was formed during the incubation of 24 hours in our system. After 24 hours, the amount of degraded ß-Amyloid (1-40) was determined by means of a TCA-precipitation. For comparison, we

diluted ß-Amyloid (1-40) into fresh medium and added these ß-Amyloid (1-40) samples to wells either with confluent SH-SY5Y cells or to wells lacking cellular material. Results are the average of two experiments made in duplicates.

As we can see in figure 49, the conditioned medium from a dry run ("24h culture medium") was able to degrade ß-Amyloid (1-40) to a greater extent than fresh medium alone without cells. This is strong evidence for the occurrence of extracellular degradation of ß-Amyloid (1-40) aggregates in our system. Moreover, the measured amount of degradation in this "low-conditioned medium" was lower than in fresh medium in the presence of cells. Therefore, we can assume that ß-Amyloid (1-40) was also partially degraded intracellularly in our system.

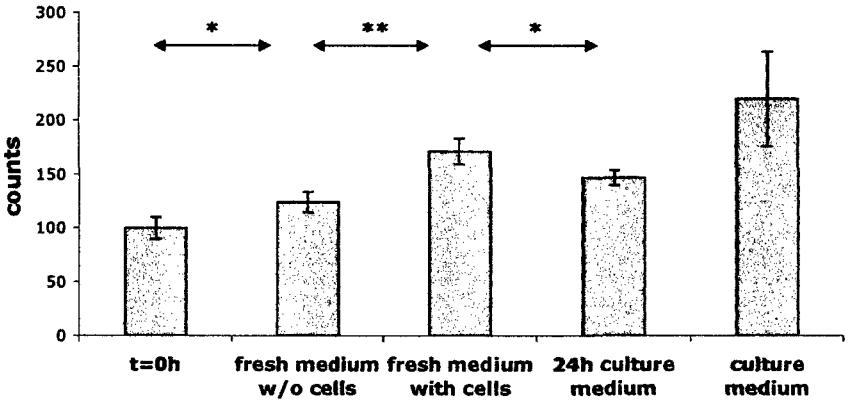

*Fig. 49: Degradation of aggregated ß-Amyloid (1-40) under different conditions gives evidence for extra- as well as intra cellular degradation by SH-SY5Y cells (*P<0.01, **P<0.001)*

Intracellular degradation of ß-Amyloid (1-40)

Data above give hint that ß-Amyloid (1-40) might be degraded *in vivo* extracellularly. This is not surprising when we take into consideration the high load of cell-released substances in the cerebrospinal fluid.

So far, studies on ß-Amyloid clearance have focused on astrocytes and microglial cells as putatively the most prominent actors in ß-Amyloid clearance *in vivo*. Little is known about the role of neurons in contributing to the ß-Amyloid degradation *in vivo*. To address the question if a part of the degraded ß-Amyloid (1-40) in our experiment was

also degraded intracellularly, we added chloroquine to the cells prior to ß-Amyloid (1-40)-addition. Chloroquine is a well-known inhibitor of lysosomal degradation. Addition of chloroquine therefore blocks successfully lysosomal ß-Amyloid (1-40) degradation, which should be reflected in a reduced amount of total degradation of ß-Amyloid (1-40) in our system if lysosomal ß-Amyloid (1-40) degradation occured indeed.

Briefly, SH-SY5Y were plated into 6-well plates and grown to confluence for 23 hours. Then, the supernatant was removed and fresh cultivation medium supplemented with chloroquine at different applied concentrations added to the cells. After one hour of chloroquine pretreatment, the cells were washed briefly with binding medium and fresh binding medium with preaggregated ß-Amyloid (1-40) (preaggregation at 140µM for 24 hours) and with chloroquine at the same concentration as during pretreatment added to the cells. After 24 hours, the amount of degraded ß-Amyloid (1-40) aggregates in the different samples was determined by means of a TCA-precipitation. Results are the average of two experiments made in duplicates.

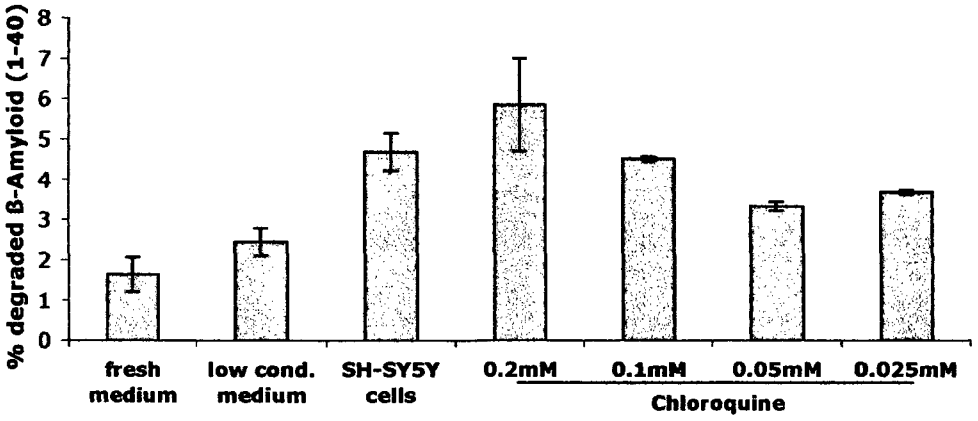

Fig.50: Addition of chloroquine at 0.05M blocks intracellular ß-Amyloid (1-40) degradation by SH-SY5Y cells successfully

Addition of chloroquine at an applied concentration of 0.05mM reduced successfully the amount of degraded ß-Amyloid (1-40) in the supernatant (see figure 50). Higher concentrations of chloroquine (0.1mM and 0.2mM chloroquine) did not further block ß-Amyloid (1-40) degradation. We assume that the great extent of ß-Amyloid (1-40) degradation at 0.1mM and 0.2mM chloroquine was a consequence of cell death leading to cell disruption and release of proteases into the extracellular medium. At a concentration of 0.2mM chloroquine, decreased cellular viability after 24 hours was

easily detectable morphologically on a microscope. Such death induction of chloroquine was also observed in the work of Ard and coworkers (1996).

We assume therefore that in our cellular system ß-Amyloid (1-40) was degraded partially intracellularly, as addition of chloroquine at 0.1mM to either fresh medium without cells or to low-conditioned medium without cells was not able to reduce extracellular ß-Amyloid (1-40) degradation in the absence of cells (see figure 51).

In summary, we gathered strong evidence that ß-Amyloid (1-40) aggregates were partially degraded intracellularly via the lysosomal pathway and partially extracellularly by SH-SY5Y-released proteases to approximately equivalent extent. These facts let us assume that neurons are able to contribute to ß-Amyloid-degradation *in vivo* and that neurons are possibly even playing a crucial role in ß-Amyloid clearance *in vivo*.

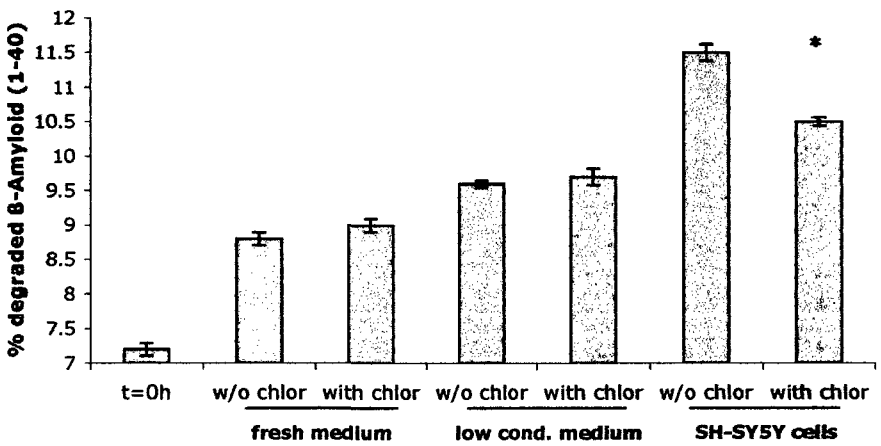

*Fig.51: Addition of chloroquine to fresh medium without cells or conditioned medium without cells does not reduce extracellular ß-Amyloid (1-40) degradation (*P<0.001)*

As the amyloid cascade hypothesis assumes a net increase in ß-Amyloid in the brain, the question, if this increase is due to increased ß-Amyloid production or reduced ß-Amyloid degradation is prevalent and still has to be elucidated. It has been shown that some forms of APP can be degraded via the ubiquitin-pathway (Gregon et al., 1994), thus removing potential ß-Amyloid. Here, we show that the product of APP, ß-Amyloid, can be degraded partially by the neurons themselves via the lysosomal pathway. Protease candidates for ß-Amyloid degradation are a serine protease-α2-macroglobulin complex (Qiu et al., 1996) and a metalloprotease secreted by CHO and BV-2 microglia cells (Qiu et al., 1997).

Aggregates of ß-Amyloid (1-40) decrease the membrane fluidity in SH-SY5Y cells

We hypothesized that ß-Amyloid perturbs membrane physical properties in ways that adversely affect function of receptors, ion channel proteins, adhesion proteins, and other cell-surface proteins. Proper functioning of integral membrane proteins and signal transduction pathways are sensitive to the local bilayer environment. For example, decreased membrane fluidity disrupts the CCK receptor-G protein complex in rat cortical membranes (Rinken et al., 1998) and alters Na^+/K^+-ATPase activity (Deliconstantinos, 1995). The latter observation is of particular interest to this work in light of reports that ß-Amyloid reduces Na^+/K^+-ATPase activity (Mark et al., 1995). Changes in membrane physical properties have been associated with Alzheimer disease in a few reports; in particular, Mecocci and coworkers (1997) observed significant decreases in Alzheimer disease mitochondrial membrane fluidity compared to age-matched controls. Müller and coworkers (2001) observed alterations of fluidity in mouse and rat brain membranes induced by rather low concentrations of ß-Amyloid (1-40).

We further hypothesized that membrane perturbation is a function of ß-Amyloid assembled state. Two types of experiments support this hypothesis. First, aggregated but not monomeric ß-Amyloid (1-40) associates with lipid components of rat cortical homogenates and mixed synthetic vesicles (Good and Murphy, 1995). Second, aggregated but not monomeric ß-Amyloid (1-40) causes a dose-dependent decrease in membrane fluidity of large unilamellar vesicles (Kremer et al., 2000, previous experiments).

Our aim was to further define the details of the relationship between ß-Amyloid assembled state, ß-Amyloid-membrane association, and ß-Amyloid-mediated perturbation of membrane structure, providing a potential link between ß-Amyloid assembled state and ß-Amyloid induced toxicity.

Previously, we and others have shown that ß-Amyloid altered the membrane fluidity in liposomes and cell homogenates if aggregated, whereas there was no effect of monomeric ß-Amyloid. The question, if this alteration of membrane fluidity is of relevance for ß-Amyloid toxicity, is still unanswered. Therefore, we investigated in the effect of toxic

species of ß-Amyloid (1-40) in alteration of cellular membrane fluidity in a cellular system as a more relevant set up. We chose the neuronal cell line SH-SY5Y as model for neurons, as this cell line is widely used in Alzheimer disease research and as it is susceptible to ß-Amyloid (1-40) toxicity.

Preliminary experiment

First, we loaded the cellular membrane of viable SH-SY5Y cells with the fluorescent dye DPH as described in Material&Methods. Thereby, it is believed that DPH is incorporated into the inner core of the membrane bilayer. Then, we added different amounts of ß-Amyloid (1-40) preaggregated under urea conditions (pH 7, 140µM for 24 hours) diluted in PBS with 5% glucose to the cells and measured the total fluorescence of DPH (spectrofluorometer without polarizators) and the anisotropy of DPH (spectrofluorometer with polarizators installed) after 30 minutes and after two hours.

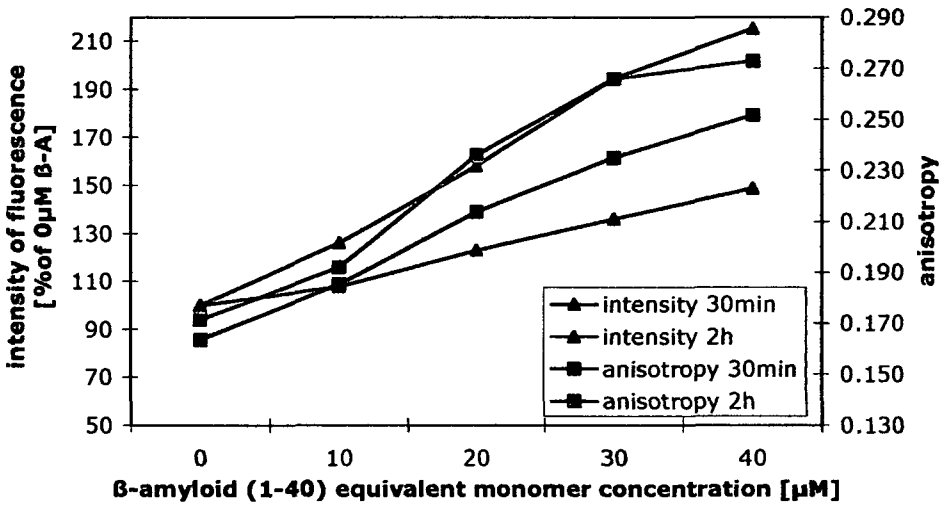

Fig.52: Addition to ß-Amyloid (1-40) aggregates to DPH-labeled SH-SY5Y cells induces an increase in total fluorescence intensity and anisotropy of DPH

On the left y-axis of figure 52, the intensity of the fluorescence (measured without polarizators) is represented. On the right y-axis, the values of DPH-anisotropy are shown (measurements with polarizators). We see clearly an increase in intensity as well as an increase in anisotropy in the SH-SY5Y cells. Increases in intensity and anisotropy were detectable as soon as 30 minutes after adding ß-Amyloid (1-40) and reached a maximum

after two hours incubation. DPH-measurements after two hours did not further increase intensity or anisotropy (data not shown).

Whereas the increase in anisotropy of DPH can be interpreted as an interaction between DPH and ß-Amyloid (1-40) aggregates, the origin of the increase of the fluorescence intensity is not obvious.

DPH-anisotropy reached after two hours incubation with aggregated ß-Amyloid (1-40) values of ≈0.29, suggesting notable loss of rotational freedom of DPH. Such high values of anisotropy are only seen in DPH-embedded liposomes, but are difficult to interpret in a cellular system, as these anisotropy-values are associated with nearly total loss of rotational freedom of DPH, suggesting a complete rigid membrane. As the cellular viability measured by means of trypan blue exclusion was not affected by this treatment (data not shown, see Material&Methods for more detail) we are confident that the DPH-anisotropy is definitely not a measure of membrane fluidity when using this protocol.

ß-Amyloid (1-40)-induced decrease of membrane fluidity in SH-SY5Y

It is evident that the anisotropies of DPH measured above were not correlated to a measure of membrane fluidity. Assuming that this discrepancy between realistically expectable and measured values for DPH-anisotropy in a cellular system arised from the interaction of DPH with aggregated ß-Amyloid (see Results/ Characterization of ß-Amyloid (1-40)/ Qualitative estimation of the hydrophobicity of ß-Amyloid (1-40)), we varied our protocol in order to eliminate any fluorescence intensity from ß-Amyloid (1-40)-bound DPH in the supernatant. Therefore, we stained SH-SY5Y cells with DPH as before, washed extensively to remove any free, membrane-unbound DPH, and treated the cells with aggregated ß-Amyloid (1-40) for one hour. Then we harvested the cells and washed the cell population 4 times with PBS to remove any ß-Amyloid (1-40)-bound DPH in the supernatant. After each washing step, we measured the DPH-anisotropy on the spectrofluorometer. Results are the average of 4 experiments.

We observed that the measured DPH-anisotropy decreased with successive washing (see figure 53). After the third washing step, there was still a significant increase in DPH-anisotropy if ß-Amyloid (1-40) aggregates were added to the cells at an applied

concentration of 40µM. Further washing did not decrease the measured DPH-anisotropy, as the DPH-anisotropy values after the fourth washing step were nearly identical to DPH-anisotropy values after the third washing step. Therefore, we assume that DPH/ß-Amyloid (1-40)-complexes in the supernatant were quantitatively washed away after the third washing step and that the remaining fluorescence had as origin DPH incorporated into the inner core of the cellular membrane.

As the DPH-anisotropy was significantly different if ß-Amyloid (1-40) was added to the cells at an applied concentration of 40µM, we believe that this increase of DPH-anisotropy was the effect of ß-Amyloid (1-40)-membrane interactions. Incorporation of ß-Amyloid in the center of the lipid bilayer has been also demonstrated by Mason and coworkers (1996) by small angle x-ray diffraction approaches.

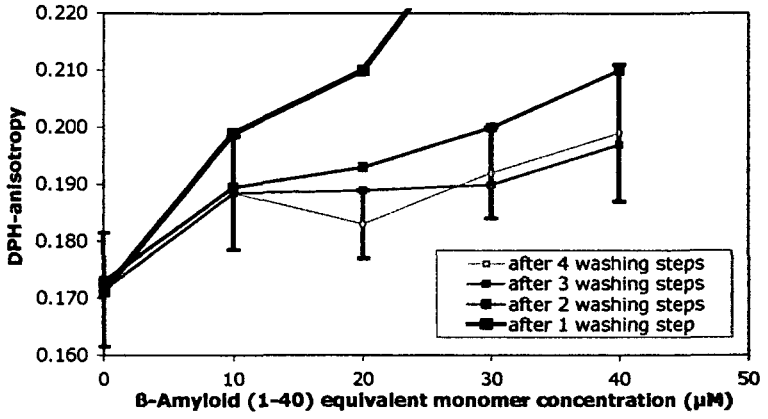

Fig.53: Aggregated ß-Amyloid (1-40) decreases membrane fluidity in SH-SY5Y cells in a dose-dependent fashion

The observed increase in DPH-anisotropy is evidence of loss of rotational freedom of DPH. As we strongly believe that in our system DPH was embedded in the inner core of the cellular membrane of SH-SY5Y cells, our results give evidence for local areas of rigidity (local decrease of membrane fluidity) in the cellular membrane, but not evidence for an overall decrease of membrane fluidity. We assume that membrane-incorporated ß-Amyloid (1-40) was bound to membrane-incorporated DPH. As these ß-Amyloid (1-40) aggregates were rather large, one can assume that the rotational freedom of these aggregates was hindered once they were embedded in the cellular membrane. This loss of rotational freedom was then reflected in the loss of rotational freedom of ß-Amyloid (1-40)-bound DPH as measured by the increase of DPH-anisotropy.

No effect of the inhibitor KLVFFK$_6$ on the ß-Amyloid (1-40)-induced increase in DPH-anisotropy

In order to determine if the incorporation of ß-Amyloid (1-40) into the inner core of the cellular membrane of SH-SY5Y cells and the induced alteration of local membrane fluidity was correlated to the toxic impact of preaggregated ß-Amyloid (1-40) in our cellular system, we added our inhibitor KLVFFK$_6$ to ß-Amyloid (1-40) prior to aggregation in order to generate non-toxic aggregates. Then, we added these ß-Amyloid (1-40)/inhibitor aggregates to the DPH-stained cells at an applied equivalent monomer concentration of 40μM, incubated for one hour, and washed extensively before measuring the anisotropy of DPH.

Furthermore, we applied freshly dissolved, monomeric ß-Amyloid (1-40) to the cells. The experiment was repeated once.

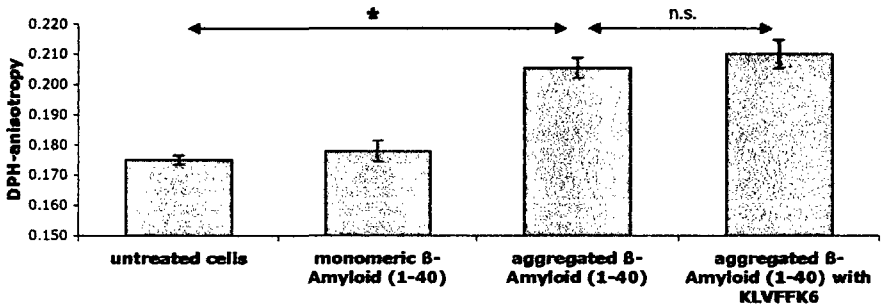

*Fig.54: Monomeric ß-Amyloid (1-40) does not alter membrane fluidity in SH-SY5Y cells; addition of the inhibitor KLVFFK$_6$ to ß-Amyloid (1-40) does not circumvent the ß-Amyloid (1-40)-induced decrease of membrane fluidity (n.s. not significant, *P<0.01)*

No effect of freshly dissolved, monomeric ß-Amyloid (1-40) on the membrane fluidity as measured by DPH-anisotropy was observed (see figure 54). Addition of the inhibitor KLVFFK$_6$ to ß-Amyloid (1-40) prior to aggregation did not circumvent the ß-Amyloid (1-40)-induced increase of DPH-anisotropy.

Therefore, we assume that the measured alterations of fluidity in the inner core of the plasma membrane of SH-SY5Y cells induced by aggregated ß-Amyloid (1-40) were not associated with its toxic impact on the cells.

Aggregates of ß-Amyloid (1-40) induce lipid leakage in SH-SY5Y

DPH-release induced by aggregated ß-Amyloid (1-40)

Fluorescence intensity and anisotropy of DPH in the supernatant

Driven by our findings that aggregated ß-Amyloid (1-40) induced calcein-leakage in liposomes, we wanted to determine the membrane-disruptive effect of ß-Amyloid (1-40) aggregates on a cellular level. We hypothesized that aggregated ß-Amyloid (1-40) disrupted the cellular membrane of SH-SY5Y neuronal cells in such way that membrane-embedded components were released into the extracellular medium.

We have shown that we were able to load SH-SY5Y cells with the fluorescent dye DPH. Furthermore, we observed that we are able to track DPH in an aqueous environment if bound to aggregated ß-Amyloid (1-40) by measuring its intensity of fluorescence and its anisotropy. Both parameters increased significantly if DPH was bound to aggregated ß-Amyloid (1-40). Thus, if species of ß-Amyloid (1-40) induced a release of DPH from the inner core of the membrane into the supernatant, DPH could easily be detected if bound to aggregates of ß-Amyloid (1-40) in the supernatant.

To elucidate if ß-Amyloid (1-40) induced the leakage of DPH from the cellular membrane of SH-SY5Y cells into the supernatant, we loaded the cells with DPH as described under Material&Methods and washed them 4 times extensively to remove any non-incorporated free DPH. Then, we added preaggregated ß-Amyloid (1-40) at different concentrations to the cells and incubated for one hour. After harvesting the cells, we retained the supernatant and measured the fluorescence intensity (spectrofluorometer without polarizers) and the anisotropy (spectrofluorometer with polarizers) of DPH in the supernatant. Results are the average of 5 experiments.

In figure 55, the intensity of fluorescence of DPH as function of the applied concentration of aggregates of ß-Amyloid (equivalent monomer concentration) is shown. We observed a linear increase of fluorescence intensity of DPH with increased concentration of aggregated ß-Amyloid (1-40). We assume therefore that aggregated ß-Amyloid (1-40)

induced the release of DPH from the cellular membrane of the cells into the supernatant in a dose-dependent manner.

No such increase of fluorescence was observed with BSA, Poly-L-lysine or monomeric ß-Amyloid (1-40) (data not shown).

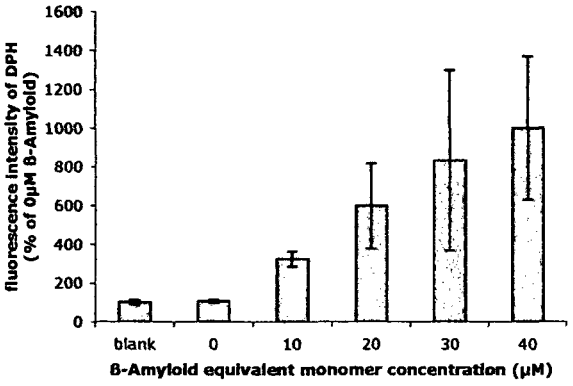

Fig.55: Addition of aggregated ß-Amyloid (1-40) induces an increase of DPH-fluorescence intensity in the supernatant

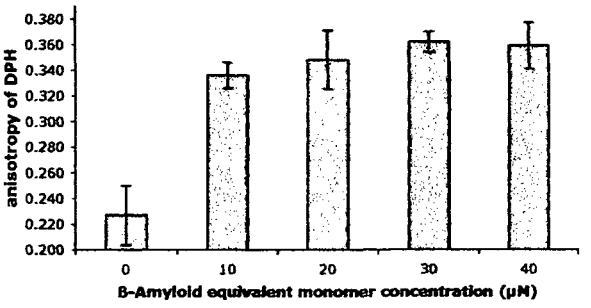

Fig.56: DPH-anisotropy values in the supernatant suggest that DPH is bound to aggregates of ß-Amyloid (1-40)

Figure 56 shows the corresponding anisotropy values of DPH in the retained supernatants. In presence of aggregated ß-Amyloid (1-40), the DPH anisotropy was approximately 0.34. This is further evidence for the presence of DPH in the supernatant associated with aggregated ß-Amyloid (1-40), as we and others (Chauhan et al., 2000) reported a DPH-anisotropy of 0.35 if bound to aggregated, "fibrillar" ß-Amyloid (1-40) in the absence of lipids.

Given these facts, we can assume that addition of aggregated ß-Amyloid (1-40) to DPH-loaded SH-SY5Y cells induced a translocation of DPH from the inner core of the membrane into the extracellular matrix, namely a release of membrane-embedded DPH into the supernatant. As it was unlikely that ß-Amyloid (1-40), if aggregated, offered a more hydrophobic environment to DPH as the cellular membrane itself, we speculate that aggregates of ß-Amyloid (1-40) induced the release of membrane fractions with embedded DPH from the cellular membrane into the supernatant. Then, once in solution, ß-Amyloid (1-40) was in sufficient vicinity to DPH for interaction, leading to an increase in anisotropy of DPH. This hypothesis is strengthened by Michikawa et al. (2001), who have shown that ß-Amyloid promotes lipid-release and that the released lipid-particles are bound to ß-Amyloid.

Remaining fluorescence intensity of DPH in the cellular membrane

To get further confirmation that aggregated ß-Amyloid (1-40) induced leakage of DPH from the membrane into the supernatant we measured the remaining intensity of DPH-fluorescence in the cells fraction. If aggregated ß-Amyloid (1-40) induced a release of DPH from the cellular membrane into the supernatant, a decrease in fluorescence intensity in the cellular membrane fraction should be detected.

Therefore, we retained DPH-loaded and ß-Amyloid (1-40)-treated cells from previous experiments, washed the cells 4 times to remove any membrane-unbound DPH, suspended the cells in PBS, and measured the intensity of fluorescence. Results are the average of 5 experiments.

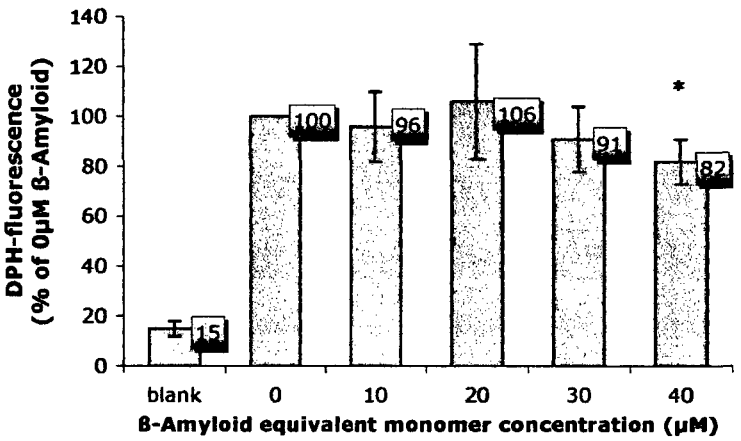

*Fig.57: The fluorescence intensity of DPH in the cell fraction, representing the amount of DPH embedded into the cellular membrane, decreases with increasing concentration of aggregated ß-Amyloid (1-40) (*P<0.01)*

Figure 57 shows the total fluorescence of DPH in SH-SY5Y cells. There was a significant decrease in intensity of DPH-fluorescence in the cellular fraction with increased concentration of aggregated peptide. This observation strengthens our hypothesis that DPH has migrated from the cellular membrane environment into the supernatant.

At 40µM equivalent monomer concentration of ß-Amyloid (1-40), 82% of the initial, fluorescence of untreated cells remained in the cell population, suggesting a loss of approximately 18%. This observation is in line with work of Koudinova and coworkers

(2000), as well of Michikawa and coworkers (2001), who observed ß-Amyloid-induced release of lipids in the same order of magnitude.

No effect of $KLVFFK_6$ on the ß-Amyloid (1-40)-induced DPH-release

The previously observed membrane-disruption by aggregates of ß-Amyloid (1-40) leading to release of DPH is definitely a novel action of ß-Amyloid, which can presumably explain the observed neuronal cell death. Thus, we wanted to answer the question if this ß-Amyloid (1-40)-induced DPH release was associated with the toxic impact on SH-SY5Y cells in our cellular toxicity studies.

Therefore, we added the inhibitor $KLVFFK_6$ to ß-Amyloid (1-40) prior to aggregation (preaggregation at 140µM for 24 hours) to generate non-toxic aggregates. Then, we added these species at an equivalent monomer concentration of 40µM to DPH-loaded SH-SY5Y cells, incubated for one hour, removed the supernatant and measured the remaining fluorescence after extensive washing. The figure 58 shows the average of three experiments.

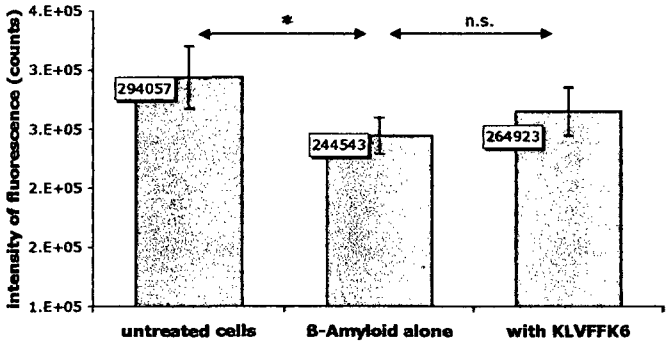

*Fig.58: No effect of the inhibitor $KLVFFK_6$ on the ß-Amyloid (1-40) induced release of DPH (n.s. not significant, *P<0.01)*

As previously, the intensity of the DPH-signal was significantly ($p<0.01$) reduced if aggregated ß-Amyloid (1-40) alone was added to the cells. Adding the inhibitor $KLVFFK_6$ lead to a higher signal, thereby less release of DPH, but the net difference was statistically not significant (see figure 58). Therefore, we assume that the inhibitor $KLVFFK_6$ was not able to circumvent the ß-Amyloid (1-40)-induced release of DPH from the membrane into the supernatant and that the observed lipid leakage as measured

by DPH-release was not the ultimate driving force for ß-Amyloid (1-40)-toxicity in our cell culture studies.

Comparison of DPH-release in SH-SY5Y and GOS-3 cells

To determine if the ß-Amyloid (1-40)-induced release of cellular membrane bound DPH was neurospecific, as we observed DPH-release in SH-SY5Y cells as model for neurons, or independent of the cellular origin, we compared the DPH-release in SH-SY5Y with the effect of aggregated ß-Amyloid (1-40) on DPH-loaded astrocytoma GOS-3 cells.
For this set of experiments, we allowed the cells to adhere on wells of 96-well-plates and to grow to confluence to offer an equal surface for ß-Amyloid (1-40) deposition and thereby avoiding differences in ß-Amyloid (1-40)-exposed cell surface as a result of differences in cell size. After staining with DPH as described in Material&Methods and successive washing, cells were incubated with ß-Amyloid (1-40) aggregates for one hour in PBS, low serum medium (1% FCS), or high serum medium (10% FCS) in a total volume of 200µL per well. Then, an aliquot of 100µL of the supernatant was retained, transferred into an empty well of the 96-well plate, and the fluorescence intensity determined on a fluorescence micro-plate reader. The experiment was repeated twice in triplicates.

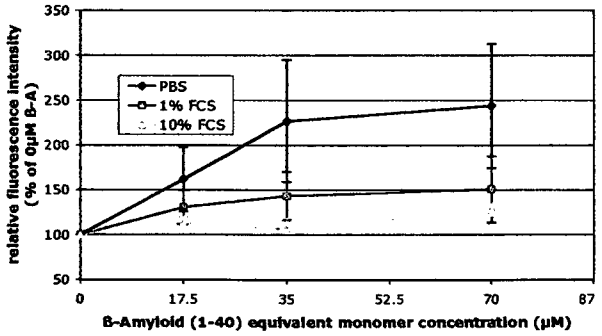

Fig.59: Aggregates of ß-Amyloid (1-40) (pre-aggregation at 140µM) induce DPH-release in adherent SH-SY5Y cells

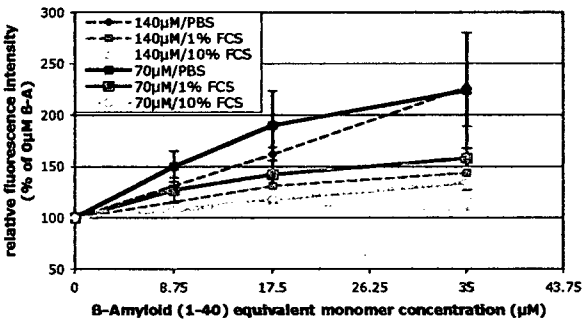

Fig.60: DPH-release by ß-Amyloid (1-40) is increased in SH-SY5 by preaggregating at 70µM instead of 140µM

ß-Amyloid (1-40) preaggregated at 140µM also induced a DPH release in SH-SY5Y cells if allowed to adhere (see figure 59). At an applied equivalent monomer concentration of

35µM ß-Amyloid (1-40), the fluorescence of DPH in the supernatant was approximately 200% of control (ß-Amyloid (1-40)-untreated cells) if ß-Amyloid (1-40) was added in PBS. DPH-release was significantly lower in medium, but still detectable.

Preaggregation of ß-Amyloid (1-40) at 70µM generated more toxic species of ß-Amyloid (1-40). When applying these ß-Amyloid species to adherent SH-SY5Y cells, we observed again a release of DPH into the supernatant (see figure 60, for comparison, DPH-release induced by 140µM preaggregated ß-Amyloid (1-40) is represented in dashed lines.). The difference in DPH-release of ß-Amyloid preaggregated at 140µM and 70µM was not significant at any ß-Amyloid (1-40) concentration or medium condition, but was consistently observed.

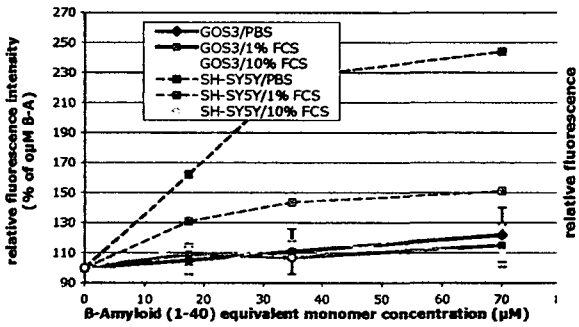

Fig.61: No significant release of DPH by ß-Amyloid (1-40) preaggregated at 140µM in GOS-3 cells

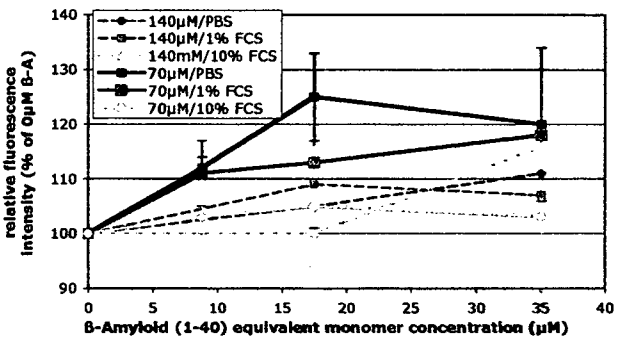

Fig.62: Only marginal release of DPH induced by ß-Amyloid (1-40) preaggregated at 70µM instead of 140µM in GOS-3 cells

Next, we applied same ß-Amyloid (1-40) aggregates (preaggregation at 70µM or 140µM for 24 hours) to GOS-3 cells.

Figure 61 shows that there was no significant release of DPH in GOS-3 cells if incubated with ß-Amyloid (1-40) preaggregated at 140µM. For comparison, data of SH-SY5Y cells are represented in dashed lines. Generating ß-Amyloid (1-40) aggregates, which were more toxic to SH-SY5Y cells (but without affecting cellular viability of GOS-3 cells, see Results/ Toxicity studies), by preaggregating the peptide at 70µM, induced weak DPH-release in GOS-3 cells, significant only at equivalent monomer concentrations above 20µM and only if incubated in PBS (see figure 62).

In summary, these observations let us assume that the ß-Amyloid (1-40)-induced DPH-release is primary a neuro-specific phenomenon.

Fluorescent lipids as probes for cellular membrane lipids

Koudinova and coworkers (2000) showed that a small, but significant amount of lipid material was released into the medium from PC12 cells incubated with ß-Amyloid (1-40). The release of lipids as novel action of the peptide was confirmed by Michikawa et al. (2001), who observed lipid release by oligomeric, but not monomeric or fibrillar ß-Amyloid (1-40). The main components of lipids released were cholesterol, phospholipids, and monosialogangliosides (GM1). Lipid release was approximately 4% in neuron-rich cultures from fetal rat brains and 3% in astrocytes. Driven by these observations and our findings showing low amounts of calcein-leakage in liposomes and release of cellular membrane-embedded DPH induced by aggregated ß-Amyloid (1-40), we wanted to investigate if ß-Amyloid (1-40) aggregated under our conditions was also able to induce lipid-leakage, presumably as cause of membrane disruption. Therefore, we loaded SH-SY5Y and GOS-3 cells with two different fluorescent lipids, added different species of ß-Amyloid (1-40) to the preloaded cells, and quantified after different incubation times the fluorescence intensity in the supernatant originating from released fluorescent lipid, as well as the remaining fluorescence intensity in the cellular fraction.

FITC-DHPE as probe for cellular membrane lipids

As described in Material&Methods, we plated SH-SY5Y cells in 24-well titer plates and let them grow to confluence in 24 hours. Then, we loaded the cells with fluorescein-DHPE as marker for lipid, by letting them sit for 20 minutes at 4°Celsius in the dark. The cells were washed twice to remove unbound lipid before addition of different loads of preaggregated ß-Amyloid (1-40) (preaggregation at pH 7 at 70µM and 140µM) in HBSS or 10% FCS cultivation-medium. After different incubation times, we removed the supernatant and measured its fluorescence.

There was no measurable amount of fluorescence intensity in the supernatant in a equivalent monomer concentration range from 0 to 35µM ß-Amyloid (1-40) preaggregated at 70µM and from 0 to 70µM ß-Amyloid (1-40) preaggregated at 140µM and a time range from one to 5 hours. We therefore concluded that either FITC-DHPE

was not a suitable probe for lipids in our system, that the amount of released lipid was below the detection limit of the fluorometer, or that there was no lipid-release under our chosen conditions. Latter explanation is sustained by work of Michikawa and coworkers (2001), who observed great differences in lipid-release-abilities of ß-Amyloid peptides from different vendors and from different batches of ß-Amyloid from the same supplier.

ß-DPH-HPC as probe for cellular membrane lipids

As described in Material&Methods, we loaded SH-SY5Y and GOS-3 cells with the fluorescent lipid ß-DPH-HPC as marker for membrane lipids, washed twice, and added freshly dissolved (monomeric) or preaggregated (at 140µM aggregation concentration) ß-Amyloid (1-40) at an applied concentration of 17.5, 35 or 70µM in 1% FCS or 10% FCS cultivation medium to the cells. After 5 hours the supernatant from each well was transferred into an empty well and fresh cultivation medium with 10% FCS added to the cells. Then, the DPH-fluorescence was determined in wells containing the retained supernatant and in the wells containing the cell monolayer on a microplate fluorometer. Results from experiments using aggregated ß-Amyloid (1-40) in low serum (1% FCS) medium are the average of three experiments made in triplicates, whereas the experiment using 10% FCS medium was done only once.

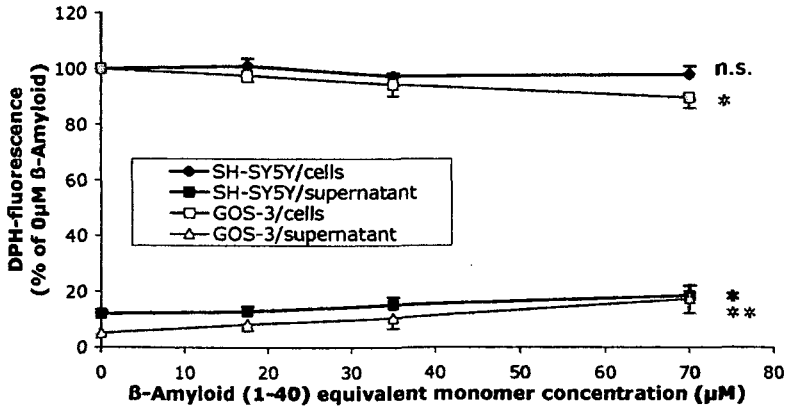

*Fig.63: Aggregates of ß-Amyloid (1-40) induce leakage of ß-DPH HPC in GOS-3, but not in SH-SY5Y cells in low serum medium (n.s. not significant, *P<0.05, **P<0.01)*

Adding monomeric ß-Amyloid (1-40) in low serum medium (1% FCS) or high serum medium (10% FCS), as well as aggregated ß-Amyloid (1-40) diluted in high serum

medium did not induce measurable ß-DPH-HPC leakage in SH-SY5Y or GOS-3 cells into the extracellular medium (data not shown).

By use of low serum medium instead of high serum medium as incubation medium, we were able to observe limited, but significant amount of ß-DPH-HPC in the retained supernatant phase of treated GOS-3 cells in a dose-dependent manner. Also, we observed a dose-dependent decrease in fluorescence intensity of ß-DPH-HPC in the wells containing GOS-3 cells (see figure 63). Prolonged incubation for more than 5 hours did not further alter fluorescence intensities in the supernatant or the cell fraction.

These data convincingly support the hypothesis that ß-Amyloid (1-40), if aggregated and diluted in low serum medium, is able to induce lipid leakage in GOS-3 cells as measured by fluorescence intensity determination of the lipid ß-DPH-HPC as model for cellular membrane lipid.

Data in SH-SY5Y were less evident. As in GOS-3 cells, we observed a slight but significant dose-dependent increase in DPH-fluorescence in the supernatant, whereas we observed only a weak, not statistically significant decrease of DPH-fluorescence in the wells containing the cells (see figure 63). Prolonged incubation of cells with aggregated ß-Amyloid (1-40) was omitted to avoid leakage of ß-DPH-HPC as a result of ß-Amyloid (1-40)-induced cell death and eventual loss of plasma membrane integrity. Therefore, these results suggest a ß-Amyloid (1-40)-induced leakage in the cell line SH-SY5Y as well, but we were not able to prove that aggregated ß-Amyloid (1-40) diluted in low serum medium induced lipid-leakage in SH-SY5Y cells significantly.

In sum, these data are evidence that ß-Amyloid (1-40)-induced lipid-leakage is not restricted to neurons, but can also occur in non-neuronal cells, as for example GOS-3 astrocytes.

Determination of lipid-release with the Stewart-assay

We observed significant ß-Amyloid (1-40)-induced release of membrane-embedded DPH as marker for membrane components and hints for release of ß-DPH-HPC as marker for membrane lipids from the cellular membrane of SH-SY5Y cells into the extracellular

medium, whereas no effect of ß-Amyloid (1-40) was detectable by using DCFH-DHP as probe for membrane lipid. Moreover, ß-DPH-HPC-release induced by the peptide was significant in GOS-3 astrocytes. These observations let us assume that ß-Amyloid-induced lipid release is possibly lipid-specific and depends on the nature of the lipid. Thus, we wanted to determine the total amount of lipid release by ß-Amyloid (1-40) to get an overall estimate of the effect of ß-Amyloid (1-40) on lipid release.

Briefly, we applied ß-Amyloid (1-40) aggregates to SH-SY5Y cells and determined the amount of lipid in the supernatant by means of the Stewart-assay, as it is a reliable method for lipid quantification. Therefore, we plated cells in 6-well plates in 2mL per well and waited 48 hours till cells reached confluence. Then, we added ß-Amyloid (1-40) aggregated at 70µM or 140µM for different amount of times. The supernatant was retained, centrifuged to remove any floating cells, and the amount of lipid quantified as described in Material&Methods.

By means of this assay, we were not able to detect any phospholipid release into the supernatant.

By using POPG to determine the standard-curve, we observed a detection limit of this method in the µg range, corresponding to an order of magnitude of 10^{15} lipid molecules. Assuming a surface area of 20Å (=20.10^{-10} M) for one single lipid in a lipid bilayer, we calculated that the surface of a well of a 6-well plate contained approximately 10^{15} lipids if covered completely with a lipid bilayer. As the cellular membrane contains also a certain amount of proteins, the actual number of lipids exposed to the supernatant containing ß-Amyloid (1-40) was even lower if the whole surface area of the well was covered with cells grown to full confluence. As only this membrane-surface was prone to immediate ß-Amyloid (1-40) membrane-disruption effects with subsequent lipid-leakage, we can assume that a release of for example 10% (the highest percentage of lipid release observed by Chauhan et al., 2000) was below the detection limit of this method and thereby not detectable.

Aggregates of ß-Amyloid (1-40) enhance H_2O_2-induced lipid peroxidation in SH-SY5Y cells

Oxidation of as little as 5% of synaptic membrane lipid can cause a 50% reduction in activity of certain plasma membrane bound enzymes as for example Ca^{2+}-ATPase (Wood et al., 1995). As there is evidence for altered activity of membrane-bound enzymes in Alzheimer disease, researchers have investigated in whether ß-Amyloid is inducing oxidation in the cellular membrane of neurons. Numerous studies have demonstrated increased levels of lipid peroxidation products such as 4-hydroxy-2-nonenal, acrolein, isoprostanes, and neuroprostanes in brain of patients with Alzheimer disease. Interestingly, immunohistochemical and biochemical studies have localized the majority of lipid peroxidation products to neurons (Montine et al., 2002). In hippocampal neurons, ß-Amyloid induced large increases of 4-hydroxynonenal, a product of lipid peroxidation (Mark et al., 1997).

When lipid peroxidation occurs, the fatty acids are peroxidized and break down to malondialdehyde and other aldehydes. They are commonly known as thiobarbituric acid (TBA) reactive substances (TBARS), because they react with TBA to form complexes that are easily detectable on a photometer. Increase of TBARS in Alzheimer disease brain has been frequently reported, but a high level of inconsistency concerning the affected regions is prevalent (Subbarao et al., 1990; Balazs and Leon, 1994; Palmer and Burns, 1994; Lovell et al., 1995; Marcus et al., 1995; Takaoma et al., 2000).

In vitro experiments have shown that ß-Amyloid increases TBARS in synaptosomal membranes (Lauderback et al., 2001). Low concentrations of unsaturated fatty acids as a result of lipid peroxidation have been shown to stimulate uptake of calcium in intestinal brush border membranes (Merrill et al., 1986) and could thereby explain the deregulated calcium homeostasis in ß-Amyloid treated cells. *In vitro* assays nevertheless have also shown that ß-Amyloid can inhibit autooxidation of liposomes prepared of polyunsaturated-fatty acids (Walter et al., 1997). Thus, the question whether lipid-peroxidation is associated with ß-Amyloid-toxicity is still a great matter of debate.

H_2O_2-induced lipid peroxidation in SH-SY5Y and GOS-3 cells

Determination of TBARS in SH-SY5Y has already been achieved successfully (Amoroso et al., 1999; Gao et al., 2001; Gasic-Milenkovic et al., 2003; Chien-Tsai Lai, personal communication; Lee et al., 2000). Prior to examining a putative role of ß-Amyloid (1-40) in lipid peroxidation, we determined the induction of lipid peroxidation by H_2O_2.

Briefly, we added H_2O_2 diluted into low serum medium (1% FCS) to adherent SH-SY5Y and GOS-3 cells grown to confluence in 12-well plates and stimulated the cells for 5 hours. Then, we determined the amount of TBARS as described in Material&Methods. Results are the average of three experiments.

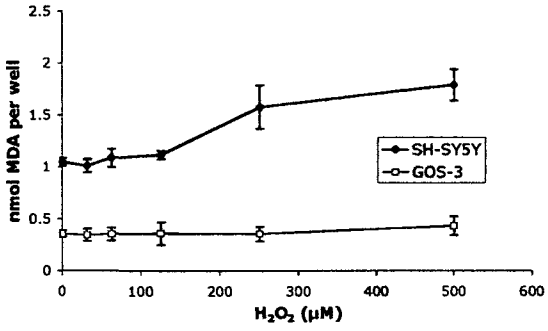

Fig.64: H_2O_2-induced lipid peroxidation in SH-SY5Y and GOS-3 cells

As we see in figure 64, the measured constitutive amount of TBARS was lower in GOS-3 cells than in SH-SY5Y cells: 0.36 nmol/well in GOS-3 cells versus 1.05 nmol/well in SH-SY5Y cells. As the measured values greatly depended on the procedure protocol, which was optimized for SH-SY5Y cells, it is not entirely reasonable to compare these absolute values. During the set up of the protocol, it was evident that differences in cell number, in cell lysis efficiency, and in extraction of MDA greatly influence the obtained values.

Of greater relevance, we observed that GOS-3 cells were less sensitive to H_2O_2-induced lipid peroxidation than SH-SY5Y cells. Whereas incubation with 500µM H_2O_2 for 5 hours induced an increase of TBARS of 70% in SH-SY5Y, the induction in GOS-3 cells was only about 20% and barely significant ($p<0.06$).

The induction of lipid peroxidation in our protocol occurred faster than previously reported. Lee and coworkers (2000) observed an increase in TBARS in SH-SY5Y cells of

50% at 500µM H_2O_2 after 24 hours, whereas we observed a 70% increase after only 5 hours. Determination of lipid peroxidation after more than 5 hours was omitted to avoid any lipid peroxidation induced by secondary oxidation pathways, e.g. release of cell-inherent reactive oxygen species as result of apoptosis-induced reduction of peroxisomal membrane integrity.

ß-Amyloid (1-40) does not induce significantly lipid peroxidation

Lot of research was undergone to determine the role of lipid peroxidation in Alzheimer disease. Evidence of increased lipid peroxidation was found in the brain of Alzheimer disease patients upon autopsy. Moreover, it has been shown that ß-Amyloid induces lipid peroxidation in brain membranes and cultured neurons.

Interestingly, as far as we know, no data was published concerning the effect of ß-Amyloid on lipid peroxidation in the neuronal cell line SH-SY5Y, even though this cell line is an often-used model for neurons in Alzheimer disease research.

To address this question, we generated different species of ß-Amyloid (1-40) (freshly dissolved or preaggregated at 140µM for 24 hours) and added these species at an applied equivalent monomer concentration of 35µM to SH-SY5Y cells as model of neurons grown to confluence in 12-well plates. After 5, 12, and 24 hours, we determined the level of TBARS as described in Material&Methods. Furthermore, we applied same aggregates to GOS-3 cells, as model for astrocytes, to determine if ß-Amyloid (1-40)-induced lipid peroxidation occurs in glial-like cells as well. Results are the average of three experiments.

Addition of ß-Amyloid aggregates to GOS-3 cells did not alter the amount of measured TBARS (see figure 65). In SH-SY5Y cells, we observed a slight increase in TBARS from 1.11nmol MDA/well at the initial time point t=0h to 1.24nmol MDA/well after 12 hours. After 24 hours, the amount of TBARS decreased again to 1.20 nmol MDA/well. This ß-Amyloid (1-40)-induced increase in TBARS was statistically barely significant ($p<0.05$ when comparing time points t=0h with time point t=12h). Addition of freshly dissolved ß-Amyloid (1-40) did not alter the amount of TBARS in SH-SY5Y or GOS-3 cells (data not shown).

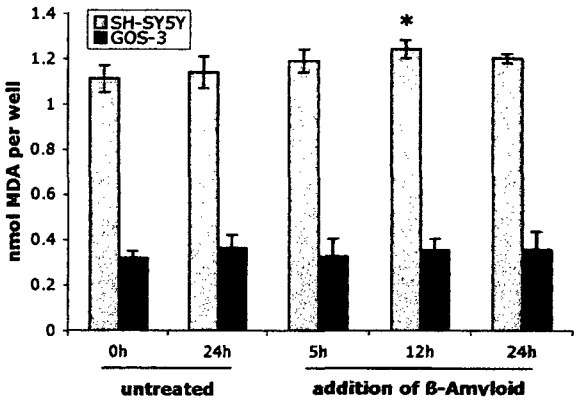

*Fig.65: ß-Amyloid (1-40) aggregates induce lipid peroxidation in SH-SY5Y, but not in GOS-3 cells (*P<0.05)*

Aggregates of ß-Amyloid (1-40) enhance H_2O_2-induced lipid peroxidation in SH-SY5Y

The brain of elderly is under constant oxidative stress. This is even more evident in brains of patients with Alzheimer disease, where extensive burst of oxidative stress has been observed several times *post mortem*. Furthermore, it has been observed that ß-Amyloid induces lipid peroxidation in cultured neurons.

We observed that ß-Amyloid (1-40) itself did only marginally induce lipid peroxidation in the neuron-like cell line SH-SY5Y. Therefore, we addressed the question whether an oxidative environment could enhance ß-Amyloid (1-40)-induced lipid peroxidation.

Therefore, we let ß-Amyloid (1-40) aggregate for 24 hours at 140µM to generate toxic species. Then, we added aliquots of the solution containing these species to low serum (1% FCS) medium with 500µM H_2O_2 to obtain ß-Amyloid (1-40)/H_2O_2 mixtures with a ß-Amyloid (1-40) equivalent monomer concentration of 35µM and a H_2O_2 concentration of 375µM. The samples were shaken briefly and directly afterwards added to confluent SH-SY5Y cells grown in 12-well plates. Thereby, the cells were incubated with ß-Amyloid (1-40) aggregates in a highly oxidative environment. For comparison, cells were incubated in the equivalent medium (low serum medium with 25% total volume PBS-buffer containing 0.4 N urea) alone, equivalent medium with H_2O_2 at 375µM, or equivalent medium with same ß-Amyloid (1-40) aggregates at same equivalent monomer concentration of 35µM. After 5 hours, the amount of TBARS was determined as before.

Results are the average of three experiments. Comparable experiments in GOS-3 cells were omitted due to financial constraints.

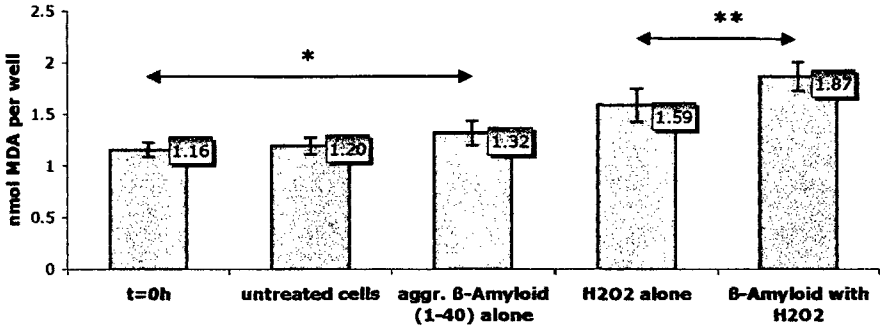

*Fig.66: Aggregated ßAmyloid (1-40) potentiates H_2O_2-induced lipid peroxidation in SH-SY5Y cells (*P<0.05, **P<0.01)*

As before, we observed that aggregated ß-Amyloid (1-40) alone at 35µM equivalent monomer concentration induced after 5 hours a slight, barely significant ($p<0.05$) increase in TBARS from 1.16 to 1.32nmol MDA per well. Furthermore, we observed that the addition of ß-Amyloid (1-40) aggregates increased the H_2O_2-induced lipid-peroxidation significantly from 1.59 to 1.87nmol MDA/well (see figure 66).

These results let us assume that ß-Amyloid (1-40) itself was barely affecting lipid peroxidation in a redox-neutral environment, whereas it induced circumstantially lipid peroxidation in an environment mimicking oxidative stress.

One possible explanation is that the aggregated ß-Amyloid peptide is able to induce lipid peroxidation only to damaged cells. This would explain why the observed lipid peroxidation induced by ß-Amyloid (1-40) alone was measurable only after few hours and significantly different from untreated cells only after 12 hours.

We also speculated if H_2O_2 oxidized ß–Amyloid (1-40) and generated thereby modified peptide(s) that were more prone to oxidize lipids of the cellular membrane of the SH-SY5Y cells than unaltered ß-Amyloid (1-40) peptides. To get proof or not for this assumption, we added freshly dissolved ß-Amyloid (1-40) to H_2O_2, mixed the solution, vortexed briefly, and added this mixture to the cells at same concentrations as before. No increase in TBARS was thereby detectable in comparison to cells treated with H_2O_2 alone (data not shown). This gave evidence that unaltered (non-oxidized) ß-Amyloid (1-40) was the lipid peroxidation-inducing moiety rather than H_2O_2-modified ß-Amyloid (1-40) peptides.

Pretreatment with ß-Amyloid (1-40) aggregates increases H_2O_2-induced lipid peroxidation

It has been shown that pretreatment of cells with sub-lethal concentrations of ß-Amyloid circumvents ß-Amyloid-induced toxicity, which is possibly mediated through lipid peroxidation. Based on these findings, we questioned whether pretreatment with ß-Amyloid (1-40) had any effect on H_2O_2-induced lipid peroxidation. This should allow us to get new insights into the role of lipid peroxidation in ß-Amyloid-induced toxicity in neurons.

Therefore, we plated SH-SY5Y cells in 12-well plates and after 24 hours, we added monomeric or preaggregated (at 140µM for 24 hours) ß-Amyloid (1-40) at a sub-lethal concentration of 17.5µM to the cells. 24 hours later the supernatant was discarded and the cells washed twice with low serum medium to remove free, unbound ß-Amyloid (1-40) quantitatively. Then, H_2O_2 diluted in low serum (1% FCS) medium was added to the cells and lipid peroxidation determined after 5 hours as before. Results are the average of three experiments.

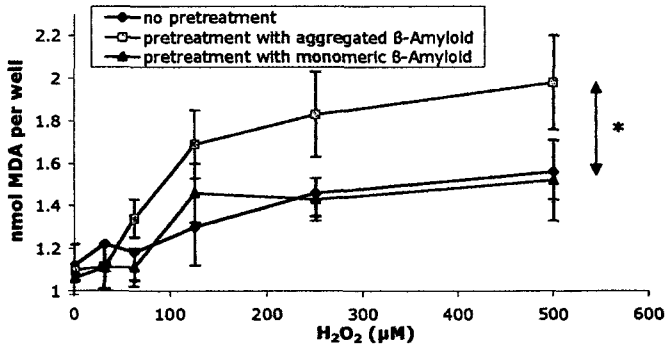

*Fig.67: Aggregated ß-Amyloid (1-40) pretreatment strongly increases H_2O_2-induced lipid peroxidation (*P<0.01)*

We observed that pretreatment of SH-SY5Y cells with freshly dissolved, monomeric ß-Amyloid (1-40) for 24 hours had virtually no effect on H_2O_2-induced lipid peroxidation, whereas pretreatment with toxic aggregates of ß-Amyloid (1-40) at sub-lethal concentration of 17.5µM for 24 hours induced a strong increase in H_2O_2-induced lipid peroxidation. At 500µM H_2O_2, ß-Amyloid (1-40) pretreatment induced a significant increase in TBARS from 1.55nmol MDA/well to approximately 2nmol MDA/well.

ß-Amyloid (1-40) circumvents H_2O_2-induced increase of oxidative stress

The question if and to what extent Alzheimer disease is linked to oxidative stress is still heavily debated. Increased oxidation of lipid and protein is detected in Alzheimer disease brain, but does also occur in other neurodegenerative dementia, as well as during aging (for references, see Introduction). If the level in oxidative burst is increased in Alzheimer disease compared to healthy elderly is not yet clear. Excessive oxidative stress could be a cause of increased burden of ß-Amyloid in the brain of patients with Alzheimer disease and thereby contribute to the onset and/or progression of the disease.

In vitro experiments have shown that ß-Amyloid toxicity to rat hippocampal neurons involves the induction of reactive oxygen species (Behl et al., 1994; Mattson and Goodman, 1995). The authors report increased free radical generation by measuring the neuronal DCF fluorescence. Oxidative stress and toxicity were circumvented by antioxidants. In contrast, other groups did observe contradictory results when adding ß-Amyloid and antioxidants, e.g. reduction of oxidative stress, but no inhibition of ß-Amyloid toxicity, or no effect of ß-Amyloid on oxidative stress at all (Lockhart et al., 1994; Pike et al, 1997; Yao et al., 1999).

Whether the ß-Amyloid-induced toxicity in the human neuronal cell line SH-SY5Y involves an elevated level of reactive oxygen species is still unknown.

Induction of oxidative stress by H_2O_2 in SH-SY5Y and GOS-3 cells

Prior to determine the effect of extracellularly added ß-Amyloid (1-40) on the level of intracellular reactive oxygen species (iROS), we characterized the response of SH-SY5Y and GOS-3 cells to H_2O_2.

Therefore we let SH-SY5Y and GOS-3 cells in 96-well plates grow to confluence, stained the cells with DCFH-DA, and added cultivation medium with 10% FCS with different amounts of H_2O_2 to the cells. At different time points, the 96-well plates were removed from the incubator, the DCF fluorescence as marker for iROS measured on a fluorescence micro-plate reader, and the cells incubated again. Thereby we were able to measure a "time-scan" of the level of iROS. Results are the average of 5 experiments.

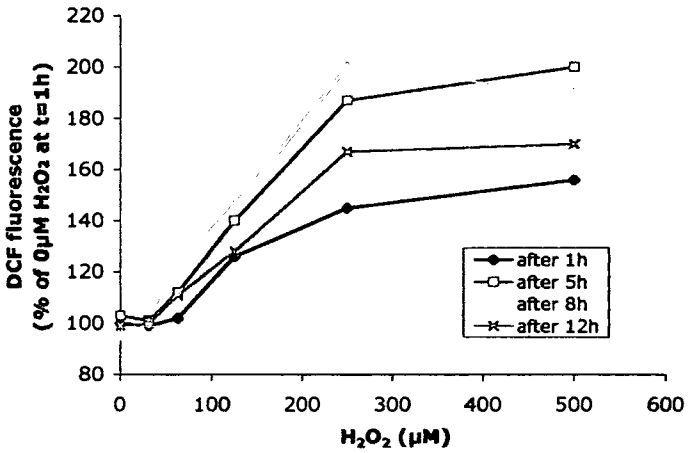

Fig.68: H_2O_2-induced increase in iROS in SH-SY5Y cells

DCF fluorescence of untreated cells did not change with time, showing that photobleaching or intracellular degradation of DCF did not occur during the time course of 12 hours.

Addition of H_2O_2 to SH-SY5Y cells induced an increase of the level of iROS in a dose-dependent manner (see figure 68). This is not surprisingly, as H_2O_2 by itself is one of the most potent oxidants that are biologically relevant and as it can diffuse through lipid bilayers. Maximal DCF fluorescence of approximately 200% of initial DCF fluorescence was observed after 8 hours of incubation with 500µM H_2O_2. 4 hour later (time point t=12h), the level decreased again. We assume that this decrease in DCF fluorescence was associated with a decrease in cellular viability and assume that DCF was thus degraded intracellularly, as there was no detectable fluorescence in the supernatant.

Using low serum medium (1% FCS) instead of 10% FCS medium did not alter the H_2O_2-induced increase of iROS significantly (data not shown).

Addition of H_2O_2 also induced an increase in iROS in GOS-3 cells, but to a lower extent (see figure 69). For comparison, data from SH-SY5Y cells are represented in dashed lines. Maximal DCF-fluorescence induction to approximately 170% of untreated cells was observed after 8 hours at an applied concentration of 500µM H_2O_2 (in comparison to 200% in SH-SY5Y cells). Assuming that there was no difference in diffusion of H_2O_2 through the cellular membranes of SH-SY5Y or GOS-3 cells, the results suggest that GOS-3 cells are equipped with a higher antioxidative capacity intracellularly. This is in agreement with the astrocytoma-like origin of GOS-3 cells. Astrocytes actively take part

in the degradation of foreign biological material, partially by the generation, peroxisomal storage, and eventual release of excessive reactive oxygen species.

The intensity of DCF-fluorescence decreased in GOS-3 cells after 12 hours only slightly in comparison to SH-SY5Y cells, strengthening the hypothesis that the significant decrease of DCF fluorescence observed in the cell line SH-SY5Y at the time point of t=12 hours is associated with a decrease in cellular viability.

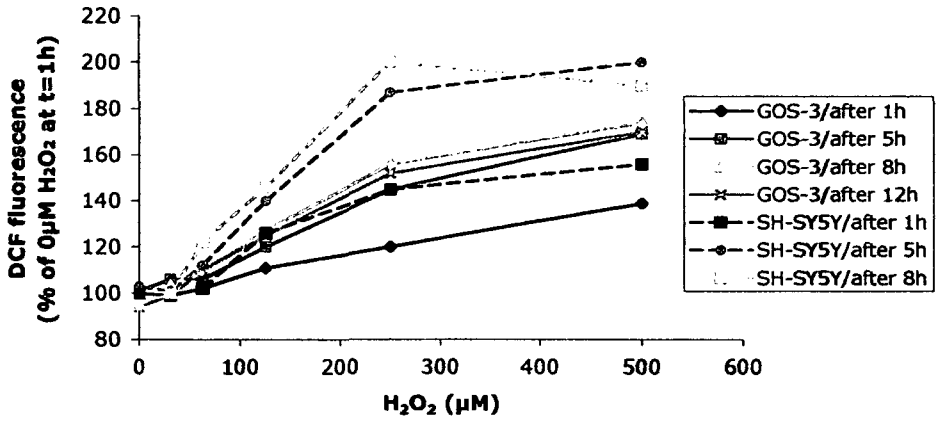

Fig.69: H_2O_2-induced increase in accumulation of iROS in GOS-3

ß-Amyloid (1-40) reduces the level of iROS in SH-SY5Y cells

Interestingly, no data so far is available if ß-Amyloid induces oxidative stress in SH-SY5Y cells, even though this cell line is very popular in ß-Amyloid research. To elucidate a possible induction of oxidative stress, we applied monomeric (freshly dissolved) or aggregated (preaggregation at 140µM for 24 hours for generation of toxic aggregates) ß-Amyloid (1-40) at different concentrations in low serum medium (1% FCS) without Phenol Red to SH-SY5Y cells for 5 hours. Then, the fluorescence of DCF was measured on a micro-plate reader.

Furthermore, we compared two protocols: 1) staining with DCFH prior to ß-Amyloid (1-40) treatment, and 2) ß-Amyloid (1-40) treatment prior to DCFH-staining. Results are the average of three experiments.

ß-Amyloid treatment with either freshly dissolved, monomeric ß-Amyloid (1-40) or preaggregated ß-Amyloid (1-40) did not alter DCF fluorescence if the cells were stained

prior to ß-Amyloid (1-40) treatment (see figure 70), suggesting *a priori* that ß-Amyloid (1-40) did not alter the level of iROS and thereby the level of oxidative stress in SH-SY5Y cells.

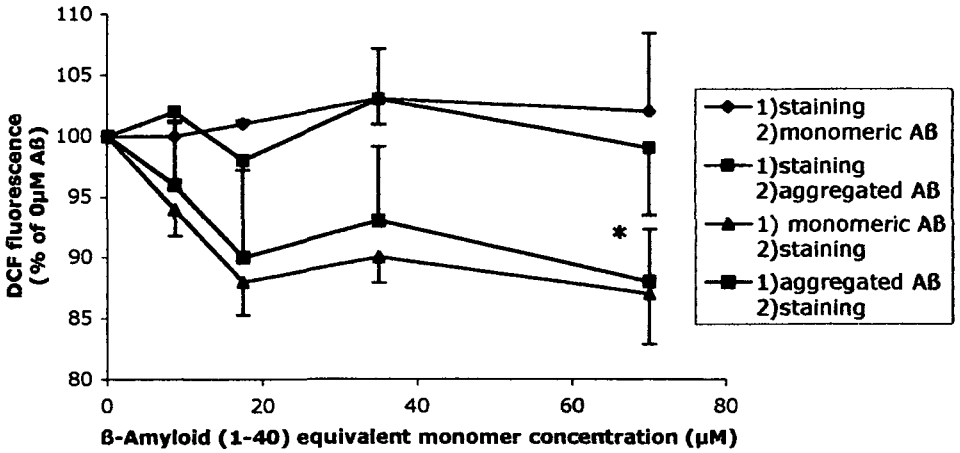

*Fig.70: Addition of monomeric or aggregated ß-Amyloid (1-40) reduces level of iROS in SH-SY5Y cells in low serum medium (*P<0.01)*

Interestingly, DCF-fluorescence intensity was noticeably reduced if cells were treated with ß-Amyloid (1-40) for 5 hours before DCFH-staining, independently of the aggregation state of the peptide. At 70µM equivalent monomer concentration of ß-Amyloid (1-40), DCF fluorescence was reduced of approximately 12% to untreated cells. These data suggest that ß-Amyloid (1-40) is able to induce a shift towards an anti-oxidative level. We assume that the pretreatment with ß-Amyloid (1-40) prior to staining with DCFH-DA reduces the amount of iROS and thereby the amount of agents that can oxidize DCFH to DCF.

Prolonged pretreatment with ß-Amyloid (1-40) did not further reduce level of iROS (data not shown).

We repeated these experiments in the GOS-3 cell line. ß-Amyloid (1-40) treatment of GOS-3 for 5 hours did not affect the level of iROS, suggesting that ß-Amyloid (1-40)-induced decrease in iROS is neuron-specific.

ß-Amyloid (1-40) pretreatment circumvents H_2O_2-induced increase of oxidative stress

As previous results suggest a certain anti-oxidative capacity of ß-Amyloid (1-40) by reducing the amount of iROS, we questioned whether ß-Amyloid (1-40) pretreatment was able to circumvent an increase of iROS induced by H_2O_2. Therefore, we pretreated SH-SY5Y cells with 17.5µM of ß-Amyloid (1-40) in low serum (1% FCS) medium without Phenol Red for 5 hours. Then we removed the supernatant and added H_2O_2 at different concentrations in low serum medium without Phenol Red for one or 8 hours. The cells were then stained with DCFH-DA and the DCF-fluorescence was then measured. Results are the average of two experiments made in 5 replicates.

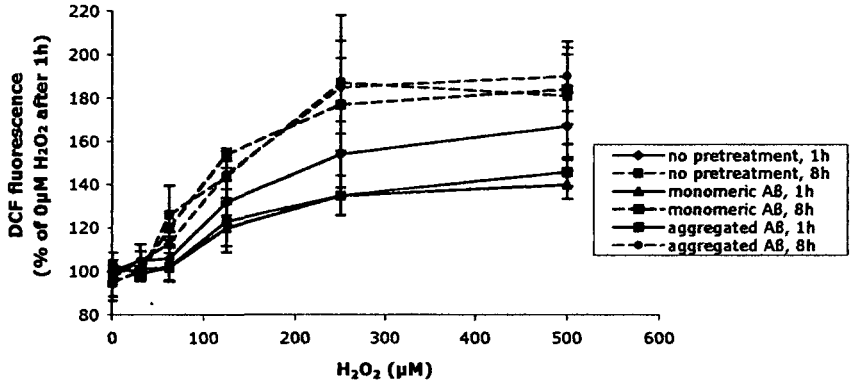

Fig.71: Pretreatment with ß-Amyloid (1-40) circumvents H_2O_2-induced accumulation of iROS in SH-SY5Y after one hour, but not after 8 hours

Pretreatment with either monomeric or aggregated ß-Amyloid (1-40) for 5 hours at a sub-lethal concentration of 17.5µM equivalent monomer concentration circumvented the H_2O_2-induced increase of iROS after one hour partially (see figure 71). Whereas H_2O_2-stimulation alone induced an increase of iROS of more than 60%, ß-Amyloid (1-40) pretreatment reduced this increase of iROS to approximately 40%. This circumvention was independent of the aggregation state of ß-Amyloid (1-40).

Prolonged incubation with H_2O_2 for 8 hours abolished this effect completely (see figure 71). There was no significant difference in DCF-fluorescence in ß-Amyloid (1-40) pretreated and ß-Amyloid (1-40) untreated cells if subsequently incubated with H_2O_2 for 8 hours.

Aggregated ß-Amyloid (1-40) induces Nuclear Factor-κB activation in SH-SY5Y cells

It was shown several times that ß-Amyloid activates the transcription factor Nuclear Factor-κB (NFκB) and NFκB-dependent pathways in microglia (Bonaiuto et al., 1997). Combs and coworkers (2001) stimulated microglia with ß-Amyloid and observed NFκB-dependent expression of inducible nitric oxide synthase (iNOS) and subsequent peroxynitrite production, leading to neuronal apoptosis.

More evidence for a role of NFκB in Alzheimer disease and the involvement of oxidative stress comes from Kaltschmidt and coworkers (1997), who observed that pro-oxidants, as well as ß-Amyloid, stimulate NFκB activity in primary neurons, as well as from the detection of nuclear translocation of NFκB in *post mortem* brains of Alzheimer disease patients (Kaltschmidt, 1997) and ß-Amyloid-resistent PC12 cells (Lezoualc'h et al., 1998).

Constitutive level of Nuclear Factor-κB activity in SH-SY5Y cells

Prior to determine if ß-Amyloid (1-40) induces an activation of NFκB, we determined the constitutive level of NFκB-activity in untreated SH-SY5Y-cells.

Therefore, cells were stained as described in Material&Methods and the fluorescence compared to the isotype-control, which quantifies the unspecific binding of the primary antibody. To compare fluorescence values, acquisition time was determined for NFκB-specific staining and was set constant for the measurement of the isotype control.

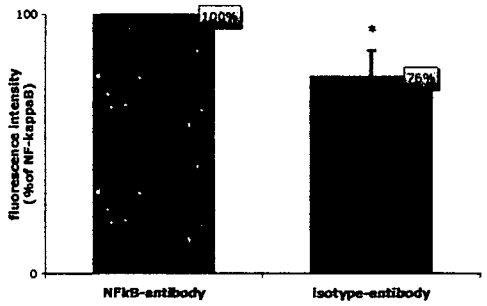

*Fig.72: Constitutive activity of NFκB in SH-SY5Y cells is detectable by immunofluorescence (*P<0.001)*

Figure 72 shows the relative intensity of fluorescence of the unspecific binding of antibody (isotype-antibody) compared to the specific binding of the antibody (NFκB-antibody). Inserts show images of one representative experiment.

As we can clearly see, the fluorescence intensity originating from the NFκB-specific antibody was stronger than the fluorescence intensity of the isotype control, which provides information about the unspecific binding of the NFκB-specific antibody.

This proves that there was a constitutive level of activated NFκB in SH-SY5Y cells, but only at low level, as the unspecific binding was only 24% lower than the NFκB-specific signal. A low but detectable level of constitutively expressed NFκB in SH-SY5Y cells was also observed by Bui and coworkers (2001).

Aggregated ß-Amyloid (1-40) induces NFκB-activation in SH-SY5Y

As we have observed that ß-Amyloid (1-40) has pro-oxidative capacities by inducing lipid peroxidation in an oxidative environment, as well as anti-oxidative capabilities by reducing the amount of intracellular reactive oxygen species in SH-SY5Y cells, we addressed the question whether and to what extent ß-Amyloid (1-40) activates the NFκB signalling pathway.

Briefly, SY-5Y cells were incubated with different amounts of preaggregated ß-Amyloid (1-40) at 140µM for 24 hours to generate toxic ß-Amyloid (1-40) species. After different time points, NFκB activation was determined by immunofluorometry. Results are the average of 5 experiments.

We observed that a treatment with aggregated ß-Amyloid (1-40) at low, subtoxic equivalent monomer concentration of 1µM significantly induced NFκB-activation in SH-SY5Y cells (see figures 74 and 75: images of untreated versus treated cells from one representative experiment). Maximal NFκB-activation was observed after one hour, then the NFκB-activity decreased again to base level after 21 hours (see figure 73). This inverted U-shaped dose response for activation of NFκB induced by aggregated ß-Amyloid (1-40) confirms data of Kaltschmidt and coworkers (1999) who also observed such dose-relationship.

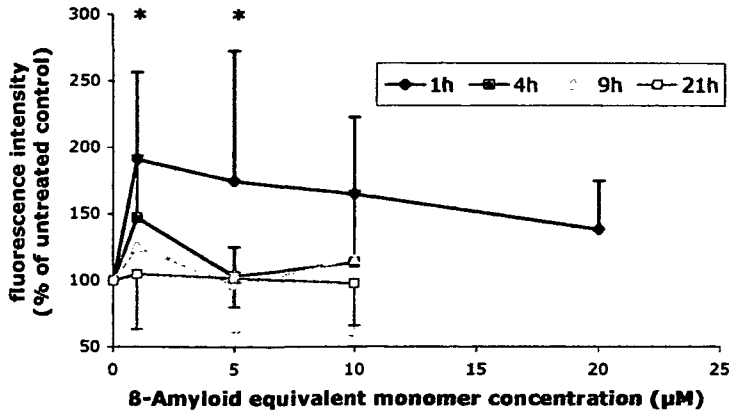

*Fig.73: Aggregates of ß-Amyloid (1-40) induce rapid activation of NFκB at low, subtoxic concentration in SH-SY5Y cells (*P<0.01)*

Fig.74: NFκB-activity in ß-Amyloid (1-40)-untreated SH-SY5Y cells

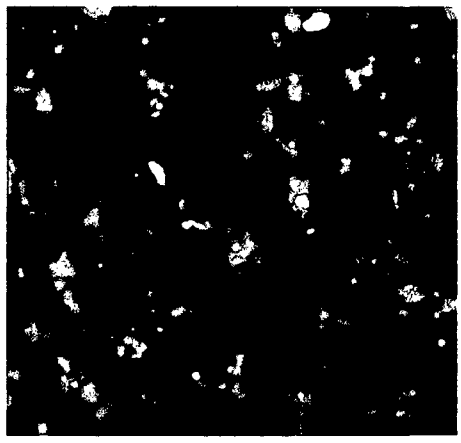

Fig.75: NFκB-activity in ß-Amyloid (1-40)-treated cells (at 1µM for one hour)

Increasing the ß-Amyloid (1-40) concentration to toxic levels continued to induce NFκB-activation, but to a lower degree. Again, maximal NFκB-activation was achieved after one hour, demonstrating again fast NFκB-response of SH-SY5Y cells to ß-Amyloid (1-40) stimulation.

The fact that we observed a reduced NFκB-activation at higher concentrations of ß-Amyloid (1-40) argues against a NFκB-activation triggered by ß-Amyloid (1-40) binding to a specific receptor as RAGE, which has been shown to activate NFκB (Huttunen et al., 1999), as we would anticipate in such case a dose-dependent activation, but not the observed inverted U-shaped dose response.

No effect of the inhibitor KLVFFK$_6$ on the ß-Amyloid (1-40)-induced activation of NFκB

Next step was to determine if the inhibitor KLVFFK$_6$ was able to alter ß-Amyloid (1-40)-induced activation of NFκB in order to elucidate the role of NFκB-activation in ß-Amyloid (1-40)-induced toxicity and the neuronal response to such an insult.

Therefore, we preaggregated ß-Amyloid (1-40) at 140µM for 24 hours alone (to generate toxic species) or in the presence of the inhibitor KLVFFK$_6$ (to generate non-toxic species) and applied these aggregates to SH-SY5Y cells at an equivalent monomer concentration of 1µM. After one hour, NFκB-activity was determined as before.

Furthermore, we compared the activation of NFκB by the ß-Amyloid (1-40)-treatment to the activation of NFκB by oxidative stress-inducing hydrogen peroxide. A concentration of 100µM H_2O_2 was chosen as this concentration induced oxidative stress (see Results/ Induction of oxidative stress by H_2O_2 in SH-SY5Y and GOS-3 cells), but did not affect cellular viability quantitatively (see Results/ H_2O_2-induced toxicity in SH-SY5Y cells). Results are the average of three experiments made in three replicates.

As before, toxic aggregates of ß-Amyloid (1-40) induced significantly activation of NFκB (see figure 76). Presence of the inhibitor KLVFFK$_6$ did not alter the ß-Amyloid-induced activation of NFκB significantly.

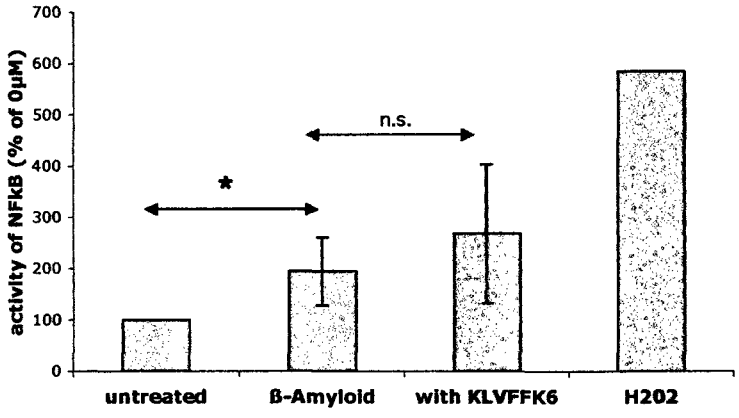

*Fig.76: The inhibitor KLVFFK$_6$ does not alter the ß-Amyloid (1-40)-induced activation of NFκB significantly (n.s. not significant, *P<0.01)*

Overall, the net activation of NFκB by toxic ß-Amyloid (1-40) was relatively minor compared to the H_2O_2-induced NFκB-activation.

Oxidative stress induces the release of ß-Amyloid (1-42) in SH-SY5Y and GOS-3 cells

The ß-Amyloid precursor protein (APP) is constitutively expressed in Alzheimer disease patients as well as in healthy individuals. It is believed that cleavage of APP leads to the net production, and possibly also to release of ß-Amyloid into the extracellular fluid. Detectable levels of ß-Amyloid are found in the cerebrospinal fluid (CSF), as well as in blood plasma.

The "Amyloid Cascade Hypothesis" postulates an increased burden of ß-Amyloid in the brain of Alzheimer disease patients, leading to ß-Amyloid aggregation and ultimately to ß-Amyloid-induced neuronal cell death. Interestingly, the level of ß-Amyloid (1-42) in the CSF is negatively correlated to the degree of cognitive function and provides thereby a prognostic tool for Alzheimer disease diagnosis, even though its use is relatively limited and only relevant if used in combination with other markers, e.g. level of hyperphosphorylated Tau-protein in the CSF.

Increased amount of ß-Amyloid reflected by accelerated deposition and decreased concentration of ß-Amyloid in the CSF are not necessarily contradictory observations: One can explain low levels of ß-Amyloid in the CSF and increased deposition of ß-Amyloid in the brains of Alzheimer disease patients by postulating that increased levels of ß-Amyloid in the brain of Alzheimer disease patients lead to accumulation of ß-Amyloid in certain, to date unknown compartments and reach thereby a threshold for aggregation and deposition, reflected by a reduction of free, soluble ß-Amyloid in the CSF.

So far the origin of increased ß-Amyloid production is unknown. Reports have shown that ß-Amyloid-related peptides are normally secreted by cultured cells (Haass et al., 1992; Seubert et al., 1992; Shoji et al., 1992). Recently, it has been shown that oxidative stress induces an increase of detectable intracellular ß-Amyloid (1-42) in the neuronal cell line SH-SY5Y (Misonou et al., 2000). We therefore investigated if oxidative stress in SH-SY5Y as model for neurons also induced a release of possibly intracellularly accumulated ß-Amyloid (1-42), giving new insights concerning the origin of excessive ß-Amyloid in the brain of Alzheimer disease patients.

Briefly, SH-SY5Y cells were plated in 24-well plates at 1E6 cells/mL. After 48 hours, cells reached confluence. Then, the cultivation medium was removed and fresh, low FCS medium (1% FCS) with different concentrations of H_2O_2 was added to the cells. After different times, the supernatant was retained. Floating cells and cell fragments were removed by centrifugation at 2500G for 10 minutes. The supernatant was then stored at -20°C till measurement for not longer than one week. The concentration of ß-Amyloid (1-42) in the supernatant was determined by a "solid-phase"-ELISA-assay as described under Material&Methods. Results are the average of 4 experiments in triplicates.

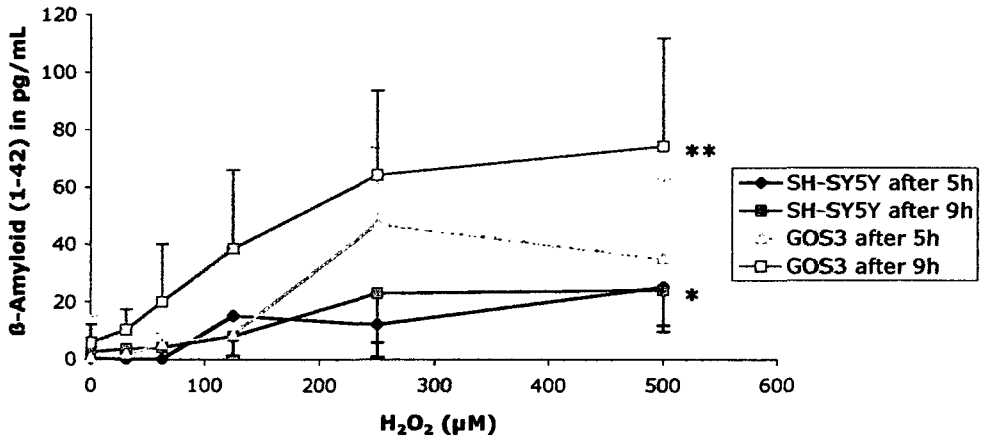

*Fig.77: Generation of oxidative stress by adding H_2O_2 induces the release of ß-Amyloid (1-42) in SH-SY5Y and GOS-3 cells in a dose-dependent manner into the supernatant (*P<0.05, **P<0.01)*

In our system, untreated SH-SY5Y and GOS-3 cells did not release ß-Amyloid (1-42) significantly into the supernatant. After 9 hours cell cultivation, only 2.5pg/mL and 5.8pg/mL released ß-Amyloid (1-42) was measured in SH-SY5Y cells, respectively in GOS-3 cells. These values are below our estimated detection limit of the ELISA-system. Induction of oxidative stress by adding H_2O_2 to low serum medium induced a significant dose-dependent release of ß-Amyloid (1-42) into the extracellular fluid in both cell lines. In SH-SY5Y cells, the H_2O_2-induced release of ß-Amyloid (1-42) was barely significant ($p<0.05$), as the measured ß-Amyloid(1-42) release is of 20pg/mL and thereby in the range of the detection limit of the assay of 20pg ß-Amyloid (1-42)/mL. This H_2O_2-induced increase in ß-Amyloid (1-42) release is in line with work from Olivieri and coworkers (2001), who observed release of ß-Amyloid (1-40), as well as to a lesser extent

release of ß-Amyloid (1-42) in SH-SY5Y cells into the extracellular medium by stimulation with 50µM or 200µM H_2O_2 for 30 minutes or with UV-light irradiation.
In comparison to SH-SY5Y cells, there was a significantly increased concentration of ß-Amyloid (1-42) in the supernatant released from stimulated GOS-3 cells (500µM H_2O_2 for 9 hours) in comparison to untreated cells (0µM H_2O_2).
These results give hint that oxidative stress is one possible origin of increased net production of ß-Amyloid (1-42). Moreover we observed quantitative ß-Amyloid (1-42)-release in an astrocytoma cell line, as well as limited ß-Amyloid (1-42)-release in a neuronal cell line. This lets us assume that a great variety of cells are potential candidates for ß-Amyloid (1-42) release if submitted to oxidative stress.
This is even more important, as it has been shown that ß-Amyloid is inducing epithelial cell monolayer permeability (Blanc et al., 1997) and that ß-Amyloid is thereby supposed to be able to cross the blood-brain-barrier.

Ex vivo addition of H_2O_2 to whole blood induces the release of ß-Amyloid (1-42)

Detectable levels of ß-Amyloid are not only found in the brains and the CSF of Alzheimer disease patients, but also in the CSF of healthy people. Moreover, it is detectable in blood plasma (Seubert et al., 1992).
Driven by our previous findings that oxidative stress induced the release of ß-Amyloid (1-42) in the neuroblastoma cell line SH-SY5Y and in the astroglioma cell line GOS-3, we addressed the question whether *ex vivo* oxidative stress in whole blood, as a model system for *in vivo* conditions in humans, also induced a quantitative release of ß-Amyloid (1-42) from blood cells into the extracellular fluid. We assumed that addition of 250µM H_2O_2 to whole blood was sufficient to generate oxidative stress.
Briefly, we added 250µM H_2O_2 to fresh whole blood collected in EDTA blood tubes and incubated the samples for 5 hours at 37°C. Then, the blood tubes were centrifuged (3000 rpm for 15 minutes on a bench centrifuge) in order to separate the plasma from the cellular material. The retained plasma was then stored at -20°C for not longer than one

month. The concentration of ß-Amyloid (1-42) in the plasma was determined as described under Material&Methods by means of a solid-phase ELISA-assay. Samples were measured in triplicates.

Fresh blood was collected from 10 randomly selected individuals, who were not obviously afflicted by Alzheimer disease. Gender distribution was equal (5 male, 5 female). The average age was 55 +/-17 years. Three individuals were diagnosed with diabetes mellitus, three other individuals with different types of malignant tumors.

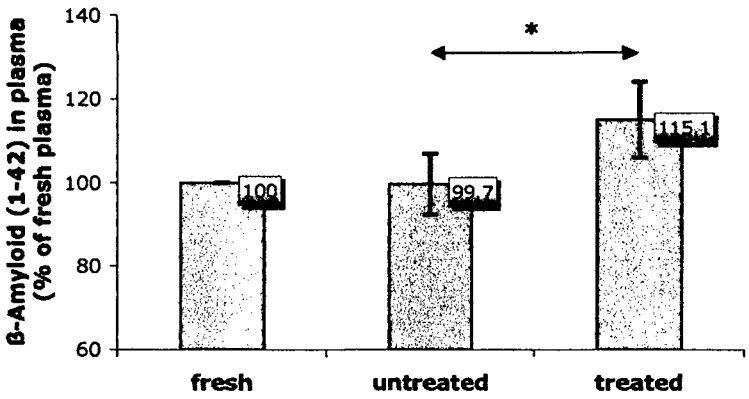

*Fig.78: Ex vivo addition of 250µM H_2O_2 to whole blood induces an increase of detectable soluble, free ß-Amyloid (1-42) in the plasma (*P<0.01)*

Average plasma concentration of ß-Amyloid (1-42) in the total population was 42.3pg/mL (±21.1pg/mL). These values are in agreement with data of Hong and coworkers (2001) who measured ß-Amyloid (1-42) plasma concentration of 21.24pg/mL (±10pg/mL) in patients afflicted with Alzheimer disease and of 16.03pg/mL (±7.25pg/mL) in healthy individuals.

As we can see in figure 78, there was a significant ($p<0.01$) increase in detectable, soluble ß-Amyloid (1-42) in the plasma of approximately 15% if whole blood was submitted to 250µM H_2O_2 for 5 hours in comparison to untreated control samples. In 7 out of the total population of 10 individuals, there was a net increase of more than 13% in the amount of detectable, free ß-Amyloid (1-42) in the plasma. In one individual, the plasma-level of ß-Amyloid (1-42) was virtually identical in treated and untreated blood. Data analysis did not reveal any correlation between ß-Amyloid (1-42)-induction and gender or specific disease.

DISCUSSION

Is ß-Amyloid the key element of Alzheimer disease?

Since 1906, the year Alois Alzheimer discovered extracellular deposits in the brains of several deceased patients with neurodementia, researchers have put strong effort in elucidating causes of and preventive actions against this disease known today as Alzheimer disease (or DAT, dementia of the Alzheimer's type).

To date a multitude of different approaches have been pursued in order to get new insights into this still incurable neurodementia, but so far only with limited success. We know that a 39 to 43 amino acid peptide called ß-Amyloid is the major player in this disease, as it constitutes more than 90% of the total weight of these abundant extracellular plaques (Selkoe, 1991). Unfortunately, this quantitative approach does not take into consideration that other, still unknown players at lesser concentration can play a more fundamental and for the onset and progression of the disease a more contributory role. After more than two decades of research on ß-Amyloid, a unambiguous causative role of this peptide in Alzheimer disease is not yet fully defined, but the mounting knowledge about the effects of ß-Amyloid on neurons and the lack of convincing alternatives allow and force us to continue our efforts in elucidating the role of ß-Amyloid in this disease.

ß-Amyloid itself is presumably not a toxin, because of its presence in the body of healthy people at all age (Plant et al., 2003). The facts that an overload of ß-Amyloid, only if aggregated, is toxic to several neuronal cell cultures grown *ex vivo* and that we find this peptide predominantly in the brains of Alzheimer disease patients in a deposited, meaning aggregated form argue for a certain toxic, more specifically neuro-toxic effect of ß-Amyloid if present in sufficient quantity and in an appropriate aggregation state (e.g. Ueda et al., 1994). Moreover, there is also a distinct correlation between its amount in the brain and the severity of mental dysfunction. This observation is apparent in late-onset dementia of Alzheimer disease, as well as in Down's syndrome, also called Trisomy 21. Interestingly, the locus of the gene coding for the precursor protein of ß-Amyloid, the so-called ß-Amyloid precursor protein (APP), is exactly located on the chromosome 21,

suggesting that excessive expression of APP leads to increased amount of its product of degradation, ß-Amyloid, which in turn becomes toxic during self-association and induces neuronal cell death, reflected by the observable progression of neurodementia. This hypothesis is very popular today and known as the "Amyloid Cascade Hypothesis" (Selkoe 1996, 1997). Unfortunately, a correlation between the amount of ß-Amyloid and progression of Alzheimer disease is not a substantial argument for a causative role of this protein. The same, the accumulated ß-Amyloid peptide in the brain of Alzheimer disease patients could result as a side-product of another, more crucial death-pathway, which does not involve ß-Amyloid *per se*. This limitation of the Amyloid cascade hypothesis led researchers to get more insight into the effects of ß-Amyloid on neuronal cells, e.g. cellular viability, cell signaling, metabolism, and ion-homeostasis. So far, a number of investigations give evidence that cells from neuronal origin are indeed more vulnerable to ß-Amyloid insult than cells from other origin, e.g. astrocytoma cells, glia.

Thus, our first goal was to determine the effect of ß-Amyloid on the cellular viability of the neuroblastoma cell line SH-SY5Y as a model for human neurons. As we already characterized the aggregation kinetics of the isoform (1-40) and as we observed ß-Amyloid (1-40)-toxicity in the rat adrenal pheochromocytoma cell line PC-12 if the peptide was applied in aggregated form, we decided to use this APP-fragment instead of the longer isoform ß-Amyloid (1-42) (Ghanta et al., 1996; Lowe et al., 2001). The observed net impact of the peptide on the cellular viability of SH-SY5Y was rather modest (maximal reduction of viability of approximately 20% after 24 hours in low serum medium, measured by means of MTT-reduction). Nevertheless, we can clearly state that this impact was neuro-specific, as same ß-Amyloid (1-40) aggregates did not alter the cellular viability in the astrocytoma cell line GOS-3 significantly. Moreover, we showed for the first time that our inhibitor $KLVFFK_6$, a hybrid compound composed of a fragment of ß-Amyloid (KLVFF) and a disruptive element (KKKKKK), circumvented to some extent ß-Amyloid (1-40)-induced toxicity in this human neuronal cell line successfully, thereby providing us with a sophisticated tool for the subsequent experimental work.

Thus, we compared in the next experiments the cellular response of SH-SY5Y and GOS-3 cells to the addition of toxic (preaggregated alone) or non-toxic (monomeric or preaggregated with the inhibitor) ß-Amyloid (1-40) species.

ß-Amyloid and its impact on membrane integrity

Another approach to elucidate the role of ß-Amyloid in Alzheimer disease puts more emphasis on the protein structure of ß-Amyloid, taking into consideration its amphiphilic nature (Sisodia and Price, 1995). In order to better understand the interactions between the (partially) lipophilic ß-Amyloid and lipid domains of the cell, e.g. the plasma membrane, researchers use synthetic liposomes as artificial models for cellular membranes. The advantage of this approach is to work under clearly defined and easily reproducible conditions. By altering the fatty acid composition of the liposomes one can readily study specific ß-Amyloid-membrane interactions in function of the nature of the fatty acids. So far, this approach has revealed some damaging effects of ß-Amyloid on the membrane integrity, e.g. alterations of membrane fluidity and loss of membrane impermeability (see Introduction for references). In our work, we focused on ß-Amyloid-membrane interactions and ß-Amyloid-induced damages on the membrane that could be eventually applied onto a cellular system: membrane binding, membrane fluidity and membrane impermeability alterations.

First, we characterized the hydrophobicity and the aggregate size of the peptide under different preaggregation conditions. We observed that the hydrophilic nature of ß-Amyloid (1-40) was more prominent if preaggregated. Aggregated, but not monomeric ß-Amyloid (1-40) did bind to the highly lipophilic fluorescent dye DPH, which is known to be virtually insoluble in aqueous conditions and fluoresces only if bound to lipid or lipid-like domains. The fact that there seems to be a correlation between the hydrophobicity and the aggregate size of the peptide (see figure 79) suggests that rather aggregated than monomeric ß-Amyloid (1-40) is prone to bind lipid domains as for example the cellular membrane. Moreover, it is highly believable that such large aggregates can successfully and compellingly alter the membrane properties in a substantial manner as the size of ß-

Amyloid aggregates is in the same order of magnitude or even greater than the thickness of biomembranes (≥10nm).

Interestingly, the intensity of fluorescence of the dye DPH if bound to ß-Amyloid (1-40) was correlated to its anisotropy (see figure 80). Thus, binding of DPH to aggregated hydrophobic ß-Amyloid (1-40) did simultaneously increase the fluorescence intensity and the anisotropy of DPH. Thereby, we had a tool to detect aggregated ß-Amyloid (1-40) if bound to DPH. Such an unconventional approach was also used successfully by Avdulov and coworkers (1997), who postulated that an increase in fluorescence intensity of fluorescent lipids in liposomes is a measure for ß-Amyloid binding to these liposomes.

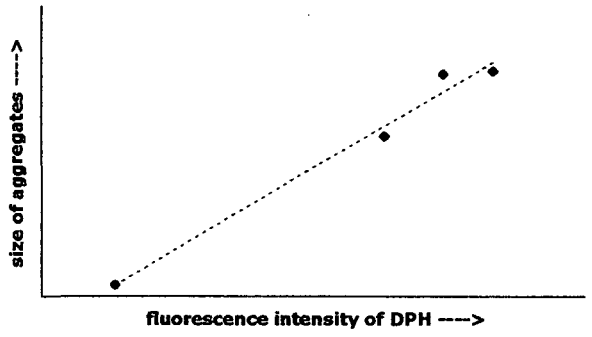

Fig.79: Data from DPH-binding and aggregation size studies reveal a possible correlation between hydrophobicity (measured by DPH-fluorescence intensity) and aggregate size(measured by means of microcentrifugation) of ß-Amyloid (1-40)species

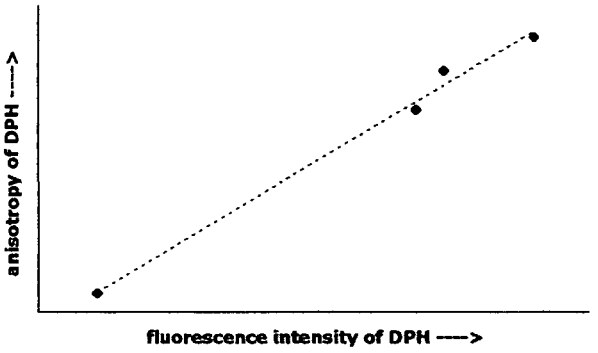

Fig.80: Correlation between anisotropy and fluorescence intensity of DPH of different ß-Amyloid (1-40) species

We not only observed DPH-binding of ß-Amyloid (1-40) in a lipid-free environment, but also ß-Amyloid (1-40)-induced alteration in DPH-anisotropy in a liposomal environment, by loading preformed liposomes with DPH and adding subsequently aggregated ß-Amyloid (1-40) to the DPH-loaded liposomes. The results of these experiments are in line with results of our previous work using DPH-preformed liposomes (Kremer et al., 2000, 2001). Both methods led to a ß-Amyloid (1-40)-induced increase in DPH-anisotropy if the peptide was allowed to aggregate prior to addition to the liposomes. The difference in the ß-Amyloid (1-40)-induced increase of DPH-anisotropy (net increase in DPH-anisotropy of less than 0.1 units in this work versus net increase in DPH anisotropy of more than 0.1 in previous work using DPH-preformed liposomes) was attributed to the different preparation procedures of the ß-Amyloid (1-40) peptide (Instead of DMSO as denaturant, we used in this work 8 M urea at pH 10) and of the liposomes, leading to

different yields of DPH-loading of the liposomes. As it is believed that this approach is a measure for the membrane fluidity of liposomes, the results could be easily interpreted as alterations in membrane fluidity in liposomes (e.g. Müller et al., 1995). Since DPH is buried deep within the acyl chain region of the lipid bilayer of the liposomes, an increase in anisotropy generally reports decreased acyl chain mobility and increased chain order in the hydrophobic core. Such changes were observed with insertion of hydrophobic peptides that share many similarities with ß–Amyloid (ß-strand fold, a fairly hydrophobic content, and propensity to aggregate), into the membrane. Therefore, we could easily assume that the ß-Amyloid (1-40) aggregates induced a decrease in membrane fluidity via the penetration of the bilayer. Our observation that aggregated ß-Amyloid (1-40) can interact directly with DPH (in the absence of membranes) raise the question to what extent this assumption is true and how to interpret these data. From a physical point of view, the anisotropy of DPH is a measure of the rotational freedom of the dye. Thus the observed increase of DPH-anisotropy if bound to aggregated ß-Amyloid (1-40) in the absence of liposomes can be interpreted as a reduced rotational freedom of excited DPH*. However, the lifetime of DPH* also influences the values of anisotropy: At same rotational freedom, a prolonged duration of a fluorophor in the excited state also increases the anisotropy. As we observed previously that the lifetime of DPH in the presence of liposomes was not significantly altered (Kremer et al., 2000) if ß-Amyloid (1-40) was present or not, we believe that the observed increase in anisotropy of DPH was a result of hindered rotation of DPH when bound to large aggregates of ß-Amyloid (1-40), that are possibly not as mobile as the small dye DPH. Therefore, we can interpret that the ß-Amyloid (1-40)-induced increase in anisotropy of liposome-embedded DPH had as origin either a specific DPH-ß-Amyloid (1-40) interaction in the inner core of the membrane as observed in a lipid-free environment, or from a traditional view a decrease in membrane fluidity that reduced the fluidity of the parallel orientated fatty acid chains of the lipids and consequently the rotational freedom of the embedded DPH. In both cases, there is indeed a reduction of fluidity, whereas locally restricted in the former. More work has to be done in order to differentiate between these two effects on the observed DPH-anisotropy. This lies beyond our expertise and not within the goals of our work.

In summary, we proved that the ß-Amyloid (1-40)-induced alteration in DPH-anisotropy in the presence of liposomes had its origin in the liposomal environment and got evidence that we were indeed measuring membrane fluidity. As only preaggregated, but not monomeric ß-Amyloid (1-40) caused this increase in DPH-anisotropy, we are free to postulate that aggregates, but not monomers of ß-Amyloid (1-40) alter the membrane fluidity of liposomes, but only future work will reveal to what extent this postulation is correct.

Eventually future work in this field could also give insights into the discrepancy between ß-Amyloid-induced alterations of membrane fluidity if measured by means of DPH-anisotropy and if measured by means of pyrene-excimer-formation. Whereas the membrane fluidity is generally decreased in the presence of ß-Amyloid if measured by means of DPH, the use of pyrene-excimer-formation as a measure for membrane fluidity reveals commonly an increase in membrane fluidity (e.g. Avdulow et al., 1997). This contradiction in the literature is not completely understood. Researchers explain this discrepancy by different vendors of ß-Amyloid, ß-Amyloid sample preparations, and other parameters. In our perception, these arguments are not very convincing.

Similarly, we observed a ß-Amyloid (1-40)-induced increase in anisotropy of cellular membrane-embedded DPH in the neuron-like cell line SH-SY5Y (Successful labeling of the plasma membrane with DPH in order to measure membrane fluidity was already achieved in lymphocytes (Shinitzky and Inbar, 1974), macrophages (Petty et al., 1987), and rat PC12 cells (Ravichandra and Joshi, 1999)). But again, one has to take into consideration the direct interaction of aggregated ß-Amyloid (1-40) with DPH. We therefore are cautious to postulate that our results are proof for membrane fluidity alterations in SH-SY5Y cells induced by aggregated ß-Amyloid (1-40). Within our technological constraints, we excluded all other possibilities as far as possible.

However, our findings are strong evidence for the localization of ß-Amyloid (1-40) in the cellular membrane. As we observed an increase of DPH-anisotropy when ß-Amyloid (1-40) was preaggregated, we can clearly assume that aggregated ß-Amyloid (1-40) inserted itself into the cellular membrane. Taking into consideration the size of our ß-Amyloid (1-40) aggregates (average contour length of 400nm or more, see Lowe et al., 2001), it is highly believable that the insertion of such large aggregates has a circumstantial impact

on physical and biochemical membrane properties. Not only membrane fluidity and integrity could be damaged, we can also assume that inserted ß-Amyloid acts directly on membrane-bound enzymes, as suggested by Lehtonen et al. (1996), thereby altering their enzymatic activity and eventually impairing membrane-located signaling pathways. This in turn could have influence on the membrane properties and thereby potentiate the direct harmful effect of the ß-Amyloid peptide itself. This is even more important, as the addition of our inhibitors, which generates non-toxic aggregates of ß-Amyloid (1-40) of approximately the same size, did not circumvent the induced increase in DPH-anisotropy in liposomes or SH-SY5Y cells.

The lack of DPH-anisotropy alteration in a liposomal or cellular system in the presence of monomeric ß-Amyloid (1-40) does not exclude the possibility that monomeric ß-Amyloid (1-40) was also incorporated into the membrane, as monomers of ß-Amyloid (1-40) did not bind DPH as measured by anisotropy and fluorescence intensity and thereby could not be tracked by this approach as easily.

To circumvent this constraint, we also determined ß-Amyloid (1-40) binding to the plasma membrane of SH-SY5Y cells by means of a more quantitative and direct approach. By adding radioactive [^{125}I]-ß-Amyloid (1-40) as a tracer to non-labeled peptide, we were able to generate easily detectable ß-Amyloid (1-40) aggregates. By adding these aggregates to either liposomes or SH-SY5Y cells, we got new insights into the interactions between ß-Amyloid (1-40) and membranes.

Whereas altering the fatty acid composition of liposomes did not significantly influence the amount of ß-Amyloid (1-40) bound to liposomes, we observed increased deposition of ß-Amyloid (1-40) aggregates on liposomes by adding the inhibitor KLVFFK$_6$ to ß-Amyloid (1-40) during preaggregation. As we excluded the possibility of specific interactions between the positively charged inhibitor and the liposomes, we assume that simple deposition-effects were the primary driving force for the membrane-binding in our system. Similar results were observed in the cell line SH-SY5Y. Interestingly, deposition of ß-Amyloid (1-40) in the same order of magnitude did also occur on iron oxide or poly-styrene surfaces, arguing again compellingly for a surface-independent, deposition-driven

membrane-binding rather than electrostatic-driven lipid-ß–Amyloid (1-40) or membrane receptor-ß-Amyloid (1-40) interaction.

Furthermore, we observed that this deposition was at least partially saturable. Calculations based on our previous observations of ß-Amyloid (1-40) aggregate size (Kremer et al., 2000) suggest a deposition leading to a monolayer of ß-Amyloid (1-40) on the membrane surface of SH-SY5Y cells. The final amount of deposited ß-Amyloid (1-40) on the surface was independent of the initial aggregate size of the peptide. If ß-Amyloid (1-40) binds indeed to a specific receptor on the cell surface as postulated from different groups (e.g. Yan et al., 1999), the measured large amount of deposited peptide would have definitely masked this specific, and quantitatively minor interaction.

This aspect shows one crucial disadvantage of any quantitative estimation of ß-Amyloid: By preaggregating ß-Amyloid, aggregates are generated with a particular size distribution. As any quantitative approach can only measure the total amount of ß-Amyloid, one cannot differentiate between the numerous species with different aggregate sizes that are present simultaneously. In other words, we were not able to prove which specific ß-Amyloid (1-40) species were covering the surface of the liposomes or the SH-SY5Y cells. This limitation is even more central, as new findings suggest that rather small intermediates than larger aggregates are the toxic moiety indeed. This is also in line with our results, showing that the addition of our inhibitors to ß-Amyloid (1-40) accelerates the aggregation kinetics of the peptide, thereby generating larger aggregates, but nonetheless with less toxic impact on PC-12 or SH-SY5Y cells. More work has to be done in order to separate different species present simultaneously without altering the aggregate size during separation. The problem thereby is that, as we have observed, aggregates, once they are generated, can either grow in size by the attachment of soluble ß-Amyloid (1-40) species from the supernatant to the aggregate, or shrink as result of re-solubilization depending on the concentration of ß-Amyloid (1-40) in the supernatant.

We encountered the same difficulty when we determined the amount of ß-Amyloid (1-40) internalized by SH-SY5Y cells. We observed no difference in internalization of different ß-Amyloid (1-40) species (toxic or non-toxic), but we cannot rule out the possibility that there was indeed a difference in internalization of one specific species of

ß-Amyloid (1-40) that accounts for its toxicity, which was masked by the overall internalization of all species present.

Based on these thoughts, there is no doubt that such quantitative approach can only have limited success, as it does not differentiate between the different species that are generated in the single sample volume. But as long as convincing alternatives are not emerging, one has to work with this restriction. Thus, we are constrained to correlate effects of ß-Amyloid (1-40) with the average size of the aggregates applied to our membrane system, without taking into account specific sub-populations.

The fact that ß-Amyloid exerts a direct damaging impact on the membrane integrity has been observed several times by measuring the release of intraliposomal or intracellular dyes, as well as of membrane components into the supernatant. We observed membrane leakage in multicomponent liposomes, in SH-SY5Y cells, and to a lesser extent in GOS-3 cells if we preaggregated ß-Amyloid (1-40) prior to addition to the experimental environment. The leakage of the encapsulated dye calcein in multi-component liposomes gives evidence for a direct impact of ß-Amyloid (1-40) aggregates on the membrane integrity that does not require cellular signaling pathways. As we did not observed calcein leakage in mono-component liposomes, we are confident to rule out an interaction between a specific fatty acid and ß-Amyloid (1-40) as ultimate cause for loss of membrane integrity. This is in line with our observation that ß-Amyloid (1-40) binding to liposomes did not depend on the fatty acid nature of the liposomes, as mentioned above. We therefore assume that a certain extent of heterogeneity in the membrane fatty acid composition is a necessary and sufficient requirement for ß-Amyloid (1-40)-induced membrane leakage. As ß-Amyloid-sensitive neurons and ß-Amyloid-insensitive glia cells share different membrane compositions, leakage as consequence of membrane damage could indeed play a crucial role in the neurotoxicity of ß-Amyloid *in vivo*. Our observation that the release of membrane-embedded DPH into the extracellular fluid was greater in neuronal SH-SY5Y than in astrocytoma GOS-3 cells strengthens this hypothesis. Nevertheless, the fact that we did not observe any circumventive effect of our inhibitor $KLVFFK_6$ within our experimental conditions of 24 hours, gives evidence that this membrane leakage was not the ultimate driving force in the reduction of cellular

viability in our toxicity studies. Moreover, we observed also significant release of the fluorescent lipid ß-DPH-HPC as marker for membrane lipids in GOS-3 cells.
Similarly to our experiments, Yang and coworkers (1998) observed loss of lysosomal membrane impermeability by monitoring the leakage of the tracer Lucifer Yellow and luminal lysosomal hydrolases from lysosomes into the cytoplasm in the presence of aggregated, but non toxic ß-Amyloid (1-40). Moreover, Oyama and coworkers (1995) observed change in membrane permeability induced by the ß-Amyloid protein fragment 25-35 in brain neurons dissociated from rats. At 1µM, ß-Amyloid (25-35) induced leakage of fluo-3 from the neurons and permeation of ethidium across the membrane in a dose-dependent manner, although both dyes are highly impermeable to the intact plasma membrane. No toxicity studies were conducted in this work, but we can certainly assume that at an applied concentration of 1µM, ß-Amyloid (25-35) was not significantly toxic.
Overall, we can only assume that impairment of the membrane integrity is a long-term toxic effect on neurons and that our findings extend the hypothesis that ß-Amyloid does not only increase the plasma membrane permeability for inorganic ions such as calcium and sodium as observed several times, but also to molecules.

Work of Avdulov and coworkers (1997) showed that the membrane integrity alterations induced by ß-Amyloid were associated with lipid peroxidation. Thus, we investigated the effect of ß-Amyloid (1-40) on lipid peroxidation in SH-SY5Y cells and GOS-3 cells. We observed only a weak, barely significant effect of ß-Amyloid (1-40) on lipid peroxidation in SH-SY5Y cells, none in GOS-3. Moreover, this effect was observed only after few hours, whereas alterations in membrane fluidity were measurable nearly immediately (within one hour of incubation) after addition of ß-Amyloid (1-40) to the cells. Therefore, we are confident to rule out a causative relationship of lipid peroxidation with membrane fluidity alteration or membrane leakage.
More interestingly, we observed that the addition of hydrogen peroxide as a means to generate an oxidative milieu enhanced ß-Amyloid (1-40)-induced lipid peroxidation in SH-SY5Y significantly. This suggests that the ß-Amyloid peptide indeed induces lipid peroxidation in neurons in oxidative stress conditions, as it occurs in the brain of Alzheimer disease patients. Moreover, we know that the brain is particularly sensitive to

free radical insults since it contains high concentrations of easily peroxidable polyunsaturated fatty acids (Halliwell, 1992) and is not particularly enriched with protective antioxidant enzymes or other antioxidant compounds. Therefore, lipid peroxidation can indeed play a crucial role in Alzheimer disease. For example, we can hypothesize that oxidative stress in the lipid environment oxidizes ß-Amyloid (and other proteins), leading eventually to protein misfolding and thereby to enhanced protein aggregation, as oxidatively modified proteins are thermodynamically unstable and assume partially unfolded tertiary structures that readily form aggregates.

The consequences of lipid peroxidation are multiple. As mentioned above, lipid peroxidation alters the biophysical properties of the membrane. Direct products of lipid peroxidation, as for example 4-HNE can cause effects observed in cell culture studies involving ß-Amyloid. It has been shown that 4-HNE did not only impair the activity of the membrane-bound enzyme Na+, K^+-ATPase, but also induced an increase in intracellular free Ca^{2+} concentration (Mark et al., 1997). It would be interesting to know if 4-HNE does not only impair Ca^{2+}-homeostasis, but also the homeostasis of other cellular components, or even membrane components. More work has to be done in order to elucidate a putative connection between lipid peroxidation and membrane leakage.

How ß-Amyloid exactly induces lipid peroxidation is currently unknown. It has been postulated that ß-Amyloid itself is a pro-oxidant. In rodent microglia and human monocytes, El Khoury and coworkers (1996) observed that ß-Amyloid-binding of membrane receptors, e.g. class-A scavenger receptor, induced the secretion of reactive oxygen species prone to peroxide membrane lipids.

In summary, we observed that ß-Amyloid (1-40), only if aggregated, caused multiple alterations in the membrane integrity that could play a fundamental role in neuronal cell death in Alzheimer disease: membrane fluidity, membrane impermeability and chemical modification of the membrane lipids as result of lipid peroxidation.

ß-Amyloid: pro-oxidant or antioxidant?

It is widely believed that ß-Amyloid causes oxidative stress-mediated neurotoxicity (Behl et al., 1994). Champions of this hypothesis argue that diagnostic, clinical, and pathological studies all support a central role for this peptide in the generation of oxidative stress as the ultimate cause for neuronal death. Observations from brain autopsies from Alzheimer disease patients showed clearly substantial evidence for oxidative stress (Markesbery, 1997; Swerdlow et al., 1997), cell culture studies demonstrated the induction of reactive oxygen species, protein and lipid oxidation when aggregated ß-Amyloid was added.

It has been shown that oxidative stress is not specific for Alzheimer, but also occurs in brain aging in healthy people, as well as in other neurodegenerative diseases such as amyotrophic lateral sclerosis (ALS) and Parkinson's disease (Olivieri et al., 2001). Schubert and coworkers (1995) showed that a variety of different amyloidal peptides share a common oxidative mechanism if a minimum amount of ß-sheet is present in the amyloid fibrils.

Nevertheless, it is unlikely that ß-Amyloid-induced oxidative stress is the ultimate cause of neuronal cell death, as this hypothesis is still heavily disputed after more than two decades of research and as several researchers observed only limited success to no impact of antioxidants in circumventing ß-Amyloid-induced toxicity (e.g. Behl, 1997; Yao et al., 1999).

In our work, we got evidence for ß-Amyloid (1-40)-induced lipid peroxidation in the neuronal cell line SH-SY5Y arguing for a pro-oxidative role of ß-Amyloid (1-40). In contrast, we did not observe an increase of intracellular reactive oxygen species (iROS) if toxic ß-Amyloid (1-40) aggregates were added to the cells. Actually, we measured a decrease in iROS if the cells were incubated with ß-Amyloid (1-40) prior to measurement. This reduction was independent of the aggregation state of the peptide. Moreover, pretreatment of the cells with ß-Amyloid (1-40) did significantly circumvent exogenous H_2O_2-induced increase of iROS. This is in line with work of Gibson and coworkers (2000), who observed in PS 1 mutant fibroblasts cells increased production of ß-Amyloid, associated with decreased production of iROS. This leads us to postulate that

the ß-Amyloid peptide has also anti-oxidative capacities that could play a role in Alzheimer disease.

In cells, numerous defense mechanisms exist to prevent the buildup of iROS, and collectively help to protect living organisms against oxidative damage. These systems include superoxide dismutase and catalase, which collectively remove superoxide ($O2^-$) and hydrogen peroxide (H_2O_2) from the cytoplasm, glutathione peroxidase and glutathione, which reduce H_2O_2 to H_2O, and vitamine E and C, which function to terminate lipid chain reactions involving peroxyl radicals. When these defense mechanisms are unable to cope with increasing burden of oxidants, the redox-state of the cell shifts towards an oxidative milieu, and the cell is exposed to oxidative stress. In Alzheimer disease, there is evidence that oxidative stress is one of, if not the earliest pathological alteration in the brain, as it has been observed that oxidative stress even emerged before the manifestation of ß-Amyloid deposits (Nunomura et al., 2001, Smith et al., 2000). It has been shown that neurons responded to such oxidative stress, as well as to UV light, both *in vitro* and *in vivo*, by increasing the production of the peptide (Yan et al., 1995). This increase in ß-Amyloid production then was associated with a consequent reduction in oxidative stress (Nunomura et al., 2000). In summary, ß-Amyloid was induced under oxidative conditions and acted to lessen oxidative damage. Thus, it is attractive to call ß-Amyloid an antioxidant.

Even though the role of ß-Amyloid as antioxidant did not attract lot of research hitherto, there is some additional evidence for this hypothesis. Nunomura and coworkers (2001) observed that the majority of the examined brains of persons over the age of 40 contained ß-Amyloid deposits where redox-alterations first manifested. An alternative view, that everyone in his mid-life is on the verge of developing Alzheimer disease is not only unsound from a biological perspective but also does not explain the large percentage of cognitively normal aged individuals whose brain contain ß-Amyloid-deposits (and also NFT) equivalent to patients with Alzheimer disease (Davis et al., 1999). The observations that the amount of ß-Amyloid correlated, albeit weakly, with Alzheimer disease severity (Knowles et al., 1998), that ß-Amyloid was often, though not always, found in regions of the brain that degenerate during the disease, do not only support the current opinion that ß-Amyloid causes the disease, but do equally sustain the alternative view that ß-Amyloid

has some protective role in Alzheimer disease (Smith et al., 2002). Indeed, new findings showed that ß-Amyloid may indeed play more neuroprotective functions than previously expected. Plant and coworkers (2003) showed that ß-Amyloid was neuroprotective in different cell lines by circumventing toxicity induced by the addition of inhibitors of secretase enzymes. Xie and coworkers (2003) observed that ß-Amyloid had a potential role in survival and function of aged spinal motor neurons after axonal injury. The observations that at methionine residue 35 oxidized, but not unoxidized ß-Amyloid generated H_2O_2 and was toxic to neurons (Barnham et al., 2003) and that certain species of ß-Amyloid reduced iron-induced toxicity in rat cerebral cortex (Bishop and Robinson, 2003) are in line with the postulation that the neuroprotective functions of the peptide are based on its anti-oxidative potential.

In this light, researchers focused on how ß-Amyloid could protect against oxidative insult. It is known that strong metal chelators are strong antioxidants. ß-Amyloid binds copper stronger than other transition metals and copper is known to be a more efficient catalyst of oxidation than any other metal. Chelation of transition metals in a redox-inactive form may theoretically serve to inhibit metal-catalyzed oxidation of biomolecules (Kontush, 2001). In view of this possibility, it has been shown recently that exogenous added ß-Amyloid inhibited metal-catalyzed oxidation of lipoproteins from CSF and plasma (Kontush et al., 2001a). This is in line with the positive correlation between CSF resistance to oxidation and its level of ß-Amyloid (Kontush et al., 2001b) and the low levels of ß-Amyloid in CSF in Alzheimer disease patients. Moreover, work of Cuajungco and coworkers (2000) has shown that ß-Amyloid by itself acted as a potent superoxide dismutase.

Therefore, it is valid to argue that these findings indicate that ß-Amyloid is not the driving force of the pathogenic process, but rather a response of the brain to the increased oxidative burst. In this line, our findings that ß-Amyloid (1-40) decreased iROS give evidence that the peptide may indeed play a neuroprotective role in fighting against oxidative insults.

To get more insights into the role of ß-Amyloid in oxidative stress, we determined the ß-Amyloid (1-40)-induced expression of the antioxidative Nuclear Factor-κB (NFκB) in

SH-SY5Y cells. NFκB-activation can prevent apoptosis induced by several different insults including exposure to oxidative insults in rat hippocampal neurons (Mattson et al., 1993). We observed fast induction of NFκB at low, sub-toxic concentrations of aggregated ß-Amyloid (1-40). These findings are in line with work of Cassarino and coworkers (2000), who found comparable induction of NFκB in SH-SY5Y cells after treatment with parkinsonian neurotoxin of approximately 200%, and of Kaltschmidt and coworkers (1997, 1999), who equally observed NFκB-activation in primary rat cerebellar neurons only at low ß-Amyloid doses. The observed inverted U-shaped dose response of NFκB activation by aggregated ß-Amyloid (1-40) suggests that high doses and/or long exposure of neurons to the peptide if aggregated could lead to an overload of oxidative stress, inactivating NFκB-driven neuroprotective gene expression, and therefore might contribute directly to pathological mechanisms. It has also been shown that NFκB-activation played a critical neuroprotective role in mouse hippocampal cultures that were treated with neurotoxic concentrations of ß-Amyloid (Barger et al., 1995). Moreover, a α-secretase-derived form of APP induced NFκB-activation in PC12 cells and protected them from being killed by ß-Amyloid (Guo et al., 1998). Also, pretreatment with antisense oligonucleotides to IκB, the inhibitor of NFκB, blocked ß-Amyloid-induced toxicity (Barger et al., 1995), and overexpression of a transdominant IκB blocked NFκB-activation and potentiated ß-Amyloid toxicity (Kaltschmidt et al., 1999), thus suggesting that activation of NFκB may play a pivotal role in neuronal survival following exposure to neurotoxic ß-Amyloid. Fast NFκB response of SH-SY5Y could be membrane-mediated: $P75^{NTR}$, the membrane-located receptor for the nerve growth factor (NGF), binds also ß-Amyloid and activates NFκB (Bono et al., 1999; Kuner et al., 1998). This in line with the observation that antisense oligonucleotides of p75 receptor potentiated ß-Amyloid toxicity (Shen et al., 1997).

How NFκB-activation circumvents ß-Amyloid-induced toxicity is currently unknown. NFκB-activation is required for the up-regulation of neuronal Bcl-xL, an antiapoptotic protein (Foehr et al., 2000). Other proteins that may be induced by NFκB-activation are tumor necrosis factor-α (TNF-α), tumor necrosis factor-ß (TNF-ß), and transforming growth factor-ß (TGF-ß), that protected cultured hippocampal neurons against ß-

Amyloid-induced toxicity (Barger et al., 1995; Prehn et al. 1996), as well as different growth factors that are known to be accumulated in senile plaques in Alzheimer's disease. (Araujo and Cotman, 1991; Pike et al., 1994).

In this view, we are able to postulate that aggregated ß-Amyloid (1-40) acts to a certain extent neuroprotective by activating NFκB and thereby activating anti-oxidative pathways. In the light that ß-Amyloid might have some anti-oxidative properties, it is of interest that Tomita and coworkers (2000) observed in COS7 cells that overexpression of X11L, a trap for NFκB, suppressed the release of ß-Amyloid (1-42), suggesting that ß-Amyloid-induced NFκB itself induced the release of ß-Amyloid (1-42). This assumption is strengthened by Kaltschmidt and coworkers (1997), who observed in brains of Alzheimer disease activated NFκB only in cells in close vicinity to early senile plaques.

Nevertheless, the situation *in vivo* is less clear as cells from different origin also show different ß-Amyloid-induced NFκB-activity. In fetal rat cortical neurons, NFκB-activity decreased after exposure to ß-Amyloid in a concentration and time dependent fashion but increased in astrocytes (Bales et al., 1998). Akama and coworkers (1998) observed that in rat astrocytes ß-Amyloid-induced increase in NFκB-activity induced nitric oxide (NO), a potent source of oxidative stress. Kuner and coworkers (1998) also observed that ß-Amyloid-induced cellular death in human SK-N-MC cells was associated with NFκB-activity. Inhibition of NFκB-activation by curcumin also abolished ß-Amyloid-induced apoptotic cell death.

In summary, one has to consider the differing effects of NFκB on cells coming from different (neuronal or glial) origin (Barger et al., 1995). Only future work will help us to fully understand the role of NFκB-activation in the cellular response to ß-Amyloid.

If ß-Amyloid has indeed some anti-oxidative functions in neurons and if oxidative stress leads to increased generation of ß-Amyloid in order to prevent excessive peroxidation of proteins and lipids, the question of the source of oxidative stress in the brains of Alzheimer disease patients becomes central to explain the onset of the disease. The list of putative sources of peroxides is virtually endless: oxidases, superoxide dismutase, xanthine oxidase, autooxidation of catecholamines, normal mitochondrial energy metabolism, lipoxygenases, cyclooxygenases, flavin oxidases, and microsomal

cytochrome oxidases could all contribute to an increase in peroxides. As the brain accounts for 20-25% of the total body oxygen consumption (and has a high glucose-driven metabolic rate), but constitutes less than 2% of the body total weight, we can assume that mitochondria are the major source of ROS in neurons that derive their energy almost completely from oxidative phosphorylation in the respiratory chain of the mitochondria. There, adenosine triphosphate is generated by the reduction of oxygen to water through the sequential addition of four electrons and four protons. During this process, a leakage of high-energy electrons can potentially cause the formation of superoxide radicals, one of the major ROS produced by the mitochondrial respiratory chain. Superoxide can also be produced from other sources, such as lipooxygenases, cyclooxygenases, and various flavin oxidases and can be further metabolized to H_2O_2 by the enzymes catalase and superoxide dismutase. Then, H_2O_2 may diffuse from the mitochondrial matrix into the cytoplasm and extracellular space, where it can react with transition metals to generate hydroxyl radicals. Moreover, H_2O_2 can be generated in the CNS by different oxidases, such as xanthine oxidase and can result from the metabolism of catecholamines and indolamines by monoamine oxidase. Another source of H_2O_2 is the non-enzymatic aytooxidation of catecholamines. As we can see, there is a plethora of possible origins for increased oxidative stress in the brain. It is worth mentioning that Alzheimer disease most strongly affects brain regions with highest metabolic rate (Mielke et al., 1998). Thus, mitochondria malfunctioning may represent a prominent source of ROS in aging and even more in Alzheimer disease. This is sustained by increased synthesis of known antioxidants in Alzheimer disease (Perry et al., 1998).

Thus, we can clearly assume that the brain is particularly sensitive to oxidative stress because it has a high glucose-driven metabolic rate, it has only low levels of antioxidant defense enzymes, it contains high concentrations of PUFA, which are potential substrates for lipid peroxidation, and as it is rich in enzymatically active transition metals, which can potentially catalyze radical formation.

Neurons play an active role in Alzheimer disease

We observed a significant impact of ß-Amyloid (1-40) on neurons: Aggregated ß-Amyloid (1-40) induced membrane damage, as observed by alterations in membrane fluidity, membrane integrity, and lipid peroxidation. These effects could play in concert to ultimately induce neuronal cell demise as observed in the brains of Alzheimer disease patients. Moreover, we have observed that ß-Amyloid (1-40) alters the amount of iROS and the level of activated NFκB in SH-SY5Y neuroblastoma cells. Taken together, these observations let us assume that neurons respond directly to ß-Amyloid.
Nevertheless, the question, to what extent neurons play actively a role in ß-Amyloid metabolism either to fight against or to contribute to neuronal cell death, remains widely open. Therefore, we examined the role of neurons in ß-Amyloid metabolism.

The "Amyloid Cascade Hypothesis" postulates that the net production of ß-Amyloid is increased in the brain of Alzheimer disease patients, either by increased production of ß-Amyloid or by decreased degradation of the peptide. Most work in ß-Amyloid-clearance has focused on microglia, as it is believed that these cells play a pivotal role in the clearance of non-self and/or toxic material. Paresce and coworkers (1996), as well as Frackowiak and coworkers (1992) observed ß-Amyloid-uptake of synthetic ß-Amyloid fibrils, ß-Amyloid microaggregates or ß-Amyloid cores from brains of Alzheimer disease patients in glia and glial-like cells, but accompanied by weak to no internal degradation of the peptide. This is in line with work of Ard and coworkers (1996) who observed intracellular accumulation of ß-Amyloid in rat microglia cells. ß-Amyloid fibrils were ingested and stored in phagosomes, but remained up to 20 days within, suggesting a very limited effectiveness of microglia in degrading ß-Amyloid fibrils (Frackowiak et al., 1992). Moreover, Chung and coworkers (1999) observed in microglial cells that after internalization intact, non-degraded ß-Amyloid was released. These observations suggest that there is only limited effectiveness of microglia in degrading ß-Amyloid, which leads us to assume that microglia are not sufficient in ß-Amyloid clearance. Other players also seem to have little contribution to ß-Amyloid-clearance. Matsunaga and coworkers (2003) observed uptake of ß-Amyloid in rat astrocytes, but no measurable degradation.

Knauer and coworkers (1992) observed in human skin fibroblasts that intracellularly accumulated ß-Amyloid remained up to three days resistant to degradation. In summary, the collection of these data suggests that rather than microglia as the sole actors a multitude of cells from different origins could contribute to ß-Amyloid-clearance (Schaffer et al., 1995). In this regard, we measured and characterized ß-Amyloid (1-40)-uptake in the neuronal cell line SH-SY5Y as model for neurons to elucidate to what extent neurons play actively a role in ß-Amyloid degradation.

As mentioned above, we observed a invariable, aggregation state-independent internalization of the ß-Amyloid (1-40) peptide in SH-SY5Y cells. This is in line with work of Lambert and coworkers (1999), who suggest that toxicity does not follow internalization, based on observations that toxicity followed surface binding followed by activation of Fyn, a tyrosine kinase in the Src family.

Moreover, we measured a substantial amount of degraded ß-Amyloid (1-40) in the extracellular medium. After 24 hours, 2% of total ß-Amyloid (1-40) applied to the cells was degraded as measured by means of TCA-precipitation. From these data, we calculated a half-life time $t_{1/2}$ of approximately one hour, in line with work of others (Burdick et al., 1997; Knauer et al., 1992; Savage et al., 1998), who observed a $t_{1/2}$ between one hour and 2.5 hours. These data a strong evidence that neurons play indeed a fundamental role in ß-Amyloid clearance, thereby contributing actively to the reduction of the load of ß-Amyloid in the brain. Kang and coworkers (2000) also provide evidence that neurons play an active role in clearance of soluble ß-Amyloid (1-40) and ß-Amyloid (1-42) via a receptor-mediated uptake, whereas they observed that microglia were more crucial in the uptake of fibrillar forms of ß-Amyloid. Ditarando and coworkers (2001) observed that internalized soluble ß-Amyloid (1-42) from the culture medium accumulated in the endosomal/lysosomal system.

This leaves the question open as to how neurons degrade ß-Amyloid. In neurons, the endocytic pathway internalizes and processes extracellular nutrients and trophic factors, recycles, modifies, and degrades receptors and other integral membrane proteins after neurotransmitter release, and directs information to intracellular biosynthetic pathways. Endocytosis enables neurons to modify or degrade molecules from the cell surface into intracellular compartments by a series of fusion and budding events. This complex of

compartments known as the central vacuolar system consists of early and late endosomes and lysosomes that have different capabilities for proteolytic processing. Most resident acid hydrolases in central vacuolar system compartments are processed in the Golgi apparatus and subsequently trafficked to acidic organelles under the regulation of mannose-6-phosphate receptors. The turnover of internalized proteins and lipids was originally thought to be limited to lysosomes, but it is known that some acid proteases are present in early endosomes and are capable of modifying endocytosed material. Early endosomes are the first major sorting station on the endocytic pathway and the site of internalization and initial processing of proteins, as probably ß-Amyloid. Indeed, our data support that approximately 50% of degraded ß-Amyloid (1-40) is degraded intracellularly, as addition of the lysosomal inhibitor chloroquine to the medium successfully decreased the amount of degraded ß-Amyloid of approximately 50%. This is in line with work of Hammad and coworkers (1997), who also observed that chloroquine (at the same applied concentration of 0.1mM) treatment successfully inhibited the cellular degradation of ß-Amyloid complexed with Apo. In contrary, Iwata and coworkers (2000) observed no effect of chloroquine and other inhibitors of lysosomal proteolysis on ß-Amyloid (1-42) injected protein in rat hippocampus, whereas inhibitors of metalloendopeptidases (phosphoramidon) caused nearly complete inhibition of ß-Amyloid-catabolism, suggesting neutral endopeptidases as the major degradation pathway of ß-Amyloid (1-42) in rat brain parenchyma.

ß-Amyloid (1-40) degradation studies in SH-SY5Y cells were conducted by Ida and coworkers (1996). At a physiological concentration of 50pg/mL, they observed that a small part of extracellularly added ß-Amyloid (1-40) accumulated in insoluble fractions of the cells and remained stable for several days. They concluded that this uptake might contribute in two different ways: either to prevent the amyloid (1-40) deposition by reducing extracellular ß-Amyloid (1-40) concentration or to promote the deposition by producing insoluble seeds for amyloid plaque formation. In the former, reduced uptake would then cause an accumulation of ß-Amyloid (1-40) leading to its aggregation and deposition, whereas in the latter enhanced uptake activity would be a cause of disease. As the extracellular concentrations are always far below aggregation-threshold, and as biochemical and immunohistochemical analyses show that the premature diffuse plaques

contain considerably amounts of N-terminally truncated ß-Amyloid (Ida et al., 1996; Knauer et al., 1992; Saido et al., 1995), we believe that the limited degradation of internalized ß-Amyloid may indeed serve as a seed for amyloid fibril formation. Western Blot assays of Ida and coworkers (1996) revealed a time-dependent decrease of ß-Amyloid in the supernatant. As degradation of ß-Amyloid was not inhibited by competition, the uptake seemed to be not mediated by a high-affinity receptor. This is in line with our work, as we observed membrane binding, which did not depend on the aggregation state of ß-Amyloid. As a protease inhibitor mixture did not change cellular clearance rate, Ida and coworkers (1996) assumed that clearance is not due to proteolytic degradation caused by extracellular released protease(s). This is in strong contradiction to our work, as we observed that conditioned medium degraded ß-Amyloid (1-40) quantitatively. Possible candidates for extracellular degradation of ß-Amyloid are serine proteases, as reported by Naidu and coworkers (1995) in CHO cells transfected with APP gene. Qiu and coworkers (1996) also observed serine-protease-degradation if complexed with α_2-macroglobulin.

In summary, more evidence from work of us and others emerges to strengthen the assumption that neurons are indeed actively contributing to ß-Amyloid clearance, especially as subtle alterations of the balance between anabolism and catabolism of a peptide over a long period of time determines circumstantially its *in vivo* amount. In this light, it is interesting that in most cases of early-onset familial Alzheimer disease cases, ß-Amyloid accumulation is caused by only approximately 50% increase in ß-Amyloid anabolism (Hardy, 1997). In contrast, most of the sporadic cases of Alzheimer disease do not seem to accompany such simple overproduction of ß-Amyloid (Scheuner et al., 1996). Therefore, aging-associated reduction of catabolism is a strong candidate mechanism that could account for the accumulation in senile brain.

As the clearance of a given peptide from the brain may also be achieved by transport to vascular systems, more work has to be done in order to estimate the impact of neuronal ß-Amyloid clearance in total peptide degradation.

Of equal importance for the net buildup of ß-Amyloid is its anabolism. Ample work demonstrated that transmembrane APP is cleaved into various fragments, including the ß-

Amyloid isoforms (1-40) and (1-42), by different secretases acting in concert (Haass and Selkoe, 1993). There is also evidence that early endosomes, which are involved in the cellular uptake and degradation of ß-Amyloid (see above), are simultaneously a major site of ß-Amyloid production in normal cells. This speculation is sustained by work of Cataldo and coworkers (2000), observing that endocytic pathway abnormalities, e.g. enlargement and elevated levels of markers of internalization as rab5, preceded ß-Amyloid deposition in neuron in brains of Alzheimer disease patients. However, these approaches do not give insight into the relevance of ß-Amyloid production *in vivo* and to what extent cells of different origin do contribute to the generation of ß-Amyloid.

Busciglio and coworkers (1993a) showed that human astrocytes generated higher levels of ß-Amyloid than any other cell type examined, thereby providing evidence that astrocytes are a major source of ß-Amyloid production in the brain. The relative abundance of the intact and truncated ß-amyloid peptides was highly dependent on cell type. Although astrocytes and neurons produced both major species of ß-Amyloid peptides, neurons generated substantially higher levels of the truncated variants.

In our work, we focused on the release of the more toxic species ß-Amyloid (1-42) in SH-SY5Y as model for neurons and GOS-3 as model for astrocytes in a cell culture system. We did not observe any constitutive release of ß-Amyloid (1-42) in a time frame of 9 hours, whereas we measured a weak release of ß-Amyloid (1-42) in neurons and a more significant release of ß-Amyloid (1-42) in astrocytes if H_2O_2 was added to the medium in order to generate oxidative stress. These results are in line with findings of Olivieri and coworkers (2001), who observed that incubation with 50μg/l mercury ($HgCl_2$) for 24 hours induced significantly oxidative stress in SH-SY5Y as measured by loss of reduced glutathione and significant release of ß-Amyloid (1-40) and (1-42) into the culture medium. The higher release of the (1-40) fragment than (1-42) reflects the balance *in vivo* in Alzheimer disease and gives further hint for a ROS-induced production of ß-Amyloid in the brain of Alzheimer disease rather than a ß-Amyloid-induced oxidative stress. Interestingly, they also observed release of both peptides after addition of the antioxidant N-acetyl-L-cysteine (NAC) with or without stressing agent. Zhang and coworkers (1997) conducted studies determining the processing of APP by western blot during H_2O_2-induced apoptosis in SH-SY5Y cells. H_2O_2 induced altered APP processing

to fragments containing ß-Amyloid. Anti-ß-Amyloid-antibodies recognized this fragment, anti-C terminal antibody not, suggesting an oxidative stress-induced shift from α- to β-cleavage of APP. H_2O_2-induced release of ß-Amyloid was also observed in monkey eye lenses (Frederikse et al., 1996).

We can only speculate how oxidative stress induces the production and/or release of ß-Amyloid. Oxidative stress appears to be a messenger provoking downstream cellular events. These include activating/deactivating transcription factors, regulating cell cycle, DNA synthesis, and apoptosis (for review, see Kamata and Hirata, 1999). Changes could then affect APP metabolism and ß-Amyloid secretion (Olivieri et al., 2000). Also, H_2O_2 could induce rapid increase of ß-Amyloid-concentration inside the cell to reach an aggregation-threshold and thereby trigger the death program. Then, the extracellular ß-Amyloid in turn could lead to more apoptosis in neighboring cells in the microenvironment. It should be pointed out that the persistent existence of the unknown initiator(s) is a pre-condition for running these vicious cycles, as the assumptions above do not explain the initial stages of Alzheimer disease. To better understand Alzheimer disease, it is of crucial importance to identify the initiator(s).

Does blood plasma ß-Amyloid contribute to the accumulation of ß-Amyloid deposits in the brain?

We observed that oxidative stress induced the release of ß-Amyloid (1-42) in SH-SY5Y cells as model for neurons and GOS-3 cells as model for astrocytes. Taking into consideration that these results suggest that cells from different origins can obviously produce/release the peptide, we addressed the question to what extent non-brain cells also contribute to the production of ß-Amyloid in the body and eventually to the formation of ß-Amyloid plaques in the brains of Alzheimer disease patients. As the brain only represents a small fraction of the total body weight, production and release of ß-Amyloid by non-cerebral cells could have a crucial impact on the overall production of ß-Amyloid. Therefore, we added H_2O_2 in order to generate oxidative stress to whole blood collected from randomly selected individuals and measured the amount of released ß-Amyloid (1-42). Indeed, we observed a significant increase in free, soluble ß-Amyloid (1-42) in the

plasma induced by the *ex vivo* addition of H_2O_2. This is strong evidence for the possibility of a substantial contribution of the body for the generation of ß-Amyloid in the brain as a specific response to oxidative stress, as activation of human platelets, which are regarded as the primary source of circulating APP and ß-Amyloid in the blood, did not release these peptides into the plasma upon stimulation with adenosin diphosphate, collagen, thrombin or similar physiological agonists of platelet activation (Olsson et al., 2003).

However, it is still unknown to what extent blood plasma ß-Amyloid can cross the blood-brain barrier in order to reach its ultimate destination. There is proof that blood ß-Amyloid is mostly bound to plasma albumin (Biere et al., 1996), the most abundant protein in both plasma and CSF (Braunwald et al., 1987). Besides its function in stabilizing the osmotic pressure of fluids, it is one of the most important physiological transport proteins. It binds and transports a variety of small molecules, including peptides and drugs, and plays a vital role in lipid metabolism by transporting fatty acids. Only a small percentage of endogenous plasma albumin crosses the intact blood brain barrier (for review, see Putnam 1975). However, this situation is altered during pathological openings of the blood-brain barrier, e.g. head trauma, which is known to play a role as a risk factor that can contribute to the development of Alzheimer disease. For example, massive cerebral ß-Amyloid accumulation has been reported in professional boxers experiencing multiple episodes of brain trauma. One can therefore speculate that an increased influx of albumin-bound ß-Amyloid across a transiently or permanently altered blood-brain barrier could play a role in accumulation of ß-Amyloid in the brain. Indeed, the ability of circulating synthetic ß-Amyloid to accrue on existing plaque has been reported in living monkeys (Ghilardi et al., 1996) and there is also evidence that iodinated ß-Amyloid (1-40) injected intravenously into rodents can pass the blood-brain barrier and accumulate within the brain parenchyma and CSF *in vivo* (Maness et al., 1994; Zlokovic et al., 1993). Moreover, it has been observed that efficient, bi-directional, receptor-mediated mechanisms could transport ß-Amyloid through the blood-brain barrier, e.g. Apo J (Shibata et al., 2000; Zlokovic et al., 1994, 1996), and conversely that exogenous ß-Amyloid was rapidly transported from CSF to plasma with an elimination half-life of some 30 minutes after intracerebral microinjection in young mice (Shibata et al., 2000).

DeMattos and coworkers (2001) have confirmed and extended this work by showing that a monoclonal antibody directed against the central domain of ß-Amyloid formed complexes with ß-Amyloid in plasma and dramatically enhanced the transfer to the peripheral circulation in the CSF.

In summary, these data allow us to postulate that blood plasma ß-Amyloid, released by still unknown agents (erythrocytes, leucocytes, trombocytes, lipoproteins or other) upon stimulation by oxidative stress, might indeed contribute to the formation of ß-Amyloid plaques in the brains of Alzheimer disease patients.

A new model for the development of Alzheimer disease

Based on our and other findings, we propose a new model to explain the progression of Alzheimer disease. In contrary to previous models, we assume that ß-Amyloid is not central, but one necessary element playing in concert with other agents in this neurodementia.

Oxidative stress is a phenomenon that occurs in the whole body and increases with age. The living organism has invented different tools to fight against this inevitable insult: for example specific enzymes that degrade peroxides in order to eliminate these putatively toxic agents. We believe that another way to fight against oxidative attack is the generation and release of soluble, monomeric amyloidogenic peptides, e.g. parkin, α-synuclein, huntingtonin, amylin, and ß-Amyloid as the most prominent example in Alzheimer disease. Thereby, multiple cellular rescue-pathways are triggered: For example, we observed that the cellular uptake of these monomeric ß-Amyloid peptides induced a decrease of intracellular reactive oxygen species in neurons. Furthermore, these amyloidogenic peptides have the inherent capacity to reduce the burden of oxidative stress by getting oxidized themselves, leading to destabilization of the protein secondary structure and eventually to an accelerated self-aggregation. Thereby, the living cell is able to circumvent the oxidative stress that would otherwise have lethal impact on the cell. In sum, the increased oxidative stress leads to increased production of amyloidogenic peptides, ß-Amyloid in the case of Alzheimer disease.

Sustained oxidative stress then induces continuous production of ß-Amyloid and subsequently enhanced ß-Amyloid-clearance. Ultimately, a point is reached where intracellular degradation pathways cannot cope with the burden of the peptide and ß-Amyloid accumulates inside the cell. Ultimately, a self-aggregation threshold concentration is reached in some intracellular compartments. Thereby, the anti-oxidative, monomeric ß-Amyloid acquires during self-association some pro-oxidative functions that are able to damage the neuron, presumably by damaging membranes, e.g. by altering membrane properties and by peroxidizing lipids. Thus, the aggregated ß-Amyloid peptide itself contributes at this point to the sustained oxidative stress. In a self-accelerating vicious cycle, the affected cell tries to fight against this oxidative insult by increasing the production of anti-oxidative, monomeric ß-Amyloid, possibly by the activation of NFκB, thereby even increasing the intracellular concentration of the peptide and enhancing its aggregation and development of pro-oxidative functions. Thus, this feedback loop eliminates one pathway of the cell in fighting against oxidative stress (by presenting monomeric ß-Amyloid to peroxides), and does even generate cell-inherent pro-oxidative agents that enhance the overall oxidative insult, leading ultimately to neuronal loss.
We can further speculate that dying neurons and excessive ß-Amyloid plaques would then activate astroglia and microglia (Araujo and Cotman, 1992), generating inflammation, which leads to increased release of peroxides. Thereby the vicious circle is accelerated and neuronal loss increased.

One premise of this attractive hypothesis is that ß-Amyloid is produced to fight against oxidative stress. Therefore, addition of soluble, monomeric ß-Amyloid to neuron-like cells in the presence of H_2O_2 as oxidative agent should circumvent cell death. Preliminary data concerning such a system were contradictory. Addition of monomeric ß-Amyloid (1-40) at low concentration did not alter H_2O_2-induced toxicity significantly. Increasing the concentration of ß-Amyloid (1-40) circumvented the toxicity partially, but not reproducibly. Further increase of ß-Amyloid (1-40) concentration seemed then to potentiate H_2O_2-induced toxicity (data not shown). We assume that the load of monomeric ß-Amyloid (1-40) that would be necessary to circumvent the lethal effect of

H_2O_2 already leads to neuronal plasma-membrane-mediated formation of aggregates which are rather pro-oxidative and toxic.

This is one example of the difficulties that a researcher encounters when simulating a decade-long process as Alzheimer disease in an acceptable time frame of only few days.

REFERENCES

Akama, K. T., Albanese, C., Pestell, R. G., and Van Eldik, L. J. (1998). Amyloid ß-peptide stimulates nitric oxide production in astrocytes through an NFκB-dependent mechanism. *Proceedings of the National Academy of Sciences of the United States of America*, **95**, 5795-5800

Amoroso, S., Gioielli, A., Cataldi, M., Di Renzo, G., and Annunziato, L. (1999) In the neuronal cell line SH-SY5Y, oxidative stress-induced free radical overproduction causes cell death without any participation of intracellular Ca^{2+} increase. *Biochimica et biophysica acta*, **1452**, 151-160

Andreasen, N., Minthon, L., Davidsson, P., Vanmechelen, E., Vanderstichele, H., Winblad, B., and Blennow, K. (2001). Evaluation of CSF-tau and CSF-Aß42 as diagnostic markers for Alzheimer Disease in clinical practice. *Archives of neurology*, **58**, 373-379

Araujo, D. M. and Cotman, C. W. (1991). ß-Amyloid stimulates glial cells in vitro to produce growth factors that accumulate in senile plaques in Alzheimer's disease. *Brain research*, **569**, 141-145

Ard, M. D., Cole, G. M., Wei, J., Mehrle, A. P., and Fratkin, J. D. (1996). Scavenging of Alzheimer's amyloid beta-protein by microglia in culture. *Journal of neuroscience research*, **43**, 190-202

Arispe, N., Pollard, H. B., and Rojas, E. (1993). Giant multilevel cation channels formed by Alzheimer disease amyloid ß-protein [Aß(1-40)] in bilayer membranes. *Proceedings of the National Academy of Sciences of the United States of America*, **90**, 10573-10577

Avdulov, N. A., Chochina, S. V., Igbavboa, U., O'Hare, E. O., Schroeder, F., Cleary, J. P., and Wood, W. G. (1997). Amyloid beta-peptides increase annular and bulk fluidity and induce lipid peroxidation in brain synaptic plasma membranes. *Journal of neurochemistry*, **68**, 2086-2091

Avdulov, N. A., Chochina, S. V., Igbavboa, U., Warden, C. S., Vassiliev, A. V., and Wood, W. G. (1997). Lipid binding to amyloid ß-peptide aggregates: preferential binding of cholesterol as compared with phosphatidylcholine and fatty acids. *Journal of Neurochemistry*, **69**, 1746-1752

Balazs, L. and Leon, M. (1994). Evidence of an oxidative challenge in the Alzheimer's brain. *Neurochemical research*, **19**, 1131-1137

Bales, K. R., Du, Y., Dodel, R. C., Yan, G.-M., Hamilton-Byrd, E., and Paul, S. M. (1998). The NF-κB/Rel family of proteins mediates Aß-induced neurotoxicity and glial activation. *Molecular brain research*, **57**, 63-72

Bales, K. R., Du, Y., Holtzman, D., Cordell, B., and Paul, S. M. (2000). Neuroinflammation and Alzheimer's disease: critical roles for cytokine/Aß-induced glial activation, NF-κB, and apolipoprotein E. *Neurobiology of aging*, **21**, 427-432

Bales, K. R., Xu, Q., Du, Y., and Paul, S. M. (1999). Amyloid ß-peptide stimulates apolipoprotein E synthesis and release in a murine microglial cell line via an NF-κB-dependent mechanism. *Abstracts - Society for Neuroscience*, **25**, 14

Barger, S. W., Hörster, D., Furukawa, K., Goodman, Y., Krieglstein, J., and Mattson, M. P. (1995). Tumor necrosis factors α and ß protect neurons against amyloid ß-peptide toxicity: Evidence for involvement of a κB-binding factor and attenuation of peroxide and Ca2+ accumulation. *Proceedings of the National Academy of Sciences of the United States of America*, **92**, 9328-9332

Barnham, K. J., Ciccotosto, G. D., Tickler, A. K., Ali, F. E., Smith, D. G., Williamson, N. A., Lam, Y. H., Carrington, D., Tew, D., Kocak, G., Volitakis, I., Separovic, F., Barrow, C. J., Wade, J. D., Masters, C. L., Cherny, R. A., Curtain, C. C., Bush, A. I., and Cappai, R. (2003). *The Journal of biological chemistry*, Epub, Aug 18

Barrow, C. J. and Zagorski, M. G. (1991). Solution structures of ß peptides and its constituent fragments: relation to amyloid deposition. *Science*, **253**, 179-182

Barrow, C. J., Yasuda, A., Kenny, P. T., and Zagorski, M. G. (1992). Solution conformations and aggregational properties of synthetic amyloid ß peptides of AD. *Journal of molecular biology*, **225**, 1075-1093

Behl, C. (1997). Amyloid ß-protein toxicity and oxidative stress in Alzheimer's disease. *Cell and tissue research*, **290**, 471-480

Behl, C., Davis, J. B., Lesley, R. and Schubert, D. (1994). Hydrogen peroxide mediates Amyloid ß protein toxicity. *Cell*, **77**, 817-827

Biedler, J. L., Helson, L., and Spengler, B. A. (1973). Morphology and growth, tumorigenicity, and cytogenetics of human neuroblastoma cells in continuous culture. *Cancer research*, **33**, 2643-2652

Biere, A. L., Ostaszewski, B., Stimson, E. R., Hyman, B. T., Maggio, J. E., and Selkoe, D. J. (1996). Amyloid ß-peptide is transported on lipoproteins and albumin in human plasma. *The Journal of biological chemistry*, **271**, 32916-32922

Bishop, G. M. and Robinson, S. R. (2003). Human Abeta (1-42) reduces iron-induced toxicity in rat cerebral cortex. *Journal of neuroscience research*, **73**, 316-323

Blanc, E. M., Toborek, M., Mark, R. J., Hennig, B., and Mattson, M. P. (1997). Amyloid ß-peptide induces cell monolayer albumin permeability, impairs glucose transport, and induces apoptosis in vascular endothelial cells. *Journal of neurochemistry*, **68**, 1870-1881

Bonaiuto, C., McDonald, P. P., Rossi, F., and Cassatella, M. A (1997). Activation of nuclear factor-κB by ß-amyloid peptides and interferon-γ in murine microglia. *Journal of neuroimmunology*, **77**, 51-56

Bono, F., Lamarche, I., Bornia, J., Savi, P., Della Valle, G., and Herbert, J. -M. (1999) Nerve growth factor (NGF) exerts its pro-apoptotic effect via the $P75^{NTR}$ receptor in a cell cycle-dependent manner. *FEBS Letters*, **457**, 93-97

Braunwald, E., Isselbacher, K. J., Petersdorf, R. G., Wilson, J. D., Martin, J. B., and Fauci, A. S. (1987). *Harrison's principles of internal medicine, 11th Ed., McGraw-Hill, New York*

Bruce-Keller, A. J., Begley, J. G., Fu, W., Butterfield, D. A., Bredesen, D. E., Hutchins, J. B., Hensley, K., and Mattson, M. P. (1998). Bcl-2 protects isolated plasma and mitochondrial membranes against lipid peroxidation induced by hydrogen peroxide and amyloid beta-peptide. *Journal of neurochemistry*, **70**, 31-39

Bruns, C. M., Hubatsch, I., Ridderstrom, M., Mannervik, B., and Tainer, J. A. (1999). Human glutathione transferase A4 crystal structures and mutagenesis reveal the basis of high catalytic efficiency with toxic lipid peroxidation products. *Journal of molecular biology*, **288**, 427-439

Bui, N. T., Livolsi, A., Peyron, J.-F., and Prehn, J. H. M. (2001). Activation of Nuclear Factor κB and *bcl-x* Survival gene Expression by Nerve Growth Factor Requires Tyrosine Phosphorylation of IκBα. *Journal of Cell Biology*, **152**, 753-763

Burdick, D., Kosmoski, J., Knauer, M. F., and Glabe, C. G. (1997). Preferential adsorption, internalization and resistance to degradation of the major isoform of the Alzheimer's amyloid peptide, Aß 1-42, in differentiated PC12 cells. *Brain Research*, **746**, 275-284

Burdick, D., Soreghan, B., Kwon, M., Kosmoski, J., Knauer, M., Henscher, A., Yates, T., Cotman, C., and Glabe, C. (1992). Assembly and aggregation properties of synthetic Alzheimer's A4/ß amyloid peptide analogs. *The Journal of biological chemistry*, **267**, 546-554

Busciglio, J., Gabuzda, D. H., Matsudaira, P., and Yankner, B. A. (1993a). Generation of ß-Amyloid in the secretory pathway in neuronal and nonneuronal cells. *Proceedings of the National Academy of Sciences of the United States of America*, **90**, 2092-2096

Busciglio, J., Lorenzo, A., Yeh, J., and Yankner, B. A. (1995). ß-Amyloid fibrils induce tau phosphorylation and loss of microtubule binding. *Neuron*, **14**, 879-888

Busciglio, J., Yeh, J., and Yankner, B. A. (1993b). Beta-Amyloid neurotoxicity in human cortical culture is not mediated by excitotoxins. *Journal of neurochemistry*, **61**, 1565-1568

Butterfield, D. A., Hensley, K., Harris, M., Mattson, M., and Carney, J. (1994). Beta-amyloid peptide free radical fragments initiate synaptosomal lipoperoxidation in a sequence-specific fashion: implications to Alzheimer's disease. *Biochemical and biophysical research communications*, **200**, 710-715

Butterfield, D. A and Kanski, J. (2002). Methionine 35 residue is critical for the oxidative stress and neurotoxic properties of Alzheimer's amyloid ß-peptide 1-42. *Peptides*, **23**, 1299-1309

Camilleri, P., Haskins, N. J., and Howlett, D. R. (1994). ß-Cyclodextrin interacts with the Alzheimer amyloid ß-A4 peptide. *FEBS Letters*, **341**, 256-258

Canning, D. R., McKeon, R. J., DeWitt, D. A., Perry, G., Wujek, J. R., Frederickson, R. C. A., and Silver, J. (1993). ß-Amyloid of Alzheimer's disease induces reactive gliosis that inhibits axonal outgrowth. *Experimental neurology*, **124**, 289-298

Carette, B., Poulain, P., and Delacourte, A. (1993). Electrophysiological effects of 25-35 amyloid-ß-protein on guinea-pig lateral septal neurons. *Neuroscience letters*, **151**, 111-114

Cassarino, D. S., Halvorsen, E. M., Swerdlow, R. H., Abramova, N. N., Parker, D., Jr., Sturgill, T. W., and Bennett, J. P. Jr. (2000). Interaction among mitochondria, mitogen-activated protein kinases, and nuclear factor-κB in cellular models of Parkinson's disease. *Journal of neurochemistry*, **74**, 1384-1392

Cassarino, D. S., Swerdlow, R. H., Parks, J. K., Parker, Jr. W. D., and Bennet, Jr. J. P. (1998). Cyclosporin A increases resting mitochondrial membrane potential in SY5Y cells and reverses the depressed mitochondrial membrane potential of Alzheimer's disease cybrids. *Biochemical and biophysical research communications*, **248**, 168-173

Cataldo, A. M., Peterhoff, C. M., Troncoso, J. C., Gomez-Isla, T., Hyman, B. T., and Nixon, R. A. (2000). Endocytic pathway abnormalities precede Amyloid ß deposition in sporadic Alzheimer's disease and Down syndrome. *American journal of pathology*, **157**, 277-286

Chauhan, V. P. S., Chauhan, A., and Wegiel, J. (2000). Fibrillar amyloid ß-protein forms a membrane-like hydrophobic domain. *Neuroreport*, **12**, 587-590

Chauhan, A., Chauhan, V. P. S., Bockerhoff, H. and Wisniewski, H. M. (1993). Effect of amyloid beta-protein on membrane properties in Alzheimer's disease. *Advances in Clinical and Basic Research, Wiley and Sons, NY*, 431-439

Chochina, S. V., Avdulov, N. A., Igbavboa, U., Cleary, J. P., O'Hare, E. O., and Wood, W. G. (2001). Amyloid ß-peptide$_{1-40}$ increases neuronal membrane fluidity: role of cholesterol and brain region. *Journal of lipid research*, **42**, 1292-1297

Choo-Smith, L.-P. and Surewicz, W. K. (1997). The interaction between Alzheimer amyloid ß(1-40) peptide and ganglioside GM1-containing membranes. *FEBS Letters*, **402**, 95-98

Chu, T., Tran, T., Yang, F., Beech, W., Cole, G. M., and Frautschy, S. A. (1998). Effect of chloroquine and leupeptin on intracellular accumulation of amyloid-ß (Aß) 1-42 peptide in a murine N9 microglia cell line. *FEBS Letters*, **436**, 439-444

Chung, H., Brazil, M. I., Soe, T. T., and Maxfield, F. R. (1999). Uptake, degradation and release of fibrillar and soluble forms of Alzheimer's amyloid ß-peptide by microglial cells. *The Journal of biological chemistry*, **274**, 32301-32308

Combs, C. K., Karlo, J. C., Shih-Chu, K., and Landreth, G. E. 92001). ß-Amyloid stimulation of microglia and monocytes results in TNFα-dependent expression of inducible nitric oxide synthase and neuronal apoptosis. *Journal of neuroscience*, **21**, 1179-1188

Copani, A., Koh, J.-Y., and Cotman, C. W. (1991). ß-Amyloid increases neuronal susceptibility to injury by glucose deprivation. *Neuroreport*, **2**, 763-765

Coyle, J. T. and Puttfarcken, P. (1993). Oxidative stress, glutamate, and neurodegenerative disorders. *Science*, **262**, 689-694

Cribbs, D. H., Pike, C. J., Weinstein, S. L., Velazques, P., and Cotman, C. W. (1997). All-D-enantiomers of ß-amyloid exhibit similar biological properties to all-L-ß-amyloids. *The Journal of biological chemistry*, **272**, 7431-7436

Cuajungco, M. P., Goldstein, L. E., Nunomura, A., Smith, M. A., Lim, J. T., Atwood, C. S., Huang, X., Farrag, Y. W., Perry, G., and Bush, A. I. (2000). Evidence that the ß-amyloid plaques of Alzheimer's disease represent the redox-silencing and entombment of Aß by zinc. *The Journal of biological chemistry*, **275**, 19439-19442

Daniels, W. M., van Rensburg, S. J., van Zyl, J. M., and Taljaard, J. J. (1998). Melatonin prevents beta-amyloid-induced lipid peroxidation. *Journal of pineal research*, **24**, 78-82

Davis, D. G., Schmitt, F. A., Wekstein, D. R., and Markesbery, W. R. (1999). Alzheimer neuropathologic alterations in aged cognitively normal subjects. *Journal of neuropathology and experimental neurology*, **58**, 376-388

Deane, R., Yan, S. D., Submamaryan, R. K., LaRue, B., Jovanovic, S., Hogg, E., Welch, D., Manness, L., Lin, C., Yu, J., Armstrong, D. L., Arnold, B., Liliensiek, B., Nawroth, P., Hofman, F., Kindy, M., Stern, D., and Zlokovic, B. (2003). RAGE mediates amyloid-ß peptide transport across the blood-brain barrier and accumulation in brain. *Nature medicine*, **9**, 907-913

Deliconstantinos, G. (1995). Cortisol effect on Na^+/K^+-ATPase activity and on bilayer fluidity of dog brain synaptosomal plasma membranes. *Neurochemical research*, **10**, 1605-1613

DeMattos, R. B., Bales, K. R., Cummins, D. J., Dodart, J. C., Paul, S. M., and Holtzman, D. M. (2001). Peripheral anti-Aß antibody alters CNS and plasma Aß clearance and decreases brain Aß burden in a mouse model of Alzheimer's disease. *Proceedings of the National Academy of Sciences of the United States of America*, **98**, 8850-8855

DeWitt, D. A., Perry, G., Cohen, M., Doller, C., and Silver, J. (1998). Astrocytes regulate microglial phagocytosis of senile plaque cores of Alzheimer's disease. *Experimental neurology*, **149**, 329-340

Ditaranto, K., Tekirian, T. L., and Yang, A. J. (2001). Lysosomal membrane damage in soluble Aß-mediated cell death in Alzheimer's disease. *Neurobiology of disease*, **8**, 19-31

Duff, K., Eckman, C., Zehr, C., Yu, X., Prada, C. –M., Perez-Tur, J., Hutton, M., Buee, L., Harigaya, Y., Yager, D., Morgan, D., Gordon, M. N., Holcomb, L., Refolo, L., Zenk, B., Hardy, J., and Younkin, S. (1996). Increased amyloid-ß42(43) in brains of mice expressing mutant presenilin 1. *Nature*, **383**, 710-713

Duffy, P. E., Rapport, M., and Graf, L. (1990). Glial fibrillary acidic protein and Alzheimer-type senile dementia. *Neurology*, **30**, 778-782

El Khoury, J., Hickman, S. E., Thomas, C. A., Cao, L., Silverstein, S. C., and Loike, J. D. (1996). Scavenger receptor-mediated adhesion of microglia to ß-amyloid fibrils. *Nature*, **382**, 716-719

Engstrom, I., Ronquist, G., Petterson, L., and Waldenstrom, A. (1995). Alzheimer amyloid ß peptides exhibit ionophore-like properties in human erythrocytes. *European journal of clinical investigation*, **25**, 471-476

Esler, W. P., Simson, E. R., Ghilardi, J. R., Vinters, H. V., Lee, J. P., Mantyh, P. W., and Maggio, J. E. (1996). In vitro growth of Alzheimer's Disease ß-Amyloid plaques display first-order kinetics. *Biochemistry*, **35**, 749-757

Esler, W. P. Stimson, E. R., Ghilardi, J. R., Felix, A. M., Lu, Y. -A., Vinters, H. V., Mantyh, P. W., and Maggio, J. E. (1997). Aß deposition inhibitor screen using synthetic amyloid. *Nature Biotechnology*, **15**, 258-63

Esterbauer H., and Cheeseman K.,H. (1991). Determination of aldehydic lipid peroxidation products: malonaldehyde and hydroxymonenal. *Methods in Enzymology. Ed Parcker L, Glazer A. New York: Academic Press*, 186(B), 407-421

Esterbauer, H., Schaur, R., and Zollner, H. (1991). Chemistry and biochemistry of 4-hydroxynonenal, malonaldehyde, and related aldehydes. *Free Radical biology & medicine*, **11**, 81-128

Felician, O., and Sandson, T. A., (1999). The neurobiology and pharmacology of Alzheimer's disease. *Journal of neuropsychiatry and clinical neurosciences*, **11**, 19-31

Ferrer, I., Marti, E., Lopez, E., and Tortosa, A. (1998). NFκB-Immunoreactivity is observed in association with ßA4 diffuse plaques in patients with Alzheimer's disease. *Neuropathology and applied neurobiology*, **24**, 271-277

Findeis, M. A., Musso, G. M., Arico-Muendel, C. C., Benjamin, H. W., Hundal, A. M., Lee, J.-J., Chin, J., Kelley, M., Wakefield, J., Hayward, N. J., and Molineaux, S. M. (1999). Modified-peptide inhibitors of amyloid ß-peptide polimerization. *Biochemistry*, **38**, 6791-6800

Foehr, E. D., Lin, X., O'Mahony, A., Geleziunas, R., Bradshaw, R. A., and Greene, W. C. (2002). NF-κB signaling promotes both cell survival and neurite process formation in nerve growth factor-stimulated PC12 cells. *Journal of neuroscience*, **20**, 7556-7563

Fraser, P. E., McLachlan, D. R., Surewicz, W. K., Mizzen, C. A., Snow, A. D., Nguyen, J. T., and Kirschner, D. A. (1994). Conformation and fibrillogenesis of Alzheimer Aß peptides with selected substitutions of charged residues. *Journal of molecular biology*, **244**, 64-73

Fraser, P. E., Nguyen, J. T., Surewicz, W. K., and Kirschner, D. A. (1991). PH-dependent structural transitions of Alzheimer amyloid peptides. *Biophysical journal*, **60**, 1190-1201

Frackowiak, J., Wisniewski, H. M., Wegiel, J., Merz, G. S., Iqbal, K., and Wang, K. C. (1992). Ultrastructure of the microglia that phagocytose amyloid and the microglia that produce beta-amyloid fibrils. *Acta neuropathologica (Berl.)*, **84**, 225-233

Frautschy, S. A., Baird, A., and Cole, G. M. (1991). Effects of injected Alzheimer ß-amyloid cores in rat brain. *Proceedings of the National Academy of Sciences of the United States of America*, **88**, 8362-8366

Frautschy, S. A., Cole, G. M, and Baird, A. (1992). Phagocytosis and deposition of vascular beta-amyloid in rat brains injected with Alzheimer beta-amyloid. *American journal of pathology*, **140**, 1389-1399

Frederikse, P. H., Garland, D., Ziegler, J. S. Jr., and Piatigorsky, J. (1996). Oxidative stress increases production of beta-amyloid precursor protein and beta-amyloid (Abeta) in mammalian lenses, and Abeta has toxic effects on lens epithelial cells. *The Journal of biological chemistry*, **271**, 10169-10174

Fukumoto, H., Tennis, M., Locascio, J. J., Hyman, B. T., Growdon, J. H., and Irizarry, M. C. (2003). Age but not diagnosis is the main predictor of plasma ß-protein levels. *Archives of neurology*, **60**, 958-964

Galdzicki, Z., Fukuyama, R., Wadhwani, K. C., Rapoport, S. I., and Ehrenstein, G. (1994). ß-amyloid increases choline conductance of PC12 cells: possible mechanisms of toxicity in Alzheimer's disease. *Brain research*, **646**, 332-336

Games, D., Adams, D., Alessandrini, R., Barbour, R., Berthelette, P., Blackwell, C., Carr, T., Clemens, J., Donaldson, T., Gillespie, F., Guido, T., Hagopian, S., Johnson-Wood, K., Khan, K., Lee, M., Leibowitz, P., Lieberburg, I., Little, S., Masliah, E., McConlogue, L., Montoya-Zavala, M., Mucke, L., Paganini, L., Penniman, E., Power, M., Schenk, D., Seubert, P., Snyder, B., Soriano, F., Tan, H., Vitale, J., Wadsworth, S., Wolozin, B., and Zhao, J. (1995). Alzheimer-type neuropathology in transgenic mice overexpressing V717F ß-amyloid precursor protein. *Nature*, **373**, 523-527

Gao, Z., Huang, K., and Xu, H. (2001). Protective effects of flavanoids in the roots of scutellaria baicalensis georgi against hydrogen peroxide-induced oxidative stress in SH-SY5Y cells. *Pharmacological Research*, **43**, 173-178

Gasic-Milenkovic, J., Loske, C., and Münch, G. (2003). Advanced glycation endproducts cause lipid peroxidation in the human neuronal cell line SH-SY5Y. *Journal of Alzheimer's disease*, **5**, 25-30

Genain, C. P., Cannella, B., Hauser, S. L., and Raine, C. S. (1999). Identification of autoantibodies associated with myelin damage and multiple sclerose. *Nature Medicine*, **5**, 170-175

Ghanta, J., Shen, C.-L., Kiessling, L. L., and Murphy, R. M. (1996). A strategy for designing inhibitors of ß-amyloid toxicity. *The Journal of biological chemistry*, **271**, 29525-29528

Ghilardi, J. R., Catton, M., Stimson, E. R., Rogers, S., Walker, L. C., Maggio, J. E., and Mantyh, P. W. (1996). Intra-arterial infusion of [125]A beta 1-40 labels amyloid deposits in the aged primate brain in vivo. *Neuroreport*, **7**, 2607-2611

Gibson, G. E., Zhang, H., Sheu, K. R., and Park, L. C. (2000). Differential alterations in antioxidant capacity in cells from Alzheimer patients. *Biochimica et biophysica acta*, **1502**, 319-329

Glenner, G. G., and Wong, C. W. (1984). Alzheimer's disease and Down's syndrome: sharing of a unique cerebrovascular amyloid fibril protein. *Biochemical and biophysical research communications*, **122**, 1131-1135

Good, T. A. and Murphy, R. M. (1995). Aggregation state-dependent binding of ß-amyloid peptide to protein and lipid components of rat cortical homogenates. *Biochemical and biophysical research commununications*, **207**, 209-215

Goodman, Y. and Mattson, M. P. (1994). Secreted forms of ß-amyloid precursor protein protect hippocampal neurons against amyloid ß-peptide-induced oxidative injury. *Experimental neurology*, **128**, 1-12

Goodman, Y., Steiner, M. R., Steiner, S. M., and Mattson, M. P. (1994). Nordihydroguaiaretic acid protects hippocampal neurons against amyloid ß-peptide toxicity, and attenuates free radical and calcium accumulation. *Brain research*, **654**, 171-176

Gould, R. J., and B. H. Ginsberg (1985). Membrane fluidity and membrane receptor function. *R. C. Aloia and J. M. Boggs (eds.), Membrane Fluidity in Biology, New York: Academic Press*, 257-280

Gregon, L., Bhasin, R., and Goldgaber, D. (1994). Ubiquitin-mediated degradative pathway degrades the extracellular but not the intracellular form of Amyloid-ß-protein precursor. *Biochemical and biophysical research communications*, **203**, 1731-1738

Gridley, K. E., Green, P. S., and Simpkins, J. W. (1997). Low concentrations of estradiol reduce beta-amyloid (25-35)-induced toxicity, lipid peroxidation and glucose utilization in human SK-N-SH neuroblastoma cells. *Brain research*, **778**, 158-165

Guan, Z., Wang, Y., Cairns, N. J., Lantos, P. L., Dallner, G., and Sindelar, P. J. (1999). Decrease and structural modifications of phosphatidylethanolamine plasmalogen in the brain with Alzheimer disease. *Journal of neuropathology and experimental neurology*, **58**, 740-747

Guo, Q., Robinson, N., and Mattson, M. P. (1998). Secreted ß-Amyloid precursor protein counteracts the proapoptotic action of mutant presenilin-1 by activation of NFκB and stabilization of calcium homeostasis. *The Journal of Biological Chemistry*, **273**, 12341-12351

Haass, C. A. and Selkoe, D. J. (1993). Cellular processing of ß-Amyloid precursor protein and the genesis of Amyloid ß-peptide. *Cell*, **75**, 1039-1042

Haass, C. A., Schlossmacher, M. G., Hung, A. Y., Vigo-Pelfrey, C., Mellon, A., Ostaszewski, B. C., Lieberburg, I., Koo, E. H., Schenk, D., Teplow, D. B., and Selkoe, D. J. (1992). Amyloid beta-peptide is produced by cultured cells during normal metabolism. *Nature*, **359**, 322--325

Halfter, H., Kremerskothen, J., Weber, J., Hacker-Klom, U., Barnekow, A., Ringelstein, E. B., and Stogbauer, F. (1998a). Growth inhibition of newly established human glioma cell lines by leukemia inhibitory factor. *Journal of neuro-oncology*, **39**, 1-18

Halfter, H., Lotfi, R., Westermann, R., Young, P., Ringelstein, E. B., and Stogbauer, F. T. (1998b). Inhibition of growth and induction of differentiation of glioma cell lines by Oncostatin M (OSM). *Growth Factors*, **15**, 135-147

Halliwell, B. (1992). Reactive oxygen species and the central nervous system. *Journal of neurochemistry*, **59**, 1609-1623

Hammad, S. M., Ranganathan, S., loukinova, E., Twal, W. O., and Aegraves, W. S. (1997). Interaction of Apolipoprotein J-Amyloid ß-peptide Complex with Low Density Lipoprotein Receptor-related Protein-2/Megalin. *The Journal of biological chemistry*, **272**, 18644-18649

Hardy, J. (1997). Amyloid, the presenilins and Alzheimer's disease. *Trends in neurosciences*, **20**, 154-159

Hardy, J. A. and Higgins, G. A. (1992). Alzheimer's disease: The Amyloid cascade hypothesis. *Science*, **256**, 184-185

Harper, J. D. and Lansbury, P. T. (1997). Models of amyloid seeding in Alzheimer's Disease and scrapie. *Annual review of biochemistry*, **66**, 385-407

Hartley, D. M., Walsh, D. M., Ye, Ch. P., Diehl, T., Vasquez, S., Vassilev, P. M., Teplow, D. B., and Selkoe, D. S. (1999). Protofibrillar intermediates of amyloid ß-protein induce acute electrophysiological changes and progressive neurotoxicity in cortical neurons. *Journal of neurosciences*, **19**, 8876-8884

Hartmann, H., Eckert, A., and Müller, W. E. (1993). ß-Amyloid protein amplifies calcium signaling in central neurons from the adult mouse. *Biochemical and biophysical research communications*, **194**, 1216-1220

Hartmann, H., Eckert, A., and Müller, W. E. (1994). Apolipoprotein E and cholesterol affect neuronal calcium signaling: the possible relationship to ß-amyloid neurotoxicity. *Biochemical and biophysical research communications*, **200**, 1185-1192

Heese, K., Hock, C., and Otten, U. (1998). Inflammatory signals induce neurotrophin expression in human microglial cells. *Journal of neurochemistry*, **70**, 699-707

Helmer, C., Joly, P., Letenneur, L., Commenges, D., and Dartigues, J. F. (2001). Mortality with dementia: results from a French prospective community-based cohort. *American journal of epidemiology*, **154**, 642-648

Hensley, K., Carney, J. M., Mattson, M. P., Aksenova, M., Harris, M., Wu, J. F., Floyd, R. A., and Butterfield, D. A. (1994). A model for ß-amyloid aggregation and neurotoxicity based on free radical generation by the peptide: relevance to Alzheimer's disease. *Proceedings of the National Academy of Sciences of the United States of America*, **91**, 3270-3274

Hensley, K., Aksenova, M., Carney, J. M., Harris, M., and Butterfield, D. A. (1995a). Amyloid ß-peptide spin trapping I: peptide enzyme toxicity is related to free radical spin trap reactivity. *Neuroreport*, **6**, 493-496

Hensley, K., Aksenova, M., Carney, J. M., Harris, M., and Butterfield, D. A. (1995b). Amyloid ß-peptide spin trapping II: evidence for decomposition of the PBN spin adduct. *Neuroreport*, **6**, 489-492

Hilbich, C., Kisters-Woike, B., Reed, J., Masters, C. L., and Beyreuther, K. (1991). Aggregation and secondary structure of synthetic amyloid ßA4 peptides of Alzheimer's disease. *Journal of molecular biology*, **218**, 149-163

Hilbich, C., Kisters-Woike, B., Reed, J., Masters, C. L., and Beyreuther, K. (1992). Substitutions of hydrophobic amino acids reduce the amyloidogenicity of Alzheimer's Disease ßA4 peptides. *Journal of molecular biology*, **228**, 460-473

Holcomb, L., Gordon, M. N., McGowan, E., Yu, X., Benkovic, S., Jantzen, P., Wright, K., Saad, I., Mueller, R., Morgan, D., Sanders, S., Zehr, C., O'Campo, K., Hardy, J., Prada, C.-M., Eckman, C., Younkin, S., Hsiao, K., and Duff, K. (1998). Accelerated Alzheimer-type phenotype in transgenic mice carrying both mutant amyloid precursor protein and presenilin-1 transgenes. *Nature medicine*, **4**, 97-100

Hong, Z., Haung, M.-S., and Zhou, B. (2001). The association of insulin and the plasma concentration of ß-Amyloid in Alzheimer's disease. *Hong Kong Medical Journal*, **7**, 19

Howlett, D. R., George, A. R., Owen, D. E., Ward, R. V., and Markwell, R. E. (1999a). Common structural features determine the effectiveness of carvedilol, daunomycin, and rolitetracycline as inhibitors of Alzheimer ß-amyloid fibril formation. *The Biochemical journal*, **343**, 419-423

Howlett, D. R., Perry, A. E., Godfrey, F., Swatton, J. E., Jennings, K. H., Spitzfaden, C., Wadsworth, B., Wood, S. J., and Markwell, R. E. (1999b). Inhibition of fibril formation in ß-amyloid peptide by a novel series of benzofurans. *The Biochemical journal*, **340**, 283-289

Hsiao, K., Chapman, P., Nilsen, S., Eckman, C., Harigaya, Y., Younkin, S., Yang, F., and Cole, G. (1996). Correlative memory deficits, Aß elevation, and amyloid plaques in transgenic mice. *Science*, **274**, 99-102

Huang, T. H. J., Yang, D.-S., Plaskos, N. P., Go, S., Yip, C. M., Fraser, P. E., and Charkrabartty, A. (2000). Structural studies of soluble oligomers of the Alzheimer ß-amyloid peptide. *Journal of molecular biology*, **297**, 73-87

Huttunen, H. J., Fages, C., and Rauvala, H. (1999). Receptor for advanced glycation end products (RAGE)-mediated neurite outgrowth and activation of NFκB require the cytoplasmatic domain of the receptor but different downstream signaling pathways. *The Journal of biological chemistry*, **274**, 19919-19924

Ida, N., Masters, C. L., and Beyreuther, K. (1996). Rapid cellular uptake of Alzheimer amyloid ßA4 peptide by cultured human neuroblastoma cells. *FEBS Letters*, **394**, 174-178

Iversen, L. L., Mortishire-Smith, R. J., Pollack, S. J., and Shearman, M. S. (1995). The toxicity in vitro of beta-amyloid protein. *The Biochemical journal*, **311**, 1-16

Iwata, N., Tsubuki, S., Takaki, Y., Watanabe, K., Sekiguchi, M., Hosoki, E., Kawashima-Morishima, M., Lee, H.-J., Hama, E., Sekine-Aizawa, Y., and Saido, T. C. (2000). Identification of the major Aß1-42-degrading catabolic pathway in brain parenchyma: Suppression leads to biochemical and pathological deposition. *Nature Medicine*, **6**, 143-150

Iwatsubo, T., Mann, D. M., Odaka, A., Suzuki, N., and Ihara, Y. (1995). Amyloid beta protein (Aß) deposition: Aß 42(43) precedes Aß 40 in Down syndrome. *Annals of neurology*, **37**, 294-299

Iwatsubo, T., Saido, T. C., Mann, D. M., Lee, V. M., and Trojanowski, J. Q. (1996). Full-length amyloid-ß (1-42(43)) and amino-terminally modified and truncated amyloid-ß 42(43)) deposit in diffuse plaques. *American journal of pathology*, **149**, 1823-1830

Jalava, A. M., Heikkila, J., Akerlind, G., Pettit, G. R., and Akerman, K. E. (1990). Effects of bryostatins 1 and 2 on morphological and functional differentiation of SH-SY5Y human neuroblastoma cells. *Cancer research*, **50**, 3422-3428

Jarrett, J. T., Berger, E. P., and Lansbury, P. T. J. (1993). The carboxy terminus of the ß amyloid protein is critical for the seeding of amyloid formation: implications for the pathogenesis of Alzheimer's Disease. *Biochemistry*, **32**, 4693-4697

Jarrett, J. T. and Lansbury, P. T. (1993). Seeding "one-dimensional crystallization" of amyloid: a pathogenic mechanism in Alzheimer's disease and scrapie? *Cell*, **73**, 1055-1058

Jellinger, K. A. (1996). Structural basis of dementia in neurodegenerative disorders. *Journal of neural transmission. Supplementum*, **47**, 1-29

Jimenez, J.L., Guijarro, J.I., Orlova, E., Zurdo, J., Dobson, C.M., Sunde, M. and Saibil, H. (1999) Cryo-electron microscopy structure of an SH3 amyloid fibril and model of the molecular packing. *The EMBO journal*, **18**, 815-821

Joachim, C. L., Morris, J. H., and Selkoe, D. J. (1987). Clinically diagnosed Alzheimer's disease. Autopsy results in 150 cases. *Annals of neurology*, **24**, 50-56

Joachim, C. L. and Selkoe, D. J. (1992). The seminal role of beta-amyloid in the pathogenesis of Alzheimer disease. *Alzheimer disease and associated disorders*, **6**, 7-34

John, V., Latimer, L. H., Tung, J. S., and Dappen, M. S. (1997). Alzheimer's disease: recent advances on the amyloid hypothesis. *Annual reports in medicinal chemistry*, **32**, 11-20

Johnson-Wood, K., Lee, M., Motter, R., Hu, K., Gordon, G., Barbour, R., Khan, K., Gordon, M., Tan, H., Games, D., Lieberburg, I., Schenk, D., Seubert, P., and McConlogue, L. (1997). Amyloid precursor protein processing and Aß42 deposition in a transgenic mouse model of Alzheimer disease. *Proceedings of the National Academy of Sciences of the United States of America*, **94**, 1550-1555

Joslin, G., Krause, J. E., Hershey, A. D., Adams, S. P., Fallon, R. J., and Perlmutter, D. H. (1991). Amyloid-ß peptide substance P, and bombesin bind to the serpin-enzyme complex receptor. *The Journal of biological chemistry*, **266**, 21897-21902

Kaltschmidt, B., Uherek, M., Volk, B., Baeurle, P., and Kaltschmidt, C. (1997). Transcription factor NF-kappa-B is activated in primary neurons by amyloid peptides and in neurons surrounding early plaques from patients with Alzheimer's disease. *Proceedings of the National Academy of Sciences of the United States of America*, **94**, 2642-2647

Kaltschmidt, B., Uherek, M, Wellmann, H., Volk, B., and Kaltschmidt, C. (1999). Inhibition of NF-κB potentiates amyloid ß-mediated neuronal apoptosis. *Proceedings of the National Academy of Sciences of the United States of America*, **96**, 9409-9414

Kamata, H. and Hirata, H. (1999). Redox regulation of cellular signaling. *Cellular signaling*, **11**, 1-14

Kanfer J. N., Sorrentino, G., and Sitar, D. S. (1999). Amyloid beta peptide membrane perturbation is the basis for its biological effects. *Neurochemical research*, **24**, 1621-1630

Kang, D. E., Pietrzik, C. U., Baum, L., Chevallier, N., Merriam, D. E., Kounnas, M. Z., Wagner, S. L., Troncoso, J. C., Kawas, C. H., Katzman. R., and Koo, E. H. (2000). Modulation of amyloid ß-protein clearance and Alzheimer's disease susceptibility by the LDL receptor-related protein pathway. *The Journal of clinical investigation*, **106**, 1159-1166

Kang, J. G. L. H., Unterbeck, A., Salbaum, J. M., Masters, C. L., Grzeschik, K. H., Multhaup, G., Beyreuther, K., and Muller-Hill, B. (1987). The precursor of Alzheimer's disease amyloid A4 protein resembles a cell-surface receptor. *Nature*, **325**, 733-736

Katzman, R. and Saitoh, T. (1991). Advances in Alzheimer's disease. *The FASEB journal*, **5**, 278-286

Kelly. J. W. (1996). Alternative conformations of amyloidogenic proteins govern their behavior. *Current opinion in structural biology*, **6**, 11-17

Keston, A. S. and Brandt, R. (1965). The fluorometric analysis of ultramicro quantities of hydrogen peroxide. *Analytical biochemistry*, **11**, 1-5

Kim, E. S., Kim, R. S., Ren, R. F., Hawver. D. B., and Flanders, K. C. (1998). Transforming growth factor-ß inhibits apoptosis induced by ß-amyloid peptide fragment 25-35 in cultured neuronal cells. *Brain research. Molecular brain research*, **62**, 122-130

Kimura, H. and Schubert, D. (1993). Amyloid ß-protein activates tachykinin receptors and inositol trisphosphate accumulation by synergy with glutamate. *Proceedings of the National Academy of Sciences of the United States of America*, **90**, 7508-7512

Kisilevsky, R., Lemieux, L. J., Fraser, P. E., Kong, X., Hultin, P. G., and Szarek, W. A. (1995). Arresting amyloidosis in vivo using small-molecule anionic sulphonates or sulphates: implications for Alzheimer's disease. *Nature medicine*, **1**, 143-148

Kirschner, D. A., Abraham, C., and Selkoe, D. J. (1986). X-ray diffraction from intraneuronal paired helical filaments and extraneuronal amyloid fibers in Alzheimer disease indicates cross-ß conformation. *Proceedings of the National Academy of Sciences of the United States of America*, **83**, 503-507

Klein, W. L., Krafft, G. A., and Finch, C. E. (2001). Targeting small Aß oligomers: the solution to an Alzheimer's disease conundrum? *Trends in neurosciences*, **24**, 219-224

Klunk, W. E., Debnath, M. L., Koros, A. M. C., and Pettegrew, J. W. (1998). Chrysamine-G, a lipophilic analogue of congo red, inhibits Aß-induced toxicity in PC12 cells. *Journal of life science*, **63**, 1807-1814

Knauer, M. F., Soreghan, B., Burdick, D., Kosmoski, J., and Glabe, C, G. (1992). Intracellular accumulation and resistance to degradation of the Alzheimer amyloid A4/ß protein. *Proceedings of the National Academy of Sciences of the United States of America*, **89**, 7437-7441

Knowles, R. B., Gomez-Isla, T., and Hyman, B. (1998). Aß associated neuropil changes: correlation with neuronal loss and dementia. *Journal of neuropathology and experimental neurology*, **57**, 1122-1130

Koh, J.-Y., Yang, L. L., and Cotman, C. W. (1990). ß-Amyloid protein increases the vulnerability of cultured cortical neurons to excitotoxic damage. *Brain research*, **533**, 315-320

Kohno, T., Kobayashi, K., Maeda, T., Sato, K., and Takashima, A. (1996) Three-dimensional structures of the amyloid ß peptide 925-35) in membrane-mimicking environment. *Biochemistry*, **35**, 16094-16104

Kontush, A. (2001). Amyloid-ß: An antioxidant that becomes a pro-oxidant and critically contributes to Alzheimer's disease. *Free racical biology & medicine*, **31**, 1120-1131

Kontush, A., Berndt, C., Weber, W., Akopyan, V., Arlt, S., Schippling, S., and Beisiegel, U. (2001a). Amyloid-beta is an antioxidant for lipoproteins in cerebrospinal fluid and plasma. *Free radical biology & medicine*, **30**, 119-128

Kontush, A., Donarski, N., and Beisiegel, U. (2001b). Resistance of human cerebrospinal fluid to in vitro oxidation is directly related to its amyloid-beta content. *Free radical research*, **35**, 507-517

Koo, E. H., Lansbury, P. T., Jr., and Kelley, J. W. (1999). Amyloid diseases: abnormal protein aggregation in neurodegeneration. *Proceedings of the National Academy of Sciences of the United States of America*, **96**, 9989-9990

Koudinova, N. V., Koudinov, A. R., and Yavin, E. (2000). Alzheimer's Aß1-40 peptide modulates lipid synthesis in neuronal cultures and intact rat fetal brain under normoxic and oxidative stress conditions. *Neurochemical research*, **25**, 653-600

Kounnas, M. Z., Loukinova, E. B., Stefansson, S., Harmony, J. A. K., Brewer, B. H., Stricklnad, D. K., and Argraves, W. S. (1995). Identification of glycoprotein 330 as an endocytic receptor for apolipoprotein J/clusterin. *The Journal of biological chemistry*, **270**, 13070-13075

Kowall, N. W., McKee, A. C., Yankner, B. A., and Beal, M. F. (1992). In vivo neurotoxicity of beta-amyloid [ß(1-40)] and the ß(25-35) fragment. *Neurobiology of aging*, **13**, 537-542

Kremer, J. J., Pallitto, M. P., Sklansky, D. J., and Murphy, R. M. (2000). Correlation of ß-amyloid aggregate size and hydrophobicity with decreased bilayer fluidity of model membranes. *Biochemistry*, **39**, 10309-10318

Kremer, J. J., Sklansky, D. J., and Murphy, R. M. (2001). Profile of Changes in lipid bilayer structure caused by ß-Amyloid peptide. *Biochemistry*, **40**, 8563-8571

Kuner, P., Schubenel, R., and Hertel, C. (1998). ß-amyloid binds to $p75^{NTR}$ and activates NFκB in human neuroblastoma cells. *Journal of neuroscience research*, **54**, 798-801

Kuner, P., Bohrmann, B., Tjernberg, L. O., Naslund, J., Huber, G., Celenk, S., Gruninger-Leitch, F., Richards, J. G., Jakob-Roetne, R., Kemp, J. A., and Nordstedt, C. (2000). Controlling polymerization of ß-amyloid and prion-derived peptides with synthetic small molecule ligands. *The Journal of biological chemistry*, **275**, 1673-1678

Lambert, M. P., Barlow, A. K., Chromy, B. A., Edwards, C., Freed, R., Liosatos, M., Morgan, T. E., Rozovky, I., Trommer, B., Viola, K. L., Wals, P., Zhang, C., Finch, C. E., Krafft, G. A., and Klein, W. L. (1999). Diffusible, nonfibrillar ligands derived from $A\beta_{1-42}$ are potent central nervous system neurotoxins. *Proceedings of the National Academy of Sciences of the United States of America*, **95**, 6448-6453

Lambert, M. P., Stevens, G., Sabo, S., Barber, K., Wang, G., Wade, W., Krafft, G., Snyder, S., Holzman, T. F., and Klein, W. L. (1994) ß/A4-evoked degeneration of differentiated SH-SY5Y human neuroblastoma cells. *Journal of neuroscience research*, **39**, 377-385

Lane, N. J., Balbo, A., Fukuyama, R., Rapoport, S. I., and Galdzicki, Z. (1998). The ultrastructural effects of ß-amyloid peptide on cultured PC12 cells: changes in cytoplasmatic and intermembraneous features. *Journal of neurocytology*, **27**, 707-718

Lansbury, P. T. (1997). Inhibition of amyloid formation: a strategy to delay the onset of Alzheimer's disease. *Current opinion in chemical biololgy*, **1**, 260-267

Lansbury, P. T., Jr. (1999). Evolution of amyloid: what normal protein folding may tell us about fibrillogenesis and disease. *Proceedings of the National Academy of Sciences of the United States of America*, **96**, 3342-3344

Lauderback, C. M., Hackett, J., Keller, J. N., Varadarajan, S., Szweda, L., Kindy, M. S., and Butterfield, D. A. (2001). Apolipoprotein E knock-out synaptosomes are vulnerable to Aß(1-40)-induced oxidative injury. *Biochemistry*, **40**, 2548-2554

Lee, H-S., Park, C.-W., and Kim, Y.-S. (2000). MPP^+ increases the vulnerability to oxidative stress rather than directly mediating oxidative damage in human neuroblastoma cells. *Experimental neurology*, **165**, 164-171

Lee, J. P., Stimson, E. R., Ghilardi, J. R., Mantyh, P. W., Lu, Y.-A., Felix, A. M., Llanos, W., behbin, A., Cummings, M., Van Criekinge, M., Timms, W., and Maggio, J. E. (1995). ^1H NMR of Aß Amyloid peptide congeners in water solution. Conformational changes correlate with plaque competence. *Biochemistry*, **34**, 5191-200

Lehtonen, J. Y. A., Holopainen, J. M., and Kinnunen, P. K. J. (1996). Activation of Phospholipase A2 by Amyloid ß-Peptides in vitro. *Biochemistry*, **35**, 9407-9414

Lezoualc'h, F., Sagara, Y., Holsboer, F., and Behl, C. (1998). High constitutive NF-kappaB activity mediates resistance to oxidative stress in neuronal cells. *The Journal of neuroscience*, **18**, 3224-3232

Li, Y.-P., Bushnell, A. F., Lee, C. -M., Perlmutter, L. S., and Wong, S. K.-F. (1996). ß-Amyloid induces apoptosis in human derived neurotypic SH-SY5Y cells. *Brain research*, **738**, 196-204

Li, W. Y., Czilli, D., and Simmons, L. (1995). Neuronal membrane conductance activated by amyloid ß-peptide: importance of peptide conformation. *Brain research*, **682**, 207-211

Lin H., Zhu, Y. J., and Lal, R. (1998). Amyloid ß protein (1-40) forms calcium-permeable, Zn^{2+}-sensitive channel in reconstituted lipid vesicles. *Biochemistry*, **38**, 11189-11196

Liu, Y., Peterson, D. A., and Schubert, D. (1998). Amyloid ß peptide alters intracellular vesicle trafficking and cholesterol homeostasis. *Proceedings of the National Academy of Sciences of the United States of America*, **95**, 13266-13271

Liu Y., Dargusch, R., and Schubert, D. (1997). Beta amyloid toxicity does not require RAGE protein. *Biochemical and biophysical research communications*, **237**, 37-40

Lockhart, B. P., Benicourt, C., Junien, J. L., and Privat, A. (1994) Inhibitors of free radical formation fail to attenuate direct beta-amyloid 25-35 peptide-mediated neurotoxicity in rat hippocampal cultures. *Journal of neuroscience research*, **39**, 494-505

Lomakin, A., Chung, D. S., Benedek, G. B., Kirschner, D. A., and Teplow, D. B. (1996). On the nucleation and growth of amyloid ß-protein fibrils: Detection of nuclei and quantitation of rate constants. *Proceedings of the National Academy of Sciences of the United States of America*, **93**, 1125-1129

Loo, D. T., Copani, A., Pike, C. J., Whittemore, E. R., Walencewicz, A. J., and Cotman, C. W. (1993). Apoptosis is induced by ß-amyloid in cultured central nervous system neurons. *Proceedings of the National Academy of Sciences of the United States of America*, **90**, 7951-7955

Lorenzo, A. and Yankner, B. A. (1994). Beta-amyloid neurotoxicity requires fibril formation and is inhibited by congo red. *Proceedings of the National Academy of Sciences of the United States of America*, **91**, 12243-12247

Lovell, M. A., Ehmann, W. D., Butler, S. M., and Markesbery, W. R. (1995). Elevated thiobarbituric acid-reactive substances and antioxidant enzyme activity in the brain in Alzheimer's disease. *Neurology*, **45**, 1594-1601

Lovell, M. A. and Markesbery, W. R. (1998). Decreased glutathione transferase in brain and ventricular fluid in Alzheimer's disease. *Neurology*, **51**, 1562-1566

Lovell, M. A., Xie, C., and Markesbery, W. R. (2001). Acrolein is increased in Alzheimer's disease brain and is toxic to primary hippocampal cultures. *Neurobiology of aging*, **22**, 187-194

Lowe, T. L., Strzelec, A., Kiessling, L., and Murphy, R. M. (2001). Structure-function relationships for inhibitors of beta-amyloid toxicity containing the recognition sequence KLVFF. *Biochemistry*, **40**, 7882-7889

Maestre, G. E., Tate, B. A., Majocha, R. E., and Marotta, C. A. (1993). Membrane surface ruffling in cells that over-express Alzheimer amyloid ß/A4 C-terminal peptide. *Brain research*, **621**, 145-149

Maggio, J. E., Stimson, E. R., Ghilardi, J. R., Allen, C. J., Dahl, C. E., Whitcomb, D. C., Vigna, S. R., Vinters, H. V., Labenski, M. E., and Mantyh, P. W. (1992). Reversible in vitro growth of Alzheimer disease beta-amyloid plaques by deposition of labeled amyloid peptide. *Proceedings of the National Academy of Sciences of the United States of America*, **89**, 5462-5466

Mandybur, I. and Chuirazzi, C. C. (1990). Astrocytes and the plaques of Alzheimer's disease. *Neurology*, **40**, 635-639

Maness, L. M., Banks, W. A., Podlisny, M. B., Selkoe, D. J., and Kastin, A. J. (1994). Passage of human amyloid beta-protein 1-40 across the murine blood-brain barrier. *Life sciences*, **55**, 1643-1650

Marcus, D. L., Thomas, C., Rodriguez, C.,, Simberkoff, K., Tsai, T. S., Strafaci, J. A., and Fremann, M. L. (1998). Increased peroxidation and reduced antioxidant enzyme activity in Alzheimer's disease. *Experimental neurology*, **150**, 40-44

Mark, R. J., Blanc, E. M., and Mattson, M. P. (1996). Amyloid ß-peptide and oxidative cellular injury in Alzheimer's disease. *Molecular neurobiology*, **12**, 211-224

Mark, R. J., Fuson, K. S., and May, P. C. (1999). Characterization of 8-epiprostaglandin F2α as a marker of amyloid ß-peptide-induced oxidative damage. *Journal of neurochemistry*, **72**, 1146-1153

Mark, R. J., Hensley, K., Butterfield, D. A., and Mattson, M. P. (1995). Amyloid beta-peptide impairs ion-motive ATPase activities: evidence for a role in loss of neuronal Ca^{2+} homeostasis and cell death. *The Journal of neuroscience*, **15**, 6239-6249

Mark, R. J., Lovell, M. A., Markesbery, W. R., Uchida, K., and Mattson, M. P. (1997). A role for 4-hydroxynonenal, an aldehydic product of lipid peroxidation, in disruption of ion homeostasis and neuronal cell death induced by amyloid ß-peptide. *Journal of neurochemistry*, **68**, 255-264

Markesbery, W. R. (1997). Oxidative stress hypothesis in Alzheimer's disease. *Free radical biology & medicine*, **23**, 134-147

Markesbery, W. R. and Lovell, M. A. (1998). 4-Hydroxynonenal, a product of lipid peroxidation, is increased in the brain in Alzheimer's disease. *Neurobiology of aging*, **19**, 33-36

Mason, R. P., Estermyer, J. D., Kelly, J. F., and Mason, P. E. (1996). Alzheimer's disease amyloid ß peptide 25-35 is localized in the membrane hydrocarbon core: x-ray diffraction analysis. *Biochemical and biophysical research communications*, **222**, 78-82

Mason, R. P., Jacobs, R. F., Walter, M. F., Mason, P. E., Avdulov, N. A., Chochina, S. V., Igbavboa, U., and Wood, W. G. (1999). Distribution and fluidizing action of soluble and aggregate amyloid ß-peptide in rat synaptic plasme membranes. *The Journal of biological chemistry*, **26**, 18801-18807

Masters, C. L., Simms, G., Weinmann, N. A. G. M., McDonald, B. L., and Beyreuther, K. (1985). Amyloid plaque core protein Alzheimer's disease and Down syndrome. *Proceedings of the National Academy of Sciences of the United States of America*, **82**, 4245-4249

Matsunaga, W., Shirokawa, T., and Isobe, K. (2003). Specific uptake of Aß1-40 in rat brain occurs in astrocytes, but not microglia. *Neuroscience letters*, **342**, 129-131

Matilla, K. M., Pirttila, T., Blemow, K., Wallin, A., Viitanen, M., and Frey, H. (1994). Altered blood-brain barrier function in Alzheimer's disease? *Acta neurologica Scandinavica*, **89**, 192-198

Mattson, M. P., Cheng, B., David, D., Bryant, K., Lieberburg, I., and Rydel, R. E. (1992). ß-Amyloid peptides destabilize calcium homeostasis and render human neurons vulnerable to excitotoxicity. *The Journal of neuroscience*, **12**, 376-389

Mattson, M. P. and Goodman, Y. (1995). Different amyloidogenic peptides share a similar mechanism of neurotoxicity involving reactive oxygen species and calcium. *Brain research*, **676**, 219-224

Mattson, M. P., Tomaselli, K., and Rydel, R. E. (1993). Calcium-destabilizing and neurodegenerative effects of aggregated ß-amyloid peptide are attenuated by basic FGF. *Brain research*, **621**, 35-49

McClure, R. J., Kanfer, J. N., Panchalingam, K., Klunk, W. E., and Pettegrew, J. W. (1994). Alzheimer's disease: membrane-associated metabolic changes. *Annals of the New York Academy of Sciences*, **747**, 110-124

McLaurin, J. and Chakrabartty, A. (1996). Membrane disruption by Alzheimer ß-amyloid peptides mediated trough specific binding to either phospholipids or gangliosides. *The Journal of biological chemistry*, **271**, 26482-26489

McLaurin, J. and Chakrabartty, A. (1997). Characterization of the interactions of Alzheimer ß-amyloid peptides with phospholipids membranes. *European journal of biochemistry*, **245**, 355-363

McLaurin, J., Franklin, T., Fraser, P. E., and Chakrabartty, A. (1998). Structural transitions associated with the interaction of Alzheimer b-amyloid peptides with gangliosides. *The Journal of biological chemistry*, **273**, 4506-4515

Mecocci, P., Beal, M. F., Cechietti, R., Polidori, M. C., Cherubini, A., Chionne, F., Avellini, L., Romano, G., and Senin, U. (1997). Mitochondrial membrane fluidity and oxidative damage to mitochondrial DNA in aged and AD human brain. *Molecular and chemical neuropathology*, **31**, 53-64

Merrill, A. R., Proulx, P., ans Szabo, A. (1986). Effects of exogenous fatty acids on calcium uptake by brush-border membrane vesicles from rabbit small intestine. *Biochimica et biophysica acta*, **855**, 337-344

Merz, P. A., Wisneiwski, H. M., Sommerville, R. A., Bobin, S. A., Masters, C. L., and Iqbal, K. (1983). Ultrastructural morphology of amyloid fibrils from neuritic and amyloid plaques. *Acta neuropathologica*, **60**, 113-124

Miatto, O., Gonzalez, R. G., Buonanno, F., and Growdon, J. H. (1986). In vitro 31P NMR spectroscopy detecs altered phospholipids metabolism in Alzheimer's disease. *The Canadian journal of neurological sciences*, **13**, 535-539

Michikawa, M., Gong, J.-S., Fan, Q. W., Sawamura, N., and Yanagisawa, K. (2001). A novel action of Alzheimer's amyloid ß-protein (Aß): oligomeric Aß promotes lipid release. *The Journal of neuroscience*, **21**, 7226-7235

Mielke, R., Kessler, J., Szelies, B., Herholz, K., Wienhard, K., and Heiss, W. D. (1998). Normal and pathological aging: findings of positron-emission-tomography. *Journal of neural transmission*, **105**, 821-837

Mills, J. and Reiner, P. B. (1999). Regulation of amyloid precursor protein cleavage. *Journal of neurochemistry*, **72**, 443-460

Misonou, H., Morishima-Kawashima, M., and Ihara, Y. (2000). Oxidative stress induces accumulation of Amyloid ß-protein (Aß) in human neuroblastoma cells. *Biochemistry*, **39**, 6951-6959

Mitchell, D. C., and Litman, B. J. (1998). Effect of cholesterol on molecular order and dynamics in highly polyunsaturated phospholipids bilayers. *Biophysical journal*, **75**, 896-908

Mirzabekov, T., Lin, M.-C., Yuan, W.-L., Marshall, P. J., Carman, M., Tomaselli, K., Lieberburg, I., and Kagan, B. L. (1994). Channel formation in planar lipid bilayers by a neurotoxic fragment of the beta-amyloid peptide. *Biochemical and biophysical research communications*, **202**, 1142-1148

Montine, T., Neely, M., Quinn, J., Beal, W., Markesbery, W., Roberts, L., and Morrow, J. (2002). Lipid peroxidation in aging brain and Alzheimer's disease (1, 2). *Free radical biology & medicine*, **33**, 620

Moran, P. M., Higgins, L. S., Cordell, B., and Moser, P. C. (1995). Age-related learning deficits in transgenic mice expressing the 751-amino acid isoform of human beta-amyloid precursor protein. *Proceedings of the National Academy of Sciences of the United States of America*, **92**, 5341-5345

Morton, A. J., Hammond, C., Mason, W. T., and Henderson, G. (1992). Characterization of the L- and N-type calcium channels in differentiated SH-SY5Y neuroblastoma cells: calcium imaging and single channel recording. *Molecular brain research*, **13**, 53-61

Müller, W. E., Kirsch, C., and Eckert, G. P. (2001). Membrane-disordering effects of ß-amyloid peptides. *Biochemical Society transactions*, **29**, 617-623

Müller, W. E., Koch, S., Eckert, A., Hartmann, H., and Scheuer, K. (1995). Beta-amyloid peptide decreases membrane fluidity. *Brain research*, **674**, 133-136

Müller, W. E., Eckert, G. P., Cairns, N. J., Maras, A., and Gattaz, W. F. (1998). Effects of ß-amyloid peptides on the fluidity of membranes from frontal and parietal lobes of human brain. High potencies of Aß1-42 and Aß1-43. *Amyloid: the international journal of experimental and clinical investigation*, **5**, 10-15

Naidu, A., Quon, D., and Cordell, B. (1995). beta-Amyloid peptide produced in vitro is degraded by proteinases released by cultured cells. *The Journal of biological chemistry*, **270**, 1369-1374

Nitsch, R. M., Blusztajan, J. K., Pittas, A. G., Slak, B. E., Growdon, J. H., and Wurtman, R. J. (1992). Evidence for a membrane defect in Alzheimer disease brain. *Proceedings of the National Academy of Sciences of the United States of America*, **89**, 1671-1675

Nunomura, A., Perry, G., Pappolla, M. A., Friedland, R. P., Hirai, K., Chiba, S., and Smith, M. A. (2000). Neuronal oxidative stress precedes amyloid-ß deposition in Down syndrome. *Journal of neuropathology and experimental neurology*, **59**, 1011-1017

Nunomura, A., Perry, G., Aliev, G., Hirai, K., Takeda, A., Balraj, E. K., Jones, P. K., Ghanbari, H., Wataya, T., Shimohana, S., Chiba, S., Atwood, C. S., Peterson, R. B., and Smith, M. A. (2001). Oxidative damage is the earliest event in Alzheimer disease. *Journal of neuropathology and experimental neurology*, **60**, 759-767

Nussbaum, R. L. and Ellis, C. E. (2003). Alzheimer's disease and Parkinson's disease. *New England journal of medicine*, **348**, 1356-1364

Olivieri, G., Baysang, G., Meier, F., Müller-Spahn, F., Stähelin, H. B., Brockhaus, M., and Brack, Ch. (2001). N-Acetyl-L-cysteine protects SHSY5Y neuroblastoma cellf from oxidative stress and cell cytotoxicity: effects on ß-amyloid secretion and tau phosphorylation. *Journal of neurochemistry*, **76**, 224-233

Olivieri, G., Brack, Ch., Müller-Spahn, F., Stähelin, H. B., Hermann, M., Renard, P., Brockhaus, M., and Hock, C. (2000). Mercury induces cell cytotoxicity, oxidative stress and increases ß-amyloid secretion, tau-phosphorylation in SHSY5Y neuroblastoma cells. *Journal of neurochemistry*, **74**, 231-236

Olsson, A., Vanmechelen, E., Vanderstichele, H., Davidsson, P., and Blennow, K. (2003). Unaltered plasma levels of ß-Amyloid (1-40) and ß-Amyloid (1-42) upon stimulation of human platelets. *Dementia and geriatric cognitive disorders*, **16**, 93-97

Oyama, Y., Chikahisa, L., Ueha, T., Hatakeyama, Y., and Kokubun, T. (1995). Change in membrane permeability induced by amyloid ß-protein fragment 25-35 in brain neurons dissociated from rats. *Japanese journal of pharmacology*, **68**, 77-83

Pahlman, S., Mamaeva, S., Meyerson, G., Mattson, M. E., Bjelfman, C. Ortoft, E., and Hammerling, U. (1990). Human neuroblastoma cells in culture: a model for neuronal cell differentiation and function. *Acta physiologica Scandinavica. Supplementum*, **592**, 25-27

Pallitto, M. M., Ghanta, J., Heinzelman, P., Kiessling, L. L., and Murphy, R. M. (1999). Recognition sequence design for peptidyl modulators of ß-amyloid aggregation and toxicity. *Biochemistry*, **38**, 3570-3578

Palmer, A. M. and Burns, M. A. (1994). Selective increase in lipid peroxidation in the inferior temporal cortex in Alzheimer's disease. *Brain research*, **645**, 338-342

Paresce, D. Ghosh, R. N., and Maxfield, F. R. (1996). Microglial cells internalize aggregates of the Alzheimer-s disease amyloid ß-protein via a scavenger receptor. *Neuron*, **17**, 553-565

Perlmutter, D. H. (1994). Microvascular pathology and vascular basement membrane components in Alzheimer's disease. *Molecular neurobiology*, **9**, 33-40

Perry, G., Castellani, R., Hirai, K., and Smith, M. A. (1998). Reactive oxygen species mediate cellular damage in Alzheimer disease. *Journal of Alzheimer's disease*, **1**, 45-55

Petty, H. R., Niebylski, C. D., and Francis, J. W. (1987). Influence of immune complexes on macrophage membrane fluidity: A nanosecond fluorescence anisotropy study. *Biochemistry*, **26**, 6340-6348

Piasecka, A., Leyko, W., Krajewska, E., and Bryszewska, M. (2000). Effect of combined treatment with perindoprilat and low-power red light irradiation on human erythrocyte membrane fluidity, membrane potential and acetylcholinesterase activity. *Scandinavian journal of clinical and laboratory investigation*, **60**, 395-402

Pike, C. J., Burdick, D., Walencewicz, A. J., Glabe, C. G., and Cotman, C. W. (1993). Neurodegeneration induced by ß-Amyloid peptides *in vitro*: the role of peptide assembly state. *Journal of neuroscience*, **13**, 1676-87

Pike, C. J., Cummings, B. J., and Cotman, C. W. (1992). ß-Amyloid induces neuritic dystrophy in vitro: Similarities with Alzheimer pathology. *Neuroreport*, **3**, 769-772

Pike, C., Cummings, B. J., Monzavi, R., and Cotman, C. W. (1994). ß-Amyloid-induced changes in cultured astrocytes parallel reactive astrocytosis associated with senile plaques in Alzheimer's disease. *Neuroscience*, **63**, 517-531

Pike, C. J., Ramezan-Arab, N., and Cotman, C. W. (1997). ß-Amyloid neurotoxicity in vitro: evidence of oxidative stress but no protection by anti-oxidants. *Journal of neurochemistry*, **69**, 1601-1611

Pike, C. J.,Walencewicz, A. J., Glabe, C. G., and Cotman, C. W. (1991a). Aggregation-related toxicity of synthetic ß-amyloid protein in hippocampal cultures. *European journal of pharmacology*, **207**, 367-368

Pike, C. J., Walencewicz, A. J., Glabe, C. G., and Cotman, C. W. (1991b). In vitro aging of ß-amyloid protein causes peptide aggregation and neurotoxicity. *Brain research*, **563**, 311-314

Pike, C. J., Walencewicz-Wasserman, A. J., Kosmoski, J., Cribbs, D. H., Glabe, C. G., and Cotman, C. W. (1995). Structure-activity analyses of ß-amyloid peptides: contributions of the ß25-35 region to aggregation and toxicity. *Journal of neurochemistry*, **64**, 253-265

Pillot, T., Goethals, M., Vanloo, B., Talussot, C., Brasseur, R., Vandekerckhove, J., Rosseneu, M., and Lins, L. (1996). Fusogenic properties of the C-terminal domain of the Alzheimer ß-amyloid peptide. *The Journal of biological chemistry*, **271**, 28757-28765

Pillot, T., Drouet, B., Queille, S., Labeur, C., Vanderkerckhove, J., Rosseneu, M., Pincon-Raymond, M., and Chambaz, J. (1999). The nonfibrillar amyloid ß-peptide induces apoptotic neuronal cell death: involvement of its C-terminal fusogenic domain. *Journal of neurochemistry*, **73**, 1626-1634

Plant, L. D., Boyle, J. P., Smith, I. A., Peers, C., and Pearson, H. A. (2003). The production of Amyloid ß peptide is a critical requirement for the viability of central neurons. *The Journal of neuroscience*, **23**, 5531-5535

Pocernich, C. B., Cardin, A., Racine, C., Lauderback, C. M., and Butterfield, D. A. (2001). Glutathione elevation and its protective role in acrolein-induced protein damage in synaptosomal membranes: relevance to brain lipid peroxidation in neurodegenerative disease. *Neurochemistry international*, **39**, 141-149

Prehn, J. H., Bindokas, V. P., Jordan, J., Galindo, M. F., Ghadge, G. D., Roos, R. P., Boise, L. H., Thompson, C. B., Krajewski, S., Reed, J. C., and Miller, R. J. (1996). Protective effect of transforming growth factor-ß1 on ß-amyloid neurotoxicity in rat hippocampal neurons. *Molecular pharmacology*, **49**, 319-329

Prasad, M. R., Lovell, M. A., Yatin, M., Dhillon, H., and Markesbery, W. R. (1998). Regional membrane phospholipids alterations in Alzheimer's disease. *Neurochemical research*, **23**, 81-88

Putnam, F. W. (1975). The plasma proteins. *2nd Ed., Academic Press, New York*

Qiu, W. Q., Borth, W., Ye, Z., Haass, C., Teplow, D. B., and Selkoe, D. J. (1996). Degradation of amyloid ß-protein by a serine protease-α2-macroglobulin complex. *The Journal of biological chemistry*, **271**, 8443-8451

Qiu, W. Q., Ye, Z., Kholodenko, D., Seubert, P., and Selkoe, D. J. (1997). Degradation of amyloid ß-protein by a metalloprotease secreted by microglia and other neural and non-neural vells. *The Journal of biological chemistry*, **272**, 6641-6646

Ravichandra, B. and Joshi, P. G. (1999). Gangliosides asymmetrically alter the membrane order in cultured PC-12 cells. *Biophysical chemistry*, **76**, 117-132

Rinken, A., Harro, J., Engstrom, L., and Oreland, L. (1998). Role of fluidity of membranes on the guanyl nucleotide-dependent binding of cholecystokinin-8S to rat cortical membranes. *Biochemical pharmacology*, **55**, 423-431

Rodrigues, C. M. P., Sola, S., Brito, M. A., Brondino, C. D., Brites, D., and Moura, J. J. G. (2001). Amyloid ß-peptide disrupts mitochondrial membrane lipid and protein structure: protective role of tauroursodeoxycholate. *Biochemical and biophysical research communications*, **281**, 468-474

Roher, A. E., Chaney, M. O., Kuo, Y. -M., Webseter, S. D., Stine, W. B., Haverkamp, L. J., Woods, A. S., Cotter, R. J., Tuohy, J. M., Krafft, G. A., Bonnell, B. S., and Emmerling, M. R. (1996). Morphology and toxicity of Aß-(1-42) dimmer derived from neuritic and vascular amyloid deposits of Alzheimer's disease. *The Journal of biological chemistry*, **271**, 20631-20635

Rosenberg, R. N. (1993). A causal role for amyloid in Alzheimer's disease: The end of the beginning. *Neurology*, **43**, 851-856

Rothwarf, D. M. and Karin, M. (1999). The NF-κB activation pathway: a paradigm in information transfer from membrane to nucleus. *Science's STKE*, **5**, 1-16

Rottkamp, C. A., Raina, A. K., Zhu, X., Gaier, E., Bush, A. I., Atwood, C. S., Chevion, M., Perry, G., and Smith, M. A. (2001). Redox-active iron mediates amyloid-ß toxicity. *Free radical biology & medicine*, **30**, 447-450

Rubinsztein, D. C. (1997). The genetics of Alzheimer's disease. *Progress in neurobiology*, **52**, 447-454

Sadler, I. J., Smith, D. W., Shearman, M. S., Ragan, C. I., Tailor, V. J., and Pollack, S. J. (1995). Sulphated compounds attenuate ß-amyloid toxicity by inhibiting its association with cells. *Neuroreport*, **7**, 49-53

Saido, T. C., Iwatsubo, T., Mann, D. M., Shimada, H., Ihara, Y., and Kawashima, S. (1995). Dominant and differential deposition of distinct beta-amyloid peptide species, Aß N3 (pE), in senile plaques. *Neuron*, **14**, 457-466

Saito, Y., Buciak, J., Yang, J., and Pardridge, W. M. (1995). Vector-mediated delivery of ^{125}I-labeled ß-amyloid peptide Aß$^{1-40}$ through the blood-brain barrier and binding to Alzheimer disease amyloid of the Aß$^{1-40}$ /vector complex. *Proceedings of the National Academy of Sciences of the United States of America*, **92**, 10227-10231

Salinero, O., Moreno-Flores, M. T., Ceballos, M. L., and Wandosell, F. (1997). ß-Amyloid peptide induced cytoskeletal reorganization in cultured astrocytes. *Journal of neuroscience research*, **47**, 216-223

Salomon, A. R., Marcinowski, K. J., Friedland, R. P., and Zagorski, M. G. (1996). Nicotine inhibits amyloid formation by the ß-Peptide. *Biochemistry*, **35**, 13568-78

Savage, M. J., Trusko, S. P., Howland, D. S., Pinsker, L. R., Mistressa, S., Reaume, A. G., Greenberg, B. D., Siman, R., and Scott, R. W. (1998). Turnover of amyloid ß-protein in mouse brain and acute reduction of its level by phorbol ester. *The Journal of neuroscience*, **18**, 1743-1752

Sayre, L. M., Zelasko, D. A., Harris, P. L., Perry, G., Salomon, R. G., and Smith, M. A. (1997). 4-Hydroxynonenal-derived advanced lipid peroxidation products are increased in Alzheimer's disease. *Journal of neurochemistry*, **68**, 2092-2097

Schaffer, L. M., Dority, M. D., Gupta-Bansal, R., Frederickson, R. C. A., Younkin, S. G.,, and Brunden, K. R. (1995). Amyloid ß protein (Aß) removal by neuroglial cells in culture. *Neurobiology of aging*, **16**, 737-745

Schenk, D. B., Rydel, R. E., May, P., Little, S., Panetta, J., Lieberburg, I., and Sinha, S. (1995). Therapeutic approaches related to amyloid-ß peptide and Alzheimer's Disease. *Journal of medicinal chemistry*, **38**, 4141-4154

Scheuner, D., Eckman, C., Jensen, M., Song, X., Citron, M., Suzuki, N., Bird, T. D., Hardy, J., Hutton, M., Kukull, W., Larson, E., Levy-Lahad, E., Vitanen, M., Peskind, E., Poorkaj, P., Schellenberg, G., Tanzi, R., Wasco, W., Lannfelt, L., Selkoe, D., and Younkin, S. (1996). Secreted amyloid ß-protein similar to that in the senile plaques of Alzheimer's disease is increased in vivo by the presenilin 1 and 2 and APP mutations linked to familial Alzheimer's disease. *Nature medicine*, **2**, 864-870

Schreck, R., Albermann, K., and Baeuerle, P. A. (1992). Nuclear factor kB: an oxidative stress-responsive transcription factor of eukaryotic cells (a review). *Free radical research communications*, **17**, 221-237

Schubert, D., Behl, C., Lesley, R., Brack., A., Dargusch, R., Sagara, Y., and Kimura, H. (1995). Amyloid peptides are toxic via a common oxidative mechanism. *Proceedings of the National Academy of Sciences of the United States of America*, **92**, 1989-1993

Schultz, J. G., Megow, D., Reszka, R., Villringer, A., Einhaupl, K. M., and Dimagl, U. (1998). Evidence that glypican is a receptor mediating ß-amyloid neurotoxicity in PC12 cells. *The European journal of neuroscience*, **10**, 2085-2093

Seilheimer, B., Bohrmann, B., Bondolfi, L., Muller, F., Stuber, D., and Dobeli, H. (1997). The toxicity of the Alzheimer's b-amyloid peptide correlates with a distinct fiber morphology. *Journal of structural biology*, **119**, 59-71

Selkoe, D. J. (1991). The molecular pathology of Alzheimer's disease. *Neuron*, **6**, 487-498

Selkoe, D. J. (1996). Amyloid ß-protein and the genetics of Alzheimer's disease. *The Journal of biological chemistry*, **271**, 18295-18298

Selkoe, D. J. (1997). Alzheimer's disease: genotypes, phenotypes, and treatments. *Science*, **275**, 630-631

Seubert, P., Vigo-Pelfrey, C., and Esch, F. Lee, M., Dovey, H., Davis, D., Sinha, S., Schlossmacher, M., Whaley, J., Swindlehurst, C., McCormack, R., Wolfert, R., Selkoe, D. J., Lieberburg, I., and Schenk, D. (1992). Isolation and quantification of soluble Alzheimer's ß-peptide from biological fluids. *Nature*, **359**, 325-327

Shearman, M. S., Ragan, C. I., and Iversen, L. L. (1994). Inhibition of PC12 cell redox activity is a specific, early indicator of the mechanism of ß-amyloid-mediated cell death. *Proceedings of the National Academy of Sciences of the United States of America*, **91**, 1470-1474

Shearman, M. S., Hawtin, S. R., and Tailor, V. J. (1995). The intracellular component of cellular 3-(4,5-dimethylthiazol-2-yl)-2,5-diphenyltetrazolium bromide (MTT) reduction is specifically inhibited by ß-amyloid peptides. *Journal of neurochemistry*, **65**, 218-227

Sheehan, S. P., Swerdlow, R. H., Miller, S. W., Davis, R. E., Parks, J. K., Parker, W. D., and Tuttle, J. B. (1997). Calcium homeostasis and reactive oxygen species production in cells transformed by mitochondria from individuals with sporadic Alzheimer's disease. *The Journal of neuroscience*, **17**, 4612-4622

Shen, C. L. and Murphy, R. M. (1995). Solvent effects on self-assembly of beta-amyloid peptide. *Biophysical journal*, **69**, 640-651

Shen, Y., Li, R., and Shiosaki, K. (1997). Inhibition of p75 Tumor Necrosis Factor Receptor by Antisense Oligonucleotides Increases Hypoxic Injury and ß-Amyloid Toxicity in Human Neuronal Cell Line. *The Journal of biological chemistry*, **272**, 3550-3553

Shibata, M., Yamada, S., Kumar, S. R., Calero, M., Bading, J., Frangione, B., Holtzman, D. M., Miller, C. A., Strickland, D. K., Ghiso, J., and Zlokovic, B. V. (2000). Clearance of Alzheimer's amyloid-ß(1-40) peptide from brain by LDL receptor-related protein-1 at the blood-brain barrier. *The Journal of clinical investigation*, **106**, 1489-1499

Shin, R. W., Ogino, K., Kondo, A., Saido, T. C. Trojanowski, J. Q., Kitamoto, T., and Tateishi, J. (1997). Amyloid beta-protein (Aß) 1-40 but not Aß1-42 contributes to the experimental formation of Alzheimer disease amyloid fibrils in rat brain. *The Journal of neuroscience*, **17**, 8187-8193

Shinitzky, M. and Inbar, M. (1974). Difference in microviscosity induced by different cholesterol levels in the surface membrane lipid layer of normal lymphocytes and malignant lymphoma cells. *Journal of molecular biology*, **85**, 603-615

Shoji, M., Golde, T. E., Ghiso, J., Cheung, T. T., Estus, S., Shaffer, L. M., Cai, X. -D., McKay, D. M., Tintner, R., Frangione, B., and Younkin, S. G. (1992). Production of the Alzheimer amyloidß protein by normal proteolytic processing. *Science*, **258**, 126-129

Siman, R., Card, J. P., Nelso, R. B., and Davis, L. G. (1989). Expression of ß-amyloid precursor protein in reactive astrocytes following neuronal damage. *Neuron*, **3**, 275-285

Simmons, L. K., May, P. C., Tomaselli, K. J., Rydel, R. E., Fuson, K. S., Brigham, E. F., Wright, S., Lieberburg, I., Becker, G. W., Brems, D. N., and Li, W. Y. (1994). Secondary structure of Amyloid ß peptide correlates with neurotoxic activity in vitro. *Molecular pharmacology*, **45**, 373-9

Simmons, M. A. and Schneider, C. R. (1993). Amyloid ß peptides act directly on single neurons. *Neuroscience letters*, **150**, 133-136

Sisodia, S. S., Price, D. L. (1995). Role of ß-amyloid protein in Alzheimer's disease. *The FASEB Journal*, **9**, 366-370

Smith, C. D., Carney, J. M., Starke-Reed, P. E., Oliver, C. N., Stadtman, E. R., Floyd, R. A., and Markesberry, W. R. (1991). Excess brain protein oxidation and enzyme dysfunction in normal aging and in Alzheimer disease. *Proceedings of the National Academy of Sciences of the United States of America*, **88**, 10540-10543

Smith, C. D., Carney, J. M., Tatsumo, T., Stadtman, E. R., Floyd, R. A., and Markesbery, W. R. (1992). Protein oxidation in aging brain. *Annals of the New York Academy of Sciences*, **663**, 110-119

Smith, M. A., Casadesus, G., Joseph, J. A., and Perry, G. (2002). Amyloid-ß and τ serve antioxidant functions in the aging and Alzheimer brain. *Free radical biology & medicine*, **33**, 1194-1199

Smith, M. A. and Perry, G. (2002). Lipid peroxidation and protein oxidation in Alzheimer's disease brain: potential causes and consequences involving amyloid ß-peptide-associated free radical oxidative stress. *Free radical biology & medicine*, **32**, 1050-1060

Smith, M. A., Rottkamp, C. A., Nunomura, A., Raina, A. K., and Perry, G. (2000). Oxidative stress in Alzheimer's disease. *Biochimica et biophysica acta*, **1502**, 139-144

Smits, H. A., van Beelen, A. J., de Vos, N. M., Rijsmus, A., van der Bruggen, T., Verhoef, J., van Muiswinkel, F. L., and Nottet, H. S. L. M. (2001). Activation of human macrophages by amyloid-ß is attenuated by astrocytes. *Journal of immunology*, **166**, 6869-6876

Snyder, S. W., Ladror, U. S., Wade, W. S., Wang, G. T., Barrett, L. W., Matayoshi, E. D., Huffaker, H. J., Krafft, G. A., and Holzman, T. F. (1994) *Biophysical journal*, **67**, 1216-1228

Solomon, B, Koppel, R., Frankel, D., and Hanan-Aharan, E. (1997). Disaggregation of Alzheimer ß-amyloid by site-directed mAb. *Proceedings of the National Academy of Sciences of the United States of America*, **94**, 4109-4112

Soto, C., Kindy, M. S., Baumann, M., and Frangione, B. (1996). Inhibition of Alzheimer's amyloidosis by peptides that prevent ß-sheet conformation. *Biochemical and biophysical research communications*, **226**, 672-680

Soto, C., Sigurdsson, E. M., Morelli, L., Kumar, R. A., Castano, E. M., and Frangione, B. (1998). ß-sheet breaker peptides inhibit fibrillogenesis in a rat brain model of amyloidosis: implications for Alzheimer's therapy. *Nature medicine*, **4**, 822-826

Stewart, J. C. (1980) Colorimetric determination of phospholipids with ammonium ferrothiocyanate. *Analytical biochemistry*, **104**, 10-14

Subbarao, K. V., Richardson, J. S., and Ang, L. C. (1990). Autopsy samples of Alzheimer's cortex show increased peroxidation in vitro. *Neurology*, **45**, 1594-1601

Subramaniam, R., Roedinger, F., Jordan, B., Mattson, M. P., Keller, J. N., Waeg, G., and Butterfield, D. A. (1997). The lipid peroxidation product, 4-hydroxy-2-trans-nonenal, alters the conformation of cortical synaptosomal membrane proteins. *Journal of neurochemistry*, **69**, 1161-1169

Sunderland T., Linker G., Mirza N., Putnam K. T., Friedman D. L., Kimmel L. H., Bergeson J., Manetti G. J., Zimmermann M., Tang B., Bartko J. J., and Cohen R.M. (2003). Decreased beta-amyloid1-42 and increased tau levels in cerebrospinal fluid of patients with Alzheimer disease. *JAMA: the journal of the American Medical Association*, **289**, 2094-103

Sung, Y. J., Cheng, C. L., Chen, C. S., Huang, H. B., Huang, F. L., Wu, P. C., Shiao, M. S., and Tsay, H. J. (2003). Distinct mechanisms account for ß-Amyloid toxicity in PC12 and differentiated PC12 neuronal cells. *Journal of biomedical science*, **10**, 379-388

Suzuki, N., Cheung, T. T., Cai, X. D., Okada, A., Otvos, L., Jr., Eckman, C., Golde, T. E., and Younkin, S. G. (1994). An increased percentage of long amyloid-ß protein secreted by familial amyloid-ß protein precursor (beta APP717) mutants. *Science*, **264**, 1336-1340

Swerdlow, R. H., Parks, J. K., Cassarino, D. S., Maguire, D. J., Maguire, R. S., Bennett, J., P., Jr., Davis, R. E., and Parker, W. D. Jr. (1997). Cybrids in Alzheimer's disease: a cellular model of the disease? *Neurology*, **49**, 918-925

Takaoma, A., Miyatake, F., Matsuno, S., Ishii, K., Nagase, S., Sahara, N., Ono, S., Mori, H., Wakabayashi, K., Tsuji, S., Takahashi, H., and Shoji, S. (2000). Apolipoprotein E allele-dependent antioxidant activity in brains with Alzheimer's disease. *Neurology*, **54**, 2319-2321

Terzi, E., Hölzemann, G., and Seelig, J. (1994). Alzheimer ß-Amyloid peptide 25-35: Electrostatic interactions with phospholipids membranes. *Biochemistry*, **33**, 7434-7441

Terzi, E., Hölzemann, G., and Seelig, J. (1995). Self-association of ß-Amyloid peptide (1-40) in solution and binding to lipid membranes. *Journal of molecular biology*, **252**, 633-642

Tomiyama, T., Shoji, A., Kataoka, K. –I., Suwa, Y., Asano, S., Kanetko, H., and Endo, N. (1996). Inhibition of amyloid ß protein aggregation and neurotoxiciy by rifampicin. *The Journal of biological chemistry*, **271**, 10205-10208

Tjernberg, L. O., Lilliehöök, C., Callaway, D. J. E., Näslund, J., Hahne, S., Thyberg, J., Terenius, L., and Norstedt (1997). Controlling amyloid ß-peptide fibril formation with protease stable ligands. *The Journal of biological chemistry*, **272**, 12601-12605

Tjernberg, L. O., Näslund, J, Lindqvist, F., Johansson, J., Karlström, A. R., Thyberg, J., Terenius, L., and Norstedt (1996). Arrest of ß-amyloid fibril formation by a pentapeptide ligand. *The Journal of biological chemistry*, **271**, 8545-8548

Tomita, S., Fujita, T., Kirino, Y., and Suzuki, T. (2000). PDZ Domain-dependent Suppression of NF-κB/p65-induced Aß42 Production by a Neuron-specific X11-like Protein. *The Journal of biological chemistry*, **275**, 13056-13060

Tomiyami, T., Shoji, A., Kataoka, K.,-I., Suwa, Y., Asano, S., Kanetko, H., and Endo, N. (1996). Inhibition of amyloid ß-protein aggregation and neurotoxicity by rifampicin. *The Journal of biological chemistry*, **271**, 10205-10208

Tucker, H. M., Rydel, R. E., Wright, S., and Estus, S. (1998). Human amylin induces "apoptotic" pattern of gene expression concomitant with cortical neuronal apoptosis. *Journal of neurochemistry*, **71**, 506-516

Ueda, K., Fukui, Y., and Kageyama (1994). Amyloid ß protein-induced neuronal cell death: neurotoxic properties of aggregated amyloid ß protein. *Brain research*, **639**, 240-244

Ueda, K., Shinohara, S., and Yagami, T. (1997). Amyloid beta protein potentiates Ca^{2+} influx through L-type voltage-sensitive Ca^{2+} channels: A possible involvment of free radicals. *Journal of neurochemistry*, **68**, 265-271

Vanderstichele, H., van Kerschaver, E., Hesse, C., Davidsson, P., Buyse, M. A., Andreasen, N., Minthon, L., Wallin, A., Blennow, K., and Vanmechelen, E. (2000). Standardization of measurement of beta-amyloid (1-42) in cerebrospinal fluid and plasma. *Amyloid: the international journal of experimental and clinical investigation*, **7**, 245-258

Van Duijn, C. M. and Hofman, A. (1991). Relation between nicotine intake and Alzheimer's disease. *BMJ*, **332**,1491-1494

Walter, M. F., Mason, P. E., and Mason, R. P. (1997). Alzheimer's disease amyloid ß peptide 25-35 inhibits lipid peroxidation as a result of its membrane interactions. *Biochemical and biophysical research communications*, **233**, 760-764

Ward, R. V., Jennings, K. H., Jepras, R., Neville, W., Owen, D. E., Hawkins, J., Chrisie, G., Davis, J. B., George, A., Karran, E. H., and Howlett, D. R. (2000). Fractionation and characterization of oligomeric, protofibrillar and fibrillar forms of ß-amyloid peptide. *The Biochemical journal*, **348**, 127-144

Weiss, J. H., Pike, J., and Cotman, C. W. (1994). Ca^{2+} channel blockers attenuate ß-Amyloid peptide toxicity to cortical neurons in culture. *The Journal of neuroscience*, **62**, 372-375

Wernyj, R. P., Mattson, M. P., and Christakos, S. (1999). Expression of calbindin-D28k in C6 glial cells stabilizes intracellular calcium levels and protects against apoptosis induced by calcium ionophore and amyloid ß-peptide. *Brain research: Molecular brain research*, **64**, 69-79

Whitson, J. S. and Appel, S. H. (1995). Neurotoxicity of Aß amyloid protein in vitro is not altered by calcium channel blockade. *Neurobiology of aging*, **16**, 5-10

Whitson, J. S., Selkoe, D. J., and Cotman, C. W. (1989). Amyloid ß protein enhances the survival of hippocampal neurons in vitro. *Science*, **243**, 1488-1490

Wong, C. W., Quaranta, V., and Glenner, G. G. (1985). Neuritic plaques and cerebrovascular amyloid in Alzheimer disease are antigenically related. *Proceedings of the National Academy of Sciences of the United States of America*, **82**, 8729-8732

Wood, W. G., Igbavboa, U., Rao, A. M., Schroeder, F., and Avdulov, N. A. (1995). Cholesterol oxidation reduces Ca^{2+} + Mg^{2+} - ATPase activity, interdigitation, and increases fluidity of brain synaptic plasma membranes. *Brain research*, **683**, 36-42

Wood, S. J., MacKenzie, L., Maleeff, B., Hurle, M. R., and Wetzel, R. (1996). Selective inhibition of Aß fibril formation. *The Journal of biological chemistry*, **271**, 4086-92

Wujek, J. R., Dority, M. D., Frederickson, R. C. A., and Brunden, K. R. (1996). Deposits of A-beta fibrils are not toxic to cortical and hippocampal neurons in vitro. *Neurobiology of aging*, **17**, 107-113

Wurtmann, R. J. (1992). Choline metabolism as a basis for the selective vulnerability of cholinergic neurons. *Trends in neurosciences*, **15**, 117-122

Xie, Y., Yao, Z., Chai, H., Wong, W. M., and Wu, U. (2003). Potential roles of Alzheimer precursor protein A4 and ß-amyloid in survival and function of aged spinal motor neurons after axonal injury. *Journal of neuroscience research*, **15**, 557-564

Xu, J., Chen, S., Hinan Ahmed, S., Chen, H., Ku, G., Goldberg, M. P., and Hsu, C. Y. (2001). Amyloid-ß peptides are cytotoxic to oligodendrocytes. *The Journal of neuroscience*, **21**, RC118, 1-5

Yan, S. D., Chen, X., Fu, J., Chen, X., Zhu, H., Roher, A., Slattery, T., Zhao, L., Nagashima, M., Morser, J., Migheli, A., Nawroth, P., Stern, D., and Schmidt, A. M. (1996). RAGE and amyloid-ß peptide neurotoxicity in Alzheimer's disease. *Nature*, **382**, 685-691

Yan, S. D., Fu, J., Soto, C., Chen, X., Zhu, H., Al-Mohanna, F., Collison, K., Zhu, A., Stern, E., Saido, T., Tohyamas, M., Ogawa, S., Roher, A., and Stern, D. (1997). An intracellular protein that binds amyloid-b peptide and mediates neurotoxicity in Alzheimer's disease. *Nature*, **389**, 689-695

Yan, S. D., Shi, Y., Zhu, H., Zhu, Y., Goibson, L., Stern, E., Collison, K., Al-Mohanna, F., Ogawa, S., Roher, A., Clarke, S. G., and Stern, D. M. (1999). Role of ERAB/L-3-hydroxyacyl-coenzyme A dehydrogenase Type II activity in Ab-induced cytotoxicity. *The Journal of biological chemistry*, **274**, 2145-2156

Yan, S. D., Yan, S. F., Chen, X., Fu, Y., Chen, M., Kuppusamy, P. Smith, M. A., Perry, G., Goodman, G. C., and Nawroth, P. (1995). Nonenzymatically glycated τ in Alzheimer's disease induces neuronal oxidant stress resulting in cytokine gene expression and release of amyloid ß-peptide. *Nature medicine*, **1**, 693-699

Yanagisawa, K., Odaka, A., Suzuki, N., and Ihara, Y. (1995). GN1 ganglioside-bound amyloid ß-protein (Aß): A possible form of preamyloid in Alzheimer's disease. *Nature medicine*, **1**, 1062-1066

Yang, A. J., Chandswangbhuvana, D., Margol, L., and Glabe, C. G. (1998). Loss of endosomal/lysosomal membrane impermeability is an early event in amyloid Aß1-42 pathogenesis. *Journal of neuroscience research*, **52**, 691-698

Yankner, B. A. (1996). New clues to Alzheimer's disease: unraveling the roles of amyloid and tau. *Nature medicine*, **2**, 850-852

Yankner, B. A., Dawes, L., Fisher, S., Villa-Komaroff, L., Oster-Granite, M. L., and Neve, R. (1989). Neurotoxicity of a fragment of the Amyloid precursor associated with Alzheimer's disease. *Science*, **245**, 417-420

Yankner, B. A., Duffy, L. K., and Kirschner, D. A. (1990). Neurotrophic and neurotoxic effects of Amyloid ß protein: reversal by tachykinin neuropeptides. *Science*, **250**, 279-282

Yao, Z.-X., Drieu, K., Szweda, L. I., and Papadopoulos, V. (1999). Free radicals and lipid peroxidation do not mediate ß-amyloid-induced neuronal cell death. *Brain research*, **847**, 203-210

Yip, C. M., Elton, E. A., Darabie, A. A., Morrison, M. R., and McLaurin, J. (2001). Cholesterol, a modulator of membrane-associated Aß-fibrillogenesis and neurotoxicity. *Journal of molecular biology*, **311**, 723-734

Yip, C. M. and McLaurin, J. (2001). Amyloid-ß peptide assembly: a critical step in fibrillogenesis and membrane disruption. *Biophysical journal*, **80**, 1359-1371

Yu, G. S. P., Hu, J., and Nakagawa, H. (1998). Inhibition of ß-amyloid cytotoxicity by midkine. *Neuroscience letters*, **254**, 125-128

Zamani, M. R. and Allen, Y. S. (2001). Nicotine and its interaction with ß-Amyloid Protein: A short review. *Biological psychiatry*, **49**, 221-232

Zamani, M. R., Allen, Y. S., Own, G. P., and Gray, J. A. (1997). Nicotine modulates the neurotoxic effect of beta-amyloid protein (25-35) in hippocampal cultures. *Neuroscience*, **88**, 755-764

Zhang, C., Lambert, M. P., Bunch, C., Barber, K., Wade, W. S., Krafft, G. A., and Klein, W. L. (1994). Focal adhesion kinase expressed by nerve cell lines shows increased tyrosine phosphorylation in response to Alzheimer's Aß peptide. *The Journal of biological chemistry*, **269**, 25247-25250

Zhang, L., Zhao, B., Yew, D. T., Kusiak, J. W., and Roth, G. S. (1997). Processing of Alzheimer's Amyloid Precursor Protein during H_2O_2-Induced Apoptosis in Human Neuronal Cells. *Biochemical and biophysical research communications*, **235**, 845-848

Zlokovic, B. V., Ghiso, J., Mackik, J. B., McComb, J. G., Weiss, M. H., and Fragione, B. (1993). *Biochemical and biophysical research communications*, **197**, 1043-1050

Zlokovic, B. V., Martel, C. L., Mackik, J. B., Matsubara, E., Wisniewski, T., McComb, J. G., Frangione, B., and Ghiso, J. (1994). Brain uptake of circulating apolipoproteins J and E complexed to Alzheimer's amyloid beta. *Biochemical and biophysical research communications*, **205**, 1431-1437

Zlokovic, B. V., Martel, C. L., Matsubara, E., McComb, J. G., Zheng, G., McCluskey, R. T., Frangione, B., and Ghiso, J. (1996). Glycoprotein 330/megalin: probable role in receptor-mediated transport of apolipoprotein J alone and in a complex with Alzheimer disease amyloid beta at the blood-brain and blood-cerebrospinal fluid barriers. *Proceedings of the National Academy of Sciences of the United States of America*, **93**, 4229-4234

Erich Pusch

Born on the 10th of July 1974 in Vienna/Austria
Nationality: Austrian
Parents: Dr. Rudolf Pusch, pediatrician, and Dr. Kveta Pusch, general practitioner

Formation

2000-2003 — Technical University Vienna, Austria
Doctor of Philosophy
Technical Chemistry, Thesis in preparation
"The dual role of the Alzheimer disease protein ß-Amyloid: Anti-oxidative ß-Amyloid (1-40) becomes a pro-oxidant during self-aggregation and damages the plasma membrane of neurons."
Institute of Process Engineering, Environmental Technology and Technical Bioengineering, Technical University Vienna, Austria, Univ. Prof. Dr. Stachelberger
Department of Chemical Engineering, UW Madison, USA, Regina Murphy, PhD
Clinic of Neurology, General Hospital Vienna, Austria, Dr. Mark Schiefermeier

1992-2000 — Technical University Vienna, Austria
Technical Chemistry, Specialization Biochemistry
Dipl.- Ing.
"Influence of in vivo and ex vivo hyperthermia on the expression of the 70kDa-heat shock protein Hsp70 in human leucocytes."
Institute of Applied Botanic, Technical Microscopy, and Organic Raw Material Science, Technical University Vienna, Univ. Prof. Dr. Stachelberger
Clinic of Surgery, General Hospital Vienna, Austria, Univ. Prof. Dr. Erich Roth

1979-1992 — Lycée Francais de Vienne, Vienna, Austria
Baccalauréat, Specialization Science
Austrian Matura Graduation with Honor

Publications

Oehler R, Pusch E, Zellner M, Dungel P, Hergovics N, Homoncik M, Eliasen MM, Brabec M, and Roth E. Cell type-specific variations in the induction of hsp70 in human leukocytes by feverlike whole body hyperthermia. Cell Stress Chaperones. 2001 Oct;6(4):306-15.

Oehler R, Pusch E, Dungel P, Zellner M, Eliasen MM, Brabec M, and Roth E. Glutamine depletion impairs cellular stress response in human leucocytes. Br J Nutr. 2002 Jan;87 Suppl 1:S17-21.

Presentations

Murphy RM, Kremer J, and Pusch E. Structural changes in lipid bilayers and cell membranes caused by adsorption of beta-amyloid peptide. AIChe Annual Meeting, 152c, 2001

Pusch E and Oehler R. Influence of glutamine on the Hsp70-Expression in human lymphocytes, Gemeinsame Jahrestagung von ÖBG und ÖGGGT 1999: 123